

**Oklahoma Water Resources Research Institute
Annual Technical Report
FY 2008**

Introduction

The Institute for Sustainable Environments (ISE) at Oklahoma State University continues to promote interdisciplinary environmental research, graduate education, and public outreach leading to better understanding, protecting, and sustainably developing the natural environment. The Oklahoma Water Resources Research Institute (OWRRI) is located within the ISE and is responsible for developing and coordinating water research funding to address the needs of Oklahoma. To guide it in meeting this objective, the OWRRI has assembled a board of state regulators, policymakers, and other water resource professionals. This board is known as the Water Research Advisory Board (WRAB).

Research Program Introduction

2008

In 2008, proposals were solicited from all comprehensive universities in Oklahoma. Proposals were received from Oklahoma State University and the University of Oklahoma. Fourteen proposals were submitted and from these, three projects were selected for funding for one year each.

- Evaluation of Water Use Monitoring by Remote Sensing ET Estimation Methods (Dr. Yang Hong, OU) evaluated and improved remote sensing ET estimation methods and adapted them for use in Oklahoma.
- An Assessment of Environmental Flows for Oklahoma (Dr. Don Turton, OSU) used the Hydroecology Integrity Assessment Process (HIP) developed by the U.S. Geological Survey to assess environmental flows in Oklahoma's perennial streams.
- Decision Support Model for Evaluating Alternative Water Supply Infrastructure Scenarios (Dr. Brian Whitacre, OSU) will develop a step-by-step procedure that rural water systems can follow to assess their water supply infrastructure needs and to plan and locate funding for needed improvements. This project experienced delays and is not complete. An interim report is included here and the final report will be submitted with next year's annual report.

2007

Also, included in this report are the final technical reports for the three projects funded in 2007. All were granted extensions due to delays in funding during 2007. These projects were:

- Subsurface Transport of Phosphorus to Streams: A Potential Source of Phosphorus not Alleviated by Best Management Practices (Dr. Garey Fox, OSU)
- Determination of Fracture Density in the Arbuckle-Simpson Aquifer from Ground Penetrating Radar (GPR) and Resistivity Data (Dr. Ibrahim Cemen, OSU)
- Decision Support Model for Optimal Water Pricing Protocol for Oklahoma Water Planning: Lake Tenkiller Case Study (Dr. Tracy Boyer, OSU)

Decision Support Model for Optimal Water Pricing Protocol for Oklahoma Water Planning: Lake Tennkiller Case Study

Basic Information

Title:	Decision Support Model for Optimal Water Pricing Protocol for Oklahoma Water Planning: Lake Tennkiller Case Study
Project Number:	2007OK78B
Start Date:	3/1/2007
End Date:	6/16/2008
Funding Source:	104B
Congressional District:	3
Research Category:	Social Sciences
Focus Category:	Economics, Surface Water, Water Use
Descriptors:	Water Pricing, Non-Market Valuation, Water Allocation
Principal Investigators:	Tracy Boyer, Larry Sanders, Arthur Stoecker

Publication

Final Report

Oklahoma Water Resources Research Institute (FY 2007)

Title: Decision Support Model for Optimal Water Pricing Protocol for Oklahoma Water Planning: Lake Tenkiller Case Study

Start Date: (3/1/2007)

End Date: (6/16/2008)

Congressional District:3

Focus Category: Water Use, Surface Water, Economics

Descriptors: ECPM; M&P, SW, WQN, WS, WU

Principal Investigators: Tracy Boyer, Agricultural Economics, Oklahoma State University; Art Stoecker, Agricultural Economics, Oklahoma State University, and Larry Sanders, Agricultural Economics, Oklahoma State University.

Publications: none

Students Trained and Supported:

Student Status	Number	Disciplines
Undergraduate	1	Agricultural Economics
M.S.	3	Agricultural Economics
Ph.D.	1	Agricultural Economics
Post Doc		
Total	5	

Section I: Problem and Research Objectives

Objectives

The objective of this study was to develop a water pricing model that could be used in the state water planning process. The model considers both monetary and opportunity costs in the allocation of surface water between competing uses. The model was constructed for Tenkiller Ferry Lake in Sequoyah and Cherokee counties. The specific purpose was to develop a water pricing protocol that

- (1) internalizes monetary and opportunity costs of water storage, treatment, and delivery systems; and
- (2) generates an sustainable supply of water over the 2010-2060 period.

Background

The lake dam is located in the Arkansas River Basin on the Illinois River in Sequoyah County. The lake is among the Oklahoma's 34 major reservoirs that store 13 million acre-feet of water. The structure was federally authorized for flood control and hydroelectric power. Construction was completed by the US Army Corps of Engineers (USACE) in 1953. The lake has 130 miles of shoreline with a mean depth of 51 feet. Capacity is 654,100 acre feet at the normal pool and 1,230,800 at the flood pool (OWRB Fact Sheet). The main beneficial uses of the lake are recreation, flood control, power generation, stream flow maintenance and municipal and industrial use.

The need for an economic model that optimizes net benefits from multiple water uses and tracks water balances for Tenkiller and other lakes is illustrated by statements from the U.S. Army Corps of Engineers (USACE) 2001 report on a proposed water treatment and conveyance study (USACE, 2001). According to the 2001 USACE report Lake Tenkiller had water rights of 29,792 acre feet with 14,739 feet allocated. Applications were pending for 172,714 acre feet. The USACE report found the 9,096 acre feet of water rights owned by the participating systems are insufficient to meet demands by the year 2050. The report further pointed out that "...having sufficient water rights does not guarantee a ... system would have enough water to meet projected demands. Water storage must also be considered"

The optimization model illustrates the tradeoffs between managing for market uses (municipal and hydropower) and managing for all uses including market and recreational uses (non-market) of surface water resources. When non-market uses, in this case, recreation, are ignored, these values are assumed to be zero in the management process. The results of this modeling process illustrate the economic importance of recreational uses by showing that when recreational values are explicitly considered in the optimization model, surface water pool levels are maintained at normal pool level during peak summer months of recreational use. Although securing water supplies, hydropower, and flood control provided the original motivation for creating Tenkiller Dam, like many other reservoirs in the Oklahoma system, the subsequent recreational values prove significant and maintenance of water rights for users and the regional economies should be also explicitly considered in the state water planning process.

Current recreational values for lake use were not available for Oklahoma. Thus this study first conducted a statewide recreational valuation study to provide as input into this model and future state water planning studies. Accordingly, the final report is divided into sub-reports to provide results on the specific objectives of the project as follows:

Section II Valuation of Oklahoma Lakes

- II.1 Problem and Research Objectives Oklahoma Lake Valuation
- II.2 Methodology of Oklahoma Lakes Survey
- II.3 Principal Findings and Significance of Oklahoma Lakes Survey

Section III Construction and Optimization of a Lake Model for Power, Municipal, and Recreation

- III.1 Objectives
- III. 2 Review of Lake Management Modeling
- III.3 Principal Findings and Significance

Section IV Extension of Research Results

- IV.1 Methodology
- IV.2 Principal Findings and Significance

Methodology

Section II. Valuation of Oklahoma Lakes

The state of Oklahoma has over 300 lakes, more man-made lakes than any other state, with over one million surface acres of water (Oklahoma Tourism and Recreation Department, 2007). Many of lakes are used for several reasons such as hydroelectric power, flood control, agriculture, and recreation. Since the mid 1950s, demand for lake recreation in Oklahoma has increased continuously due to increased convenience of transportation, communication, and other technologies such as types of vehicles and types of new watercrafts available to public (Caneday, 2000). The outdoor recreation business was reported as one of the fastest growing businesses in Oklahoma (Oklahoma Tourism and Recreation Department, 2001). Even though the demand for lake recreation in Oklahoma is increasing, few recent studies have analyzed the

demand for lake recreation as well as welfare effects from lake use in term of recreation (Jordan and Badger, 1977). Caneday and Jordan (2003) studied the behavior of Oklahomans traveling to state parks, but they did not estimate economic values for water based amenities such as quality and quantity or estimate total visitation across all water-oriented recreational activities. Therefore, currently, there is no comprehensive explanation for lake recreation demand in Oklahoma.

II.1 Problem and Research Objectives of Oklahoma Lake Valuation

This study estimated the value of lake recreation for Tenkiller as part of a statewide Oklahoma Lakes Survey conducted in 2007. The research performed in this study focuses on determining what the opportunity cost of diminished recreational value for Tenkiller recreation when there are competing uses for water. Specifically we wished to answer the following question, “What is the recreational value of a trip to Tenkiller Lake?” However, since values for recreation were scant for the entire state of Oklahoma, we wished to determine what factors influence demand for lake recreation statewide and specifically how much does willingness to pay for recreation change according to lake quality improvements?” When no value is assigned to recreational uses, then they are treated as if they were zero.

II. 2 Methodology of Oklahoma Lakes Survey

Data for this paper were collected by mail on Oklahoma Lake Use (2007) for travel cost and discrete choice experiments. The survey is provided in appendix A. Data on travel distances and lake characteristics were compiled from GIS maps from Oklahoma Water Resource Board (OWRB), lake websites, and phone interview with lake managers.

The survey was mailed to 2,000 individuals, who were randomly chosen, in every county of Oklahoma during fall 2007. A random sample was obtained from Survey Sampling Inc, Fairfield, CT, stratified across 6 regions of Oklahoma.

The survey was first distributed in September 2007 by mail. Standard Dillman procedures were used to elicit the highest possible response rate (Dillman, 2000). The cover letter and follow up letters that accompanied the survey are provided in Appendix A. From 2,000 surveys, 401 were returned. Thirty-nine of them were unusable, and allowing for 150 undeliverable surveys due to no forwarding addresses. The net response rate was 19.57 percent. The survey was designed to collect both revealed preferences for lake visits, i.e., travel cost data, and stated or hypothetical data on preferences for lake amenities. The revealed preference method is often believed to be very credible for valuation since users have actually chosen to spend money and time visiting a site. The hypothetical/stated preference method is helpful in determining potential demand for improvements or management scenarios not currently available.

Stated preference data

The Oklahoma Lakes Survey asked hypothetical or stated preference (SP) questions about potential management changes in lake amenities using a discrete choice experiment. Orthogonally designed sets of discrete choice experiments were designed to estimate willingness to pay for quality and amenity improvements at a lake similar to the lake respondents most often visited. The SP questions elicited lake visitor preferences for lake attributes, including availability of lake amenities and distance travelled to the lake. Six measurable attributes associated with lake recreation at 2 to 6 levels each as shown in Table II.1. This created 2,304 possible combinations. Each combination was then randomly paired with another combination to create different options for columns A and B. The third option from which respondents could choose was given as the respondent's most frequently visited lake, or the status quo for that person.

Each respondent was asked to answer two experimental choice questions. Each of them contains two options of hypothetical lakes, options A and B. An example is given in Figure II.1.

Table II.1. Attributes and Levels in the Discrete Choice Survey (Stated Preference)

Attribute	Factor Levels
Increase in public boat ramp	None 1 Boat ramp 2 Boat ramp 3 Boat ramp
Campsites	None Available Available with electric service
Public restroom	None Porta-potties/ Pit toilets Restroom with flush toilets Restroom with flush toilets and showers
Lodge	None Available
Water clarity	No improvement 1 foot increase of water visibility dept from surface 2 foot increase of water visibility dept from surface 3 foot increase of water visibility dept from surface
Increase in distance from home (one-way)	0 miles increase 10 miles increase 20 miles increase 30 miles increase 40 miles increase 50 miles increase

Figure II. 1. An Example of Conjoint Question

Compared to the lake you most visit, would you choose a lake such as A or B? Or would you choose to stay with the one you currently visit, C? Please choose one.

Attribute	Option A	Option B	Option C
Increase in public boat ramps	2 Boat ramp	1 Boat ramp	NO CHANGE: I would rather keep the management of this lake the way it is today
Campsites	Available with electric service	Available with electric service	
Public restrooms	Restroom with flush toilets and showers	Restroom with flush toilets and showers	
Lodges	None	Available	
Water clarity	1 foot increase of water visibility dept from surface	No improvement	
Increase in distance from home (one-way)	20 miles increase	40 miles increase	
I would choose (Please check only one)	<input type="checkbox"/> A	<input type="checkbox"/> B	<input type="checkbox"/> C (I would not want either A or B)

Given your choice above, how many trips per year would you take?

Number of single day trips same number or ___#less or ___# more

Modeling

The marginal values for the attributes listed in Table II.1 were estimated using a conditional logit model based on the Random Utility Model (RUM). We assume that when asked to choose between options A, B and the option of not choosing a lake, our respondents choose the option that gives them highest utility. If

$$U_{ij} > U_{ik} \tag{1}$$

the respondent will select option j over k only if (1) holds for all $j \neq k$.

However, we do not know real utility of the respondent. We can only observe part of the respondent’s utility denoted as V_{ij} , and the unobservable part of the utility that is unknown is denoted as ε_{ij} . Therefore, the utility can be represented as

$$U_{ij} = V_{ij} + \varepsilon_{ij} \tag{2}$$

where i denotes the respondent, j denotes the option (A, B, or neither A or B).

As mentioned above, the respondents will choose the option or lake that gives them highest utility, and we can observe V_{ij} by giving options A, B, or neither A or B to respondents. Therefore, V_{ij} can be expressed as a function of policy attributes accompanying each alternative, for the stated preference example below:

$$V_{ij} = \beta_1(R_{ij}) + \beta_2(C_{ij}) + \beta_3(CE_{ij}) + \beta_4(P_{ij}) + \beta_5(T_{ij}) + \beta_6(FS_{ij}) + \beta_7(L_{ij}) + \beta_8(WQ_{ij}) + \beta_9(F_{ij})\varepsilon_{ij} \quad (3)$$

The equation for the stated preference discrete choice model is as follows: R is the number of boat Ramps available; C is a dummy for whether a basic campsite is available; CE is whether a campsite with electricity is available; P is if porta-potties are available only; T is a dummy variable if flush toilets are available; FS is dummy variable of restroom with flush toilets and showers; and L is if a lodge is available, WQ is the water clarity measured by Secchi Disk depth, and F is the price of going to the lake (either a distance converted to a mileage rate or a fee imposed for entry, depending on the model). β 's are the parameters to be estimated. In addition, in order to calculate the marginal willingness to pay, each attribute coefficient will be divided by the estimated coefficient for distance which functions as the price paid for the trip.

Revealed preference data (Travel Cost Model)

Respondents were also asked to report their actual visitation patterns of single-day trips and multiple day trips to 144 public lakes in Oklahoma in 2007 (See Appendix B for the table of lakes in the survey). They were also asked a series of questions about their activities at lakes, features of lakes they prefer, and basic demographic data. Appendix C gives additional statistics on the activities, interest in state provided information on the lakes and demographics of the sample which were not explicitly used in the travel cost valuation.

In order to obtain the effect of water quality on lake recreation demand, water quality data were gathered from Beneficial Use Monitoring Program (BUMP) database of OWRB. Because more detailed chemical analysis data such as phosphorus, nitrate and algal levels were not available, system wide, Secchi disk depth level is used. A Secchi disk is used to measure how deep a person can see into the water. A black and white patterned disk is lowered into the lake until the observer loses sight of it. Then, the disk is raised until it reappears. The depth of the water where the disk reappears is the Secchi disk reading. Although this is a crude measure, lake users have direct visual experience with lake clarity and may not have awareness of other quality characteristics.

Data on the physical amenities available at each lake (types of restrooms, docks, campsites, boat ramp, etc.) were collected from the lake websites and/ or by phone interview with lake managers. TransCAD software was used to calculate the distance from each zip code to 144 lakes via roads. Then, the distances were expressed as round trip travel cost, which was combined with out-of-pocket expenditure and opportunity cost of time.¹

Again, as explained above in equations (1) and (2), a conditional logit, random utility travel cost model is estimated for the travel cost model. A random utility travel cost model is focused on measuring the differences in site characteristics as a function of site choice (details on measurement of environmental values and differing methods are available in Freeman, 2003). The “price” of recreation is trip cost, such as mileage in our model. It is assumed that a person chooses the lake with the characteristics that yield the highest utility (or happiness) conditional on the availability of 143 other lakes with a varied set of amenities. A single lake’s value is estimated by the formula as follows

$$CV = -\frac{1}{\beta_{TC}} \ln(\exp(v_j)) \quad (4)$$

where β_{TC} is the travel cost coefficient, and v_j is the indirect utility visiting site j . In this method, the user has reported actual trips to lakes in Oklahoma.

II.3 Principle Findings and Significance of the Oklahoma Lakes Survey

Table II.2 below gives the results from the stated preference model. All of the variables included were significantly different from zero at greater than 90% confidence levels except for increases in Boat Ramps, the presence of a state park lodge, portable potties, and improvements in water clarity. These four variables do not induce a significant willingness to pay that is different from zero. The result for park lodges is interesting since Oklahoma has an extensive lodge system that needs constant upgrading due to its age. Table II.3 translates these results into mean willingness to pay for these individual attributes. The entrance fee model shows that having basic campsites at the average lake raises a lake’s per trip value \$6.48 (2007USD) compared to having none, but campsites with electric hookups add an additional \$6.80 per trip. Flush toilets were worth \$23.47 per trip compared to having none and restrooms with showers were worth \$3.55 per trip more. These results confirm that users of lakes value more services over fewer amenities.

¹ The out-of-pocket expenditure was estimated by multiplying distance with \$0.48/ mile, and the opportunity cost of time was calculated as one third of an hourly individual’s wage rate time by travel time, which was assumed speed of 50 mile/hour.

Table II.2 Conditional Logit Entrance Fee Model (Stated Preference)

Parameter	DF	Coeff	Std	t-value	p-value
		-			
Boat ramp	1	0.015	0.064	-0.240	0.8130
Camp available	1	0.318	0.189	1.680	0.0920
Camp with electric	1	0.651	0.185	3.520	0.0004
Porta-Potties	1	0.363	0.243	1.500	0.1340
Flush toilet	1	1.150	0.223	5.150	<0.0001
Flush toilet with showers	1	1.324	0.224	5.920	<0.0001
Lodge	1	0.120	0.147	0.820	0.4140
Water clarity	1	0.099	0.067	1.500	0.1342
		-			
Entrance fee	1	0.049	0.007	-6.550	<0.0001
		-			
Constant	1	1.680	0.277	-6.080	<0.0001
Log Likelihood = -553.400					

Table II.3 Willingness to Pay for Changes in Attributes from the Entrance Fee Model

	WTP
Boat ramp	NS
Camp available	\$6.48
Camp with electric	\$13.28
Porta-Potties	NS
Flush toilet	\$23.47
Flush toilet with showers	\$27.02
Lodge	NS
Water clarity	NS

NS indicates the variables are not significantly different from zero.

Travel Cost Model

The results from the Travel Cost Model are given in Tables II.4 and II.5 which give the descriptive statistics and results respectively. Travel Cost is measured in 2007 dollars per person per trip. Travel cost is calculated as the round trip cost of road travel and time travel on the road. This was found by multiplying distance with \$0.48/ mile (AAA 2007 rate), and the opportunity cost of time was calculated as one third of an hourly individual's wage rate time by travel time, which was assumed speed of 50 mile/hour. The issue of valuing individuals' time is problematic because of differences in paid versus unpaid time off, among other issues. We take a conservative approach here and value lost time in travel to and from the site. The assumption we make here is that the trip itself is an opportunity cost, but the individual does not view time on site as a cost in lost wages. The mean expenditure for single day trips is \$186.18, and \$149.34 per trip. However, the value of each lake depends on its characteristics when using the models estimated in Table II.5. Lakes were divided regionally by quadrants dividing the state of Oklahoma by I-40 running East-West and I-35 running North-South.

Table II.4. Travel Cost Model: Variable Definitions for Oklahoma Lakes

Variable	Definition	Mean or %
<i>Travel Cost¹</i>	\$/roundtrip/person	\$186.1877 (Single Day Trip) \$149.3376 (Multiple Days Trip)
<i>Boat Ramp</i>	Number	3.3542
<i>Porta-Potties</i>	Number	3.2500
<i>Flush-Toilet</i>	Number	1.2431
<i>Flush-Toilet with Shower</i>	Number	1.6944
<i>Lodge</i>	Number	0.7153
<i>Campsite</i>	Number	83.2708
<i>Campsite with Electricity</i>	Number	60.4792
<i>Water Clarity</i>	Centimeters Secchi Depth	82.9011
<i>Shoreline</i>	Miles	69.9375
<i>Swimming Beach</i>	Available=1, 0 otherwise	40.28%
<i>Major Lake</i>	Area>5000 acres =1, 0 otherwise	15.97%
<i>North East</i>	If in NE region=1, 0 otherwise	44.44%
<i>South East</i>	If in SE region=1, 0 otherwise	30.56%
<i>South West</i>	If in SW region=1, 0 otherwise	15.97%
<i>North West</i>	If in NW region=1, 0 otherwise	9.03%

1 The out-of-pocket expenditure was estimated by multiplying distance with \$0.48/ mile, and the opportunity cost of time was calculated as one third of an hourly individual's wage rate time by travel time, which was assumed speed of 50 mile/hour.

Table II.5 gives the conditional logit valuation results for Oklahoma Lakes in 2007 by single Day Users and Multiple Day Users. The willingness to pay for each attribute on average is given in the column next to the coefficient estimate. The dependant variable is the choice of a lake for a trip given all the other substitute sites available and their characteristics.

For the day trip users, lodge and campsites are omitted from the estimation in the first model in Table II.5. Portapotties, boat ramps, and flush toilets proved insignificantly different from zero. Users preferred flush toilets with showers at \$6.50/trip per user. Water clarity proved significant and had a willingness to pay of \$0.38 per centimeter increased clarity per trip for lakes on average and \$0.03/mile increase in lake shoreline available on average. Swimming beaches were highly valued at \$56.09/trip per user. Major lakes on average are worth \$96 more than lakes that are less than 5000 acres. Among the regions, all regions were significantly preferred to the Northwestern lakes, but the Northeast had the highest value at \$59/trip with the Southwest at slightly less at \$56/trip. Results would suggest that day users greatly value swimming beaches, larger lakes, and the ability to shower at the end of the day in a full restroom facility.

The results for multiple day users in Table II.5 are similar to those for day trip users. Boat Ramps, basic campsites, and shoreline size were not significantly different from zero. Multiple-day trip users had negative values for porta-potties, lodges, and restroom facilities that lacked shower facilities. They were willing to pay \$36/trip for a lake trip where restrooms with showers were available and \$1.24 per trip more for lakes with campsites with electricity. Note that these two amenities are usually available at the same lake simultaneously, so it does not indicate that users are simply willing to pay \$1.24 to camp overnight, it is the combination of these marginal values of given amenities at a site that adds up to total willingness to pay. Water clarity is valued at \$1.70 per centimeter of clarity and a swimming beach is marginally worth \$192 per trip to the multiple day user. Large lakes are \$129 more valuable on average than lakes under 5000 acres to multiple day users. Southwestern (\$269), northeastern (\$204), and southwestern (\$200) lakes are ranked from most to least favorite for multiple day users over northwestern lakes.

Regional rankings are the one category that differs between day users and multiple day users. Multiple day users rank southwestern lakes highest whereas day users rank northeastern lakes highest. The southeastern area is ranked a distant third for day users, most likely because of the difficulty of travelling there for a day trip.

Table II.5 Conditional Logit Results for Oklahoma Lakes (2007)
(Dependant Variable is Lake Site Choice)

Variable	Single Day User	WTP for Single Day User (\$)	Multiple Day User	WTP for Multiple Days User (\$)
<i>Travel Cost</i>	-0.0111*** (-17.0800)		-0.0051*** (-3.9900)	
<i>Boat Ramp</i>	0.0143 (1.4000)	1.2895	0.0047 (0.1700)	0.9142
<i>Porta-Potties</i>	-0.0140 (-1.5000)	-1.2629	-0.0902*** (-3.7300)	-17.5267
<i>Flush-Toilet</i>	-0.0162 (-0.9400)	-1.4544	-0.0434 (-1.1300)	-8.4394
<i>Flush-Toilet with Shower</i>	0.0726*** (3.9300)	6.5331	0.1883*** (3.8500)	36.5863
<i>Lodge</i>			-0.0319** (-2.0600)	-6.1936
<i>Campsite</i>			-0.0024 (-1.1600)	-0.4603
<i>Campsite with Electricity</i>			0.0066** (2.4200)	1.2867
<i>Water Clarity</i>	0.0043*** (5.6700)	0.3884	0.0088*** (5.8700)	1.7049
<i>Shoreline</i>	0.0004*** (3.7300)	0.0381	0.0004 (1.2200)	0.0800
<i>Swimming Beach</i>	0.6233*** (4.9100)	56.0876	0.9918*** (3.4500)	192.7010
<i>Major Lake</i>	1.0749*** (8.0300)	96.7292	0.6675** (2.2600)	129.6863
<i>North East</i>	0.6615*** (3.0400)	59.5277	1.0543** (2.1700)	204.8405
<i>South East</i>	0.4407* (1.8700)	39.6550	1.0311** (2.0600)	200.3334
<i>South West</i>	0.6236** (2.4900)	56.1190	1.3873** (2.4900)	269.5271
Log-Likelihood	-2026.677		-574.311	
No. of Observation	70128		22032	

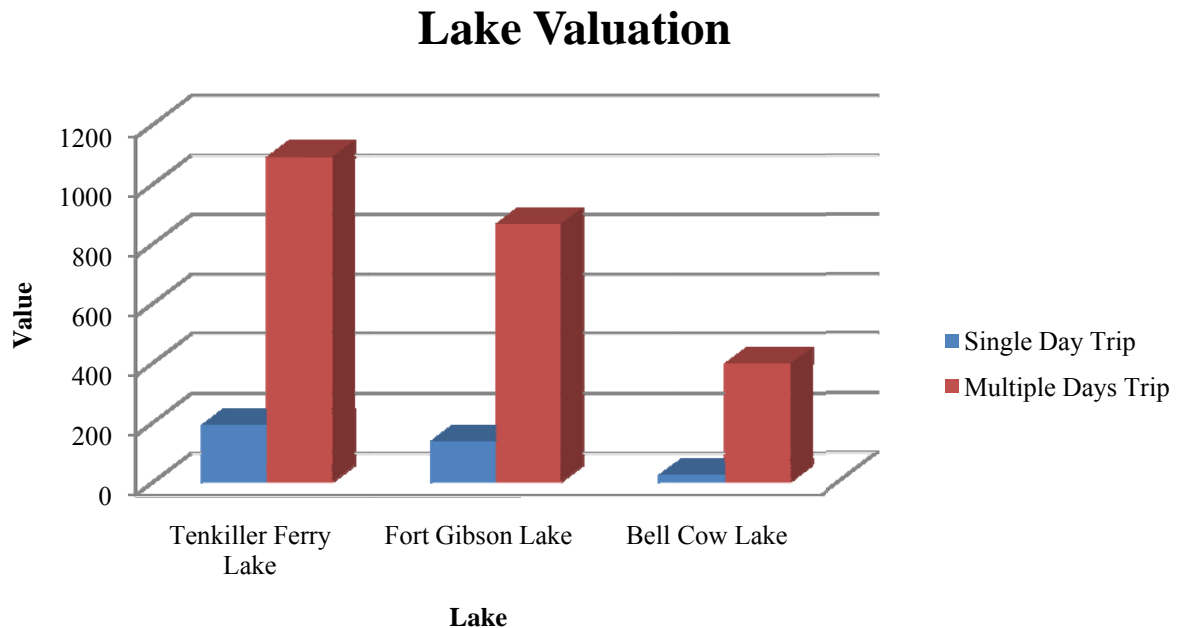
Note: ***, **, and * indicate significant level at the 1%, 5%, and 10%, respectively.

Table II.6 and Figure II.2 give examples of values computed for representative lakes in Oklahoma that might be used for other studies. The value for small lakes such as Bell Cow Lake is obviously smaller because it lacks the same amenities. However, Fort Gibson is valued at \$136/day trip which is significantly less than Tenkiller’s value at \$191/day trip. Because of their size and proximity, these lakes might be considered substitutes for each other, so this result illustrates the unique recreational value that Tenkiller holds for Oklahomans. Multiple day trips draw users from farther away and thus by nature the value of a multiple day trip is higher.

Table II.6 Estimated Individual Lakes’ Per Trip Values per User (Travel Cost)

Lake	Single Day (2007 Dollars)	Multiple Day Trips (2007 Dollars)
Tenkiller Ferry Lake	191.0226	1090.5934
Fort Gibson Lake	136.4034	865.8952
Bell Cow Lake	22.30714	396.6928

Figure II.2. Graph of Relative \$ Valuation of Tenkiller, Fort Gibson, and Bell Cow Lakes



On average, the day user in our sample visits Tenkiller Ferry Lake 2.375 times per year but the multiple day trip user visits 8 times per year as shown in Table II.7. Tenkiller Lake’s characteristics are listed in Table II.8. Note that the average value of a trip to Tenkiller is \$194.34, but the estimated per trip value taking all the substitute sites into consideration is the value of \$191/day trip as given in Table II.6. The latter value will be used in section III for the optimization model value per trip.

Table II.7 Total and Average Trip Numbers for Tenkiller Ferry Lake

Trip Characteristic	Tenkiller Ferry Lake
Average Single Day Trips/ Person	2.375
Average Multiple Day Trips/ Person	8

Table II.8 Tenkiller Ferry Lake's Characteristics

Variable	Quality
<i>Travel Cost</i>	\$194.34 (Single Day Trip) on Average \$151.45 (Multiple Days Trip) on Average
<i>Boat Ramp</i>	2
<i>Porta-Potties</i>	0
<i>Flush-Toilet</i>	0
<i>Flush-Toilet with Shower</i>	7
<i>Lodge</i>	0
<i>Campsite</i>	240
<i>Campsite with Electricity</i>	87
<i>Water Clarity</i>	217 Centimeter
<i>Shoreline</i>	130 Mile
<i>Swimming Beach</i>	1 (Available)

Results from the travel cost model for lake managers suggest that swimming beaches are a strong component of user value for both day trip and multiple day trip users and that water quality, while relatively small in value is still significant to users' value. Both models suggest that complete restroom facilities outfitted with showers are important to all users. Boat ramps were not significant which suggests that the majority of users take them for granted or do not use them. And, users on average travel farther in favor of visiting larger lakes with more shoreline and greater size. While this does not diminish the importance of local opportunities, it suggests that large lakes like Tenkiller have greater value to both day and multiple day users and should receive special attention. Figure 3 in Appendix C shows that Tenkiller is the third

most popular multiple day user lake in Oklahoma second to Blackwell and Texoma. Figure 4 shows that very few of Oklahomans responding to the survey choose to leave the state of Oklahoma. We have not included the value of non-Oklahomans who visit lakes in Oklahoma since they were not surveyed. Those values for many lakes such as Texoma are likely to be large.

More data on respondents' concerns about lakes in Oklahoma is provided in Appendix C. In light of controversy over sources of pollution leading to bacterial contamination and algal blooms, the researchers wanted to gain a sense of the public's level of concern. Figure 7 shows that respondents believe information on bacterial contamination (88%), fish contamination (87%) and crime (85%) should be provided by the state to users. Of respondents 77% said they should also be informed about algal blooms and 79% lake water levels. Greater than 60% in each of these categories said that information on these subjects would affect their likelihood to visit a lake. Therefore, a high demand for increased information on lake quality and decreased demand for recreation plus greater awareness would likely lead to increased pressure to improve water quality from local businesses dependant on recreation and users. Additional data shown in appendix C, Figure 9 shows that water quality is the highest ranked self reported factor affecting choice to visit a lake followed by crowding and park facilities. Furthermore, Figure 10 in Appendix C shows that bacterial contamination and water odor are the highest ranked water quality factors to users. As seen in the discussion above, recreational values alone can be large (\$191/day trip alone to Tenkiller) for users. These estimates only examine direct use of a resource for recreation. We have not included other components of non-market value such as ecosystem services that these users and perhaps non-users (people who stay home) may have for lake values. For one lake, Lake Tenkiller, we will show in section III, how including recreational values which are normally ignored could affect the management of lake levels if managers optimized for highest use to society.

Section III: Construction and Optimization of a Lake Model of Power, Municipal, and Recreation.

III.1 Objectives

The objective of the overall study was to develop a water pricing model that could be used in the state water planning process. The model considers both monetary and opportunity costs in the allocation of surface water between competing uses including municipal use, hydropower and recreation. The model was constructed for Tenkiller Ferry Lake in Sequoyah and Cherokee counties. The specific purpose was to develop a water pricing protocol that

- (3) internalizes monetary and opportunity costs of water storage, treatment, and delivery systems; and
- (4) generates a sustainable supply of water over the 2010-2060 period.

The information on recreational benefits for Tenkiller from section II are integrated into the maximization problem in this section. The optimization shows that pool levels will be kept at normal pool levels during the summer months of highest recreational use.

III.2 Review of Lake Management Modeling

Labadie (2008) reviews models for the optimal operation of the multi-reservoir systems. The review discusses the models and software (linear, nonlinear, and dynamic programming, neural networks, fuzzy-rural based systems, and genetic algorithms) used. The review concentrates on the linkage between multi-reservoir systems. The author notes problems related to reduced reservoir benefits at times can be traced to inadequate attention to maintenance and operation issues after completion, development of new projects not in the initial project design, such as municipal and industrial uses, and minimum stream flow requirements for ecological reasons, and recreational uses. Labadie also addresses the gap between theoretical modeling methods and real world applications. Reasons for the gap are attributed to model skepticism by lake operators, model complexity, and variability of model types, methods of solution, and data requirements.

The concept of lake management for recreational purposes is often addressed through limiting the range of lake levels during peak recreational periods (Re Velle, Labadie). The Center for Business and Economic Research (2003) estimated the value of delaying late summer drawdown on seven eastern Tennessee TVA lakes from August to September and to October. A combination of Willingness to Pay (WTP) surveys of visitors and hedonic pricing study of lake property values was used to assess net economic benefits of the delayed drawdown. Daily expenditures per person were expected to range from approximately \$9-34 among the eight lakes in the study. The authors estimated a two month delay would increase visitor related expenditures by \$12.4 million and increase net income by \$2.35 million dollars. The delay was estimated to increase jobs for September and October by 744 and to add about \$1100 to the value of each property parcel around the lakes. The WTP (or consumer surplus) values to maintain full pool lake levels during September and October ranged from \$3.12 to 11.27 per foot. The aggregate WTP values by all users to maintain full pool lake levels during September

October, and the two month period were 39.7 million, 23.6 million and 39.7 million dollars respectively. The authors did not compare the gains from recreation against any reductions in power generated.

Several models have been applied to Lake Tenkiller. Shrestha (1996) developed a fuzzy rule-based modeling system of reservoir operation. This model develops decisions in terms of releases based on lake level, time of year. The decisions are of the form "If the lake level is x feet above sea level, then release y cubic meters of water". The model mimics existing management policies but does not lend itself to an economic analysis of those policies. Ozelkan et al. (1997) developed a linear quadratic dynamic programming model of the reservoir. The authors developed optimal control releases and levels to meet contracted releases for electrical generation, maintaining volume for flood control, and for municipal use. The stochastic model (unconstrained except with respect to monthly water balances) was tested with monthly data from 1979-1989. The authors note the model was able to obtain a lower value (some improvement) than with existing management. However, the authors noted that the unconstrained model violated maximum and minimum releases about six percent of the time. McKenzie (2003) developed a model of Broken Bow Lake in Oklahoma based on the methodology developed by Re Velle (1999). The model was used to consider the possibility of water sales subject to recreational, flood control, municipal use, and minimal releases.

Badger and Harper (1975) completed an assessment of lake elevation effects on visitation and concession operations at Tenkiller Ferry Lake. The primary objective was to determine numerical effects of lake levels ranging from 640 feet above sea level to 620 feet or less. Marina operators were asked whether changing mean storage levels 632, 635, and 640 feet above sea level would increase or reduce gross sales. All felt the 632 level would increase gross revenue and most felt the higher levels would reduce gross sales. All favored restricting drawdown to no more than 620 feet. Reasons cited were that reduced fluxions would reduce operating expenses, lead to an increased public use of marina facilities, and make the lake more attractive due to smaller exposures of defoliated areas (Badger and Harper, 1975). The authors developed regression equations to estimate overall lake attendance but did not relate attendance levels directly to lake levels. Warner et al. (1973) used the zonal travel cost method to estimate the value of a visitor day at \$4.67 in 1972 prices. This would be worth about \$24 in 2008 prices (McMahon, 2008).

Structure of a Monthly Lake Management Model for Lake Tenkiller Ferry

The basic form of the model developed in this study is based on models discussed in the book, *Optimizing Reservoir Resources* by ReVelle (1999). The model was also used in a previous OSU study by McKenzie (2003). The basic model described by ReVelle (1999) is described below.

It is assumed the purpose of a lake management model is to maximize net benefits from market and non-market products. Net Benefits are measured in terms of Consumers' Surplus + Producers' Surplus + Net Government Revenue. The model can be stated as maximizing the sum of total net monthly benefits from municipal and industrial use, flood control, power generation.

$$\text{Max TNB} = \sum_m (\text{BM}_m, \text{BF}_m, \text{BP}_m, \text{BS}_m)$$

Subject to

$$\text{Af}_{m+1} = \text{Af}_m + \text{In}_m - \text{Rl}_m - \text{Pr}_m - \text{Ml}_m - \text{Ev}_m$$

$$\text{Af}_m \leq \text{Vmax}_m$$

$$\text{Af}_m \geq \text{Vmin}_m$$

Where the value variables are:

BM_m is the average benefit from municipal and industrial use in month m .

BF_m is the average flood control benefit in month m ,

BP_m is the average power generation in month m , and

PS_m is the average downstream benefit from releases in month m .

Where the monthly quantity variables (measured in acre feet) are:

Af_m is the volume of water in the lake in month m ,

In_m is the inflow of water into the lake in month m ,

Rl_m is the amount of water released for reasons other than power generation in month m ,

Pr_m is the amount of water released for hydropower in month m ,

Ml_m is the amount of water withdrawn for municipal and industrial use in month m ,

Ev_m is amount of water lost from evaporation and seepage in month m , and

Vmax_m and Vmin_m are monthly maximum and minimum volumes in month m .

The multi-period model is obtained by expanding the annual model and by linking the end of year volume of the lake to the beginning volume for the next year. Future net-benefits are discounted. The models defined by ReVelle (p91-95, 1999) recommended meeting recreation objectives by keeping the range of lake levels as narrow as possible. However this guideline does not allow the operator to either determine the optimal range of lake level nor does it provide any assurance that the benefit of maintaining lake levels within an arbitrary range exceeds the opportunity cost of reducing other uses. An objective of this study is to include the value of recreational benefit as an explicit variable when determining the optimal lake use.

Monthly Lake Balance

The monthly lake balance is calculated as a simple inventory equation.

The beginning balance + inflow + rain fall =
evaporation + releases for power + releases for power + ending inventory.

It was necessary to develop a monthly model of lake inflows, retained volume, and releases. Daily data for the period beginning November 1, 1994 and ending March 31, 2007 were downloaded from the USACE website, <http://www.swt-wc.usace.army.mil/TENKcharts.html>. During this period of record the single day minimum level was 619.6 feet and the single day maximum level was 652.6 feet. The average daily volume for this 4534 day period was 650,913 acre feet and the average daily lake level was 631.58 feet above sea level.

The variables used from the daily data were the hour_2400_lake_level (feet), volume (acre-feet), releases for power, other releases, surface inches of evaporation, inches of rainfall at dam, and inflow. Data in DSF units for inflow and power releases were converted to acre feet by using the conversion factor 1 af = 1.983439 DSF supplied by the USACE. It was necessary to convert estimates for evaporation and rainfall to acre feet.

A simple double log regression model was used to relate the depth of the lake to volume in acre feet. The form was $\ln(\text{vol}) = a + \ln(\text{depth})$. With values in natural log form the obtained equation was,

$$\ln(\text{volume af.}) = -66.485 + 12.386 \ln(\text{depth in feet})$$

(-2535) (3045)

R-square = .99, with 4532 observations. T values are in parentheses.

After taking the antilog, the equation is $\text{Vol af} = \text{Vo} D^{12.386}$, where $\text{Vo} = \exp(-66.485)$ and D is depth in feet. The average, maximum, minimum, and standard deviation of average lake levels for each month were calculated as a method of determining the implicit range of operating parameters upon the lake. The average beginning volume and average inflow and outflow for each month are shown below in Table III.1.

Table III.1.Beginning of Month Volume and Average Inflow and OutFlow from Lake Tenkiller
November 1994-March 2007.

Month	LakeVolume (Beg.OfMo) ^b	Inflow ^a AcreFeet	Releases ^b Power	Other	Evap and Seepage
Jan	644,642	139,529	86,551	38,101	5,517
Feb	654,002	115,190	82,287	9,345	14,776
Mar	662,784	134,488	100,303	23,780	6,055
Apr	667,134	152,338	104,362	25,362	14,218
May	675,530	141,149	86,434	30,778	10,956
Jun	688,511	132,882	70,359	22,275	15,446
Jul	713,313	65,106	83,979	39,984	11,902
Aug	642,554	27,618	53,020	3,130	7,433
Sep	606,589	35,776	21,650	2,266	9,477
Oct	608,972	34,665	29,806	2,168	1,557
Nov	610,106	95,504	49,364	6,846	9,497
Dec	639,903	93,730	75,611	8,231	5,149

^a Includes rainfall

^b Average for the month

The average monthly levels and the variability the lake levels are shown below in Table III.2 and in Figure III.2. In Table III.2, the average daily level, the standard deviation of the level, the lowest daily observed along with the highest level observed are presented.

Table III.2 Average Daily Level Tenkiller Ferry from November 1994 through 2007, Along with the Standard Deviation, Minimum Level by Month.

Month	Average Daily Level	Standard Deviation	Minimum Level	Maximum Level
Feet above sea level				
Jan	632.5	5.50	619.9	649.6
Feb	631.6	4.30	619.7	647.3
Mar	632.6	4.70	619.9	646.7
Apr	632.9	4.50	621.8	650.2
May	634.5	5.10	623.7	650.2
Jun	635.1	5.20	630.6	652.6
Jul	633.6	5.20	626.3	651.9
Aug	629.6	3.10	622.5	637.0
Sep	627.8	3.10	621.7	637.4
Oct	628.3	3.50	620.8	637.1
Nov	629.8	4.30	620.1	641.0
Dec	630.8	4.40	619.6	641.3

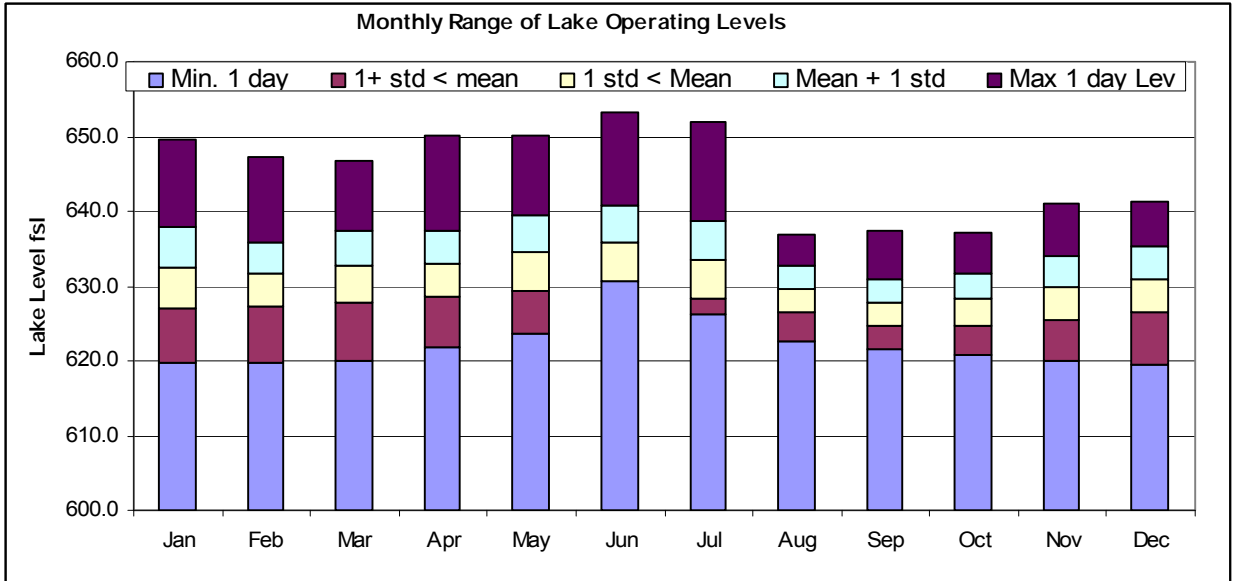


Figure III.1. Operating range of Tenkiller Ferry Lake showing Minimum One day level, Range of One Standard Deviation Below and Above the Mean, and the Maximum One Day Level Observed. (November 1994 - March 2007).

The data in Table III.2 and Figure III.1 above show the highest average lake level occurred during April while the lowest average lake level occurred during September. The smallest deviation of lake levels occurred during August and September. When the mean minus one deviation is compared to the absolute minimum it shows there is a concentrated effort to prevent the lake level from dropping below 620 feet during the heavily used June, July, and August recreation period.

Lake Visitation Data.

Current total monthly visitor numbers were obtained from the USACE for the period from 2001 through 2006. Six years is a fairly short for a time model to cover 50 years of projected use, so historic data were also used. Similar data were published by Badger and Harper (1975) covered the period 1955 through 1974. An average of 2.25 million people visited Lake Tenkiller Ferry during the period from 1955 to 1974 and from 2000 through 2004. The peak number of visits occurred from May through August (1.35 million) with an average .4 million visits occurred in July. These data are shown below in Figure III.2.

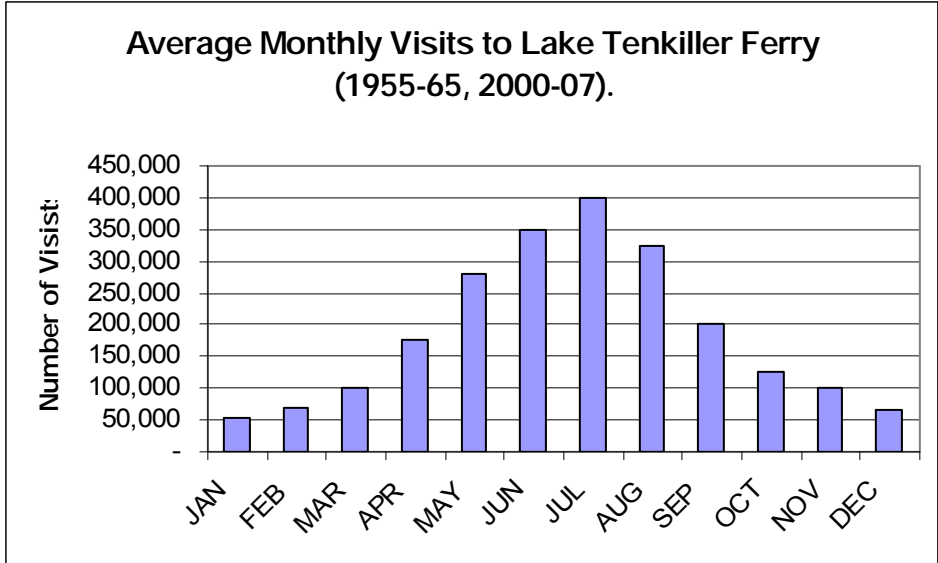


Figure III.2. Average Number of Visitor Days to Lake Tenkiller by Month (1955-1965 and 2000-2007).

The monthly visitor data was regressed against the lake level for the same month to estimate the effect of varying lake levels on visitor attendance. The estimated regression equation used in this study was,

$$\begin{aligned}
 \text{Visits} = & 103733 + 83400\text{Apr}^* + 182031\text{May}^* + 337142 \text{ June }^* + 401425 \text{ July}^* + \\
 & \quad (4.46) \quad (9.57) \quad (13.26) \quad (15.31) \\
 & 316164 \text{ Aug}^* + 117626 \text{ Sep}^* + 2642 \text{ ALkLv}^* + 5227\text{LvJun}^* + 2654 \text{ Tsumr }^* + \\
 & \quad (12.97) \quad (6.32) \quad (3.28) \quad (1.57) \quad (4.30) \\
 & -254 \text{ Lv}_{\text{Jn}}^{2*} - 1072 \text{ Lv}_{\text{Jly}}^{2*} - 254 \text{ Lv}_{\text{Aug}}^{2*}, \quad r^2 = 0.66 \\
 & \quad (-1.95) \quad (-2.51) \quad (-1.95)
 \end{aligned}$$

*Variables significant at 10 percent level or less

- The variables Apr, May, June, July, Aug and Sep are 0-1 dummy variables which are 1 in the indicated months and zero otherwise.
- Tsumr is a time (2000 = 0) trend for months June, July, and August. The other months were not found to significantly vary with time.
- ALkLv is the Average monthly lake level – 632.
- Lv_{Jun} is a discrete variable to test if visits to the lake in June are more sensitive to lake levels than in other months.
- Lv_{Jn}² is the square of the June lake level – 632, = [Lake level – 632]²
- Lv_{Jly}² is the square of the July lake level – 632, = [Lake level – 632]², and
- Lv_{Aug}² is the square of the August lake level – 632, = [Lake level – 632]².

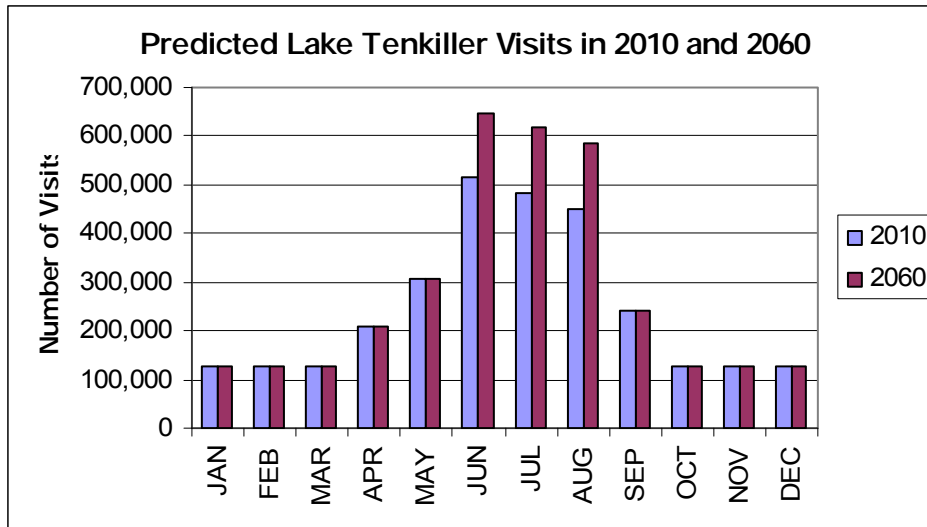


Figure III.3. Regression prediction of Visitor Days in 2010 and 2060.

Value of a Visitor Day at Lake Tenkiller.

The recreational value of Lake Tenkiller was as estimated as part of a larger random utility travel cost model for all lakes in Oklahoma as explained in section II . The value or “price” of the trip is the travel cost to a site given its amenities and those of other substitute sites. . Estimation of the trips taken as a function of the fee and lake levels is derived from Roberts et al (2008) is used to show adjust visit value from the travel cost as a function of lake level.

The value of a visitor day to Lake Tenkiller, Lake Fort Gibson, and Bell Cow Lake were estimated to be \$191, \$136, and \$22 per day respectively. Previous analysis had show that values of visitor day as low as \$8 per day were sufficient to reduce releases of water for power generation during the summer months in order to hold lake levels near normal levels of 632 feet. In the following analysis, the value of a visitor day at normal lake levels was placed \$50 per day. This is a conservative value, well below the estimated value of \$191 per day. The study by Roberts et al. (2006) had shown the willingness to pay for a visitor day declined by \$0.81 for each foot the lake was below the normal level of 632. The lowest level tested was 624 feet. The value of a visitor day used in this model was taken to be,

- \$50 per day if the lake level \geq 632 feet,
- $\$43 + \$.82(\text{Lake Level} - 624)$ if the lake level is > 624 and < 632 ,
- \$43 per day if the lake level is ≤ 624 feet.

A graphical view of the recreational value used in the model is shown below in Figure III.4.

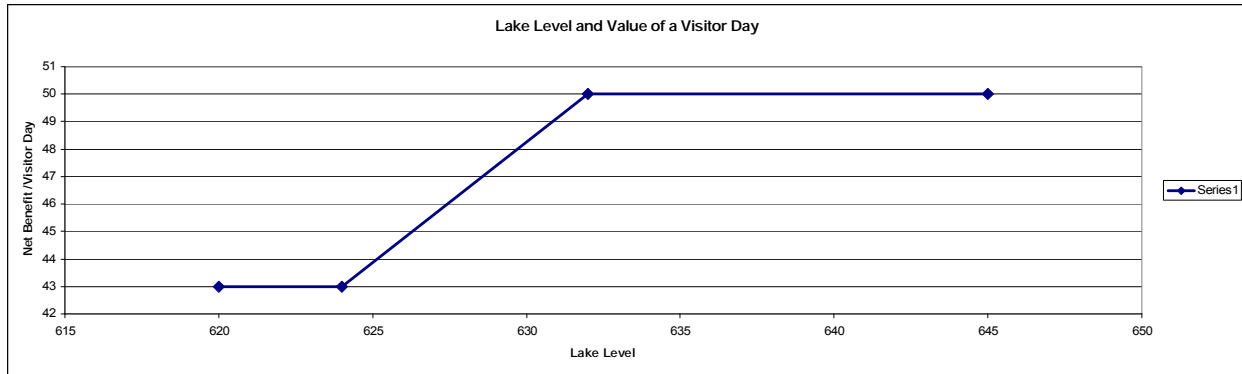


Figure III.4. Value of a Visitor Days as a Function of Lake level Given a Maximum Value of \$50.

Power Generation.

Power Generation was one of the beneficial uses for which the Lake Tenkiller Ferry dam was constructed (USACE, 1999). The amounts of electricity generated shown below in Table III.3 were summed and averaged from daily values provided by the USACE (2008) for the 1995-2000 time period.

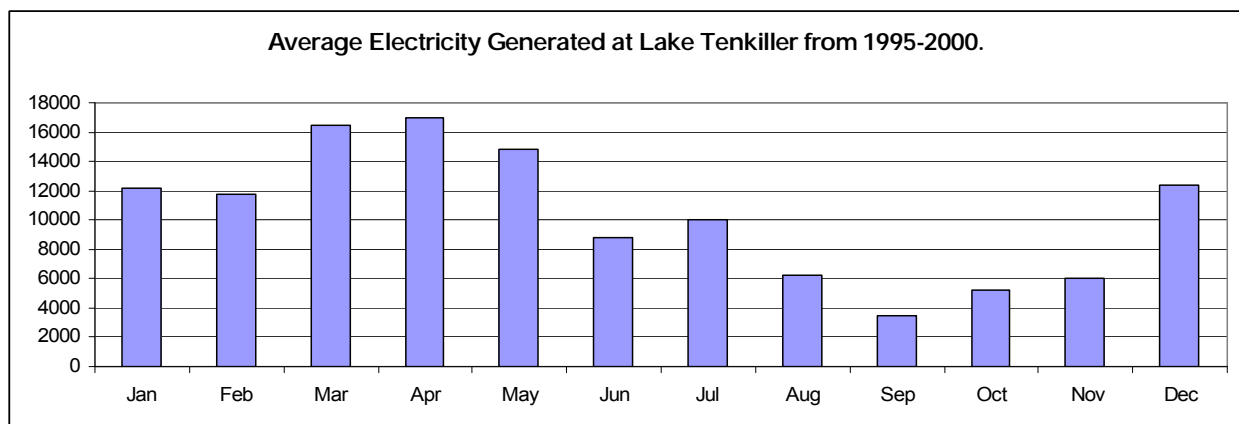


Figure III.5. Average Monthly Hydropower Generated at Lake Tenkiller from 1995-2000 in Thousand kwh.

Table III.3. Electricity Produced by Tenkiller Ferry Lake From 1995-2006.

Year	Jan	Feb	Mar	Apr	May	Jun	Jul	Aug	Sep	Oct	Nov	Dec	Year
	Thousand kwh												
1995	16835	15072	21273	20089	28422	11070	22754	10205	2228	2189	2099	3904	156140
1996	10928	5568	3912	14107	20078	6106	3719	3447	4663	14052	21855	27039	135474
1997	6154	12508	25122	18592	6750	9447	7958	5663	3146	706	3432	16170	115648
1998	27852	17652	18316	26991	8646	5706	4389	3953	2911	4574	4953	10998	136941
1999	7470	15670	23222	17357	15625	0	0	4269	2675	4090	1935	477	92790
2000	3487	4010	6823	4899	9678	20411	21524	9616	5373	5626	2196	15761	109404
Average	12121	11747	16445	17006	14867	8790	10057	6192	3499	5206	6078	12392	124400
Std. Dev	8977	5656	8918	7305	8282	6851	9701	2978	1235	4678	7813	9551	22751

Figure III.5 shows that most of the electricity is generated during the months of March through May with the lowest amount of electricity being produced in September. However the results in Table III.3 indicate considerable variability in monthly production from one year to the next. In a previous study of the economic impacts of the Lake Tenkiller, Warner et al. (1973) reported that annual electrical power generation varied from 16.4 to 156.6 million kilowatt hours for the

period from 1960-1971. Annual Sales of Electricity varied from 194 to 628 thousand dollars per year for the same period.

ReVelle (1999) presents the formula for power generation as a nonlinear function depending on the product of Release x Head. The function can be expressed as $P = aQH$ where

- Q is the volume of water released through the turbines.
- H is the height of the water above the turbines. The top of the turbines was assumed to be 486.5 feet above sea level.
- a is constant reflecting gravity, viscosity, and turbine efficiency.

Data were available from the USACE website on the daily volume of water released for power and on the amount of power generated from January 1955 through December of 2000. The average lake level for each day was calculated for this period. The head available for power generation on day t was then calculated as $(\text{level}_t + \text{level}_{t+1})/2 - 486.52$. The height of the top of the turbines is given as 486.52 feet above sea level. The head was multiplied by the quantity of water released. A simple plot of the quantity of electricity produced plotted against the product of head x Quantity released is shown below.

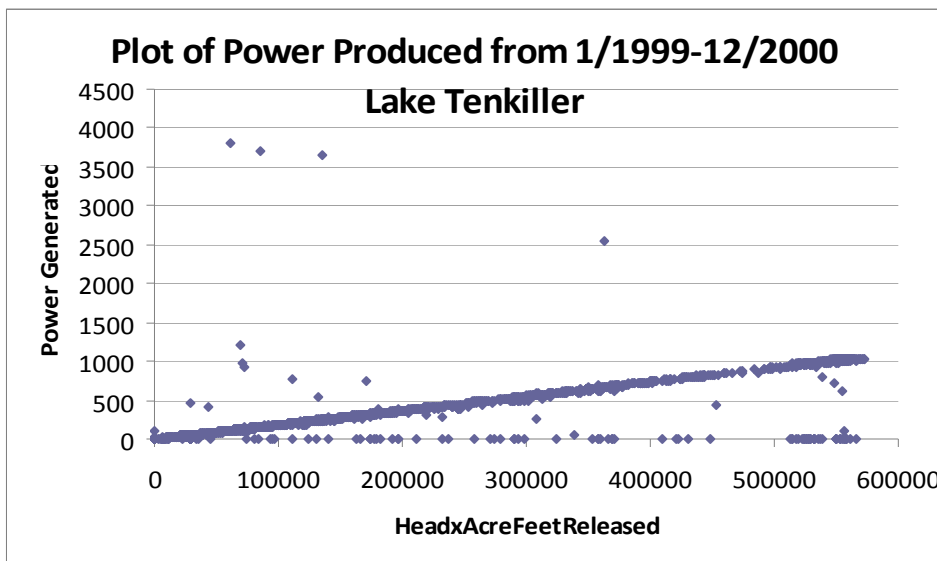


Figure III.6. Historical Relation between Power Generated and the Product of Head times Acre Feet Released.

There are releases for power when no power was generated and sometimes estimates for power generation that are much too high to have been generated by the quantity of water released. These outliers were deleted and an equation of the electrical values along the line in the above Figure III.6 were used to derive the estimate,

$$KW = 0.232457 (\text{Head} \times \text{Acre Feet Released}), \quad R\text{-Square} = 0.99$$

(1152)

The t-value is in the parenthesis.

This equation was used to estimate the quantity of electricity generated based on average monthly lake level or head times the number of acre feet released for power generation for the month. Power generated under long term contract is more reliably priced than power generated on the spot market. To simulate long term contracts, it was assumed the electrical authority could sell electricity in one or more of a series of four month contracts. The simulated contracts were for January-April, March-June, May-August, July-October, September-December and/or November-February.

Electricity was valued using monthly prices from the year 2000 through 2007 obtained from wholesale prices compiled by the U.S. Department of Energy.

Lake Tenkiller Wholesale Water Distribution Study

The USACE conducted a study of providing wholesale water to cities and rural water districts to the northwest and to the east of Lake Tenkiller. They estimated the cost of supplying water to some thirty cities and rural water systems at \$2.25 per thousand gallons

Water System Simulation Models

A hydraulic simulation model for a water system is a key tool that can be used to assist rural water districts (RWDs) in long term planning. In general, construction of these models can be expensive, time consuming and out of the reach of smaller RWDs. This study takes advantage of the Oklahoma Rural Water Systems GIS (geographical information systems) data set developed by the Oklahoma Water Resources Board (OWRB) which contains pipelines, facilities and general system capacity information. The available GIS files contain data on the length and diameter of each pipeline. The pipeline shape files have been overlaid on USGS 1/3 second elevation files. This step provides elevation data at points along the pipelines which is essential for estimation of pumping costs. Software programs have been developed to help with editing the apparently unused data set. Editing problems include missing pipes, mislabeled pipes, duplicate pipes, and duplicate nodes. Once the data files have been edited, an input file to EPANET is generated. The simulation model is capable of estimating pressure zones and system performance under various population levels and spatial distributions of that population. The pressure zone data over the area served by a system under alternative population levels can be used to estimate costs for capital investments in pipelines and water treatment facilities. Pipeline files, district boundary files, facility files, and management files have been downloaded, for the water systems below.

Burnt Cabin	Cherokee County Rural Water District (RWD) #1
Cherokee County RWD #2 (Keys)	Cherokee County RWD #3
Cherokee County RWD #7	Cherokee County RWD #8
Cherokee County RWD #13 (Cookson)	Town of Vian
East Central Oklahoma Water Authority	Fin and Feather Water Association
Lake Tenkiller Harbor	Lost City RWD
Muskogee County RWD #4	Muskogee County RWD #7
Paradise Hills, Inc.	Sequoyah County Water Association
Sequoyah County RWSG & SWMD #7	Stick Ross Mountain Water Company
Summit Water	Tahlequah Public Works
Lake Region Electric Development	Tenkiller Aqua Park
Tenkiller State Park	Town of Gore

Monthly Water Demands

The initial set future water demands in each of the areas was based on the average daily consumption levels calculated for the individual users in the USACE Wholesale Supply study (2001). The estimated average daily values for each user are shown below in Table III.4.

Table III.4. Actual and Projected Water Demands by User Based on Projections by the US Army Corps of Engineers

Year	2000	2010	2020	2030	2040	2050	2060
	(Thousand gallons per day)						
Muskogee RWD#4	74	82	85	88	93	97	105
Lost City RWD RWD11	215	239	248	255	269	282	303
Cherokee RW 1	75	84	87	89	94	99	106
Muskogee RWD#7	144	160	166	171	180	189	203
Cherokee RW 8	108	119	124	128	134	141	152
Cherokee RW 7	108	119	124	128	134	141	152
Cherokee RW 3	189	209	217	223	235	247	265
Tahlequah Water	653	722	760	792	841	900	955
Stick Ross Mt. Water System	215	239	248	255	269	282	303
Cherokee RW2	86	95	99	102	107	113	121
LRED east	61	68	71	73	77	81	87
Summit Water	72	80	83	86	90	94	101
Cherokee RW13	75	84	87	89	94	99	106
LRED east	47	53	55	56	59	62	67
Tenkiller State Park	19	21	22	23	24	25	27
Sequoyah WW	1492	1653	1714	1768	1859	1951	2098
LRED west	59	66	68	70	74	77	83
Burnt Cabin	32	36	37	38	40	42	45
Lake Tenkiller Harbor	32	36	37	38	40	42	45
Fin & Feather Water	38	42	43	45	47	49	53
Paradise Hills	24	26	27	28	30	31	33
Tenkiller Aqua Park	11	12	12	13	13	14	15
Vian	194	215	223	230	242	254	273
Gore	292	323	335	346	364	382	411
East Central OK	205	227	235	242	255	268	288
Total	4520	5010	5207	5376	5664	5962	6397

The data in Table III.4 differ from those in the USACE 2001 study in that projections were made for 2060 and because demands for Sallisaw, Muldrow, and Roland were deleted. A series of monthly water demands were derived based on precipitation and temperature elasticities obtained from another water demand simulation program IrrMain developed by the USACE. Since the area is mostly residential the single family dwelling elasticities were used. The elasticities used for each month along with the average monthly temperature and precipitation data for the area are given below in Table III.5.

Table III.5. Average Monthly Temperature and Precipitation Values and Elasticities Used to Derive Monthly Water Demands for the Tenkiller Study Area.

	Jan	Feb	Mar	Apr	May	Jun	Jul	Aug	Sep	Oct	Nov	Dec
Rainfall (in)	2.4	2.4	4.2	4.1	5.7	5.2	3.5	3.2	5.3	4.3	4.7	3.2
Temperature (F)	36.8	42.4	51.5	60.3	67.9	75.6	80.4	80	72.4	61.7	49.5	39.9
Rainfall Elasticity	-0.25	-0.25	-0.25	-0.25	-0.02	-0.02	-0.02	-0.02	-0.02	-0.25	-0.25	-0.25
Temp Elasticity	0.45	0.45	0.45	0.45	1.5	1.5	1.5	1.5	1.5	0.45	0.45	0.45
Price Elasticity	-0.04	-0.04	-0.04	-0.04	-0.25	-0.25	-0.25	-0.25	-0.25	-0.04	-0.04	-0.04

Source: IRRWMain, Davis etal. 1987.

The base consumption for month m was assumed to be given by the relation,

$$Q_m = Q_a T_m^{em} R_m^{er} \text{ and that } \sum_m Q_m = Q_a.$$

This is enforced by letting $r = \sum_m Q_m / 12Q_a$, where r is a ratio that requires the sum of the monthly. The value of r was calculated to be 0.88. The estimated base level of demand for each month was $Q_m = r Q_a T_m^{em} R_m^{er}$.

The total monthly demands shown below were projected using the monthly temperature and rainfall elasticities. The monthly and annual values for each ten year period from 2010 through 2060 are given Table III.6 below. The annual demands increase from 5.6 thousand acre feet per year in 2010 to 7.1 thousand acre feet by 2060. These are similar the USACE projections under alternative 1 which also excluded the Sallisaw area.

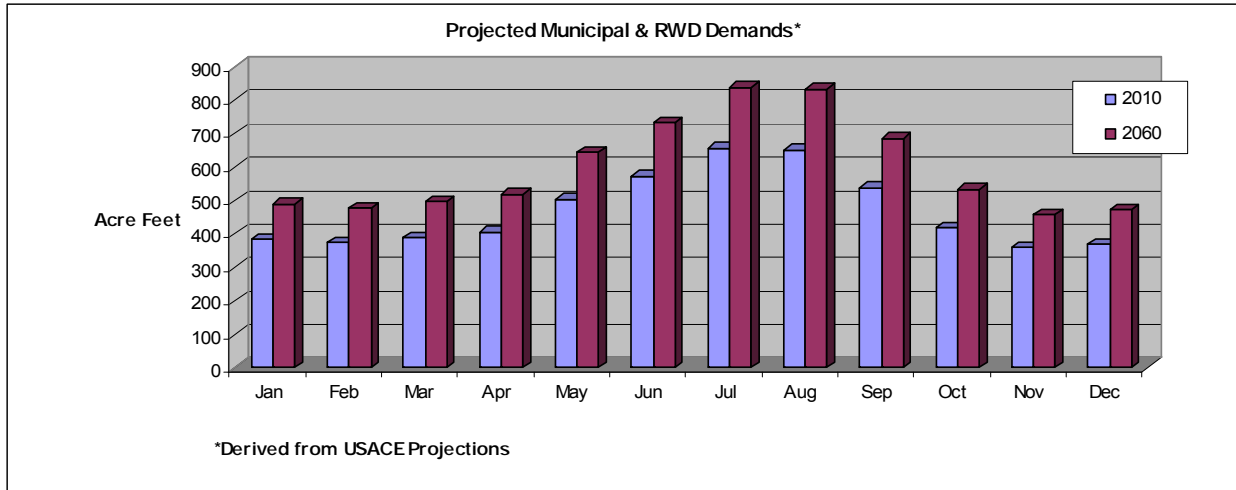


Figure III.7. Projected Municipal and Rural Water District Demand Based on Annual Consumption Estimated Adjusted by Rainfall and Temperature Elasticities.

Table III.6. Projected Monthly Estimates of Water Use by Municipal and Rural Water Districts from Lake Tenkiller from the Year 2010 to 2060.

Year	Jan	Feb	Mar	Apr	May	Jun	Jul	Aug	Sep	Oct	Nov	Dec	Total
	Acre Feet												
2010	384	373	388	406	504	574	655	652	537	418	359	370	5619
2020	399	387	403	422	523	596	681	677	559	435	373	385	5840
2030	412	400	416	435	540	616	703	699	577	449	385	397	6030
2040	434	421	439	459	569	649	741	737	608	473	405	419	6353
2050	457	444	462	483	599	683	780	775	640	498	427	441	6687
2060	490	476	496	518	643	733	837	832	686	534	458	473	7175

Net Benefits or Consumers and Producers Surplus from Water Consumption

Linear demand equations were constructed from the quantities shown above in Table III.6 by using the price elasticities from Table III.5 and by using an estimated final price for water. The process uses the definition of a price elasticity ρ , in month m as

$$\rho = \frac{dq P_m \cdot}{dp Q_m}$$

The desired slope (d_{1m}) for the demand equation of the form $P_m = d_{0m} + d_{1m}Q_m$, where $d_{1m} = (dp_m/dq_m) \rho$. P_m is the retail price of water and Q_m is the quantity consumed. The intercept is then calculated as $d_{0m} = P_m - d_{1m}Q_m$. The first part of the equation for net social benefits from the consumption of Q units of water is obtained by integrating over the price flexibility equation with respect to Q to get $CS' = d_0Q + .5 d_1 Q^2$. The equation for $CS + PS$ is obtained by subtracting the total cost of delivering Q units of water. The equation for $CS+PS = d_0Q + 0.5 d_1Q^2 - Cost(Q)$. In the case where the total cost of delivering water to the customer is linear, the term in the objective function for the net benefits of delivering water is

$$NSBm = d_{0m}Q_m + 0.5 d_1 Q^2 - c_0 - c_1Q_m.$$

Use of EPANET Simulation to Estimate Water Distribution Costs

The monthly values shown above in Table III.6 were simulated in an EPANET pipeline simulation model. The demands for each of the 12 months were simulated for the years, 2010, 2020, 2030, 2040, 2050, and 2060. The purpose was to determine the power and pumping capacity and the average daily pumping cost over the 50 year planning period.

An outline of the pipeline map is shown below in Figure III.8. The map has been overlaid on a USGS 1/3 second elevation file for the region. The pipeline serves communities around the lake along with the towns of Gore and Vian to the south. The pipeline also partially serves the city of Tahlequah and other RWDs to the north. From the mean lake level of 632 the pipeline reaches 1000 feet at points northwest and southeast of Lake Tenkiller.

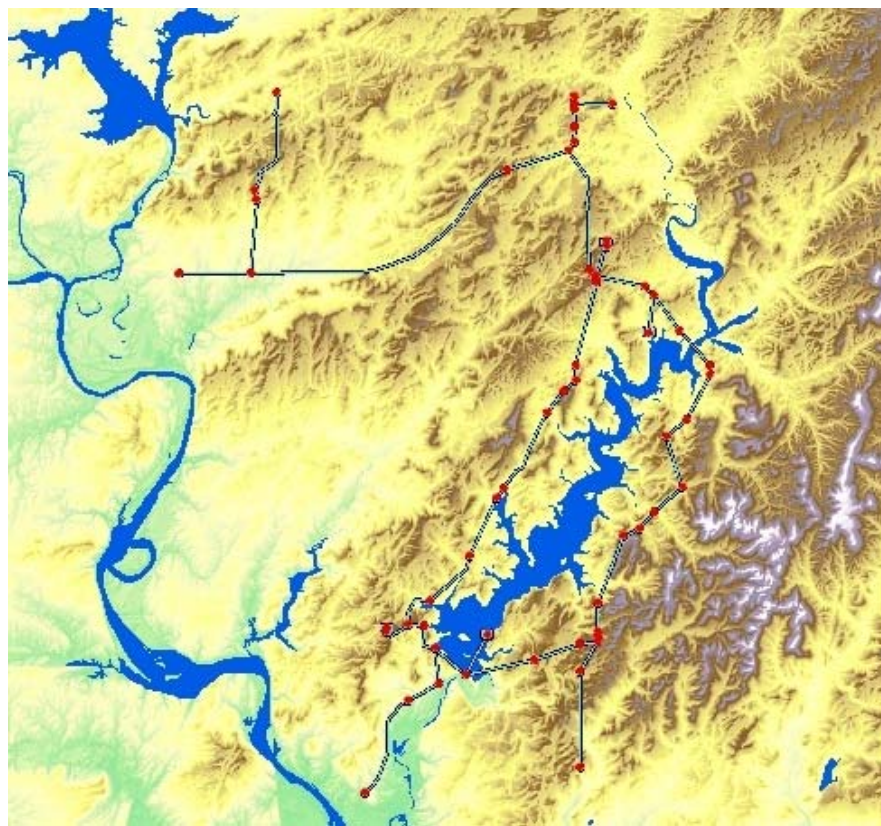


Figure III.8. Pipeline System Serving Municipalities and Rural Water Districts (Represented by Nodes) from Lake Tenkiller.

The variable energy cost of pumping as given by the EPANET model over the 60 year period as given by the following linear equation,

$$\text{Cost} = -458. + \$257.64 \text{ AF}, R^2 = .99.$$

(2.5) (760)

The variable Cost is the total cost of pumping AF (dollars per acre feet) for the entire system in a month. The values in parentheses are t-values. Since the relationship is linear, the pump efficiency in the EPANET may not be modeled correctly but specific pump curves would be required to improve the estimate. The final delivered price includes payments to amortize the system cost and also local distribution costs by each system. The final marginal delivery cost was derived as shown in Table III.7 below.

Table III.7. Delivery Cost of Water to Municipal and Rural Water Districts Users.

<u>Item</u>	<u>Cost/1000 Gal</u>	<u>Cost/AF</u>
Variable pumping cost	\$ 0.79	\$ 257.67
Amortized Capital cost of the Regional System	\$ 1.43	\$ 465.97
Local Administration and distribution cost	<u>\$ 1.28</u>	<u>\$ 416.84</u>
<u>Final delivered (retail) Price</u>	<u>\$ 3.50</u>	<u>\$1,140.48</u>

The cost of local administration and distribution cost was taken as the difference between the costs as supplied by the Oklahoma Municipal League (2002) and the wholesale cost of \$1.22 per 1000 gallons.

III.3 PRINCIPAL FINDINGS AND SIGNIFICANCE

The first part of this section of results deals with the effect of maximizing net benefits with recreation as one of the variables in the objective function, as opposed to maximizing benefits to municipal and power generation subject to maintaining summer lake levels above between 620 and 632 feet above sea levels. In the latter case, the value of recreation is explicitly estimated from the resulting lake levels after the optimal power and municipal uses have been determined. The first part of the results section establishes that there are gains to be made by directly including recreation values in the objective function of the model. The second part of the results discusses the changes in the monthly and annual allocations of water over the 2010 to 2060 period when recreation values are directly included in the objective function.

The approach in this study was to determine the allocation of Lake Tenkiller water resources among uses for power generation, municipal and rural water demands, and recreational uses. A series of solutions were obtained in which monthly demands were met for the years 2010, 2020, 2030, 2040, 2050, and 2060. Two monetary values for a visitor day were used. The value of \$191 per visitor day (obtained from the state-wide survey described above) and as a sensitivity test, a lower value of \$50 per day was used. The lower value was used in all solutions because it was sufficient to show that changes could be made in lake level management that would increase overall net public benefits from the lake resources.

Effect of Directly Including Recreational Values in the Objective Function

For this analysis recreation was valued at \$50 per visitor day. The model was solved for the years 2010, 2020, 2030, 2040, 2050, and 2060. The values for years between the dates were determined by interpolation. NPV were determined by discounting over the 50 year period at 4.875 percent, the discount rate indicated by the Water Resources Council for water projects (2008). The results are shown in Table III.8 below.

Table III.8. Comparison of NPV of Net Benefits from 2010 to 2060 from Lake Tenkiller when Recreational Values are Not Included and When Recreational Values are Directly Included in the Objective Function (Values in thousand dollars)*.

<u>Recreational Values Post Solution</u>		<u>Recreational Values in Objective Function</u>	
<u>Item</u>	<u>Value</u>	<u>Item</u>	<u>Value</u>
Power Generation	\$ 16,120	Power Generation	\$ 15,536
Municipal	900,180	Municipal	873,618
		Recreation	2,510,667
Objective Function	916,300	Objective Function	3,399,821
Recreation	2,422,446		
<u>Total All Values</u>	<u>\$3,338,746</u>	<u>Total All Values</u>	<u>\$ 3,399,821</u>

*Recreation valued at \$50 per visitor day.

On the left the visitor days were calculated from the lake levels determined by optimizing for power and municipal use. With the recreational visitor day valued at \$50, the recreation values were much larger than the values for power generation and municipal use. The results are interesting since neither municipal nor recreation were listed as primary uses when the dam was built. As expected, when recreational values are directly included in the objective function, it is possible to gain nearly 61 million dollars of additional value from the lake resource over the 50 year period. The values in Figure III.10 indicate that the gain in recreation values (at \$50/visitor day) that an additional 88 million dollars in recreation benefits are gained with a reduction of \$26.6 million in municipal benefit and \$0.6 million in power generation over the 50 year period in present value terms. This gives a 3.24 benefit to cost ratio, i.e., for every dollar lost in municipal and hydropower generation in 2007 dollars, 3.25 dollars are gained in recreation. If the value of a recreational day had been placed at \$191, rather than the conservative value of \$50/visitor day, the value of recreational benefits would have been near \$300 million over the 50 year period.

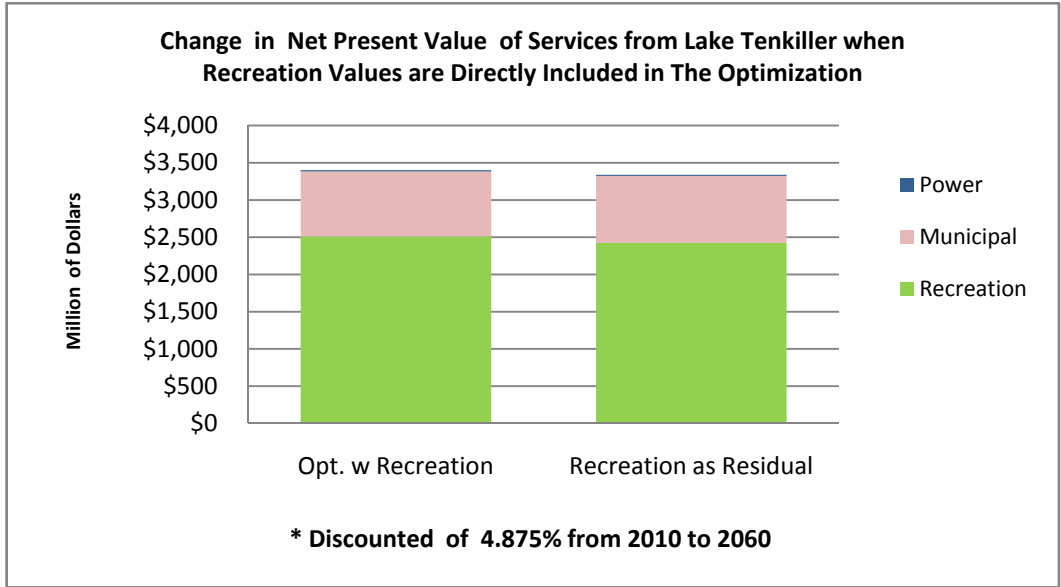


Figure III.9. Comparison in Net Present Value of Services from Lake Tenkiller when Recreation Values are Directly Included in the Optimization, (Recreation Valued at \$50).

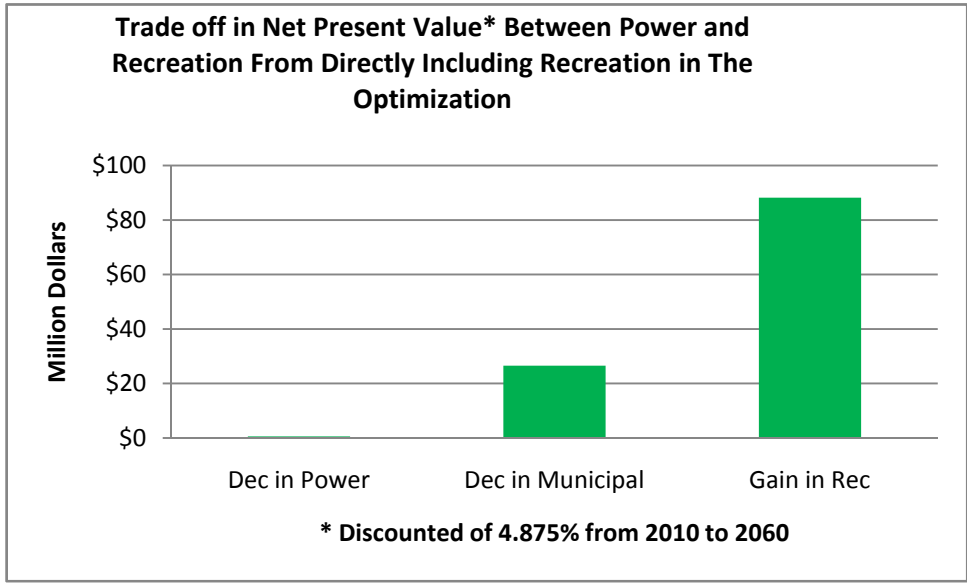


Figure III.10. Tradeoff in the Net Present Value between Power and Recreation Values when Recreation Values are Included in the Objective Function of the Optimization Model.

Long Term Implications of Directly Including Recreation Values in the Objective Function.

The results indicate that Lake Tenkiller is capable of meeting the power needs, municipal and rural water district consumption and recreational services. The demands for municipal and RWDs is very inelastic with respect to price. The estimated levels of consumption for the years 2010 and 2060 are shown below. The monthly consumption levels for each of the 10 year period are shown below in Table III.9.

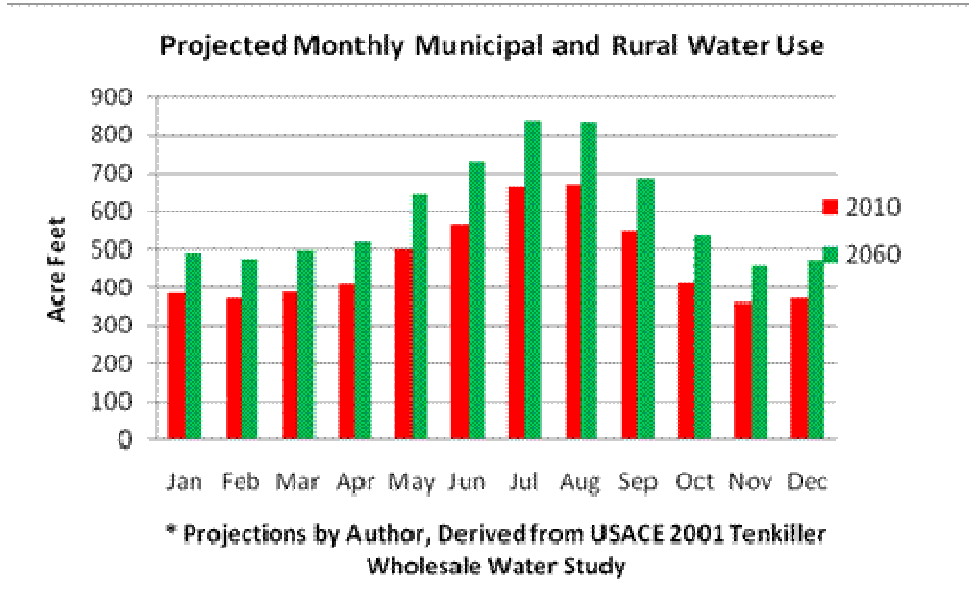


Figure III.11 Estimated Public Water Consumption from Lake Tenkiller for the Years 2010 and 2060.

Table III.9. Estimated Public Water Consumption from Lake Tenkiller by Municipal and Rural Water Districts.

	<u>2010</u>	<u>2020</u>	<u>2030</u>	<u>2040</u>	<u>2050</u>	<u>2060</u>
	Acre Feet					
Jan	384	398	415	434	471	490
Feb	372	387	400	421	458	476
Mar	388	403	414	439	474	496
Apr	408	422	434	458	495	518
May	498	525	536	570	718	643
Jun	567	598	611	649	811	733
Jul	661	681	702	739	951	837
Aug	668	677	699	737	947	832
Sep	550	558	572	607	780	686
Oct	413	435	451	473	512	534
Nov	360	373	385	406	441	458
Dec	371	385	398	418	451	473

Lake Levels

The greatest changes in the resource allocation were in the timing of releases for power generation and the resulting effect on recreation visitors. That is the model tended to maximize benefits to recreational users by maintaining lake levels very close to the “normal lake level” of 632 feet above sea level. The lake levels for the years 2010 and 2060 are compared with historical levels in Figure III.12 below.

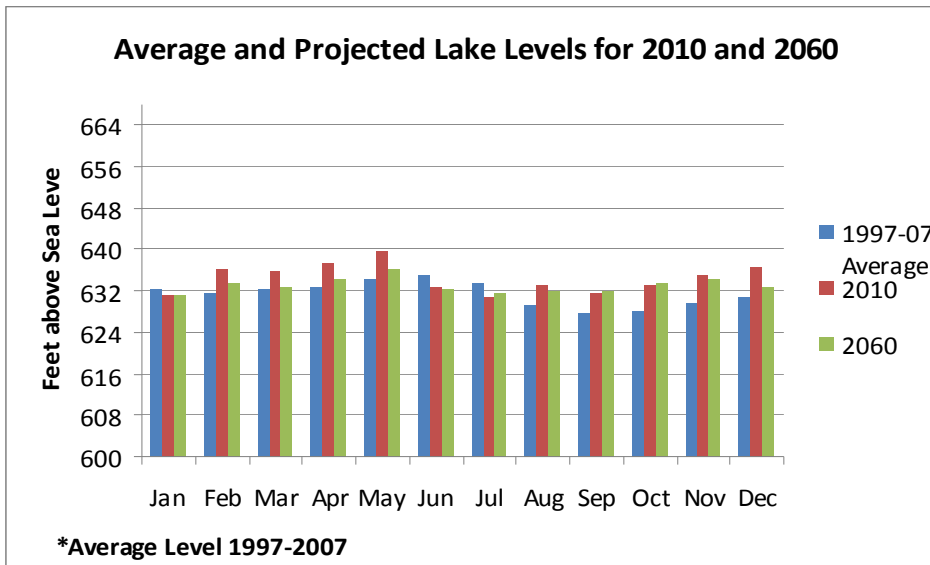


Figure III.12 Estimated Optimal Lake Levels in each month for 2010 and 2060.

The main change from the historical level is that with optimization, the lake levels during the summer months of June, July, and August are maintained very close the normal pool 632 foot level. Lake levels are slightly higher than historical levels for all other months except June.

Releases for Power Generation

The main visible change in the releases for power generation is the reduction of releases during June, July, and August when recreation is specifically included in the optimization. The reduction in power generation during the summer months is made up in part by increased generation during the remaining months of the year though total power releases are reduced.

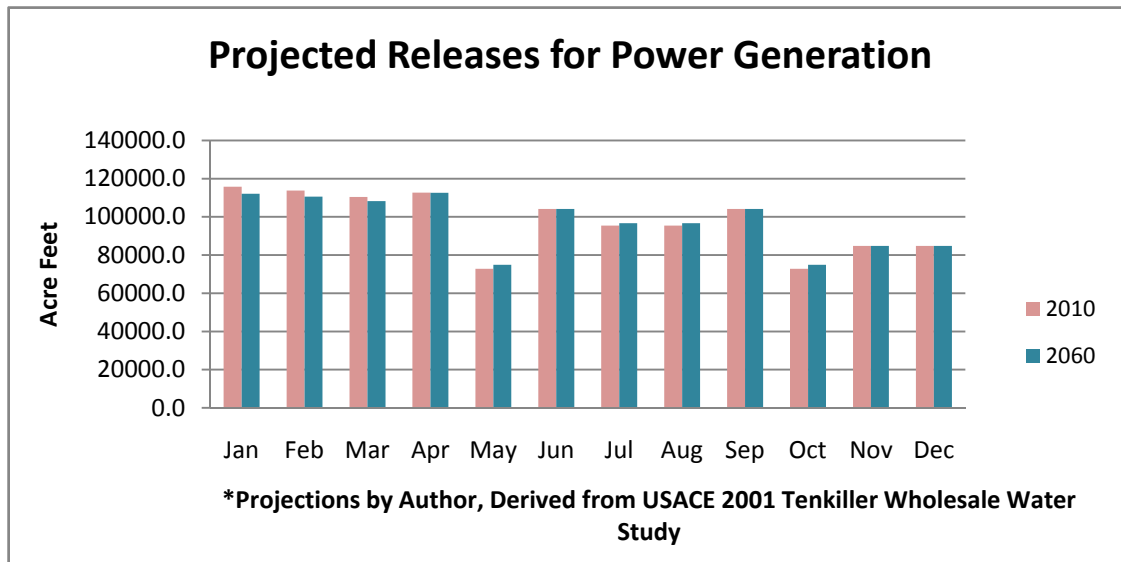


Figure III.13. Optimal Releases of Water for Power Generation in the Years 2010 and 2060.

Table III.10. Actual and Projected Releases for Power Generation for the Years 2010 to 2060.

	<u>Average*</u>	<u>2010</u>	<u>2020</u>	<u>2030</u>	<u>2040</u>	<u>2050</u>	<u>2060</u>
		Acre Feet					
Jan	86,551	115752	109975	109975	112061	112061	112061
Feb	82,287	113769	109754	109754	110619	110619	110619
Mar	100,303	110465	109386	109386	108216	108216	108216
Apr	104,362	112709	113860	113860	112580	112580	112580
May	86,434	72781	75822	75822	74909	74909	74909
Jun	70,359	104132	104132	104132	104132	104132	104132
Jul	83,979	95444	76191	76191	96666	96666	96666
Aug	53,020	95444	76191	76191	96666	96666	96666
Sep	21,650	104132	104132	104132	104132	104132	104132
Oct	29,806	72781	75822	75822	74909	74909	74909
Nov	49,364	84773	104132	104132	84778	84778	84778
Dec	75,611	84773	104132	104132	84778	84778	84778
Total	843,726	1166954	1163529	1163529	1164446	1164446	1164446

* Average Years 1999-2007

Lake Visitors

The regression analysis indicated the number of lake visitors were dependent upon lake levels between 624 and 632 feet. The value of a visitor day was placed at \$43 when the lake level was 624 feet or less and \$50 per day when the level is 632 feet or more. Between those levels the price was increased linearly when the level was between 624 and 632 feet. Reductions in the number of lake visitors when lake levels were above or below the above levels were not found to be significant except for the months of June, July, and August. July visitors were projected to exceed 600,000 per in the month of July by the year 2060. The solution estimates for the years 2010 and 2060 are shown below in Figure III.14. The greatest increases are in the months of June, July, and August which were the only months where the historical data indicated there were significant time increases. Table III.11 indicates total visitor days increased from a historical average of 2.2 to 3.1 million per year by 2060.

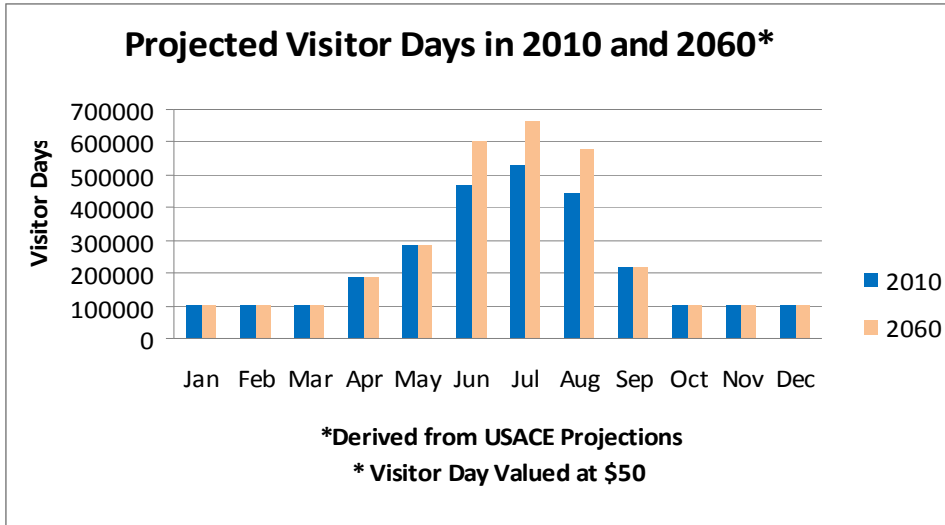


Figure III.14. Optimal Number of Visitor Days in 2010 and 2060.

Table III.11. Actual and Estimated Visitor Days for Lake Tenkiller (2010 – 2060)

Month	Average	2010	2020	2030	2040	2050	2060
Visitor Days							
Jan	54388	103733	103733	103733	103733	103733	103733
Feb	68579	103733	103733	103733	103733	103733	103733
Mar	101286	103733	103733	103733	103733	103733	103733
Apr	176077	187133	187133	187133	187133	187133	187133
May	281455	285764	285764	285764	285764	285764	285764
Jun	350397	467415	493955	520495	547035	573575	600115
Jul	398482	531698	558238	584778	611318	637858	664398
Aug	324280	446437	472977	499517	526057	552597	579137
Sep	202888	221359	221359	221359	221359	221359	221359
Oct	125943	103733	103733	103733	103733	103733	103733
Nov	101211	103733	103733	103733	103733	103733	103733
Dec	66944	103733	103733	103733	103733	103733	103733
Total	2251931	2762204	2841824	2921444	3001064	3080684	3160304

IV. Extension of Research Results

IV.1 Methodology

- Results from the recreational survey were presented at the Oklahoma Clean Lakes and Water Association meeting in Tulsa, Ok from April 9-11, 2008 to individuals from state agencies, volunteer environmental groups, and academics.
- An in service workshop in Kellyville, OK, provided an opportunity for delivery of Lake Tenkiller research findings to OCES professionals from the counties in and around the Lake Tenkiller area. The program included presentations on:
 1. Current water rights and law, and the potential for changes as the Comprehensive State Water Plan is underway;
 2. The economics of water use in Oklahoma, including the Tenkiller region;
 3. A comparison of water rates by selected water district; and,
 4. Lake and river recreation and non-market valuation in the Tenkiller area.
- A presentation of the optimization results was given at the Oklahoma Water Resources Research Institute Symposium, October 29, 2008 entitled, “Managing Water Resources Given Competing Uses - A Lake Tenkiller Case Study.” In Midwest City, OK.
- A poster entitled, “Optimal Allocation of Reservoir Water” by Deepayan Debnath, Art Stoecker, Tracy Boyer, and Larry Sanders was presented at the Oklahoma Water Resources Research Institute Symposium, October 29, 2008.

IV.2 Principal Findings of Extension

These presentations stimulated discussion on competing uses for the region’s water resources, as well as the need for future research and development of extension and outreach programs outside of this grant activity. As a result, several activities are planned:

1. A survey of the rural water districts in the Tenkiller to determine the factors that affect water rates;
2. Meetings with the water districts and the public to discuss results of the Boyer, Stoecker, Sanders research, and the water rates survey results;
3. Development of fact sheets, other educational materials, a website and public meetings to address the perceived needs of county educators.
4. Further research and extension projects and proposals to follow up on questions brought about by this research indicated a need for further study.

References

- Badger, D.D. and W.M. Harper, 1975. "Assessment of Pool Elevation Effects on Recreation and Concession Operations at Tenkiller Ferry Lake". Prepared for U.S. Army Corps of Engineers Tulsa District, Department of Agricultural Economics, Oklahoma State University, AE 7503.
- Caneday, L., and D. Jordan. "State Park Visitor Survey: 2002-2003." Working Paper, Leisure Studies, College of Education, Oklahoma State University.
- Center for Business and Economic Research, 2003. Economic Effects of Lake Management Policy in East Tennessee, Center for Business and Economic Research, University of Tennessee, May.
- Davis, W.Y., D.M. Rodrigo, E.M. Optiz, B. Dziegielewski, D.D. Baumann, and J.J. Boland, 1987. IWR-MAIN Water Use Forecasting System, Version 5.1: User's Manual and System Description, Prep. for U.S. Army Corps of Engineers, Planning and Management Consultants, Ltd., Carbondale Ill., Dec.
- Dillman, D.A. 2000. *Mail and Internet Surveys: The Tailored Design Method*. 2nd Edition, New York: John Wiley & Sons.
- Freeman, A. M, 2003. *The Measurement of Environmental and Resource Values*. Resources for the Future Press, Washington, D.C.
- Hoff-Hisey, H.K and M.D. Woods, 1994. Lake Tenkiller Region Data Study, Rural Development, Oklahoma Cooperative Service, Oklahoma State University.
- Jordan, Edward and Badger, Daniel. "Management considerations in operating municipal lake recreation enterprises in Oklahoma." Agricultural Experiment Station, Oklahoma State University. Technical Report. 1977.
- Labadie, J.W., 1999. Reservoir System Optimization Models, Water Resources Update, The Universities Council on Water Resources (UCOWR), Issue 108, Southern Illinois Univ.
- Labadie, J.W., 2004. Optimal Operation of Multireservoir Systems: State-of-the-Art Review, J. of Water Resources Planning and Management, March/April.
- McCroy, M. and W Schieffer, 2004. Facilitating the Tenkiller Utilities Authority Public Water Decision Project, Oklahoma Water Resources Research Institute, (2003OK19B).
- McMahon, T., 2008. Historical CPI, Inflation.Com, [hppt://inflationdata.com/inflation/consumer](http://inflationdata.com/inflation/consumer), June.

- McKenzie, R.W., 2003. Examining Reservoir Management Practices: The Optimal Provision of Water Resources under Alternative Management Scenarios, Ph.D. Dissertation, Edmond Low Library, Oklahoma State University.
- Oklahoma Municipal League, 2008. "Oklahoma Municipal Utility Costs", Report of Oklahoma Conference of Mayors, Oklahoma Municipal League, Inc and Municipal Electric Systems of Oklahoma, 2002, 2008.
- Oklahoma Water Resources Board, 2008. Tenkiller Ferry Lake Oklahoma Water Resources Board Website, www.owrb.state.ok.us .
- ReVelle, C. 1999. Optimizing Reservoir Resources: Including a New Model for Reservoir Reliability, John Wiley & Sons, Inc., New York.
- Ozelkan, E.C., A. Galambosi, E. Ferandez-Gaucherand, and L. Duckstein, 1997. Linear Quadratic Dynamic Programming for Water Reservoir Management. Applied Mathematical Modeling, (21)591-598.
- David Roberts, Tracy Boyer, and Jayson Lusk, "Environmental Preferences Under Uncertainty." *Ecological Economics* 2008. Vol 66: 584-593.
- Rossman, L. A., 2000. EPANET 2: Users Manual, EPA/600/R-00/057, Water Supply and Water Resources Division, National Risk Management Research Laboratory, USEPA, September.
- Shrestha, B.P., 1966. Fuzzy-Rule Based Modeling of Reservoir Operation. Journal of Water Resources Planning and Management. ASCE, P122-124.
- USACE, 2001. Tenkiller Wholesale Water Treatment and Conveyance System Study: Phase III- Additional Preliminary Designs and Cost Estimates. Planning Assistance to States Program, Prepared for Tenkiller Utilities Authority through Oklahoma Water Resources Board, Tulsa District, U.S. Army Corps of Engineers. January 2001.
- USACE, 2008. TENO2: Tenkiller Lake, Real Time Lake Information, Web <http://www.swt-wc.usace.army.mil/TENK.lakepage.html>.
- Warner, L., D.D. Badger, and G.M. Lage, 1973. "Impact study of the Construction and Operation of the Tenkiller Ferry Lake, Oklahoma". Research Foundation, Oklahoma State University.
- Wolff, N.C., 1973. Demand and Economic Impact Recreation at Lake Tenkiller, M.S. Thesis, Dept. of Agricultural Economics, Oklahoma State University

Appendices

Appendix A: Letter to Oklahoma Lakes Survey Respondents

Appendix B: Oklahoma Lakes Survey 2007

Appendix C: Oklahoma Lakes Survey 2007: Additional Statistics on Responses

Appendix A

First Cover Letter

Name and Address of addressee

September x, 2007

Dear X

Would you do us a favor?

I am writing to ask you to help in a study of recreational lakes in Oklahoma. This study examines how lakes are used and what factors influence people's selection of lakes to visit.

We are contacting a random sample of residents from every county in the state to ask whether they visit lakes in Oklahoma, how often, and why.

Your participation will require several minutes to complete the enclosed questionnaire. Results from the survey will help Oklahoma agencies such as the Oklahoma Water Resources Board and Oklahoma State Parks manage and protect our lake resources. Even if you do not visit Oklahoma lakes, your response to the survey will help us understand why you have not visited the lakes and improve your satisfaction with them.

Your answers will remain completely confidential, and no individual's answers can be identified. Your information will be stored securely and will be available only to persons conducting the study. No reference will be made on written reports which could link you to the study. After this study is completed, your name will be deleted and never connected to your answer in any way. This survey is voluntary. There are no known risks associated with this survey which are greater than those ordinarily encountered in daily life. Your answers will help us very much to share your lake visiting experience. If for some reason you prefer not to respond, please let us know by returning the blank questionnaire in the enclosed stamped envelope.

If you have questions about your rights as a research volunteer, you may contact Dr. Sue C. Jacobs, IRB Chair, 219 Cordell North, Stillwater, OK 74078, 405-744-1676 or irb@okstate.edu.

Thank you very much for helping with this important study.

Sincerely,

Tracy Boyer

Assistant Professor

Tracy.Boyer@okstate.edu

Postcard Reminder

In the last two weeks, a questionnaire seeking your opinion about Oklahoma Lakes was mailed to you.

If you have already completed and returned the questionnaire to us, please accept our sincere thanks. If not, please do so today. We are especially grateful for your help because it is only by asking people like you to share experiences that we can understand why people decide to visit or not visit lakes in state of Oklahoma. If you did not visit any lakes recently your response is still important and we'd appreciate answers to questions 1 and 14-25!

If you did not receive a questionnaire, or if it was misplaced, please call us at (405) 744-6169 or email us at Tracy.boyer@okstate.edu, and we will get another one in the mail to you.

Tracy Boyer

Assistant Professor
Department of Agricultural Economics

Oklahoma State University

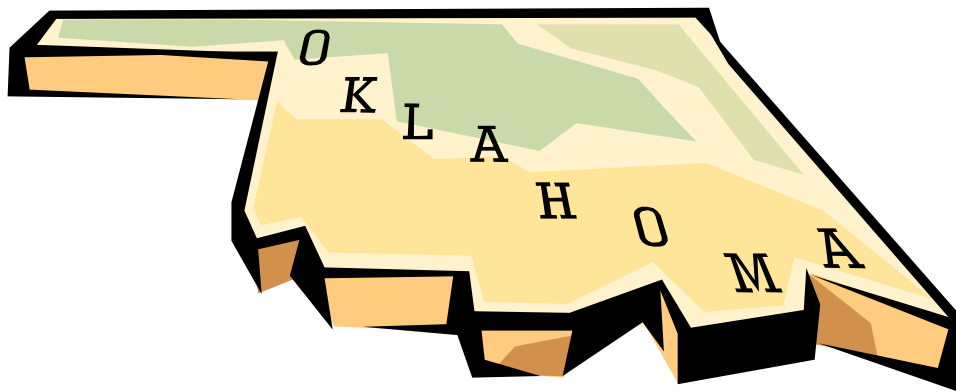
Stillwater, OK 74078

Appendix B
Oklahoma Lakes Survey



Oklahoma Lakes Survey 2007

order to make sound decisions concerning the future of Oklahoma lakes, it is important to understand how the lakes are used, as well as what factors influence your selection of lakes to visit. The answers you give to the questions in this survey are very important. Even if you have not visited any lakes in Oklahoma, please complete and return the questionnaire. It is critical to understand the characteristics and views of both those who use and those who do not use the lakes



Participating in this survey will take only a few minutes of your time.

Your participation is voluntary and answers will remain strictly confidential.

Department of Agricultural Economics

Oklahoma State University

In this first section, we would like to find out which of the lakes you visited and what you did there. A map is provided at the end of the survey if you need it.

- 1. Please indicate how often you or other members of your household visited each of the following lakes in the current and past year. Also, indicate the number of trips you anticipate making to each of the lakes in 2008. If you have not visited any lakes in Oklahoma, and do not plan to visit any in the upcoming year, please check this box and skip to question 2.**

I have not, and do not plan to visit any lakes in Oklahoma

If you visited lakes in Oklahoma that are not on this list, please count them in the “other” category at the end of the list.

Name of Lake	County	Number of visits (January-December) in:					
		2006 (last year)		2007 (this year)		2008 (next year)	
		Single day	Over night	Single day	Over night	Single day	Over night
<i>Example (Perry Lake)</i>	<i>Nobel</i>	<i>2 trips</i>	<i>3 trips</i>	<i>7 trips</i>	<i>0 trips</i>	<i>4 trips</i>	<i>1 trip</i>
Altus/Lugert Lake	Kiowa						
American Horse Lake	Blaine						
Arbuckle Lake	Murray						
Arcadia Lake	Oklahoma						
Ardmore City Lake	Carter						
Atoka Lake	Atoka						
Bell Cow Lake	Lincoln						
Birch Lake	Osage						
Bixhoma Lake	Wagoner						
Bluestem Lake	Osage						
Boomer Lake	Payne						
Broken Bow Lake	McCurtain						
Brushy Creek Lake	Sequoyah						
Burtschi Lake	Grady						
Canton Lake	Rogers						
Carl Albert Lake	Latimer						
Carl Blackwell Lake	Payne						
Carlton Lake	Latimer						
Carter Lake	Marshall						
Cedar Lake	Canadian						
Chambers Lake	Beaver						
Chandler Lake	Lincoln						
Chickasha Lake	Caddo						
Chouteau Lake	Nowata						
Claremore Lake	Rogers						
Clayton Lake	Pushmataha						
Clear Creek Lake	Stephens						
Cleveland City Lake	Cleveland						
Clinton Lake	Washita						

Name of Lake	County	Number of visits (January-December) in:					
		2006 (last year)		2007 (this year)		2008 (next year)	
		Single day	Over night	Single day	Over night	Single day	Over night
Example (Perry Lake)	Nobel	2 trips	3 trips	7 trips	0 trips	4 trips	1 trip
Coalgate City Lake	Coal						
Comanche Lake	Comanche						
Copan Lake	Washington						
Crowder Lake	Washita						
Cushing Municipal Lake	Payne						
Dave Boyer Lake	Cotton						
Dead Indian Lake	Roger Mills						
Dripping Springs Lake	Okmulgee						
Duncan Lake	Stephens						
El Reno Lake	Canadian						
Elk City Lake	Beckham						
Ellsworth Lake	Alfalfa						
Elmer Lake	Kingfisher						
Elmer Thomas Lake	Comanche						
Etling Lake	Cimarron						
Eucha Lake	Delaware						
Eufaula Lake	Pittsburg						
Fairfax City Lake	Osage						
Fort Cobb Lake	Caddo						
Fort Gibson Lake	Cherokee						
Fort Supply Lake	Woodward						
Foss Lake	Custer						
Frances Lake	Marshall						
Frederick Lake	Tillman						
Fuqua Lake	Stephens						
Grand Lake	Delaware						
Great Salt Plains Lake	Alfalfa						
Greenleaf Lake	Muskogee						
Guthrie Lake	Logan						
Hall Lake	Harmon						
Healdton City Lake	Carter						
Hefner Lake	Oklahoma						
Henryetta Lake	Okmulgee						
Heyburn Lake	Creek						
Holdenville Lake	Hughes						
Hominy Municipal Lake	Osage						
Hudson Lake	Osage						
Hugo Lake	Choctaw						
Hulah Lake	Osage						
Humphreys Lake	Stephens						
Jap Beaver Lake	Jefferson						
Jean Neustadt Lake	Carter						
John Wells Lake	Haskell						
Kaw Lake	Choctaw						
Keystone Lake	Pawnee						
Konawa Lake	Seminole						

Name of Lake	County	Number of visits (January-December) in:					
		2006 (last year)		2007 (this year)		2008 (next year)	
		Single day	Over night	Single day	Over night	Single day	Over night
Example (Perry Lake)	Nobel	2 trips	3 trips	7 trips	0 trips	4 trips	1 trip
Langston Lake	Logan						
Lawtonka Lake	Comanche						
Liberty Lake	Logan						
Lloyd Church Lake	Latimer						
Lone Chimney Lake	Payne						
McAlester Lake	Pittsburg						
McGee Creek Lake	Atoka						
McMurtry Lake	Noble						
Meeker Lake	Lincoln						
Mountain Lake	Carter						
Murray Lake	Carter						
Nanah Waiya Lake	Pushmataha						
New Spiro Lake	Le Flore						
Newt Graham Lake	Oklahoma						
Okemah Lake	Okfuskee						
Okmulgee Lake	Okmulgee						
Oologah Lake	Nowata						
Optima Lake	Texas						
Overholser Lake	Oklahoma						
Ozzie Cobb Lake	Pushmataha						
Pauls Valley City Lake	Garvin						
Pawhuska Lake	Osage						
Pawnee Lake	Pawnee						
Perry Lake	Noble						
Pine Creek Lake	McCurtain						
Ponca Lake	Kay						
Prague City Lake	Lincoln						
Purcell Lake	McClain						
Quanah Parker Lake	Comanche						
R.C. Longmire Lake	Garvin						
Raymond Gary Lake	Choctaw						
Robert S. Kerr Lake	Sequoyah						
Rock Creek Lake	Carter						
Rocky Lake	Washita						
Sahoma Lake	Creek						
Sardis Lake	Latimer						
Schooler Lake	Choctaw						
Shawnee Twin Lake	Pottawatomie						
Shell Lake	Osage						
Skiatook Lake	Osage						
Sooner Lake	Noble						
Spavinaw Lake	Mayes						
Sportsman Lake	Custer						
Spring Creek Lake	Roger Mills						
Stanley Draper Lake	Oklahoma						
Stroud Lake	Lincoln						
Talawanda Lake	Pittsburg						
		Number of visits (January-December) in:					

Name of Lake	County	2006 (last year)		2007 (this year)		2008 (next year)	
		Single day	Over night	Single day	Over night	Single day	Over night
<i>Example (Perry Lake)</i>	<i>Nobel</i>	<i>2 trips</i>	<i>3 trips</i>	<i>7 trips</i>	<i>0 trips</i>	<i>4 trips</i>	<i>1 trip</i>
Taylor Lake	Nowata						
Tecumseh Lake	Pottawatomie						
Tenkiller Ferry Lake	Cherokee						
Texoma Lake	Cleveland						
Thunderbird Lake	Cleveland						
Tom Steed Lake	Kiowa						
Vanderwork Lake	Washita						
Veterans Lake	Murray						
Vincent Lake	Ellis						
W.R. Holway Lake	Mayes						
Watonga Lake	Blaine						
Waurika Lake	Osage						
Waxhoma Lake	Osage						
Wayne Wallace Lake	Latimer						
Webbers Falls Lake	Muskogee						
Weleetka Lake	Okfuskee						
Wes Watkins Lake	Oklahoma						
Wetumka Lake	Hughes						
Wewoka Lake	Seminole						
Wiley Post Memorial Lake	McClain						
Wister Lake	Le Flore						
Yahola Lake	Tulsa						

OUTSIDE OF OKLAHOMA:

2. Please indicate how often you or other members of your household visited lakes or rivers in each of the following locations in the current and past year. Also, indicate the number of trips you anticipate making to each of these locations in 2008.

Lake Name	Number of Visits January-December					
	2006 (last year)		2007 (this year)		2008 (next year)	
	Single Day	Overnight	Single Day	Overnight	Single Day	Overnight
<i>Example (Lake in Alaska)</i>	<i>0 trips</i>	<i>2 trips</i>	<i>0 trips</i>	<i>1 trip</i>	<i>0 trips</i>	<i>1 trip</i>
Lakes in Kansas						
Lakes in Texas						
Lakes in Arkansas						
Lakes in Missouri						
Lakes in Colorado						
Lakes in Mississippi						
Other Lakes						

If you chose other Lakes, what state(s) were these lakes in? _____

3. What is your 5 digit postal ZIP code at your permanent residence? _____

4. What activities did you and your family typically engaged in when visiting a lake?
Please Check all that apply.

- | | | |
|--------------------------------------|---|---|
| <input type="checkbox"/> Boating | <input type="checkbox"/> Jet-skiing/wave running | <input type="checkbox"/> Picnicking |
| <input type="checkbox"/> Camping | <input type="checkbox"/> Sailing | <input type="checkbox"/> Fishing |
| <input type="checkbox"/> Hunting | <input type="checkbox"/> Canoeing/Kayaking | <input type="checkbox"/> Swimming and Beach Use |
| <input type="checkbox"/> Golfing | <input type="checkbox"/> Nature appreciation/wildlife viewing | <input type="checkbox"/> Other _____ |
| <input type="checkbox"/> Sightseeing | <input type="checkbox"/> Hiking | |

5. How frequently do you or your family swim in Oklahoma lakes?

- Never Rarely Sometimes Frequently

In this section we would like to find out what features of lakes are important to you.

6. To what extent do you agree or disagree with the following statement: “Potential crowding and congestion affect my choice of lake and/or the days of the week or weekends of the year to visit my favorite lake?”
Please circle a number below to indicate your answer (1 being strongly disagree and 10 being strongly agree).

Strongly disagree			Neutral				Strongly agree		
1	2	3	4	5	6	7	8	9	10

7. Indicate whether you believe the state should provide public information on lakes with respect any of these factors.

Factor	Should it be provided?		Would it affect your decision to visit a lake?	
	<input type="checkbox"/> Yes	<input type="checkbox"/> No	<input type="checkbox"/> Yes	<input type="checkbox"/> No
Public safety (crime rate)	<input type="checkbox"/> Yes	<input type="checkbox"/> No	<input type="checkbox"/> Yes	<input type="checkbox"/> No
Fish contamination	<input type="checkbox"/> Yes	<input type="checkbox"/> No	<input type="checkbox"/> Yes	<input type="checkbox"/> No
Bacterial or related lake water contamination	<input type="checkbox"/> Yes	<input type="checkbox"/> No	<input type="checkbox"/> Yes	<input type="checkbox"/> No
Algal blooms/turbidity	<input type="checkbox"/> Yes	<input type="checkbox"/> No	<input type="checkbox"/> Yes	<input type="checkbox"/> No
Lake water levels	<input type="checkbox"/> Yes	<input type="checkbox"/> No	<input type="checkbox"/> Yes	<input type="checkbox"/> No

8. How important are the following factors for you in choosing a lake for recreation? Please circle appropriate number to indicate your answer on a scale of 1-10 (1 being not important and 10 being very important).

	Not important				Neutral			Very important			
Sandy or hard bottom in swimming area	1	2	3	4	5	6	7	8	9	10	
Diversity of fish species/habitat	1	2	3	4	5	6	7	8	9	10	
Quantity of fish caught	1	2	3	4	5	6	7	8	9	10	
Crowding/ Congestion	1	2	3	4	5	6	7	8	9	10	
Distance to where you live	1	2	3	4	5	6	7	8	9	10	
Park facilities	1	2	3	4	5	6	7	8	9	10	
Activities at the lake	1	2	3	4	5	6	7	8	9	10	
Activities in Town nearby	1	2	3	4	5	6	7	8	9	10	
Water quality	1	2	3	4	5	6	7	8	9	10	
Location of friends/relatives	1	2	3	4	5	6	7	8	9	10	
Other (please specify) _____	1	2	3	4	5	6	7	8	9	10	

9. This question asks for the importance of water quality in lakes. Please rank each of the following water quality factors with regard to influence you in choosing a lake for recreation. Please rank them 1st, 2nd, 3rd, and 4th in their relative importance to your choice.

- _____ Lack of water odor
- _____ Bacteria/ contamination at levels posing health risks
- _____ Increase in water clarity
- _____ No algal boom

In the section starting on the next page, we would like to ask you several questions about potential management scenarios being considered to improve Oklahoma lake recreation. There are four different sets of management scenarios (question 10 to 13). Please consider one as a separate question.

Turn over page and please answer questions in the next section. → → → → → → → →

10. Compared to the lake you most visit, would you choose a lake such as A or B? Or would you choose to stay with the one you currently visit, C? Please choose one.

Attribute	Option A	Option B	Option C
Increase in public boat ramps	1 Boat ramp	1 Boat ramp	<p>NO CHANGE: I would rather keep the management of this lake the way it is today</p>
Campsites	Available with electric service	Available with electric service	
Public restrooms	Restroom with flush toilets and showers	Restroom with flush toilets and showers	
Lodges	Available	Available	
Water clarity	1 foot increase of water visibility dept from surface	1 foot increase of water visibility dept from surface	
Increase in distance from home (one-way)	40 miles increase	40 miles increase	
I would choose (Please check only one)	<input type="checkbox"/> A	<input type="checkbox"/> B	<input type="checkbox"/> C (I would not want either A or B)

Given your choice above, how many trips per year would you take?

Number of single day trips same number or ___#less or ___# more

Number of multiple day trips same number or ___# less ___# more

11. Compared to the lake you most visit, would you choose a lake such as A or B? Or would you choose to stay with the one you currently visit, C? Please choose one independent of your previous choices.

Attribute	Option A	Option B	Option C
Increase in public boat ramp	1 Boat ramp	1 Boat ramp	<p>NO CHANGE: I would rather keep the management of this lake the way it is today.</p>
Campsites	Available with electric service	Available with electric service	
Public restrooms	Restroom with flush toilets and showers	Restroom with flush toilets and showers	
Lodges	Available	Available	
Water clarity	1 foot increase of water visibility dept from surface	1 foot increase of water visibility dept from surface	
Increase in distance from home (one-way)	40 miles increase	40 miles increase	
I would choose (Please check only one)	<input type="checkbox"/> A	<input type="checkbox"/> B	<input type="checkbox"/> C (I would not want either A or B)

Given your choice above, how many trips per year would you take?

Number of single day trips same number or ___#less or ___# more

Number of multiple day trips same number or ___# less ___# more

12. Compared to the lake you most visit, would you choose a lake such as A or B? Or would you choose to stay with the one you currently visit, C? Please choose one independent of your previous choices.

Attribute	Option A	Option B	Option C
Increase in public boat ramp	1 Boat ramp	1 Boat ramp	<p>NO CHANGE: I would rather keep the management of this lake the way it is today.</p>
Campsites	Available with electric service	Available with electric service	
Public restrooms	Restroom with flush toilets and showers	Restroom with flush toilets and showers	
Lodges	Available	Available	
Water clarity	1 foot increase of water visibility dept from surface	1 foot increase of water visibility dept from surface	
Increase in entrance fee/ camping fee (per trip)	\$30 increase	\$30 increase	
I would choose (Please check only one)	<input type="checkbox"/> A	<input type="checkbox"/> B	<input type="checkbox"/> C (I would not want either A or B)

Given your choice above, how many trips per year would you take?

Number of single day trips same number or ___#less or ___# more

Number of multiple day trips same number or ___# less ___# more



13. Compared to the lake you most visit, would you choose a lake such as A or B? Or would you choose to stay with the one you currently visit, C? Please choose one independent of your previous choices.

Attribute	Option A	Option B	Option C
Increase in public boat ramp	1 Boat ramp	1 Boat ramp	<p>NO CHANGE: I would rather keep the management of this lake the way it is today.</p>
Campsites	Available with electric service	Available with electric service	
Public restrooms	Restroom with flush toilets and showers	Restroom with flush toilets and showers	
Lodges	Available	Available	
Water clarity	1 foot increase of water visibility dept from surface	1 foot increase of water visibility dept from surface	
Increase in entrance fee/ camping fee (per trip)	\$30 increase	\$30 increase	
I would choose (Please check only one)	<input type="checkbox"/> A	<input type="checkbox"/> B	<input type="checkbox"/> C (I would not want either A or B)

Given your choice above, how many trips per year would you take?

Number of single day trips same number or ___#less or ___# more

Number of multiple day trips same number or ___# less ___# more

Information about you and other members of your household will help us better understand how household characteristics affect an individual's use of Oklahoma lakes and attitudes towards changes in them. It will also help us to determine how representative respondents are of people in the state of Oklahoma.

All of your answers are strictly confidential. The information will only be used to report comparisons among groups of people. We will never identify individuals or households with their responses. Please be as complete as possible. Thank you.

14. What is your age in years?

- | | |
|-----------------------------------|----------------------------------|
| <input type="checkbox"/> Under 18 | <input type="checkbox"/> 50 – 59 |
| <input type="checkbox"/> 18 – 25 | <input type="checkbox"/> 60 – 75 |
| <input type="checkbox"/> 26 – 34 | <input type="checkbox"/> 76 + |
| <input type="checkbox"/> 35 – 49 | |

15. Are you

- Male Female

16. What is the highest level of schooling that you have completed? (Please check only one)

- Some high school or less
 High school graduate
 Some college or trade/vocational school
 College graduate (B.A., B.S.)
 Advanced degree (M.D., J.D. M.A., M.S., or PhD)

17. How many adults (including yourself) live in your household? _____

18. How many children live in your household (18 or under)? _____

19. If you are currently employed, how many hours a week do you typically work? _____

20. If you are currently employed, do you have the option of working additional hours to increase your total income?

- No
 Yes—if so, what would your hourly wage be? \$ _____ per hour

21. If you answered “no” to question 20, and you could have the option of working more or less hours, which would you prefer?

- Work more hours
- Work the same number of hours
- Work less hours

22. What was your total household income (before taxes) for 2006?

- | | |
|--|--|
| <input type="checkbox"/> Under \$10,000 | <input type="checkbox"/> \$40,000-\$49,999 |
| <input type="checkbox"/> \$10,000-\$14,999 | <input type="checkbox"/> \$50,000-\$59,999 |
| <input type="checkbox"/> \$15,000-\$19,999 | <input type="checkbox"/> \$60,000-\$74,999 |
| <input type="checkbox"/> \$20,000-\$24,999 | <input type="checkbox"/> \$75,000-\$99,999 |
| <input type="checkbox"/> \$25,000-\$29,999 | <input type="checkbox"/> \$100,000-\$124,999 |
| <input type="checkbox"/> \$30,000-\$34,999 | <input type="checkbox"/> \$125,000-\$149,999 |
| <input type="checkbox"/> \$35,000-\$39,999 | <input type="checkbox"/> Over \$150,000 |

23. Do you own a home on or near a lake in Oklahoma?

- No
- Yes, →If yes, are you a year-round resident?
 - Yes
 - No

24. Do you own a home on a lake outside of Oklahoma?

- Yes
- No

25. Do you belong to a lake protection association?

- Yes
- No

COMMENTS? COMMENTS ABOUT LAKES AND RECREATION IN OKLAHOMA?

THANK YOU!

If you have any questions about this survey, please contact:

Tracy Boyer, Assistant Professor

Department of Agricultural Economics

321 Agriculture Hall

Oklahoma State University

Stillwater, OK 74078

(405) 744-6169

Tracy.boyer@okstate.edu

MAP OF LAKES INCLUDED IN SURVEY HAS BEEN OMITTED

APPENDIX C

**OKLAHOMA LAKES SURVEY 2007:
ADDITIONAL STATISTICS ON RESPONSES**

Table 1: Day and Multiple Day Trips and Visitors Averages

	Total Single day trips	Total Multiple day trip
Total	2,777	1,053
Average/person	14	10

Figure 1: Percentages of respondents by Single and Multiple Day Trips

■ Single day trips ■ Multiple day trips ■ Repondents who have never visited lakes

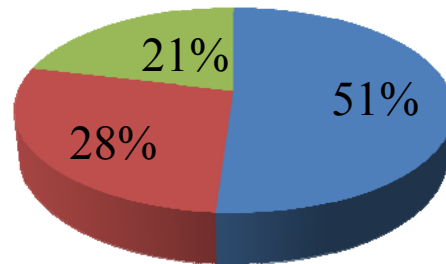


Figure 2: Top 15 Most Popular Lakes for Single Day Trips (no of visits in sample)

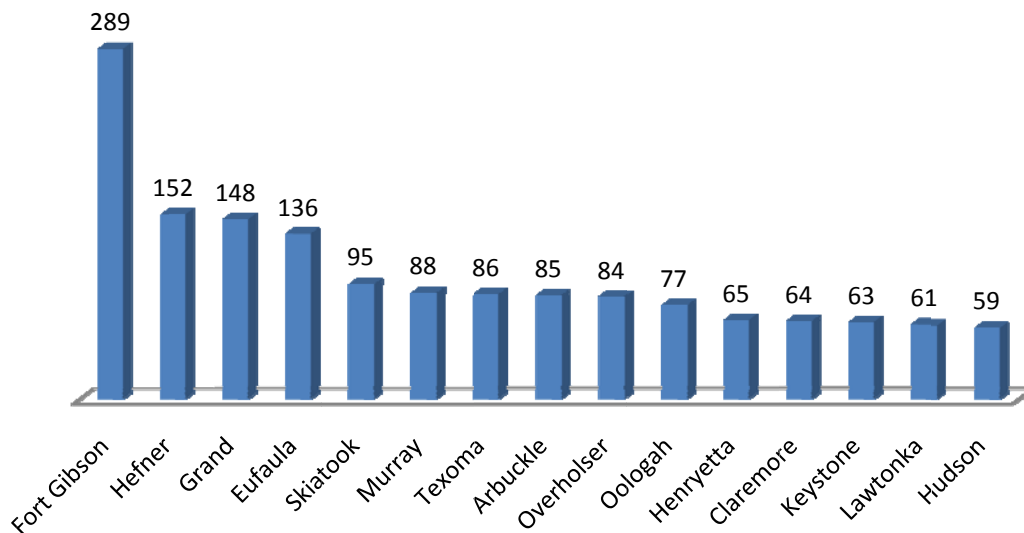


Figure 3: Top 15 Most Popular Lakes for Multiple Day Trips (# of visits in sample)

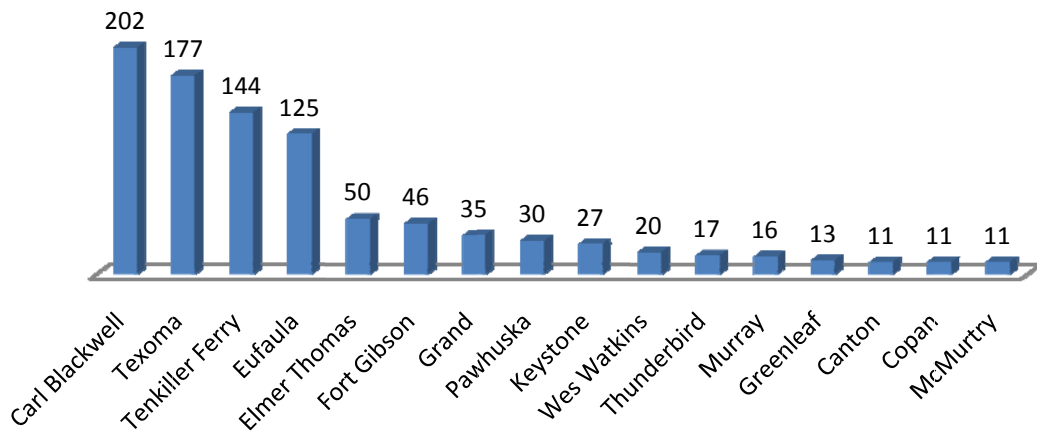


Figure 4: Percentage of Total Trips Reported to Lakes Outside of Oklahoma in 2007(as a percentage of all trips in and out of state)

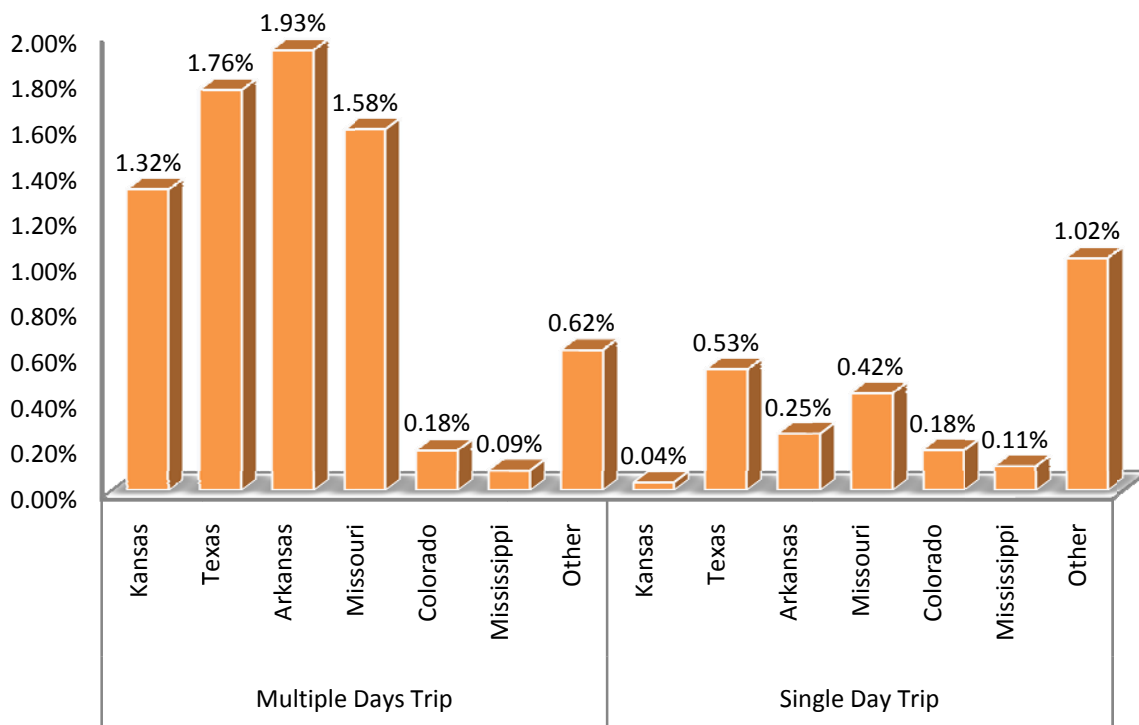


Figure 5: Activities at Lakes Ranked

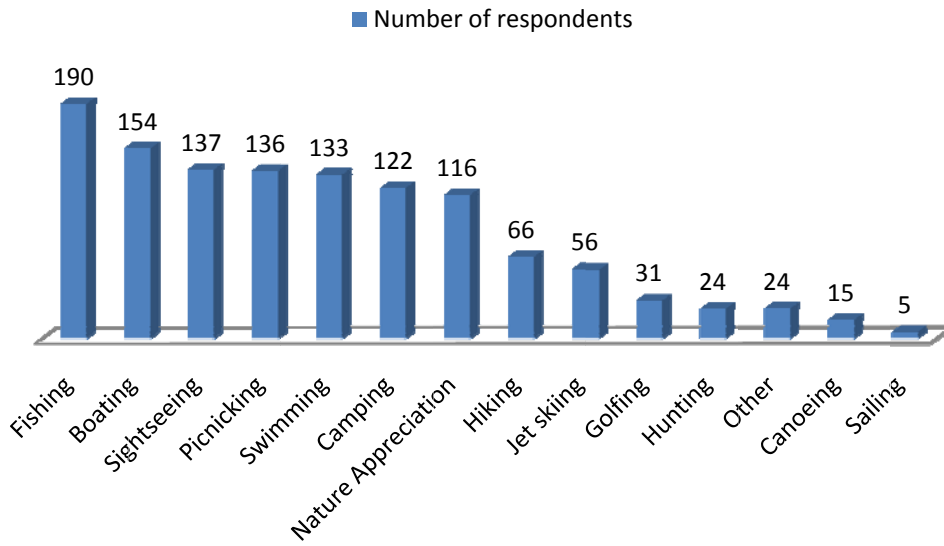


Figure 6: Reported Frequency of Swimming in Oklahoma Lakes by Percentage of Respondents Visiting Lakes

■ Never ■ Rarely ■ Sometimes ■ Frequently

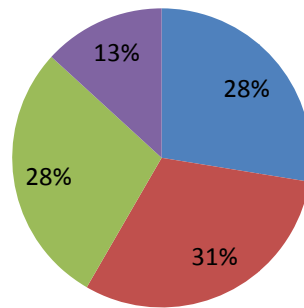


Figure 7: Percentage of All Respondents Who Believe Lake Condition Information Should Be Provided by the State by Subject

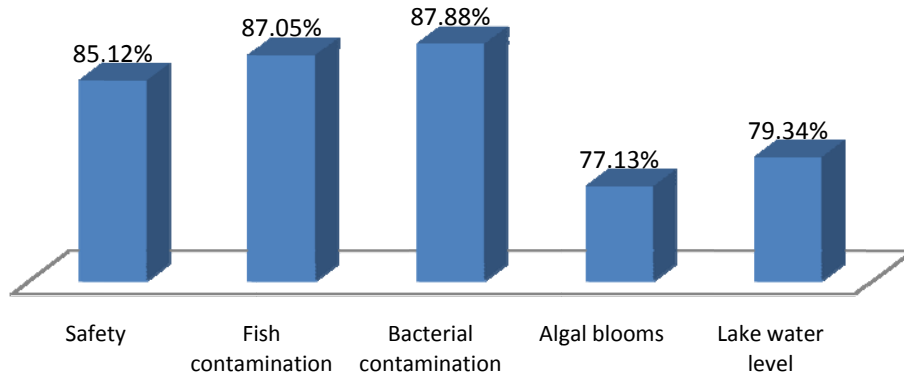


Figure 8: Percentage of All Respondents Who Believe Lake Condition Information Given by the State Would Affect Their Visitation Rate by Subject

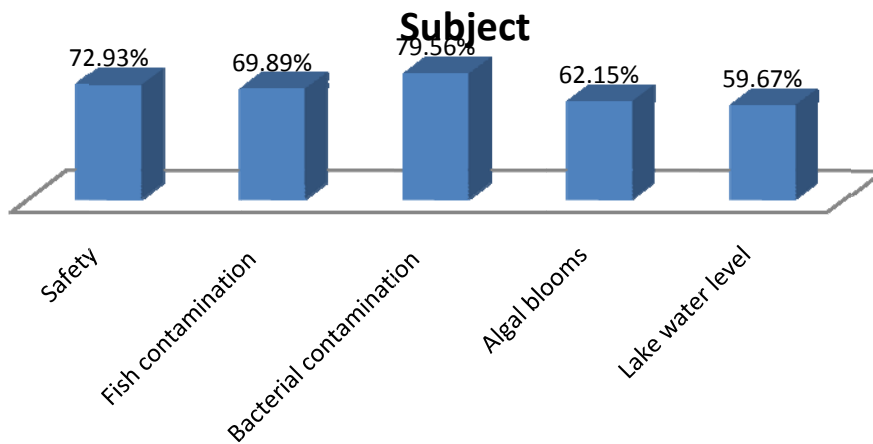


Figure 9: Average Score of Factors Affecting Choice to Visit Lakes

Scale of 1-10

(1 =not important and 10=very important, 5= neutral)

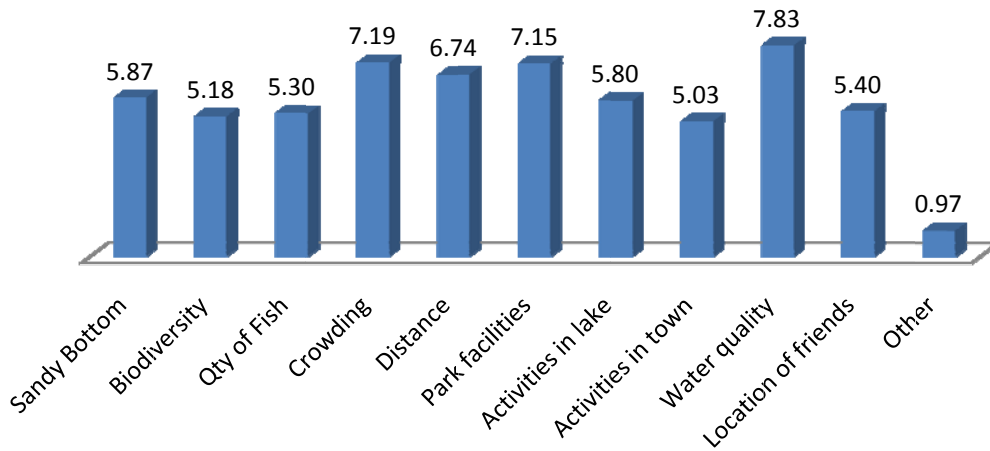


Figure 10: Average Rank of Water Quality Factors: Ranked 1st, 2nd, 3rd in Importance to Choice of Lake to Visit

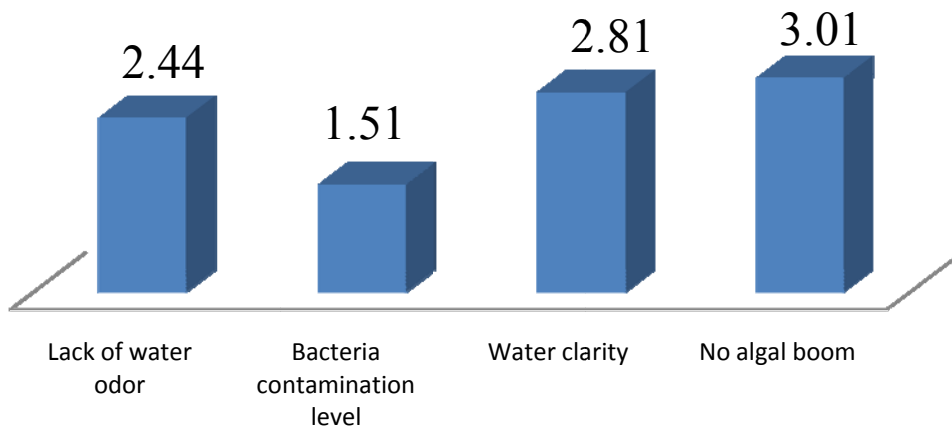


Figure 11: Respondent Age Categories by Percentage (Years)

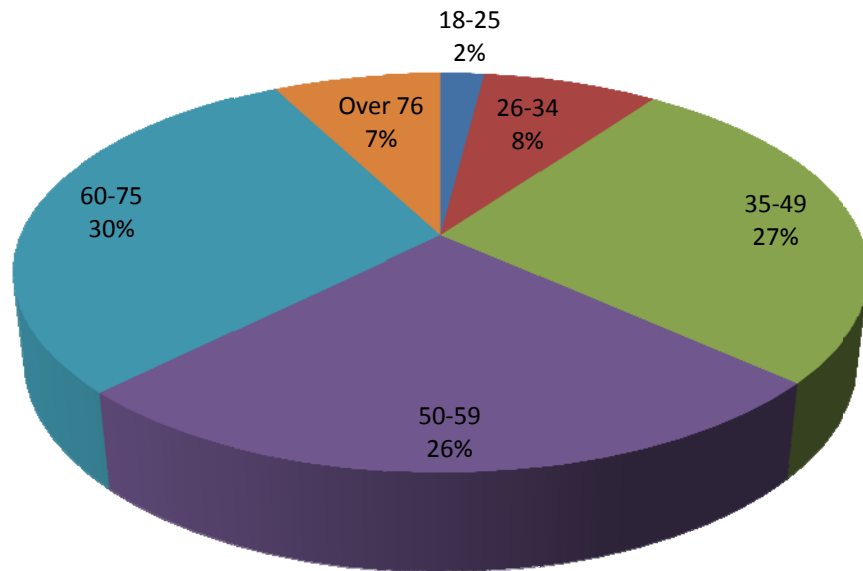


Figure 12: Gender structure of sample

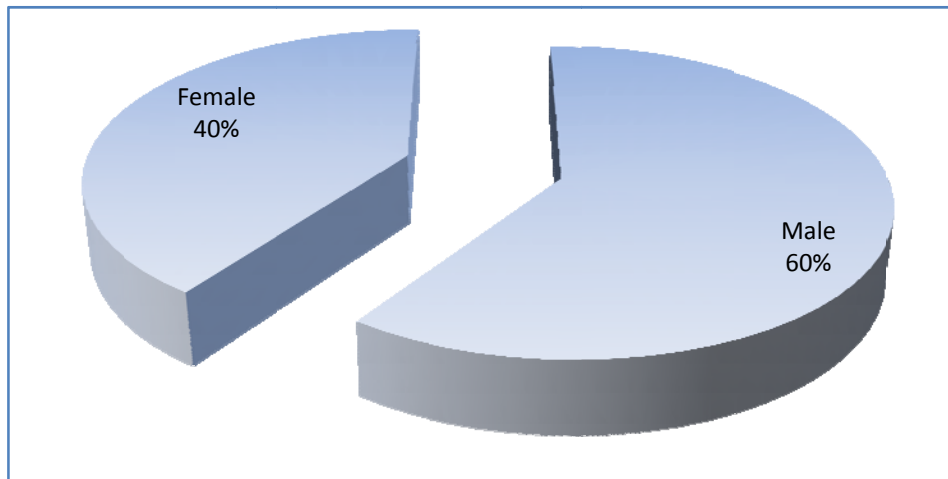
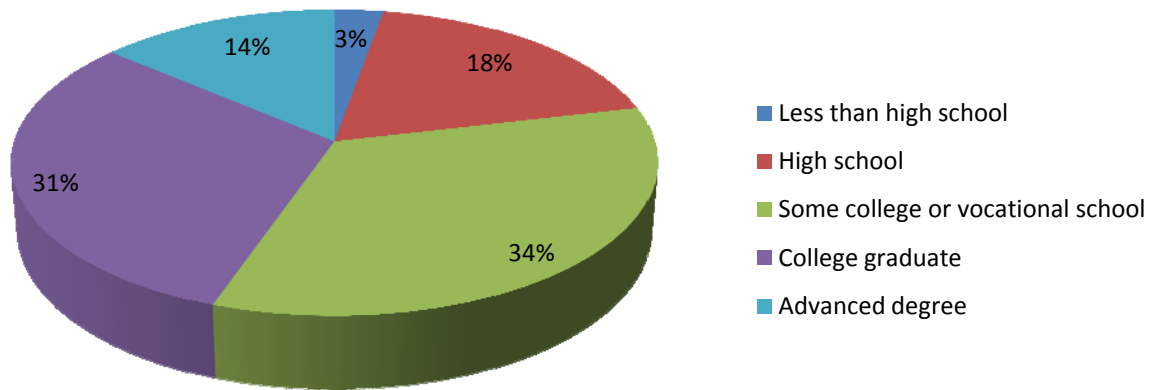


Figure 13: Education Levels of Respondents



**Figure 14:
Income levels of Respondents' Households by
Percentage (USD 2007)**

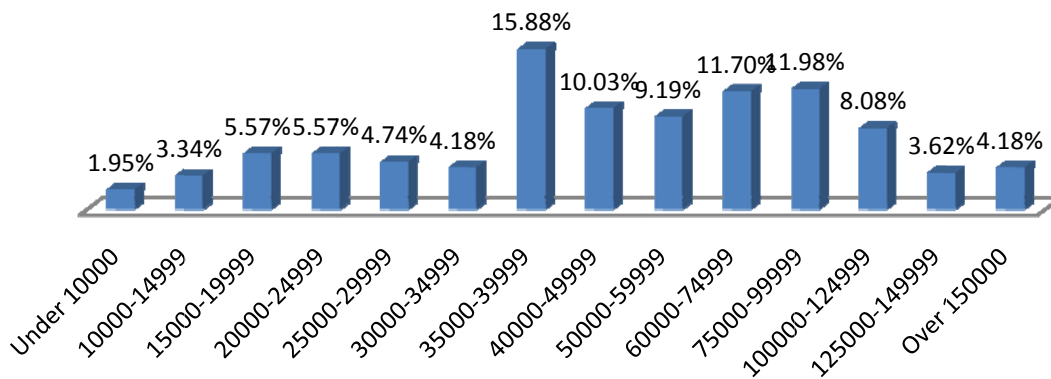
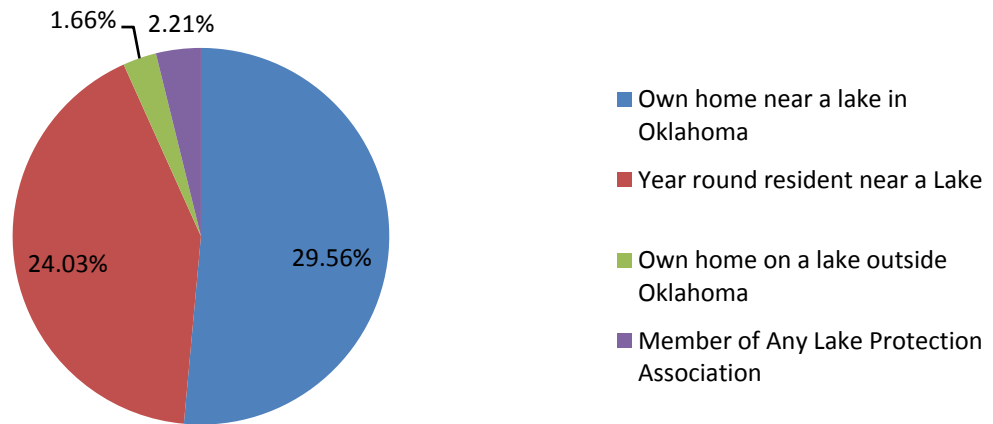


Figure 15: Percentage of Respondents Closely Linked to Lakes



Subsurface Transport of Phosphorus to Streams: A Potential Source of Phosphorus not Alleviated by Best Management Practices

Basic Information

Title:	Subsurface Transport of Phosphorus to Streams: A Potential Source of Phosphorus not Alleviated by Best Management Practices
Project Number:	2007OK79B
Start Date:	3/1/2007
End Date:	7/31/2008
Funding Source:	104B
Congressional District:	3
Research Category:	Ground-water Flow and Transport
Focus Category:	Water Quality, Nutrients, Groundwater
Descriptors:	Phosphorus, Subsurface flow, Cherty/Clarksville soils, Best Management Practices, Non-point source pollution
Principal Investigators:	Garey Fox, Chad Penn, Daniel E. Storm

Publication

1. Fuchs, J.W., G.A. Fox, D. Storm, C. Penn, and G.O. Brown. 2008. Subsurface transport of phosphorus in riparian floodplains: Tracer and phosphorus transport experiments. ASABE Paper No. 084614. St. Joseph, Mich.: ASABE.
2. Fuchs, J.W., G.A. Fox, D.E. Storm, C. Penn, and G.O. Brown. 2009. Subsurface transport of phosphorus in riparian floodplains: Influence of preferential flow paths. Journal of Environmental Quality 38(2): 473-484.
3. Heeren, D.M., R. Miller, G.A. Fox, D.E. Storm, C.J. Penn, and T. Halihan. 2009. Preferential Flow Path Effects on Subsurface Contaminant Transport in Alluvial Floodplains. ASABE Annual International Conference, Reno, NV, June 21-25, 10 pages.

FY 2007 Oklahoma Water Resources Research Institute Grant Final Technical Report

Title:

Subsurface Transport of Phosphorus to Streams: A Potential Source of Phosphorus not Alleviated by Best Management Practices (BMPs)

Start Date:

March 1, 2007

End Date:

October 15, 2008

Congressional Districts:

02 – Tahlequah, Oklahoma
03 – Stillwater, Oklahoma State University

Focus Category:

AG, GEOMOR, GW, HYDROL, NPP, NU, SW, WQL

Descriptors:

Ground Water, Phosphorus, Preferential Flow, Riparian Floodplain, Subsurface Transport

Principal Investigators:

Garey A. Fox, Ph.D., P.E., Department of Biosystems and Agricultural Engineering, Oklahoma State University; Daniel E. Storm, Ph.D., Department of Biosystems and Agricultural Engineering, Oklahoma State University; Chad J. Penn, Ph.D., Department of Plant and Soil Sciences, Oklahoma State University; Glenn O. Brown, Ph.D., P.E., Department of Biosystems and Agricultural Engineering, Oklahoma State University

Publications:

Fuchs, J.W., G.A. Fox, D.E. Storm, C. Penn, and G.O. Brown. Subsurface transport of phosphorus in riparian floodplains: Influence of preferential flow paths. *Journal of Environmental Quality* (Accepted for Publication, In Press).
Fuchs, J.W., G.A. Fox, D. Storm, C. Penn, and G.O. Brown. 2008. Subsurface transport of phosphorus in riparian floodplains: Tracer and phosphorus transport experiments. ASABE Paper No. 084614. St. Joseph, Mich.: ASABE.

TABLE OF CONTENTS

List of Figures	iii
List of Tables	iv
Summary Table of Student Support.....	v
Abstract	vi
I. PROBLEM AND RESEARCH OBJECTIVES	1
1.1 Subsurface Nutrient Transport Studies	1
1.2 Hydraulic Conditions Promoting Subsurface Phosphorus Transport	2
1.3 Objectives.....	2
II. METHODOLOGY	3
2.1 Soil Sampling	4
2.2 Tracer and Phosphorus Injection Experiments	6
2.3 Laboratory Column Experiments.....	7
III. PRINCIPLE FINDINGS AND SIGNIFICANCE	9
3.1 Soil Properties	9
3.2 Tracer and Phosphorus Injection Experiments	11
3.3 Laboratory Flow Experiments	20
4.4 Research Implications	23
IV. CONCLUSIONS AND FUTURE WORK	23
V. ACKNOWLEDGEMENTS.....	24
VI. REFERENCES	24
APPENDIX. AERIAL PHOTO OF FIELD SITE ALONG BARREN FORK CREEK.....	27

LIST OF FIGURES

Figure 1. Field site located approximately 25 km east of Tahlequah, Oklahoma adjacent to the Barren Fork Creek.....	3
Figure 2. (a) Location of the trench and piezometers and (b) illustration of piezometers relative to the location of the trench. Photograph was taken from piezometer D looking northeast towards piezometers A and E.	4
Figure 3. Laboratory flow-through experimental setup. The experimental setup follows that of DeSutter et al. (2006).....	7
Figure 4. Particle size distribution for gravel subsoil in the riparian floodplain. D_{10} , D_{30} , D_{50} , and D_{60} are the diameter of soil particles in which 10, 30, 50, and 60%, respectively, of the sample is finer.	9
Figure 5. Laboratory data fit to Langmuir isotherm, where Q^o is the mass of phosphorus sorbed per unit soil mass at complete surface coverage and b is the binding energy, for fine soil material (i.e., less than 2.0 mm). The distribution coefficient, K_d , for the.....	10
Figure 6. (a) Rhodamine WT concentrations for non-preferential flow piezometers located 2-3 m and 7-8 m from trench during experiment 1. (b) Rhodamine WT concentrations in preferential and non-preferential flow piezometers during experiment 1. Note: Concentrations greater than 300 ppb were above detection limit of field fluorometer.	12
Figure 7. Rhodamine WT concentrations in trench (a) compared to non-preferential flow piezometers (b) and (c) and preferential flow piezometers (d), (e), and (f) during experiment 2.....	13
Figure 8. Box plots of background phosphorus (P) concentration in preferential flow versus non-preferential flow piezometers prior to P injection experiment (i.e., experiment 3). 25th and 75th percentiles = boundary of the box; median = line within the box; 10 th and 90 th percentiles = whiskers above and below the box.....	16
Figure 9. Phosphorus concentrations in trench (a) compared to non-preferential flow piezometers (b) and (c) and preferential flow piezometers (d), (e), and (f) during experiment 3.....	17
Figure 10. Phosphorus (P) concentrations detected in outflow (C) versus (a) dimensionless time and (b) mg P added per kg of soil, where Q is the flow rate, V_{ps} is the pore space volume, C_b is the background P concentration released from the soil, C_o is the inflow P concentration, and t_b^* is the dimensionless breakthrough time.....	21

LIST OF TABLES

Table 1. Summary of Rhodamine WT and phosphorus (KH ₂ PO ₄) injection experiments. Water was injected at a rate of approximately 0.0044 m ³ /s.....	6
--	---

SUMMARY TABLE OF STUDENT SUPPORT

Student Status	Number	Disciplines
Undergraduate	2	Geology, Biosystems and Agricultural Engineering
M.S.	1	Biosystems and Agricultural Engineering
Ph.D.		
Post Doc		
Total	3	

ABSTRACT

For phosphorus (P) transport from upland area to surface water systems, the primary transport mechanism is typically considered to be surface runoff with subsurface transport assumed negligible. However, certain local conditions can lead to an environment where subsurface transport may be significant. The objective of this research was to determine the potential of subsurface transport of P along streams characterized by cherty or gravel subsoils, especially the impact of preferential flow paths on P transport. At a field site along the Barren Fork Creek in northeastern Oklahoma, a trench was installed with the bottom of the trench at the topsoil/alluvial gravel interface. Fifteen piezometers were installed at various locations surrounding the trench in order to monitor flow and transport. In three experiments, water was pumped into the trench from the Barren Fork Creek to maintain a constant head. At the same time, a conservative tracer (Rhodamine WT) and/or potassium phosphate solution were injected into the trench at concentrations at 3 and 100 mg/L for Rhodamine WT and at 100 mg/L for P. Laboratory flow-cell experiments were also conducted on soil material less than 2 mm in size to determine the effect that flow velocity had on P sorption. Rhodamine WT and P were detected in some piezometers at equivalent concentrations as measured in the trench, suggesting the presence of preferential flow pathways and heterogeneous interaction between streams and subsurface transport pathways, even in non-structured, coarse gravel soils. Phosphorus transport was retarded in non-preferential flow paths but not in preferential flow pathways. Breakthrough times were approximately equivalent for Rhodamine WT and P suggesting no colloidal-facilitated P transport. Results from laboratory flow-cell experiments suggested that higher velocity resulted in less P sorption for the alluvial subsoil. Therefore, with differences in flow rates between preferential and non-preferential flow pathways in the field, variable sorption was hypothesized to have occurred. The potential for nutrient subsurface transport shown by this alluvial system has implications regarding management of similar riparian floodplain systems.

SUBSURFACE TRANSPORT OF PHOSPHORUS TO STREAMS: A POTENTIAL SOURCE OF PHOSPHORUS NOT ALLEVIATED BY BEST MANAGEMENT PRACTICES (BMPS)

I. PROBLEM AND RESEARCH OBJECTIVES

The adverse impact of increased nutrient loadings on surface water quality has drawn considerable attention in recent years. Polluted drinking water, excessive algal growth, taste and odor issues, and fish kills are only a few of the negative effects that can result from an overload of nutrients. While nitrogen is a concern, phosphorous (P) is generally considered the most limiting nutrient. Daniel et al. (1998) found that concentrations of P critical for terrestrial plant growth were an order of magnitude larger than concentrations at which lake eutrophication may occur. Excessive soil P concentrations can increase potential P transport to surface waters or leaching into the groundwater and have negative implications.

1.1 Subsurface Nutrient Transport Studies

Subsurface P transport is a less studied and understood transport mechanism compared to transport by overland flow, although numerous studies have reported P in groundwater and subsurface P transport (Turner and Haygarth, 2000; Kleinman et al., 2004; Nelson et al., 2005; Andersen and Kronvang, 2006; Hively et al., 2006). For example, from research on four grassland soils, Turner and Haygarth (2000) documented that subsurface P transfer, primarily in the dissolved form, can occur at concentrations that could cause eutrophication. Kleinman et al. (2004) noted that the P leaching is a significant, but temporally and spatially variable transport pathway. Nelson et al. (2005) indicated that P leaching and subsurface transport should be considered when assessing long-term risk of P loss from waste-amended soils. Andersen and Krovang (2006) modified a P Index to incorporate potential P transport pathways of tile drains and leaching in Denmark. Hively et al. (2006) considered transport of total dissolved P (TDP) for both baseflow and surface runoff. Other researchers are beginning to emphasize colloidal P transport in the subsurface, as P attaches to small size particles capable of being transported through the soil pore spaces (de Jonge et al., 2004; Heathwaite et al., 2005; Ilg et al., 2005).

The potential for subsurface nutrient transport in association with vegetated buffer strips (VBS) along the riparian areas of surface water systems has recently been emphasized. The VBS can be either grass or forested, and act as a zone in which runoff is captured and/or sediment trapped, inhibiting sediment-bound nutrient transport to the stream. However, some studies have shown these VBS systems promote subsurface nutrient loading to streams (Osborne and Kovacic, 1993; Vanek, 1993; Cooper et al., 1995; Polyakov et al., 2005). Polyakov et al. (2005) examined current research regarding riparian buffer systems and their ability to retain nutrients. Their findings suggested that conditions, such as the spatial variability in soil hydraulic conductivity, the presence of preferential flow pathways, and limited storage capacity in the riparian zone's soil, could subvert the buffer system's ability and allow for increased nutrient transport. Osborne and Kovacic (1993) showed VBS could actually act like a nutrient source, releasing dissolved and total P into the groundwater. Another study conducted in Sweden showed that the soil

in riparian zones had almost no P retention capacity due to a natural calcium leaching process which started over 3000 years ago (Vanek, 1993). Also, a study by Cooper et al. (1995) showed a high P availability for groundwater transport due to saturation of the riparian zone.

There have been several studies conducted in which observation wells were used to monitor the flow of nutrients in groundwater in riparian zones (Vanek, 1993; Carlyle and Hill, 2001; McCarty and Angier, 2001). Vanek (1993) noted groundwater P concentrations taken from 12 wells in a lake riparian zone ranged from 0.4 to 11.0 mg/L with an average of 2.6 mg/L. Carlyle and Hill (2001) monitored the behavior of P in the subsurface in a river riparian zone and suggested that riparian areas can become saturated with P. They noticed higher soluble reactive phosphorus (SRP) concentrations (0.10 to 0.95 mg/L) in areas characterized by having soils with higher hydraulic conductivities buried under the top soils. They suggested that riparian areas might actually be contributing to the release of P because they increase the redox potential. McCarty and Angier (2001) studied preferential flow pathways in riparian floodplains. Their findings showed increased biological activity in these pathways and could lead to reduced conditions, which, in turn, decrease the ability to remove nutrients.

It should be noted that surface runoff usually consists of high flows over a short period of time, whereas subsurface flow is characterized by lower flow rates over long periods of time. The point is that even though surface runoff has shown higher concentrations in many field studies (i.e., Owens and Shipitalo, 2006), low-concentration subsurface flow occurring over a long period of time could still be making a viable contribution to the total nutrient load of a surface water body. The findings mentioned above show that there is a potential for subsurface nutrient transport. Therefore, there is a need for more research devoted to monitoring and understanding subsurface P transport.

1.2 Hydraulic Conditions Promoting Subsurface Phosphorus Transport

As noted earlier, local or regional conditions can lead to conditions where subsurface transport is significant (Andersen and Kronvang, 2006). Areas such as riparian floodplains commonly consist of alluvial deposits with gravelly soils possessing hydraulic properties conducive to the subsurface transport of P. Gravel or cherty soils are common throughout the Ozark region of Oklahoma, Arkansas, and Missouri. In eastern Oklahoma, cherty soils adjacent to rivers consist of gravelly silt loam to gravelly loam substrate below a thin layer of organic matter. Sauer and Logsdon (2002) studied the hydraulic properties of some of these cherty soils (Clarksville and Nixa series) and concluded that relatively subtle morphological factors can have a disproportionate impact on water flow in the soils, suggesting the need for further research regarding their hydraulic properties. These soils possess infiltration rates as high as 1.22 to 3.67 m/d according to USDA Soil Surveys. Therefore, the potential for subsurface transport is significant.

1.3 Objectives

More research pertaining to the role of subsurface P transport is needed, especially in riparian floodplains. Current best management practices aimed at reducing P load through surface runoff may be ineffective if subsurface flow is a significant transport mechanism and therefore could impact long-term planning of available water supplies. This research attempts to quantify the potential for subsurface alluvial transport of P in a

riparian floodplain, especially the impact of preferential flow paths on P transport. If subsurface P transport is important on these landscapes, questions need to be answered regarding what impact, if any, current best management practices are having on this transport mechanism.

II. METHODOLOGY

In order to study the potential for subsurface transport in a riparian floodplain (Figure 1), a trench-piezometer system was installed in a riparian area (latitude: 35.90°, longitude: -94.84°) approximately 20 m adjacent to the Barren Fork Creek near Tahlequah, OK (Figure 2). The trench system was designed to induce a constant water head and a tracer/P injection source on the subsurface alluvial gravel with subsequent monitoring of flow, tracer, and P transport in the piezometer field. The dimensions of the trench were approximately 0.5 m wide by 2.5 m long by 1.2 m deep. The bottom of the trench was located approximately 25 to 50 cm below the interface between the topsoil and gravel layers, thereby short-circuiting flow and tracer/P directly into the gravel. A bracing system consisted of a frame constructed with 5 cm by 13 cm studs and covered with 2 cm plywood. Fifteen piezometers were installed at various locations around the trench with the majority of the piezometers located between the trench and the river (Figure 2). The piezometers were approximately 6 m (20 ft) long and were constructed of Schedule 40 PVC. Each consisted of at least a 3 m screened section at the base. The piezometers were installed using a Geoprobe® (Kejr, Inc.) drilling machine. Fuchs (2008) discussed additional details on piezometer installation.

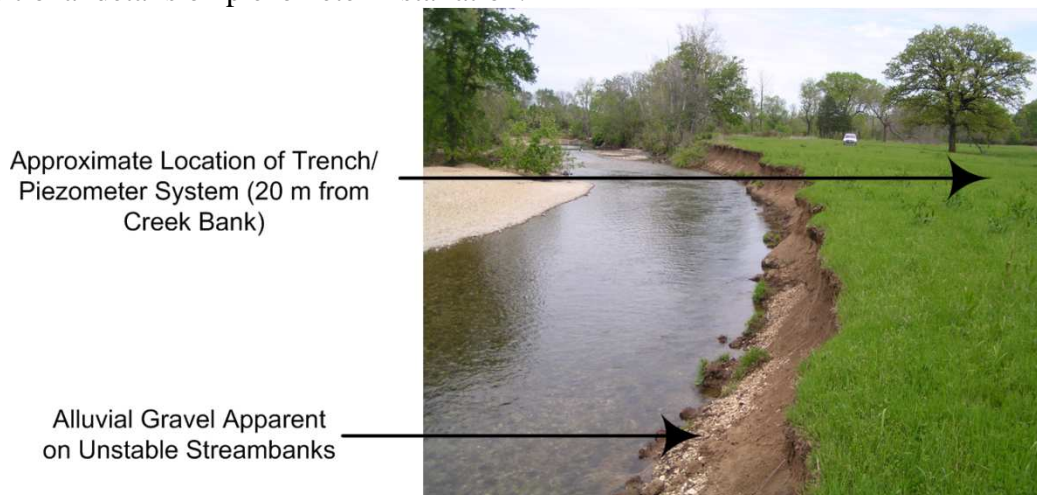


Figure 1. Field site located approximately 25 km east of Tahlequah, Oklahoma adjacent to the Barren Fork Creek.

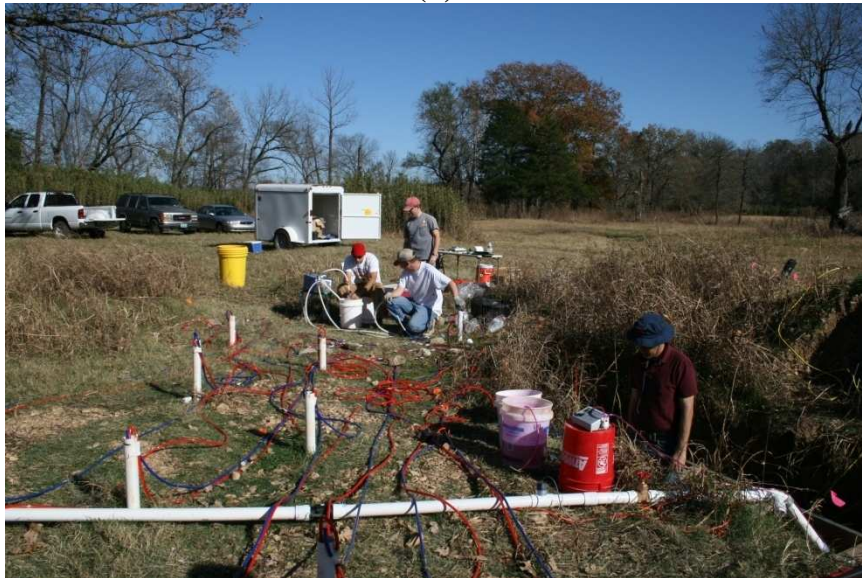
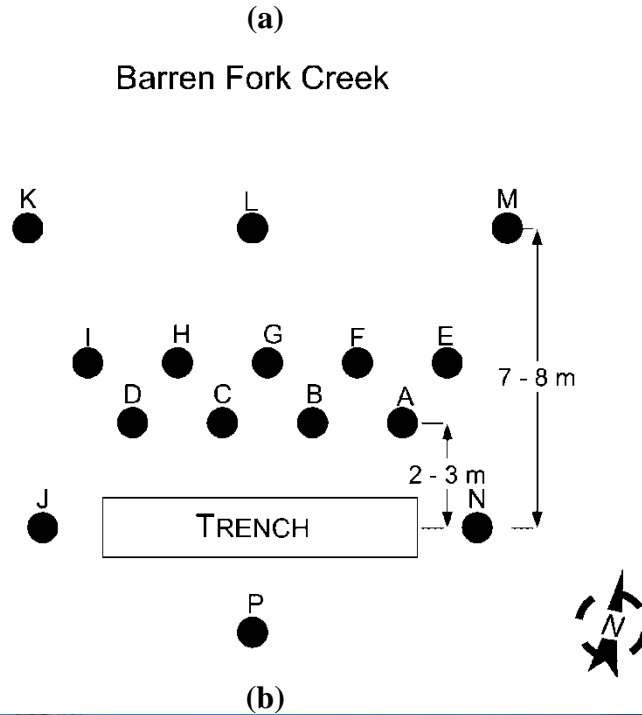


Figure 2. (a) Location of the trench and piezometers and (b) illustration of piezometers relative to the location of the trench. Photograph was taken from piezometer D looking northeast towards piezometers A and E.

2.1 Soil Sampling

Samples from the surface of the alluvial gravel were taken when installing the trench since the unconsolidated gravel was unstable. Although these samples were disturbed, they still provided a reasonable representation of the subsoil. The samples taken from the gravel layer were first sieved to determine the particle size distribution for the

gravel subsoil. After oven drying the sample, the coarse gravel was first separated out using a stack of five sieves ranging from 25.4 mm to 4.75 mm (No. 4). Next, the smaller particles were sieved using a sieve stack as follows: 4.75 mm (No. 4), 2.0 mm (No. 10), 0.85 mm (No. 20), 0.6 mm (No. 30), 0.425 mm (No. 40), 0.25 mm (No. 60), 0.15 mm (No. 100), and 0 mm (pan).

The particle size distribution was analyzed to determine the D_{10} , D_{30} , D_{50} , and D_{60} (i.e., diameter of soil particles in which 10, 30, 50, and 60%, respectively, of the sample is finer). Once the particle size was known, the diameters were used with an empirical equation proposed by Alyamani and Sen (1993) to estimate the hydraulic conductivity of the soil:

$$K = 1300[I_0 + 0.025(D_{50} - D_{10})]^2 \quad (1)$$

where K is the hydraulic conductivity in m/d, D_{50} and D_{10} are in mm, and I_0 is the intercept of the line formed by D_{50} and D_{10} with the grain size axis. This estimate for hydraulic conductivity was compared to another estimate obtained using a falling head test (Landon et al., 2001; Fox et al., 2004). The falling head test was performed by filling the trench with water until steady state conditions were reached, shutting off water to the trench, and recording water levels over time as the trench drained. Data obtained from the falling head experiment were then used with the Darcy equation to estimate the vertical hydraulic conductivity:

$$K_v = \frac{L}{t_1 - t_0} \ln \frac{H_0}{H_1} \quad (2)$$

where K_v is the vertical hydraulic conductivity of the soil in m/d, L is the sediment interval being tested in m (i.e., 0.25 to 0.50 m for the trench system), and H_0 and H_1 are the displacement in m of the water at time t_0 and t_1 respectively (Landon et al., 2001; Fox et al., 2004).

After sieving the soil sample, particles with a diameter less than 2.0 mm were further analyzed for P sorption. Adsorption isotherms were estimated by adding different levels of P (0, 1, 5, 10, 25, 50, 100, 200, 400, and 800 mg P/L) to 2.0 g soil samples. The samples were shaken for 24 hours using a reciprocating shaker and then centrifuged for 10 minutes at 10,000 rpm. The P in solution was then quantified using ICP-AES analysis. Data were fit to linear (equation 3) and Langmuir (equation 4) isotherms to provide information in regard to the ability of the fine sediment fraction of the alluvial soils to adsorb P from solution:

$$q_e = K_d C_e \quad (3)$$

$$q_e = Q^0 \frac{bC_e}{1 + bC_e} \quad (4)$$

where q_e is the mass of P sorbed per unit mass of soil, C_e is the equilibrium, dissolved phase concentration, K_d is the distribution coefficient, and Q^0 and b are parameters of the Langmuir isotherm (i.e. Q^0 is the mass of P sorbed per unit mass of soil at complete surface coverage and b is the binding energy).

An ammonium oxalate extraction was also performed on the fine material to determine the degree of P saturation, which is the ratio of P to the total amount of iron and aluminum (McKeague and Day, 1966; Iyengar et al., 1981; Pote et al., 1996). This procedure dissolved the non-crystalline forms of aluminum and iron in the material,

considered to be the main sink for P among acidic soils. Therefore, selective dissolution of these amorphous minerals liberates any P associated with them into solution.

2.2 Tracer and Phosphorus Injection Experiments

Two Rhodamine WT tracer and one P (potassium phosphate, KH_2PO_4) injection experiments were performed to monitor subsurface solute transport from the trench (Table 1). Prior to the injection, each piezometer and the Barren Fork Creek was sampled and analyzed for background P levels. Also, a water level indicator was used to determine the depth to the water table in each piezometer prior to injection. Experiments were performed near base flow conditions in the Barren Fork Creek with ground water tables approximately 3.5 m below ground surface. Next, water was pumped from the Barren Fork Creek into the trench at approximately $0.0044 \text{ m}^3/\text{s}$ (i.e., 4.4 L/s) in order to induce water movement. The steady-state water level in the trench was held as constant as possible at approximately 40 to 60 cm above the bottom of the trench. Water levels in the piezometers surrounding the trench were monitored over time. Pumping continued until the system reached pseudo-steady state conditions, which was verified when the water levels in the piezometers remained constant.

Rhodamine WT or P (KH_2PO_4) was injected into the trench at a constant rate using a variable rate chemical pump (Table 1). Once the injection began, samples were taken from the piezometers for the duration of the experiment in order to monitor the movement of the Rhodamine WT tracer and P. To sample the piezometers, a peristaltic pump was used. In order to obtain water samples at two different depths for experiment 2 and 3, two hoses were run to each of the piezometers. One hose was lowered to a depth 10 cm below the water table, while another was lowered to a depth 1.10 m below the water table.

Table 1. Summary of Rhodamine WT and phosphorus (KH_2PO_4) injection experiments. Water was injected at a rate of approximately $0.0044 \text{ m}^3/\text{s}$.

Experiment No.	1	2 ^a	3 ^a
Injection Compound	Rhodamine WT	Rhodamine WT	KH_2PO_4
Concentration (mg/L)	100	3	100
Compound Injection Duration (min)	60	90	90
Duration of Water Injection (min)	120	200	200
Average Water Level in Trench (cm)	44	60	60

^a Experiments 2 and 3 were performed simultaneously.

The samples were placed into small bottles and then put into a refrigerated cooler and transported back to the laboratory where they were analyzed for Rhodamine WT, P and other cations such as calcium and aluminum. Each sample was analyzed for Rhodamine WT content using a Turner model 111 fluorometer and an Aquaflor handheld fluorometer. Samples were then analyzed for P content using two different methods. The Murphy-Riley (1962) method was used to measure the dissolved inorganic P present in the

samples, and an inductively coupled plasma atomic emission spectroscopy (ICP-AES) machine was used to measure the total dissolved P.

2.3 Laboratory Column Experiments

The fine material (i.e., less than 2.0 mm) obtained from the sieve analysis was also used in laboratory flow-cell experiments (DeSutter et al., 2006) to investigate the P sorption characteristics with respect to the flow velocity. The use of a uniform layer of fine material removed physical non-equilibrium effects due to spatial uniformity in dispersivity. Approximately 5.0 g of the fine material was placed in each of six flow-through cells (Figure 3). This corresponded to a soil depth of approximately 2.3 mm. A Whatman 42 filter was placed at the bottom of each cell to prevent the fine material from passing through the bottom. Each cell had a nozzle at the bottom with a hose running from the nozzle to a peristaltic pump. The pump pulled water with a predetermined P concentration through the cells and fine material at a known flow rate (mL/min) (Figure 3). Two different speeds on the peristaltic pump were used to evaluate the effect that flow velocity had on P sorption. The flow rates used averaged 0.4 mL/min for three low flow experiments and 14 mL/min for three high flow experiments. These flow rates corresponded to average flow velocities of 1.3 and 46 m/d, respectively.

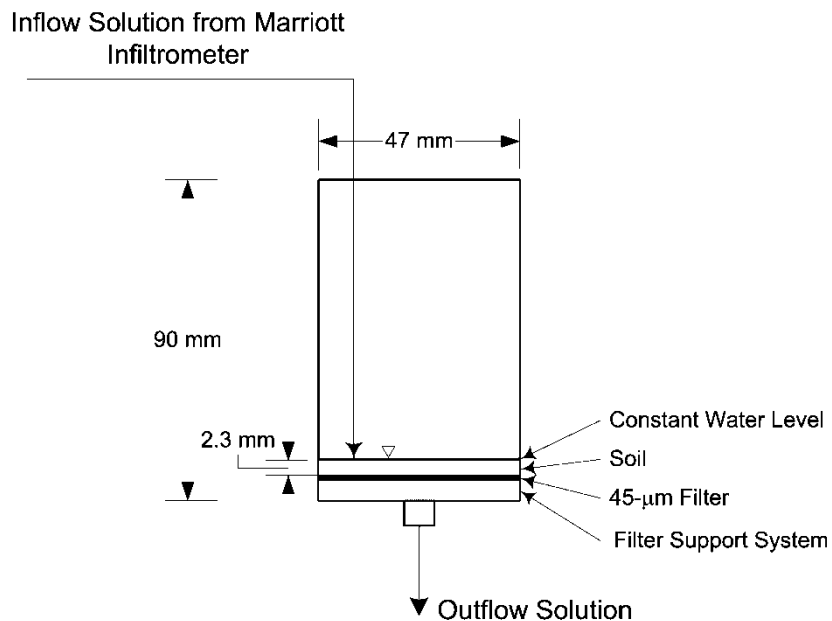


Figure 3. Laboratory flow-through experimental setup. The experimental setup follows that of DeSutter et al. (2006).

First, 20 mL of deionized water was pulled through the soil to determine the background P that was removed from the soil. Next, a KH_2PO_4 solution was injected into each cell at 1.0 mg/L and kept at a constant head using a Mariott bottle system (Figure 3). The low flow experiment was run for approximately 8 hours, while the high flow

experiment was run for 1 hour. This was done to achieve approximately equal P loads to each system. Samples were taken periodically throughout each experiment. The samples were analyzed in the laboratory for P and Ca using both the Murphy-Riley (1962) method and ICP-AES analysis.

The solution dissolved P concentrations obtained from the ICP-AES analysis were then used to evaluate the effect flow velocity on P sorption. Two scientific perspectives were used to analyze these data. The first method was based on contaminant transport theory and compared the outflow dissolved P concentrations from both low flow and high flow velocities over time. The dissolved P concentrations determined by ICP-AES analysis were plotted versus a dimensionless injection time, t^* , where $t^* = tQ/V_{ps}$, where Q is the inflow rate and V_{ps} is the pore volume. From the curve produced from outflow dissolved P concentration versus t^* , a breakthrough time, t_b^* , was estimated for each of the flow velocity experiments. This was assumed to be the time at which 50% of the inflow concentration was detected in the outflow solution.

A sorbing contaminant moves through porous media at a retarded flow velocity, as suggested by the following advection-dispersion-retardation equations:

$$\begin{aligned} R \frac{\partial c}{\partial t} &= -v \frac{\partial c}{\partial x} + D_L^{(h)} \frac{\partial^2 c}{\partial x^2} \\ \frac{\partial c}{\partial t} &= -v_s \frac{\partial c}{\partial x} + \alpha_L v_s \frac{\partial^2 c}{\partial x^2} \end{aligned} \quad (5)$$

where x is the direction along the length of the column, c is the concentration, v is the pore water velocity, $D_L^{(h)}$ is the hydrodynamic dispersion coefficient, α_L is the dispersivity, and v_s is the sorbed contaminant velocity. The sorbed contaminant velocity is simply the groundwater velocity divided by the retardation factor, R :

$$R = 1 + \left(\frac{K_d \rho_b}{\varepsilon} \right) \quad (6)$$

where ρ_b is the soil bulk density and ε is porosity. Solutions to equation 5 were given by Ogata and Banks (1961) and Hunt (1978):

$$C(x,t) = \frac{C_0}{2} \operatorname{erfc} \left(\frac{x - v_s t}{2\sqrt{\alpha_L v_s t}} \right) \quad (7)$$

These data from the flow-through experiments were then used with this equation to inversely estimate v_s and α_L by minimizing the sum of squared errors between predicted and observed outflow concentrations (i.e., $x = 0.23$ cm). With this estimated v_s , the average flow velocity measured during the experiment (v) was used to estimate R and then K_d . The K_d values estimated from low-flow and high-flow velocity experiments were compared.

Based on the one-dimensional advection-dispersion equations, a ratio relating the breakthrough times and flow velocities was derived assuming the length of the columns were equivalent between flow velocity experiments:

$$\frac{v_h}{v_l} = \frac{t_{b_l}}{t_{b_h}} \quad (8)$$

where t_{b_l} and t_{b_h} are the breakthrough times and v_h and v_l are the velocities for the high flow and low flow tests, respectively. If the ratios differed between experiments, then variable P sorption was occurring and the flow velocity had an effect on the sorption characteristics of the fine (i.e., less than 2.0 mm) material.

These flow-cell data were also analyzed based on the concentrations of dissolved P in the outflow compared to the total amount of P added to the system. If an equal mass of P was added to each system, the measured dissolved P concentrations in the outflows would be approximately equal if flow velocity did not have an effect on sorption. The mass of P added per kg of soil (mg P/kg soil) was found by multiplying Q (mL/min) by the inflow P concentration (mg/L) and by the elapsed time of the experiment (min). These data were plotted against the dissolved P concentrations (mg/L) detected in the outflow solutions for both flow velocities. If velocity had an effect on sorption, the curve for the low velocity data set would be lower than the curve for the high velocity data set.

III. PRINCIPLE FINDINGS AND SIGNIFICANCE

3.1 Soil Properties

From the particle size analysis of the gravel subsoil, it was found that roughly 81% of the material by mass was larger than 2.0 mm (Figure 4). This was significant because 2.0 mm is generally the upper limit used when attempting to characterize the sorption properties of a material. In other words, 81% of the gravel subsoil would likely be considered to have negligible sorption capabilities. According to the Wentworth (1922) scale, this gravel subsoil is classified as coarse gravel. The uniformity coefficient, defined as the ratio of D_{60} (i.e., 19 mm) to D_{10} (i.e., 0.9 mm), equaled 22 and suggested a fairly well-graded soil.

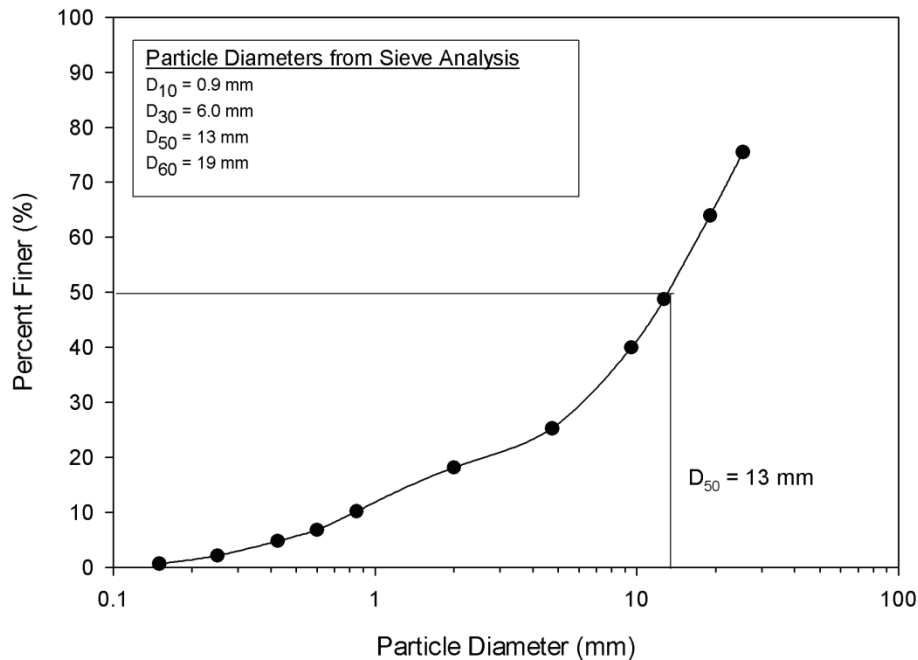


Figure 4. Particle size distribution for gravel subsoil in the riparian floodplain. D_{10} , D_{30} , D_{50} , and D_{60} are the diameter of soil particles in which 10, 30, 50, and 60%, respectively, of the sample is finer.

The particle size distribution was also used to estimate the hydraulic conductivity, K , of the gravel subsoil. Using a D_{50} of 13 mm, a D_{10} of 0.9 mm and I_0 equal to 0.4 mm, the K was estimated to be 640 m/d. Estimates for K_v obtained from the falling head test ranged from 140 to 230 m/d. It should be noted that most of the equations used to calculate K and K_v previously focused on soils with much smaller grain sizes (Landon et al., 2001). As indicated in the particle size distribution, the alluvial system tested here had a large percentage of gravels greater than 10 mm in diameter. Although the estimates for K and K_v obtained from the particle size distribution and falling head test may be elevated representations, they still demonstrate how conductive the gravel subsoil was and could be used as an indicator of the potential for rapid water and nutrient transport in the alluvial system.

The fraction of alluvial deposit less than 2.0 mm (i.e. about 19%) was found to possess considerable sorption capability based on linear ($K_d = 4.5$ L/kg based on C_e less than 10 mg/L) and Langmuir ($Q^0 = 125$ mg/kg and $b = 0.048$ L/kg) isotherms (Figure 5). When compared to other Oklahoma surface soils analyzed for P sorption properties, the Q^0 determined for our sample (125 mg/kg) was slightly lower than the range in Q^0 (191 to 772 mg/kg) of other surface soils analyzed in eastern Oklahoma (Fuhrman, 1998). A weighted linear K_d calculated based on the fraction of material above and below 2 mm resulted in a K_d of 0.9 L/kg. This weighted K_d suggested a P sorption R of 18 to 24 based on estimates of ρ_b for the gravel material of 1.5 to 1.8 g/cm³ and ϵ of 0.35 to 0.40.

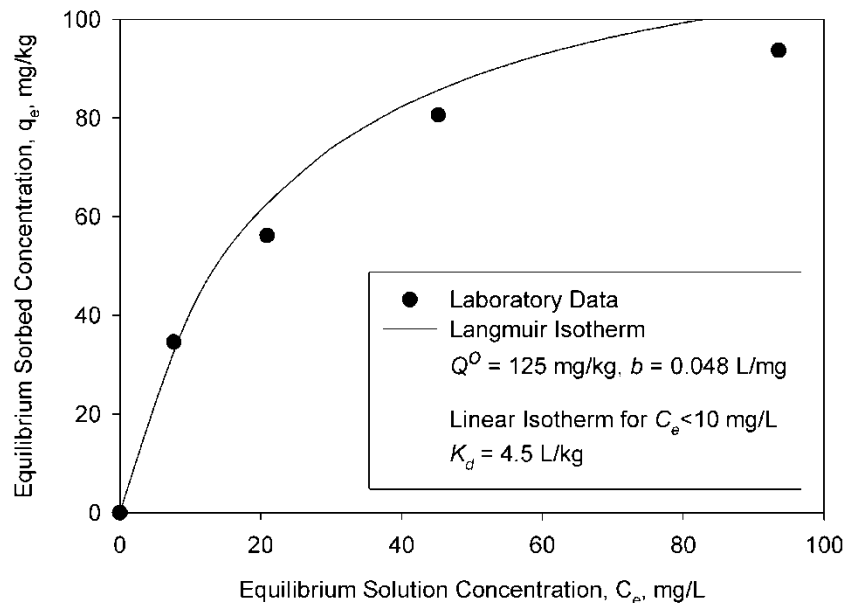


Figure 5. Laboratory data fit to Langmuir isotherm, where Q^0 is the mass of phosphorus sorbed per unit soil mass at complete surface coverage and b is the binding energy, for fine soil material (i.e., less than 2.0 mm). The distribution coefficient, K_d , for the

Results from the ammonium oxalate extractions showed a degree of P saturation of 4.2% when not including the α factor of 0.5 (Beauchemin and Simard, 1999). This α factor has been used to adjust the total amount of iron and aluminum that could be available in different soil types. The value was derived from a given set of soils and

laboratory conditions. Thus, it may not be appropriate to use it for all cases. When incorporating the α factor of 0.5, the degree of P saturation for the fine soil was found to be 8.4%. Both P saturation values could be considered lower than agricultural topsoils with a history of P applications beyond crop needs. This suggested that the fine soil material would be capable of sorbing a considerable amount of P. However, this only pertains to the fine material in the gravel subsoil, which is only about 19% of the entire size fraction.

3.2 Tracer and Phosphorus Injection Experiments

In the first experiment, Rhodamine WT was injected at 100 mg/L (Table 1). Samples analyzed from this experiment showed detectable concentrations in all of the piezometers. Concentrations detected in piezometers located 2 to 3 m from the trench (i.e. piezometers A, B, and C) peaked at 36 $\mu\text{g/L}$ with peak concentrations occurring approximately 30 min after injection. Detected levels in piezometers located 7 to 8 m from the trench (i.e., piezometers K, L, and M) were generally less than 30 $\mu\text{g/L}$ with peak concentrations occurring approximately 50 min after initiation of injection (Figure 6a).

Also, Rhodamine WT concentrations detected in piezometers D, I, and J for the first experiment were much higher than those detected in all other piezometers (Figure 6b). Sample concentrations from these piezometers all exceeded 300 $\mu\text{g/L}$, which was the upper detection limit on the field fluorometer. After dilution in the laboratory, the concentrations in these wells were found to be close to the injected concentration of 100 mg/L. Piezometers D, I, and J were hypothesized to be located in a preferential flow pathway which was more conductive than other subsurface material (Figure 6b).

In the second experiment, Rhodamine WT was injected at approximately 3.0 mg/L with the intent of staying within the range of detection for the field fluorometer (Figure 7). Sample analysis showed a pattern similar to the first injection, with detection levels in piezometers D, I, and J approximately equivalent to the injected concentration of 3.0 mg/L (Figure 7). However, there was no Rhodamine WT detected in any of the other piezometers. This was hypothesized to be due to the fact that the injected concentration of 3.0 mg/L (compared to 100 mg/L in the first experiment) was diluted near the detection limit by the time it reached the outer piezometers.

The results from the second Rhodamine WT injection supported the hypothesis that a highly conductive preferential flow pathway existed in the coarse gravel subsoil. The Rhodamine WT concentrations detected in the preferential flow pathway, i.e. Figures 7 (d), (e), and (f), were roughly two orders of magnitude larger than the concentrations detected in the non-preferential flow piezometers, i.e. Figures 7 (b) and (c). This demonstrated the potential for rapid subsurface transport in this alluvial system.

Another trend visible from the Rhodamine WT injections was that samples taken from 10 cm below the water table showed significantly higher concentrations than samples taken 110 cm below the water table for the piezometers considered to be in the preferential flow pathway (Figure 7). These data supported the possibility of layering (i.e., vertical anisotropy) in the subsoil. These findings also support those of previous researchers, such as Poole et al. (2002), that such preferential flow pathways may be located at specific elevations within the alluvial floodplain. However, unlike the study by Poole et al. (2002), the preferential flow pathway in this research did not correspond to topographic elements on the surface.

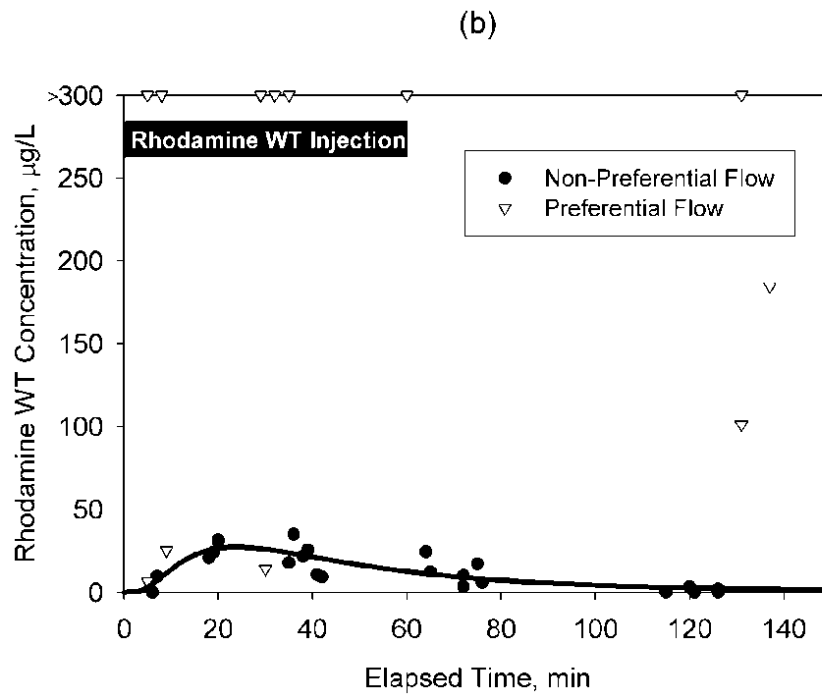
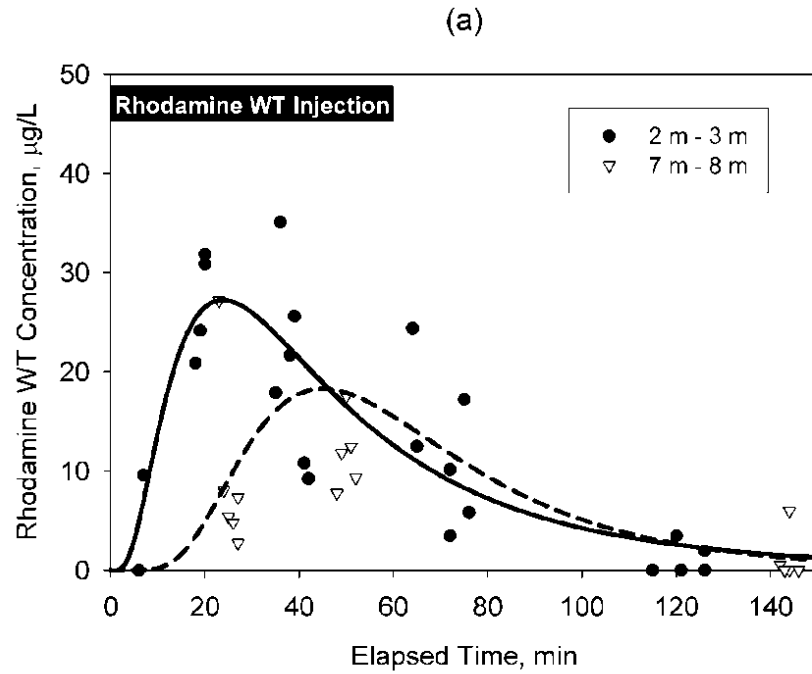


Figure 6. (a) Rhodamine WT concentrations for non-preferential flow piezometers located 2-3 m and 7-8 m from trench during experiment 1. (b) Rhodamine WT concentrations in preferential and non-preferential flow piezometers during experiment 1. Note: Concentrations greater than 300 ppb were above detection limit of field fluorometer.

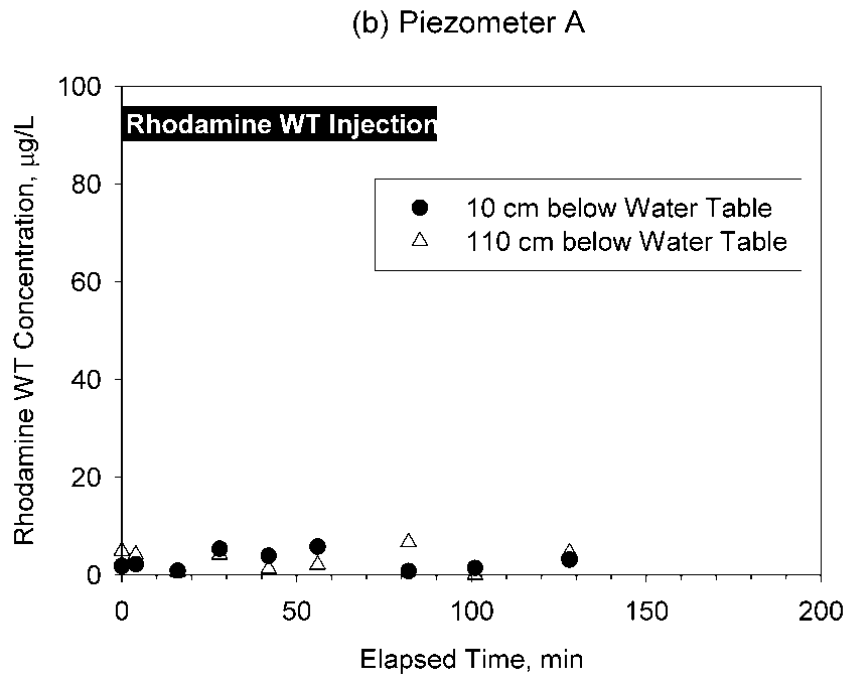
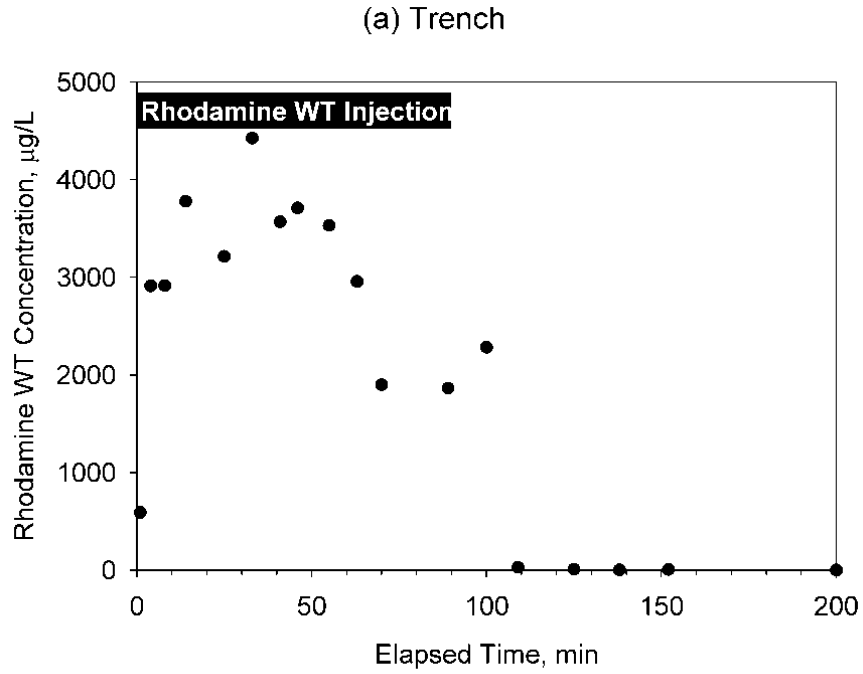
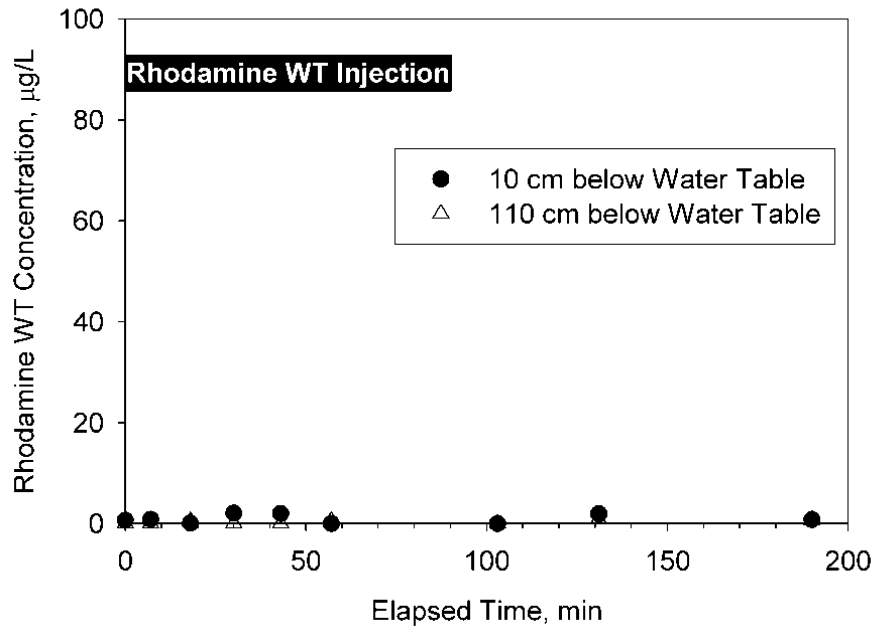


Figure 7. Rhodamine WT concentrations in trench (a) compared to non-preferential flow piezometers (b) and (c) and preferential flow piezometers (d), (e), and (f) during experiment 2.

(c) Piezometer C



(d) Piezometer D

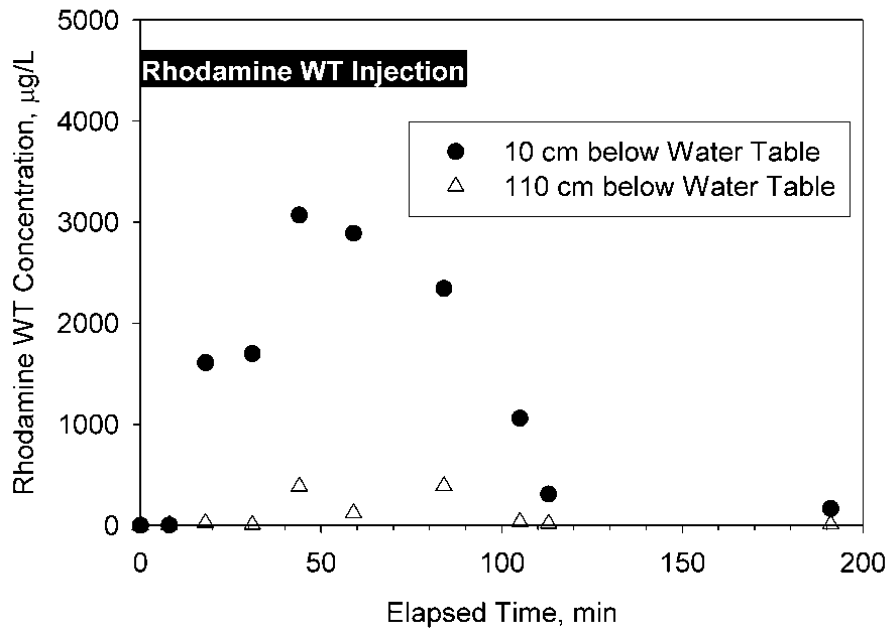
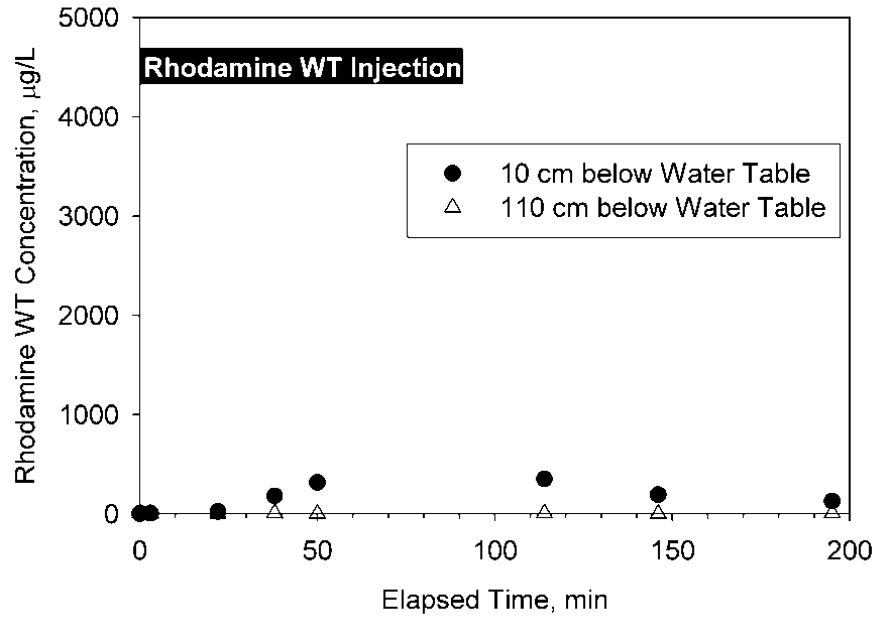


Figure 7 (Continued). Rhodamine WT concentrations in trench (a) compared to non-preferential flow piezometers (b) and (c) and preferential flow piezometers (d), (e), and (f) during experiment 2.

(e) Piezometer I



(f) Piezometer J

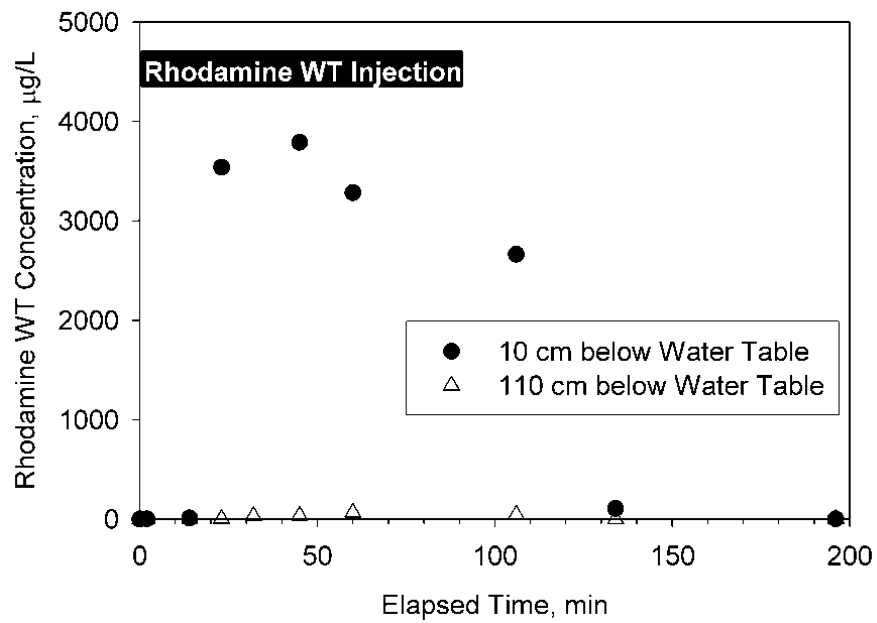


Figure 7 (Continued). Rhodamine WT concentrations in trench (a) compared to non-preferential flow piezometers (b) and (c) and preferential flow piezometers (d), (e), and (f) during experiment 2.

Prior to the injection experiments, the water levels detected in each piezometer showed minor differences (i.e., less than 1 cm). Therefore, a minimal hydraulic gradient existed which was directed towards the preferential flow pathway. However, during injection, water level readings from two of the piezometers (i.e., D and J) in the preferential flow pathway suggested that water was flowing down the side of the piezometer. This qualitative evidence again supports the hypothesis of vertical anisotropy with a confining layer or bottom of the preferential flow pathway located between 1.7 m (i.e., the elevation of the bottom of the trench at the topsoil/gravel interface) and 3.5 m (i.e., the original water table elevation).

Background dissolved P samples prior to the last injection were grouped according to the observed piezometer flow response from the Rhodamine WT experiments: (1) preferential flow piezometers versus (2) non-preferential flow piezometers. A statistically significant difference ($\alpha = 0.05$, p-value = 0.013) was noted between the background dissolved P concentration in preferential versus non-preferential flow piezometers (Figure 8). Concentrations of dissolved P in the Barren Fork Creek were approximately 1.8 times higher than those observed in the piezometers. The difference between piezometer groupings suggested potential for the preferential flow piezometers to be more directly connected to the stream channel and non-point source loads in the stream.

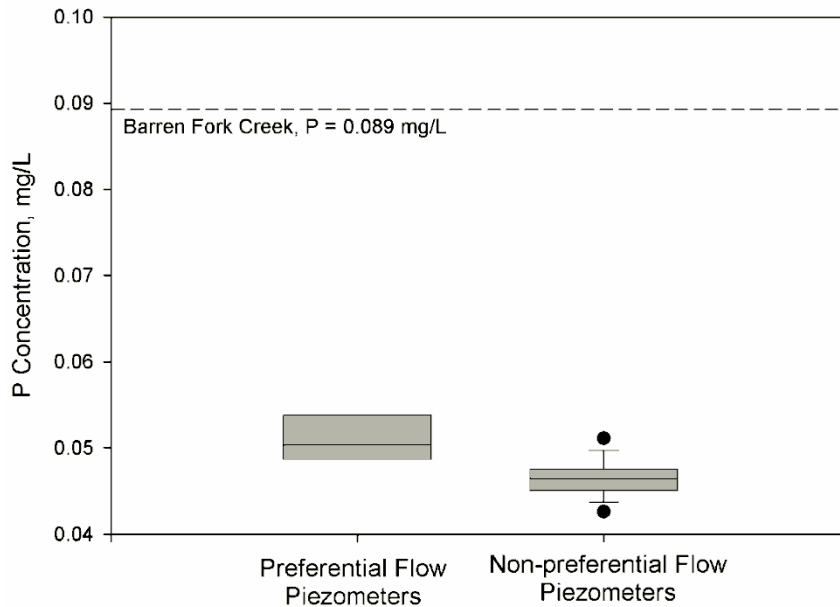


Figure 8. Box plots of background phosphorus (P) concentration in preferential flow versus non-preferential flow piezometers prior to P injection experiment (i.e., experiment 3). 25th and 75th percentiles = boundary of the box; median = line within the box; 10th and 90th percentiles = whiskers above and below the box.

In the third experiment, P was injected into the trench at a concentration of 100 mg/L, as shown in Figure 9. Similar to the Rhodamine WT injections, dissolved P concentrations in preferential flow piezometers again mimicked concentrations injected into the trench: Figures 9 (d), (e), and (f). Also, the breakthrough time of dissolved P in preferential flow piezometers was approximately equivalent to the breakthrough time of

Rhodamine WT. Dissolved P and Rhodamine WT were detected at 50% of the injected concentration approximately 20 to 30 min after injection.

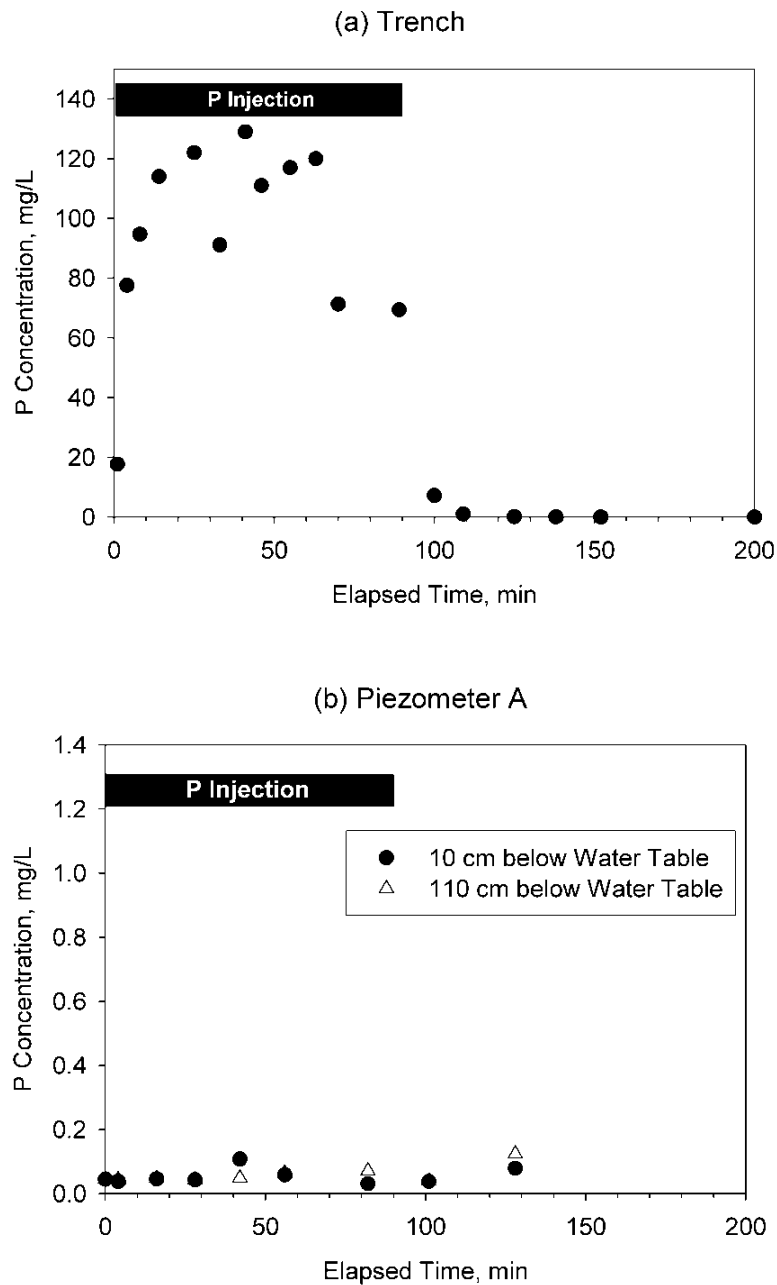


Figure 9. Phosphorus concentrations in trench (a) compared to non-preferential flow piezometers (b) and (c) and preferential flow piezometers (d), (e), and (f) during experiment 3.

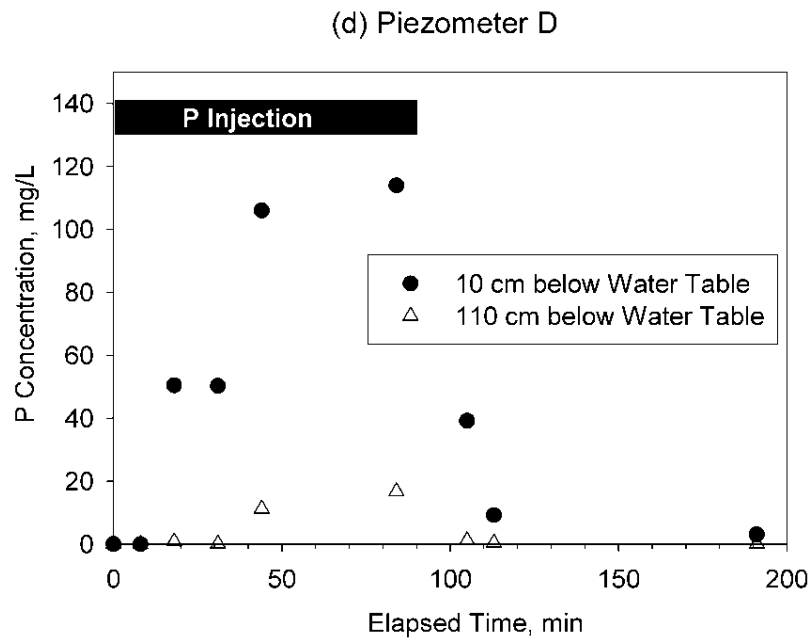
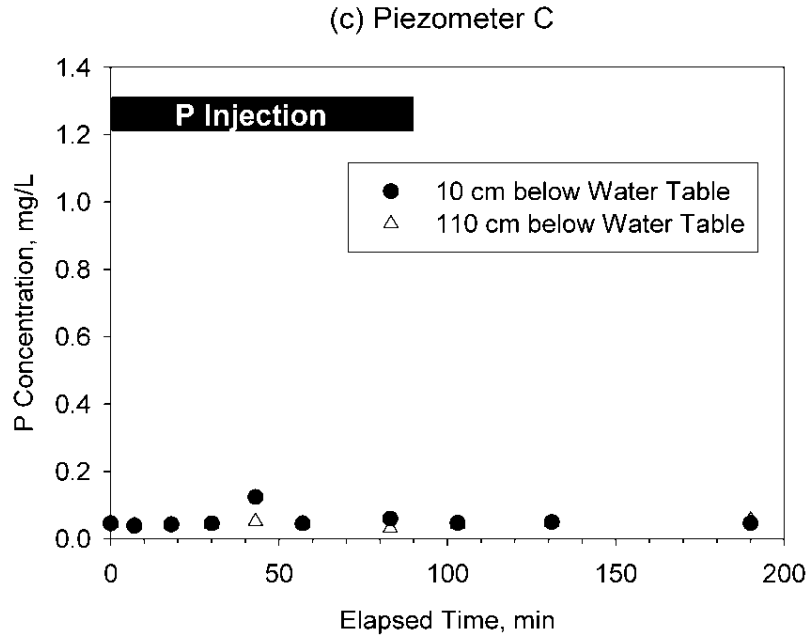
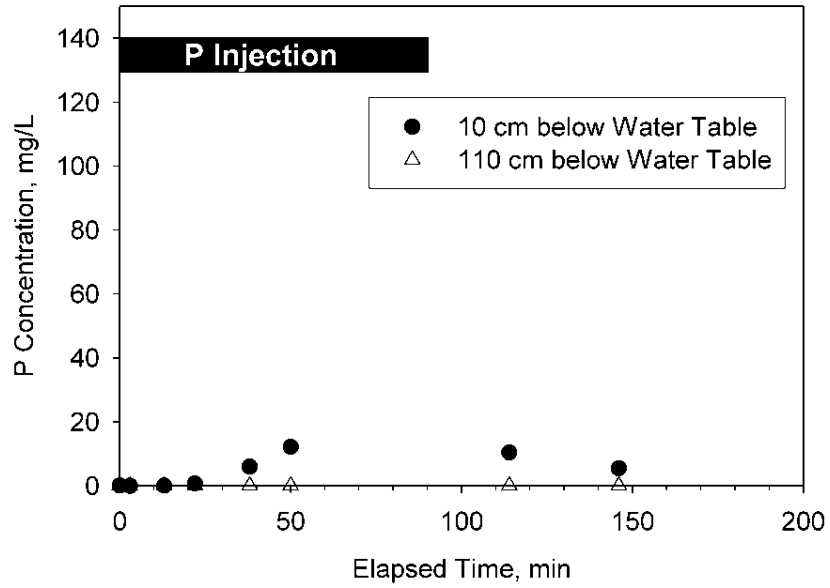


Figure 9 (Continued). Phosphorus concentrations in trench (a) compared to non-preferential flow piezometers (b) and (c) and preferential flow piezometers (d), (e), and (f) during experiment 3.

(e) Piezometer I



(f) Piezometer J

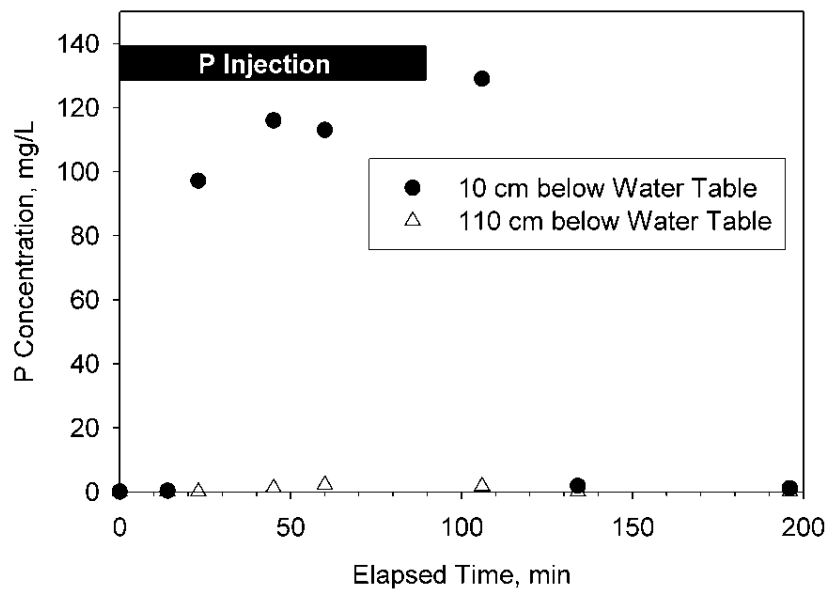


Figure 9 (Continued). Phosphorus concentrations in trench (a) compared to non-preferential flow piezometers (b) and (c) and preferential flow piezometers (d), (e), and (f) during experiment 3.

Such results suggested no enhanced transport of P with colloids. In fact, no visible colloids were observed on a 0.45- μm filter during sampling. Negligible colloids were also supported by the approximately equivalent P concentrations between the Murphy-Riley (1962) and ICP-AES methods. Had colloids been present in this system, the transport velocity of the colloids may have been equivalent to the average groundwater flow velocity in the preferential flow paths due to the fact that the colloid size would be much smaller than the soil pore size in this coarse gravel (McCarthy and Zachara, 1989; Ramaswami et al., 2005).

The long tailings shown in both the Rhodamine WT and P preferential flow piezometer data suggested that the alluvial system experienced non-equilibrium conditions. Direct comparison of Rhodamine WT and dissolved P in specific preferential flow wells indicated that P and Rhodamine WT possessed equivalent periods of detection. Both dissolved P and Rhodamine WT reached background levels at approximately 120 min in piezometers D and J, as shown in Figures 7(d), 7(f), 9(d), and 9(f), and approximately 200 min in piezometer I, as shown in Figures 7(e) and 9(e). These results signaled the presence of heterogeneities in aquifer dispersivity, a result that is not unexpected in such geomorphologically active alluvial stream systems, and/or chemical kinetics.

In non-preferential flow piezometers, dissolved P was not detected above background concentrations (i.e., 40 $\mu\text{g/L}$) even in piezometers 2 to 3 m from the trench. Rhodamine WT was detected in non-preferential flow piezometers 2 to 3 m from the trench at concentrations near 40 $\mu\text{g/L}$. This result suggested that sorption retarded the movement of P to these non-preferential flow piezometers, and that no significant sorption was observed for piezometers D and J. Two hypotheses were proposed for the lack of sorption that was suggested in piezometers considered to be in the preferential flow pathway: (1) the presence of fewer particles with significant P sorption capability and/or (2) lack of contact time between aqueous and solid phases due to the higher flow velocities. To evaluate the first hypothesis, undisturbed soil cores would be needed from the preferential flow path. However, this was difficult to obtain in the coarse gravel substrate. Therefore, this hypothesis was not evaluated. The second hypothesis was evaluated using flow-cell experiments in the laboratory.

3.3 Laboratory Flow Experiments

Both the contaminant transport and load perspectives suggested that flow velocity had an effect on the sorption capabilities of the system. Figure 10a shows the dissolved P concentrations for both velocities plotted versus dimensionless time. Concentrations detected in the outflow solution for the high velocity experiment are approximately 90% of the inflow dissolved P concentration after less than 1 min. Therefore, the breakthrough time, t_b , for the experiment is less than 1 min. The exact time at which 50% of the sample was detected is not known because the first sample (i.e., at 0.5 min) corresponded to 60% of the inflow concentration. The exponential fit to these data (Figure 10a) was used to estimate a t_b^* of 2.7, which corresponded to a t_b of 0.4 min. For the low flow experiment, the outflow concentration gradually increased with time and reached approximately 75% of the inflow concentration after 8 hours of injection. The t_b determined for the low flow experiment was approximately 155 min, which corresponded to a t_b^* of 25.4 (Figure 10a).

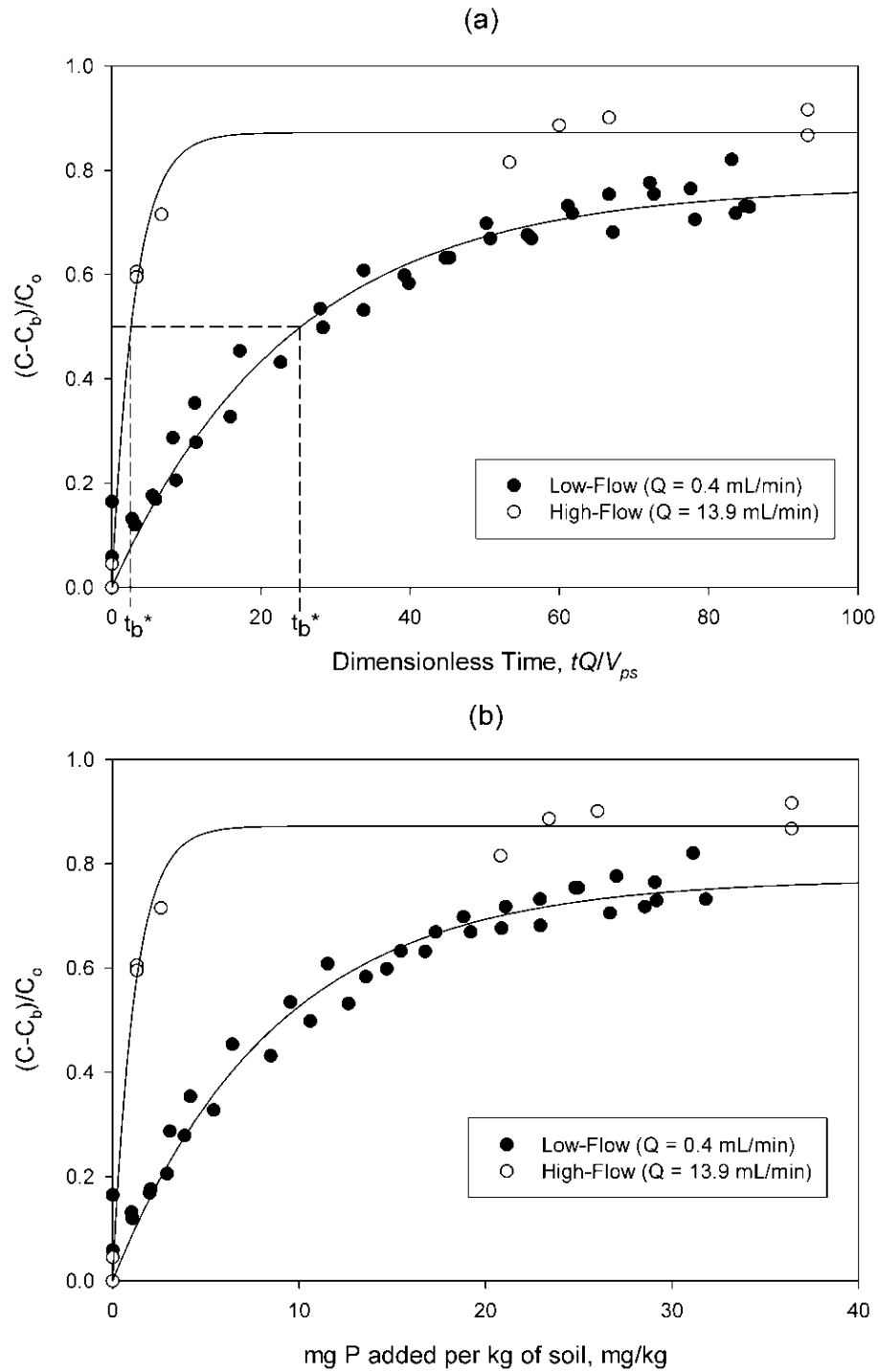


Figure 10. Phosphorus (P) concentrations detected in outflow (C) versus (a) dimensionless time and (b) mg P added per kg of soil, where Q is the flow rate, V_{ps} is the pore space volume, C_b is the background P concentration released from the soil, C_o is the inflow P concentration, and t_b^* is the dimensionless breakthrough time.

These data suggested that increased P sorption was occurring in the low flow experiment. Specifically, the velocity ratio between the high flow and low flow experiments was approximately 36 when using average flow velocities of $v_h = 46$ and $v_l = 1.3$ m/d, respectively. Compared to the ratio of the breakthrough times of approximately 390, additional P sorption was occurring during the low-flow experiment. This could likely be due to the small reaction time between the P and soil surfaces during the high-flow experiment. In previous laboratory studies, differences were observed in water soluble P extraction at two different shake times (i.e., 1 hr and 16 hr) indicating that kinetics played a significant role in desorption/adsorption. Even though there was no visible preferential flow pathways (i.e., edge flow) in the laboratory flow-cell experiments, such pathways may have existed. If pathways existed, they were consistent among three replicates at the high flow velocity.

These flow-cell data were also analyzed by comparing the total mass of P added to the dissolved P concentrations detected in the outflow, as shown in Figure 10b. Variables such as inflow P concentration, mass of P added and mass of soil sample were held constant. The only parameter changed between the two experiments was flow velocity. From Figure 10b, it is noticeable that the outflow P concentrations detected for the low flow experiment were consistently less than the concentrations obtained during the high flow experiment at the same mg of P added per kg of soil. Similar to the contaminant transport analysis, these data also suggest that more P sorption was occurring during low flow velocity experiments and that flow velocity had an effect on sorption.

This fine (i.e., less than 2.0 mm) material consists of secondary minerals with larger surface areas, such as kaolinite and non-crystalline Al and Fe oxyhydroxides, and is characterized by valence-unsatisfied edge hydroxyl groups. Due to the valency, these edge hydroxyl groups are highly active and account for the majority of P sorption in the material. Although isotherm data on the fine material showed that material had lower sorption properties than other surface soils in Oklahoma, it did suggest that the material was capable of sorbing P. Therefore, the finding that P was sorbing in the low flow experiment is reasonable.

The flow-cell experiments suggested that neither variation in fine particle distribution nor P sorption kinetics could be eliminated as factors hypothesized to contribute to the field-observed increased sorption in non-preferential pathways compared to preferential flow pathways. Most likely, a combination of both the presence of fewer fine particles (i.e. soil particles less than 2.0 mm in diameter which possess greater P sorption capability) and the lack of contact time between aqueous and solid phases due to the higher flow velocities in the preferential flow path contributed to the variability in P sorption observations. Estimates for K_d obtained from the Ogata and Banks (1961) and Hunt (1978) equations were 11 L/kg and 0.9 L/kg for the low flow and high flow experiments, respectively. It should be noted that direct comparisons of K_d between the batch and flow-cell experiments is difficult. The batch sorption and flow-cell experiments are different tests with non-similar soil to solution ratios. Furthermore, reaction products were being removed during the flow-cell experiments, but not during the batch experiment. Removal of reaction products allowed the reaction to continue to proceed more easily.

The differences in the K_d values suggested that nonequilibrium processes were occurring in the system. These processes can be divided into physical and chemical nonequilibrium. Physical non-equilibrium is the result of dissolved P moving into the

micropores between the soil particles. Because there was not a large amount of fine clay in the material, the effect of microporosity is likely negligible. Therefore, the differences in the K_d are likely due to a chemical kinetics, meaning that the amount of sorption observed varies due to the time associated with the reaction between dissolved P and the soil surfaces. If one was attempting to derive parameters for a predictive model as opposed to simply demonstrating the presence and influence of chemical kinetics, a non-equilibrium model, such as those discussed by Pang and Close (1999) and McGechan and Lewis (2000), would be more appropriate for analyzing the column data than the equilibrium model used in this research.

4.4 Research Implications

This research demonstrated that preferential flow pathways can occur even in non-structured, coarse gravel substrates and demonstrated that the heterogeneity in the riparian floodplain subsoil can promote significant subsurface nutrient transport. This research directly confirmed previous research findings by Carlyle and Hill (2001) and McCarty and Angier (2001). Preferential flow pathways may create direct hydraulic connections between nonpoint source loads in the stream and the alluvial gravel subsoil. These direct connections could lead to a transient storage mechanism, where nutrient loads concurrent with large storm events could potentially migrate from the stream into the adjacent floodplain, contaminating the alluvial storage zone. Second, a direct connection may exist between upland sources of P and the streams such that a significant nonpoint source load may not be currently considered in analyzing for the impact of P application and management on such landscapes. Future research should be aimed at quantifying the preferential flow path length, where this research only identified relatively short flow paths (i.e., 2 to 3 m), and likelihood of connectivity with the stream. Tools which may prove effective at quantifying such characteristics include geophysical techniques such as electrical resistivity imaging (Sima et al., 2008).

This research has wide reaching implications for how riparian floodplains are managed. Millions of dollars are spent each year to mitigate surface runoff and sediment and nutrient loads. Although these management plans can be effective, this research has shown that subsurface P transport could also be a contributing factor in certain conditions. Because the nutrient load studied here was input directly into the subsurface, the overall subsurface load contribution could not be quantified. The next step is determining if similar conditions like this are common and if a direct connection exists between nutrient sources on the surface and the conductive subsurface material.

IV. CONCLUSIONS AND FUTURE WORK

This research demonstrated that subsurface movement of P can be an important transport mechanism, especially in areas such as riparian floodplains with hydraulic conditions conducive to the rapid transport of P. The movement of water and contaminants in riparian floodplains, even those classified as non-structured, coarse gravel, is not homogeneous and can be impacted by the presence of preferential flow pathways. In the presence of preferential flow paths, P could be transported through alluvial groundwater without any reduction in its concentration. In contrast, in the absence of preferential flow paths, P transport was hindered.

Minimal sorption of P to subsoil material in the preferential flow pathways occurred because of two hypothesized factors: (1) the presence of fewer fine particles (i.e. soil particles less than 2.0 mm in diameter) and (2) lack of contact time between aqueous and solid phases due to the higher flow velocities. Laboratory flow experiments suggested that higher velocity of flow through the subsoil resulted in less P sorption. These findings suggested that high concentrations of dissolved P (i.e., concentrations mimicking the injected concentration) detected in the piezometers located in the preferential flow pathway were a result of the greater flow velocity. The velocity, in turn, likely led to a smaller reaction time between the dissolved P and soil surfaces, prohibiting measurable sorption. The lack of dissolved P above background concentrations in piezometers outside of the preferential flow pathway may have been a result of the P solution moving much slower through the subsoil and therefore sorbing to the fine material.

Because of the quantity of data generated during the field tracer studies, future research is underway to better understand the water quality changes in the alluvial ground water during the injection experiments. Future work is also aimed at investigating the preferential flow pathways in more detail. Electrical resistivity mapping will be used at the field site to attempt to identify and map the preferential flow pathways.

V. ACKNOWLEDGEMENTS

This material is based upon work supported by a FY 2007 Oklahoma Water Resources Research Institute and the Oklahoma Water Resources Board grant. The co-PIs acknowledge Dan Butler of the Oklahoma Conservation Commission for providing access to the riparian floodplain property along the Barren Fork Creek. The co-PIs also acknowledge the assistance of Drs. Alex Simms and Todd Halihan, Geology Department, Oklahoma State University.

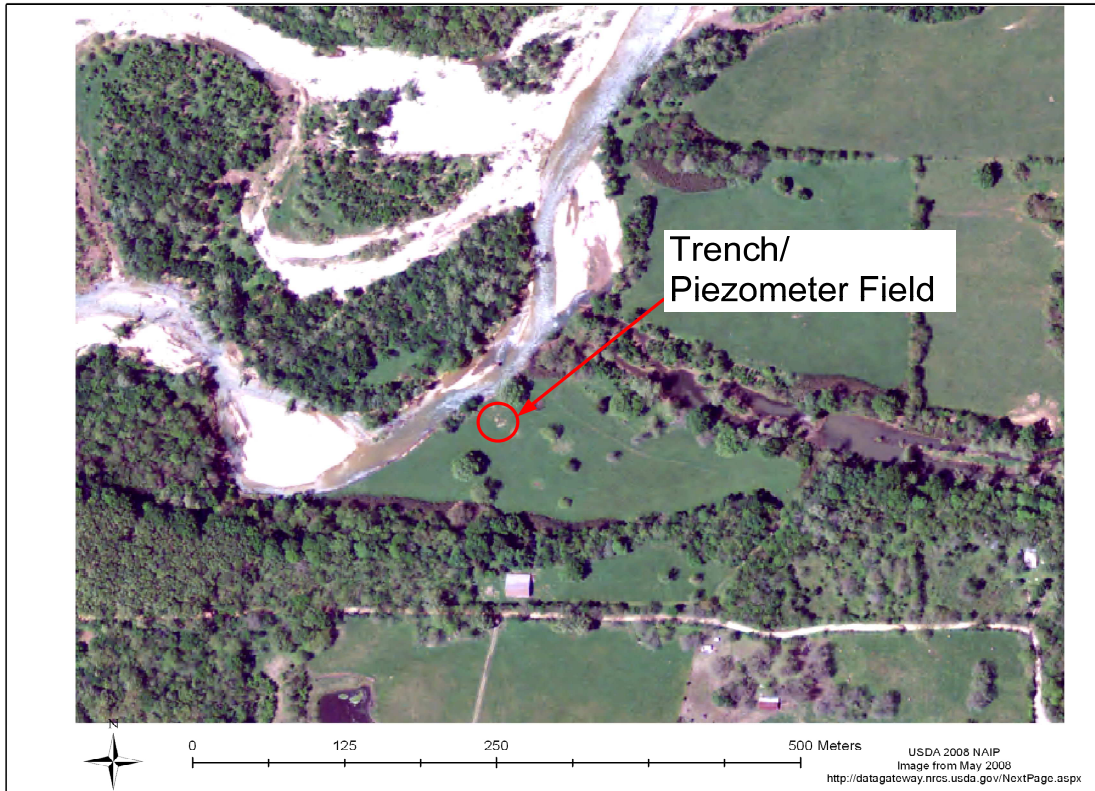
VI. REFERENCES

- Alyamani, M.S., and Z. Sen. 1993. Determination of hydraulic conductivity from complete grain-size distribution curves. *Ground Water* 31(4):551-555.
- Andersen, H.E., and B. Kronvang. 2006. Modifying and evaluating a P index for Denmark. *Water Air and Soil Poll.* 174(1-4): 341-353.
- Beauchemin, S., and R.R. Simard. 1999. Soil phosphorus saturation degree: Review of some indices and their suitability for P management in Quebec, Canada. *Can. J. Soil Sci.* 79: 615-625.
- Carlyle, G.C., and A.R. Hill. 2001. Groundwater phosphate dynamics in a river riparian zone: Effects of hydrologic flow paths, lithology, and redox chemistry. *J. Hydrol.* 247: 151-168.
- Cooper, A.B., C.M. Smith, and M.J. Smith. 1995. Effects of riparian set-aside on soil characteristics in an agricultural landscape: Implications for nutrient transport and retention. *Agr. Ecosyst. Environ.* 55: 61-67.
- Daniel, T.C., A.N. Sharpley, and J.L. Lemunyon. 1998. Agricultural phosphorus and eutrophication: A symposium overview. *J. Environ. Qual.* 27:251-257.
- de Jonge, L.W., C. Kjaergaard, and P. Moldrup. 2004. Colloids and Colloid-Facilitated Transport of Contaminants in Soils: An Introduction. *Vadose Zone J.* 3: 321-325.
- DeSutter, T.M., G.M. Pierzynski, and L.R. Baker. 2006. Flow through and batch methods

- for determining calcium-magnesium and magnesium-calcium selectivity. *Soil Sci. Soc. Am. J.* 70:550-554.
- Fox, G.A. 2004. Evaluation of a stream aquifer analysis test using analytical solutions and field data. *J. Am. Water Resour. As. (JAWRA)* 40(3): 755-763.
- Fuchs, J.W. 2008. Subsurface Transport of Phosphorus in Riparian Floodplains: Tracer and Phosphorus Transport Experiments. M.S. Thesis. Oklahoma State University, Stillwater.
- Fuhrman, J.K., 1998. Phosphorus sorption and desorption characteristics of Oklahoma soils. M.S. Thesis. Oklahoma State University, Stillwater.
- Heathwaite, L., P. Haygarth, R. Matthews, N. Preedy, and P. Butler. 2005. Evaluating colloidal phosphorus delivery to surface waters from diffuse agricultural sources. *J. Environ. Qual.* 34 (1): 287-298.
- Hively, W.D., P. Gerard-Marchant, and T.S. Steenhuis. 2006. Distributed hydrological modeling of total dissolved phosphorus transport in an agricultural landscape II. Dissolved phosphorus transport. *Hydrol. Earth Syst. Sc.* 10(2): 263-276.
- Hunt, B. 1978. Dispersive sources in uniform ground-water flow. *J. Hydraul. Eng.-ASCE* 104(HY1): 75-85.
- Ilg, K., and M. Kaupenjohann. 2005. Colloidal and dissolved phosphorus in sandy soils as affected by phosphorus saturation. *J. Environ. Qual.* 34: 926-935.
- Iyengar, S.S., L.W. Zelazny, and D.C. Martens. 1981. Effect of photolytic oxalate treatments on soil hydroxyl interlayered vermiculites. *Clay. Clay. Miner.* 29: 429-434.
- Kleinman, P.J.A., B.A. Needelman, A.N. Sharpley, and R.W. McDowell. 2004. Using soil phosphorus profile data to assess phosphorus leaching potential in manured soils. *Soil Sci. Soc. Am. J.* 67 (1): 215-224.
- Landon, M.K., D.L. Rus, and F.E. Harvey. 2001. Comparison of instream methods for measuring hydraulic conductivity in sandy streambeds. *Ground Water* 39(6): 870-885.
- McCarthy, J., and J. Zachara. 1989. Subsurface transport of contaminants. *Environ. Sci. Technol.* 23(5): 496-502.
- McCarty, G., and J. Angier. 2001. Impact of preferential flow pathways on ability of riparian wetlands to mitigate agricultural pollution. p. 53-56. In D. Bosch and K. King (ed.) Proc. 2nd Int. Symp. Preferential Flow: Water Movement and Chemical Transport in the Environment, Honolulu, HI. 3-5 Jan. 2001. American Society of Agricultural Engineers, St. Joseph, MI.
- McGechan, M.B., and D.R. Lewis. 2002. Sorption of phosphorus by soil: I. Principles, equations and models. *Biosyst. Eng.* 82(1): 1-24.
- McKeague, J., and J.H. Day. 1966. Dithionite and oxalate-extractable Fe and Al as aids in differentiating various classes of soils. *Can. J. Soil Sci.* 46: 13-22.
- Murphy, J., and J.R. Riley. 1962. A modified single solution method for the determination of phosphate in natural waters. *Anal. Chim. Acta* 27: 31-36.
- Nelson, N.O., J.E. Parsons, and R.L. Mikkelsen. 2005. Field-scale evaluation of phosphorus leaching in acid sandy soils receiving swine waste. *J. Environ. Qual.* 34(6): 2024-2035.

- Ogata, A., and R.B. Banks. 1961. A solution of the differential equation of longitudinal dispersion in porous media. U.S. Geological Survey Prof. Paper 411-A.
- Osborne, L.L., and D.A. Kovacic. 1993. Riparian vegetated buffer strips in water-quality restoration and stream management. *Freshwater Biol.* 29(2): 243-258.
- Owens, L.B., and M.J. Shipitalo. 2006. Surface and subsurface phosphorus losses from fertilized pasture systems in Ohio. *J. Environ. Qual.* 35: 1101-1109.
- Pang, L., and M.E. Close. 1999. Field-scale physical nonequilibrium transport in an alluvial gravel aquifer. *J. Contam. Hydrol.* 38(4): 447-464.
- Polyakov, V., A. Fares, and M. H. Ryder. 2005. Precision riparian buffers for the control of nonpoint source pollutant loading into surface water: A review. *Environ. Rev.* 13: 129-144.
- Poole, G.C., J.A. Stanford, C.A. Frissell, and S.W. Running. 2002. Three-dimensional mapping of geomorphic controls on flood-plain hydrology and connectivity from aerial photos. *Geomorphology* 48: 329-347.
- Pote, D.H., T.C. Daniel, A.N. Sharpley, P.A. Moore, Jr., D.R. Edwards, and D.J. Nichols. 1996. Relating extractable soil phosphorus to phosphorus losses in runoff. *Soil Sci. Soc. Am. J.* 60: 855-859.
- Ramaswami, A., J.B. Milford, and M.J. Small. 2005. Chapter 9: Models of transport in individual media: Soil and groundwater. P. 315-377. In A. Ramaswami et al. (ed.) *Integrated Environmental Modeling: Pollutant Transport, Fate, and Risk in the Environment*, John Wiley & Sons, Inc., New Jersey.
- Sauer, T.J., and S.D. Logsdon. 2002. Hydraulic and physical properties of stony soils in a small watershed. *Soil Sci. Soc. Am. J.* 66:1947-1956.
- Sima, A., T. Halihan, K. Thompson, G. Fox, and D. Storm. 2008. Transient electrical resistivity imaging of a Phosphorus/Rhodamine WT tracer test, Tahlequah, OK. Geological Society of America (GSA) South-Central Section Meeting, Hot Springs, Arkansas, 30 March-1 April.
- Turner, B.L., and P.M. Haygarth. 2000. Phosphorus forms and concentrations in leachate under four grassland soil types. *Soil Sci. Soc. Am. J.* 64 (3): 1090-1099.
- Vanek, V. 1993. Transport of groundwater-borne phosphorus to Lake Bysjon, South Sweden. *Hydrobiologia* 251(1-3): 211-216.
- Wentworth, C.K. 1922. A scale of grade and class terms for classic sediments. *J. Geol.* 30: 377-392.

APPENDIX. AERIAL PHOTO OF FIELD SITE ALONG BARREN FORK CREEK



Determination of Fracture Density in the Arbuckle-Simpson Aquifer from Ground Penetrating Radar (GPR) and Resistivity Data

Basic Information

Title:	Determination of Fracture Density in the Arbuckle-Simpson Aquifer from Ground Penetrating Radar (GPR) and Resistivity Data
Project Number:	2007OK80B
Start Date:	3/1/2007
End Date:	8/15/2008
Funding Source:	104B
Congressional District:	3 & 4
Research Category:	Ground-water Flow and Transport
Focus Category:	Water Supply, Hydrology, Models
Descriptors:	Fractures, GPR, resistivity
Principal Investigators:	Ibrahim Cemen, Todd Halihan, Roger Young

Publication

FINAL TECHNICAL REPORT

OWRRI PROJECT
DETERMINATION OF FRACTURE
DENSITY IN THE ARBUCKLE-SIMPSON
AQUIFER FROM GROUND PENETRATING
RADAR (GPR) AND RESISTIVITY DATA

AUGUST 2008

Prepared for:

Oklahoma Water Resources Research Institute
003 Life Sciences East, OSU
Stillwater, Oklahoma 74078-3011

Prepared by:

Ibrahim Cemen
OSU School of Geology
105 Noble Research Ctr
Stillwater, OK 74078

Roger Young
University of Oklahoma
School of Geology and
Geophysics
100 East Boyd St. Ste 810
Norman, OK 73019

Todd Halihan
OSU School of Geology
105 Noble Research Ctr
Stillwater, OK 74078

Table of Contents

Report

Appendices

Appendix A	Data processing flow---A-S Ranch
Appendix B	Coherent noise reduction---A-S Ranch
Appendix C	Velocity determination----A-S Ranch
Appendix D	Data processing flow---Devil's Den
Appendix E	Coherent noise reduction---Devil's Den
Appendix F	Velocity determination----Devil's Den

1.0 Introduction

The ground water resources of Oklahoma are vital to the economic well being of the state. In order to properly manage these resources, an understanding of the discharge and recharge of aquifers is necessary. Fractures in aquifer rocks affect the flow of water. Therefore, numerical modeling of the fluid flow requires an understanding of the geometry and density of fractures that have a great influence on the discharge and recharge mechanisms.

1.1 Project Objective

The Arbuckle-Simpson aquifer of southern Oklahoma is a major source of drinking water for communities in the south-central part of the state. In outcrops, the carbonate units of the Arbuckle-Simpson are highly fractured. The basement rocks underlying the Arbuckle-Simpson aquifer are also highly fractured in outcrop. However, the orientation and density of fractures are different in the basement than the Arbuckle-Simpson aquifer. For example, the granites exposed in the Devil's Den area near Tishomingo, Oklahoma exhibit extensive fracturing and faulting. The carbonates of the Arbuckle-Simpson aquifer in the Spear's ranch contain only fractures. Moreover, fracture densities are very different within the two areas. The characterization of fractures in the basement is also important for ground water modeling work currently underway at both the Oklahoma Water Resources Board (OWRB) and the United States Geological Survey (USGS). Therefore, mapping fracture density from geophysical data such as Ground Penetrating Radar (GPR), Electrical Resistivity Imaging (ERI), and seismic data would provide timely information for these modeling studies. When tied to outcrop fracture data, significant information can be obtained regarding the fracture properties of these formations.

1.2 Application of GPR Techniques in Fractured Rock Environments

Characterization of fracture systems in competent rocks by the GPR method is effective in evaporates and in crystalline basement rocks. Young and Ramirez (2007) show that electromagnetic ray paths that cross fractures in evaporates at different angles of incidence will travel at different velocities and this, then, gives a means of determining fracture orientation. Holloway et al. (1992) used both surface and borehole GPR to examine Precambrian granite of the Canadian Shield in order to rank sites for subsurface radioactive waste disposal in Manitoba. They found a correlation between reflections and large aperture, open fractures on the one hand and between reflection swarms and multiple small fractures on the other.

GPR wavefields penetrate to depths of several tens of meters in carbonates and granites but where there is attenuation due to higher conductivity lithologies, such as a soil mantle or heavily weathered epikarst, detection of geological targets is restricted to shallower depths. Lower frequency antennas maximize the depth of investigation, but at the same time, diminish resolution. Our antenna choice in the surveys of this project was 100 MHz unshielded antennas.

Processing flow

The first processing step increases the signal strength during recording. GPR waves travel at a large fraction of the speed of light and therefore take very little time to travel from the transmitter to the receiver. This permits vertical stacking of the GPR traces in real time, that is, the superposition of up to 1024 traces at each location during the survey thereby increasing the signal/noise ratio considerably.

Processing of raw GPR data is necessary to remove noise further and to enhance signal by restoring signal strength lost to spherical spreading and frequency-dependent attenuation (spherical and exponential correction). Artifacts of the recording process must also be removed (dewow). Unlike a seismic survey, the time at which the GPR trace begins is not the instant the transmitter fires. Removing this delay is termed time-zero correction. Finally, bandpass filtering also helps separate signal from noise.

Although stacking decreases *random* noise, spurious reflections and diffractions from metal objects clutter up the desired image of the subsurface. Due to the high dielectric contrast between air or soil and metal, these unwanted signals are often much stronger than the reflections from geological boundaries—stratigraphic and structural—being sought. Because such objects are time invariant, stacking is ineffective.

Coherent noise reduction

Young and Sun (1999) devised an effective method for removing locally recognized, coherent noise from a GPR section and named this process *the domain filter*. It has proven very effective in removing coherent noise events. The principle coherent noise at the A-S Ranch is due to a buried pipe. At both the A-S Ranch and Devil's Den very shallow stratigraphy and fractures, respectively, are obscured by a noise mode traveling directly through the air from transmitter to receiver. We remove both the pipe response and the air wave using the domain filter.

Velocity analysis

Velocities characterize lithology thereby helping to identify a geologic unit traversed by a GPR wave. Velocity is also important to convert recorded two-way reflection travel times to depth. Velocity can be determined by using the method of velocity semblance developed for seismic reflection analysis. Velocity can also be found by constructing the linear traveltimes curve, $T(X)$, for the wave traveling at the earth's surface directly through the ground from a source location to a receiver location.

1.3 Application of ERI techniques in fractured rock environments

Fractured and karstic aquifers have been described for many years, but few field techniques to adequately characterize these complex aquifers exist. Much of our understanding of the flow in these aquifers has been generated from field experiments using wells or outcrops. The lack of characterization data generally comes from the cost involved in drilling, completing, maintaining and sampling wells. This cost is higher in fracture and karstic aquifers due to the higher drilling costs and the heterogeneous flow fields typically require more data than are available from discrete sampling techniques which provide only limited 2- or 3-dimensional data.

To resolve these difficulties, data are required that allow areas or volumes of the subsurface to be examined, instead of solely relying on discrete sampling data. Most importantly, methods employed need to be economical when compared to alternative techniques.

Existing methods of characterizing these aquifers have relied on two detection and monitoring strategies. The first strategy involves discrete point sampling of fluids using wells, springs or multilevel piezometers whose data is integrated and interpreted. The second strategy uses indirect measurements through surface or borehole geophysical techniques.

The difficulty with point sampling techniques is that sufficient sampling can be expensive because of drilling costs, sampling time, sample analysis and data integration and interpretation time. Additionally, determining whether fractures or karst features exist between sampling locations using piezometers can be difficult to impossible to determine. This point sampling method can miss conduits not sampled by wells, or barriers to flow like vertical faults that are not sampled with a traditional piezometer monitoring grid.

A solution to some of these sampling problems in the vadose and phreatic zones is the utilization of electrical resistivity imaging (ERI) to provide more complete site data coverage. A temporary surface system for site evaluation can be used as an evaluation of a 2-D or 3-D portion of subsurface or cable can be installed in boreholes to image to deeper depths with higher resolution. Cables can be permanently installed in shallow trenches or in boreholes for long-term monitoring applications.

Electrical resistivity measurements have been used since the 1830's to interpret the geology of the earth (Van Nostrand and Cook, 1966). The technique introduces current into the ground and the potential field is measured. ERT (Electrical Resistance Tomography) is a method of obtaining resistivity measurements that determines the electrical conductivity of the ground using subsurface electrodes (Daily et al., 2004). In contrast, a multielectrode array uses electrodes only on the surface. Electrical Resistivity Imaging (ERI) is a general term used to indicate that a high resolution electrical resistivity technique is being used without naming each electrode configuration differently.

An electrical resistivity image is an inverted model of hundreds to thousands of four electrode resistivity measurements. A single electrical measurement does not yield significant information, similar to a single pixel on a digital photo. However, hundreds of measurements of a site can produce a 2-D or 3-D electrical image of the subsurface.

This technique is occasionally used for site characterization, but it can be inefficient, expensive, or worse, ambiguous (Ramirez et al., 1993).

In general, flow features (such as faults that conduct fluids) and higher porosity lithologies are indicated by low resistivity anomalies. Additionally, the hydraulic parameters of the formation may be estimated using electrical methods (Purvance and Andricevic, 2000a, b). The electrical data produced from this type of study may help characterize heterogeneity, fractures, and aquifer parameters (Herwanger et al., 2004; Niwas and de Lima, 2003).

2.0 Site Description

Two sites were evaluated as part of this study. They include the Arbuckle Simpson Ranch west of Connerville, OK and the Devil's Den site south of Reagan, OK. The first site is Arbuckle-Simpson Ranch in southern Oklahoma. Dolomite of the Lower Arbuckle Group in this area is extensively fractured in outcrops in this area. The second site is in the Devil's Den area of Tishomingo, Oklahoma where Precambrian age granite is exposed at the surface. These granites are about 1.35 to 1.4 billion years old and form much of the basement rocks of southern Oklahoma (Suneson, 1997). The granite is highly fractured in places and is an excellent site for our work because of the absence of conductive overburden which limits the depth of penetration of GPR signal and electrical current. The granitic environment does present a challenge for drilling holes to plant electrodes in the ground for electrical resistivity work.

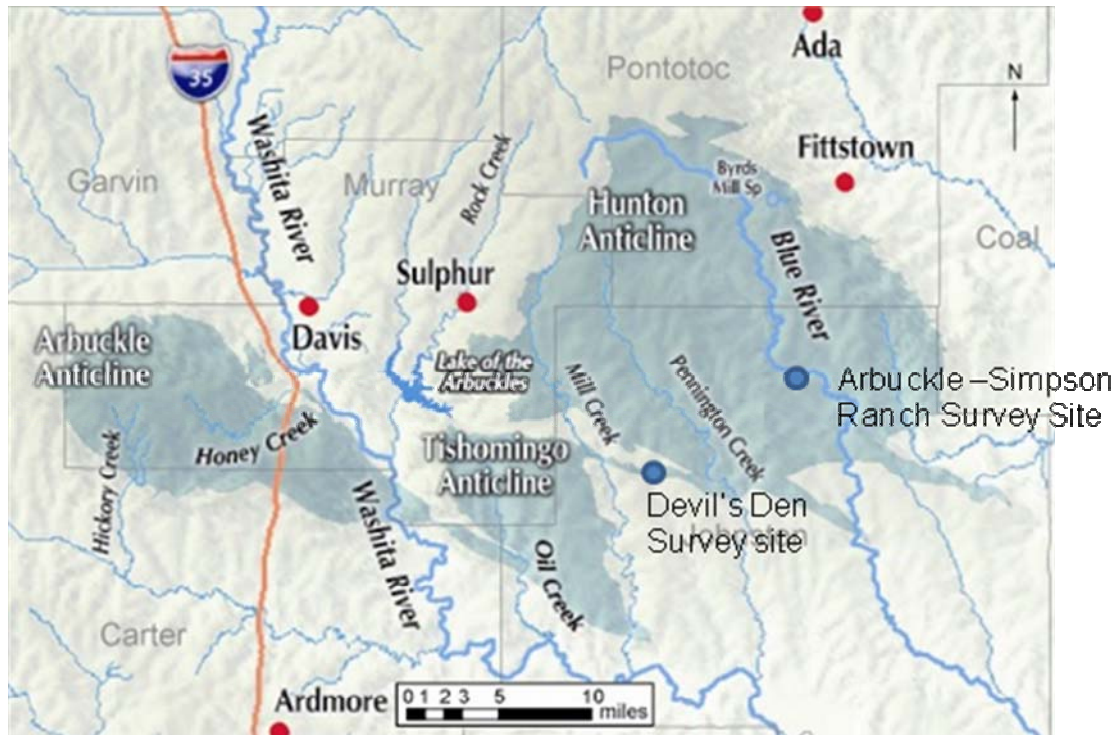


Figure 1: Map showing the locations of the Arbuckle-Simpson and Devil's Den sites surveyed during this investigation

3.0 GPR Data

3.1 GPR Data Collection

Description of pulseEKKO Pro 100 GPR system

Ground Penetrating Radar (GPR) measurements consist of recordings of an electromagnetic wave directed into the earth at a transmitter antenna and recorded at a receiver antenna. The downgoing wave is reflected from boundaries at which there is a change in dielectric permittivity. As with seismic waves, the greater the difference in permittivity across the boundary, the larger is the reflection coefficient and the stronger is the reflection recorded by the receiver antenna. Attenuation proportional to distance traveled (spherical spreading) and conversion of wave energy into heat (absorption) both diminish recorded reflection amplitudes. High electrical conductivity is the physical property most responsible for attenuation, and it is most often high conductivity that limits the depth to which GPR can see geological boundaries.

An EKKO Pro 100 system of Sensors and Software, Inc., recorded all GPR data acquired in the present project. Table 1 shows the survey and recording parameters for both sites at which data was acquired.

Arbuckle Simpson Ranch Survey

Line Name	Transmitter Voltage (Volts)	Source-Receiver Separation (m)	Station Spacing (m)	Record Length (ns)	Sample Interval (ns)	Vertical Stack Fold	Nominal Frequency (Hz)
GPR 1	400	1	0.5	200	0.8	64	100
GPR 2	400	1	0.5	200	0.8	64	100

Table 1a Survey and recording parameters at the A-S Ranch

Devil's Den Survey

Line Name	Transmitter Voltage (Volts)	Source-Receiver Separation (m)	Station Spacing (m)	Record Length (ns)	Sample Interval (ns)	Vertical Stack Fold	Nominal Frequency (Hz)
Line 1	400	1	0.5	200	0.8	64	100
Line 2	400	1	0.5	200	0.8	64	100
Line 3	400	1	0.5	200	0.8	64	100
Line 4	400	1	0.5	200	0.8	64	100
Line 5	400	1	0.5	200	0.8	64	100
Line 6	400	1	0.5	200	0.8	64	100
Line 7	400	1	0.5	200	0.8	64	100
Line 8	400	1	0.5	200	0.8	64	100
Line 9	400	1	0.5	200	0.8	64	100
Line 10	400	1	0.5	200	0.8	64	100
Line 11	400	1	0.5	200	0.8	64	100
Line 12	400	1	0.5	200	0.8	64	100
Line 13	400	1	0.5	200	0.8	64	100
Line 14	400	1	0.5	200	0.8	64	100
Line 15	400	1	0.5	200	0.8	64	100
Line 16	400	1	0.5	200	0.8	64	100
Line 17	400	1	0.5	200	0.8	64	100
Line 18	400	1	0.5	200	0.8	64	100
Line 19	400	1	0.5	200	0.8	64	100
Line 20	400	1	0.5	200	0.8	64	100
Line 21	400	1	0.5	200	0.8	64	100
Line 22	400	1	0.5	200	0.8	64	100
Line 23	400	1	0.5	200	0.8	64	100
Line 24	400	1	0.5	200	0.8	64	100
Line 25	400	1	0.5	200	0.8	64	100

Table 1b Survey and recording parameters at the Devil's Den

Survey sites

The present project recorded coincident GPR and ERI data at two geologically distinct locations, the Arbuckle-Simpson Ranch and Devil's Den (Figure 1). The A-S Ranch is on the south side of the Hunton Anticline. Here the geology is characterized by a relatively thick soil mantle overlying epikarst of the Arbuckle-Simpson Group. The GPR targets were the sub-horizontal boundaries between soil mantle and epikarst as well as the base of the epikarst seen in the resistivity profiles from the ERI surveys. In addition, we sought

to compare the ability of GPR to locate a sub-vertical boundary, namely, a fault detected by the ERI surveys of Halihan and coworkers and originally mapped by Ham (1964).

The Devil's Den area near Tishomingo, OK, lies south of the Hunton Anticline and is stratigraphically beneath the Arbuckle-Simpson Group(Figure 1). It consists of Precambrian granitic basement, which is highly faulted and fractured. The geological target at Devil's Den is the fractures as no lithologic layering is expected within the basement. Vertical fractures, on the other hand, can be seen clearly on the surface of the large outcrop over which we conducted the GPR measurements. We planned to assess the fracture density within the epikarst by GPR measurements and compare this to mapped fracture patterns obtained by Cemen (2008, personal communication) and co-workers.

3.2 GPR Data Reduction

The Arbuckle-Simpson Ranch 2D profiles

Our acquisition strategy at the A-S Ranch was to reoccupy the ERI lines surveyed by Halihan and students and to use GPR to image the same cross-sections of the subsurface in order to achieve a comparison between the two geophysical methods. This would establish whether the information from ERI and GPR is complementary in delineating horizontal contrasts in stratigraphy and in locating vertical discontinuities. **Figure Y1** shows the line locations of all ERI and GPR profiles acquired at the A-S Ranch.

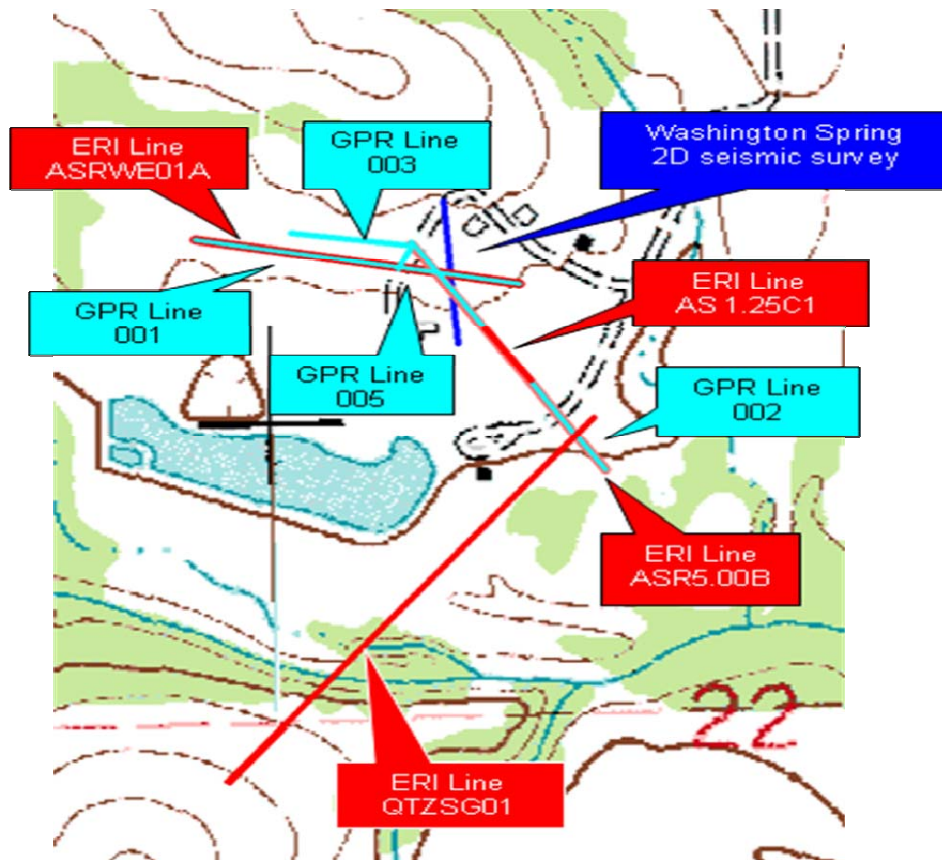


Figure 2: Map of all geophysical survey lines at the A-S Ranch

Processing flow

Processing of the A-S Ranch profiles is illustrated in Appendix A by a diagram showing how a segment of GPR Line 2 is changed by the different stages of processing. The final stage of processing (Figure A1e) shows that a 30 m long basinal feature exists at a time of 50-75 ns beneath the western half of the data segment. However, a coherent, westward dipping noise event still exists in the data (Figure A1e).

Another measure of success at noise reduction in processing is shown in Figure A2. After bandpass filtering, the frequency range in which signal occurs stands out more strongly from the frequency range of the noise.

Methods of coherent noise reduction

Appendix B shows the application of the domain filter to remove the dipping, non-geologic event left after processing (Figure B1a). This event is interpreted to be noise, possibly due to a reflection from a buried pipe. Before processing (Figure B1a), the

event overprints reflections of geologic significance. By transforming the selected event to the FK domain (Figure B2a), transforming it back to the X-T domain (Figure B2b) and subtracting it from the original data, the dipping event is removed. Figure B3 shows that after subtraction, a stratigraphic sag is now apparent.

Methods of velocity analysis

Auxiliary GPR surveys consisting of CMP gathers of traces were collected at the A-S Ranch in order to perform velocity semblance analysis. Two of these velocity analyses along GPR Line 2 are shown in Appendix C. Results for 8 CMP locations are shown in Table Y2. The average RMS velocity corresponding to a time of approximately 50 ns is .16 m/ns. Because most of the reflection raypath is in the uppermost epikarst-- and not in the much slower soil mantle-- this velocity for a carbonate rock should be consistent with the generally cited value of .12 m/ns (Annan, 2005). Our result is appreciably higher, but the difference may be that the Annan figure is for carbonates with appreciable porosity. The corresponding depth to the reflecting boundary within the epikarst is approximately 3.7 m. Figure C2 is a plot of the direct ground wave traveling through the soil mantle. The average velocity from two CMP gathers is approximately .05 m/ns

CMP Location	Time (ns)	Velocity (m/ns)
1	58	0.16
2	47	0.16
3	60	0.17
4	N/A	N/A
5	57	0.17
6	60	0.15
7	61	0.15
8	N/A	N/A
9	43	0.18
9	54	0.15
	<i>Average Velocity</i>	0.16

Table 2: RMS velocity at all A-S Ranch CMP locations

Devil's Den 3D survey

The GPR data at Devil's Den was acquired on an area of granite outcrop bearing no soil cover. Figure 3 shows the 25 parallel lines, each 100 m long, constituting the 3D survey. The absence of soil cover hindered transmission of low frequency current into the ground for the ERI survey, but a coupling problem did not exist for transmission of GPR waves.

Processing flow

Processing of data at Devil's Den followed the same steps as at the A-S Ranch: dewow application, spherical and exponential correction, time-zero correction, and bandpass filtering (Appendix D). Figure D1e shows the presence of sub-horizontal reflections most likely due to variations in mineral banding within the granite. Bandpass filtering relieves both high and low frequency noise components.

There are also many steeply dipping events corresponding to diffractions from fractures in the granite. Migration will be applied to collapse these events back to the location of the fractures.

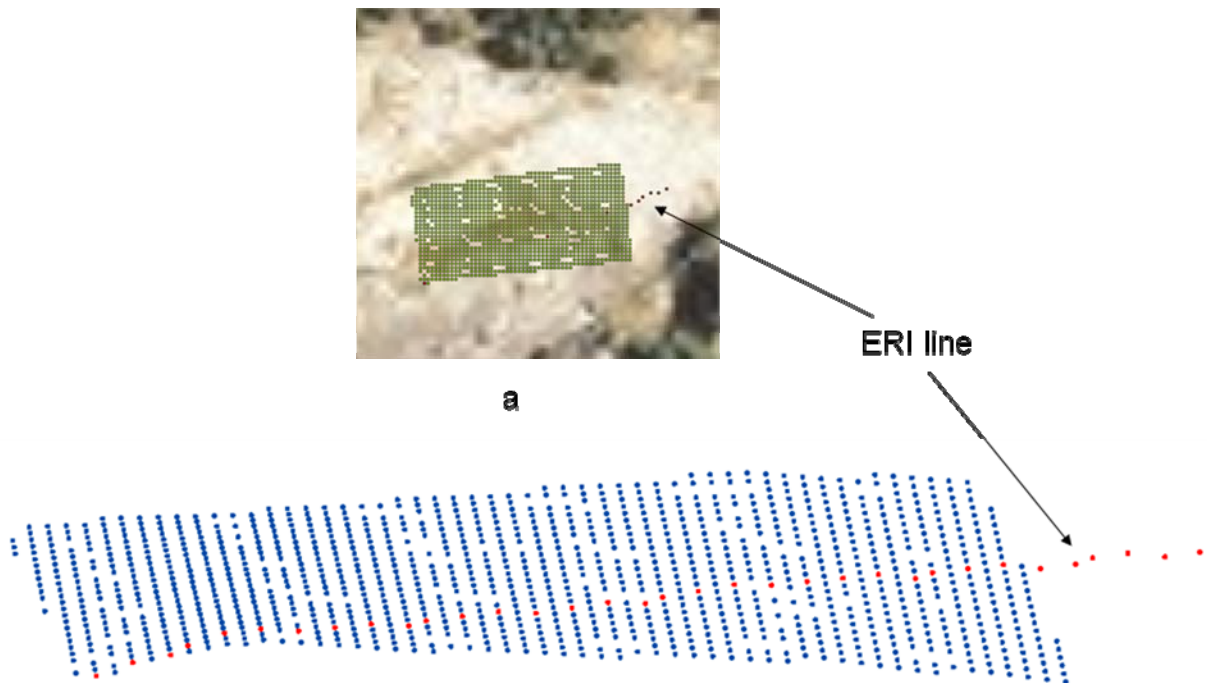


Figure 3: 3D GPR survey grid at Devils Den

Coherent noise reduction

The domain filter is used (Appendix E) to remove the airwave seen in Figure D1e so that very shallow underlying fractures can be seen. After filtering, diffractions from very shallow fractures (red circles, Figure E3b) extend the fracture imaging into an area formerly obscured by the airwave.

Velocity analysis

Because coherent reflections are absent from the data collected in the granite, the direct ground wave must be used to find the velocity of the granite. Figure F1 shows that velocities of the granite vary but are approximately .11 m/ns. This is somewhat lower than the average figure of .13 m/ns given by Annan (2005). We suspect that the occurrence of felsic dikes and extensive fracturing may play a role in determining the bulk velocity at this outcrop. Because we have chosen to profile across, rather than along, the predominant direction of fracturing, we would expect slower velocities as the GPR waves are impeded by these obstructions. Measurement made at many antenna orientations for each station have been successful in defining this velocity anisotropy in evaporates (Young and Ramirez, 2008) and this verification could be tried at Devil's Den.

3.3 GPR Data Interpretation

Principles of GPR interpretation

Both ERI and GPR measurements made on the ground's surface are indirect indicators of the underlying stratigraphy and degree of fluid saturation. Ground truth is absolutely necessary in order to pin a geological or lithological identity on either a resistivity boundary or a permittivity boundary.

At the A-S Ranch, Geoprobe cores and logs of a closely spaced sequence of five boreholes (Sample, 2008) provide shallow control, but no deeper ground truth is available. At Devil's Den, no ground truth is available. Due to this paucity of control, this report, for the most part, can point out correspondence of geophysical anomalies to mapped features but cannot confirm it. *Figure 4a shows location of Interpreted GPR section at A-S Ranch*

Interpretation of GPR Line 2 at the A-S Ranch

The purpose of the following section is to present one entire GPR line from the A-S Ranch and its interpretation. (Interpretation of the Devil's Den data is in Chapter 5 *Geophysical and Geological Data Integration*.)

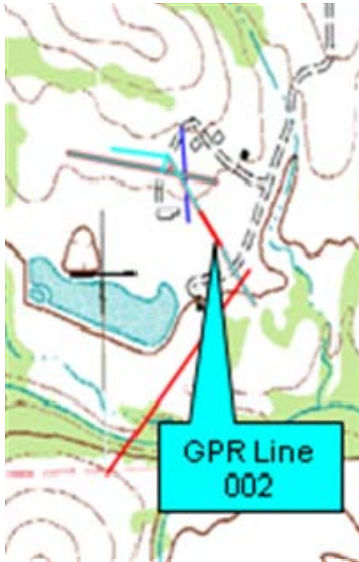


Figure 4a: Showing the location of Interpreted GPR section at A-S Ranch

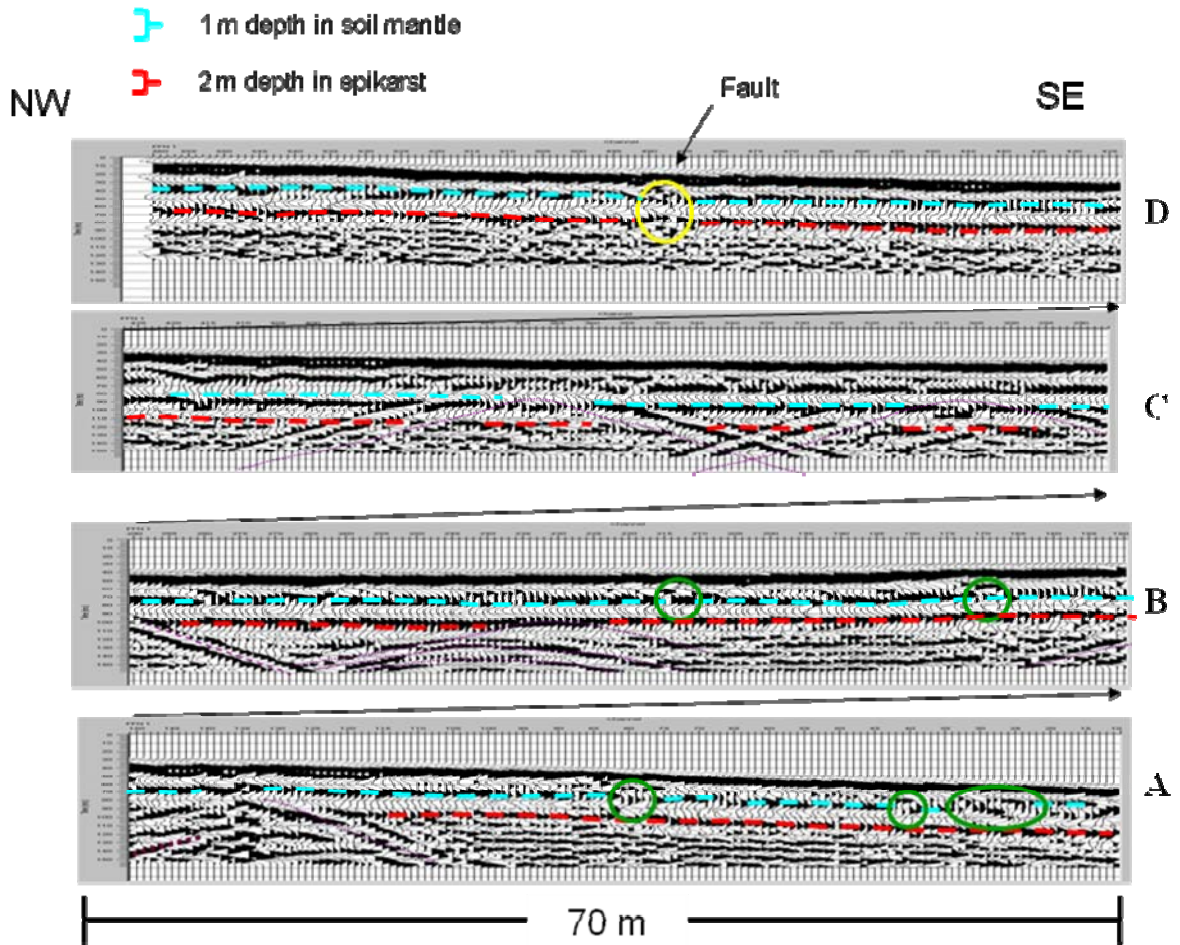


Figure 4b: Interpreted GPR section at A-S Ranch

Figure 4b consists of 560 GPR traces collected from SE to NW. In addition to the processing described in the appendices, the section has been topographically corrected. The line is spread out into four segments for detailed viewing. The vertical axis is in two-way time, but approximate conversion to depth is possible by using the scale bars at the top of the plot. Because velocity differs in soil and in epikarst, two scales are necessary.

Reflections from the base of the soil mantle (blue) and from a boundary within the epikarst (red) can be seen across the entire line. At places one or both boundaries are disrupted. The yellow circle shows disruption of both boundaries at a location corresponding to a mapped fault location (Todd Halihan, personal communication). Furthermore, it is in agreement with a fault (blue line, Figure 4b) seen on a near-surface seismic reflection survey (Kennedy and Young, in preparation) and on GPR line 1 where it intersects Line 2 (Figure 2). The green circles (Figure 4b) show shallow disruptions of the contact between the soil mantle and the epikarst. The large ellipse near the start of segment A indicates a portion of a basinal sedimentary feature where the soil mantle thickens.

The strong events (purple) cutting across segments A, B, and C are noise and are not of geological significance. Appendix B shows an example of how these features can be removed by further processing.

4.0 ERI Data

4.1 ERI Data Collection

An Advanced Geosciences, Inc. SuperSting R8 Earth Resistivity Meter (SuperSting) direct-coupled resistivity system was used to collect seven transects of ERI data at the study sites (Figure 5).



Figure 5: ERI surface electrodes and cables deployed to collect ERI Line AS1.25C1. Lower left: SuperSting R8 Earth Resistivity meter

The system consisted of 56 stainless steel electrodes (3/8-inch diameter) that were hammered in to the ground along a straight line at a specific spacing between electrodes. The total length of each of the lines varied from 68.75 meters to 495 meters (Figures 5, 6 and 7). Table 2 shows the ERI dataset information for both study sites.

The spacing used on each line was determined to provide the appropriate depth of imaging for the study area along with sufficient lateral distance to meet the project objectives. The depth of imaging at the site also varied from approximately 14 meters to 99 meters below the surface. The electrodes were connected via geophysical cables and the cables were connected to an AGI SuperSting resistivity meter and its components.

Site	Dataset	Electrode spacing (m)	Total Line Length (m)	~Depth of image (m)
Arbuckle Simpson Ranch	AS2.5A1	2.5	137.5	28
	AS1.25C1	1.25	68.75	14
	ASR5.00B	5	275	55
	ASRWE01A	5	275	55
	QTZSG01	9	495	99
Devil's Den	DEV0102	1.25	68.75	14
	DEV03	1.5	82.5	17

Table 2: ERI dataset information for both study sites.

Once each of the survey lines were laid out in the field, the resistivity instrument gathered a significant amount of data related to the electrical properties of the subsurface. Seven ERI datasets were collected during 2007- 2008. OSU collected ERI data using a proprietary high resolution ERI survey technique (developed by Oklahoma State University) known as the Halihan-Fenstemaker Technique (Halihan et al, 2005). The data was checked for quality and integrity in the field; full data reduction and processing were performed off-site.

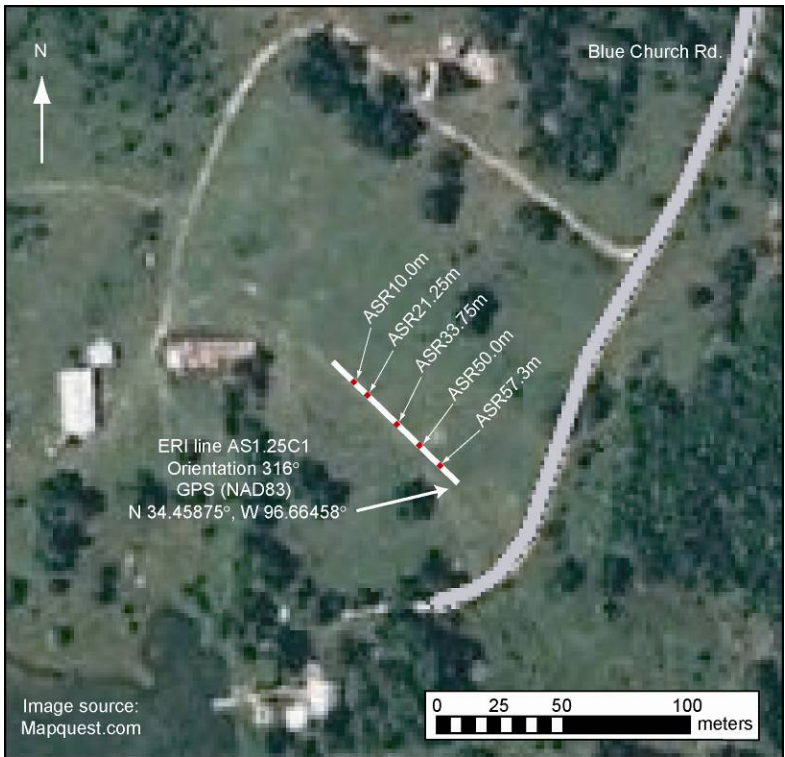


Figure 6: ERI line locations and drilling targets at the Arbuckle-Simpson Ranch site

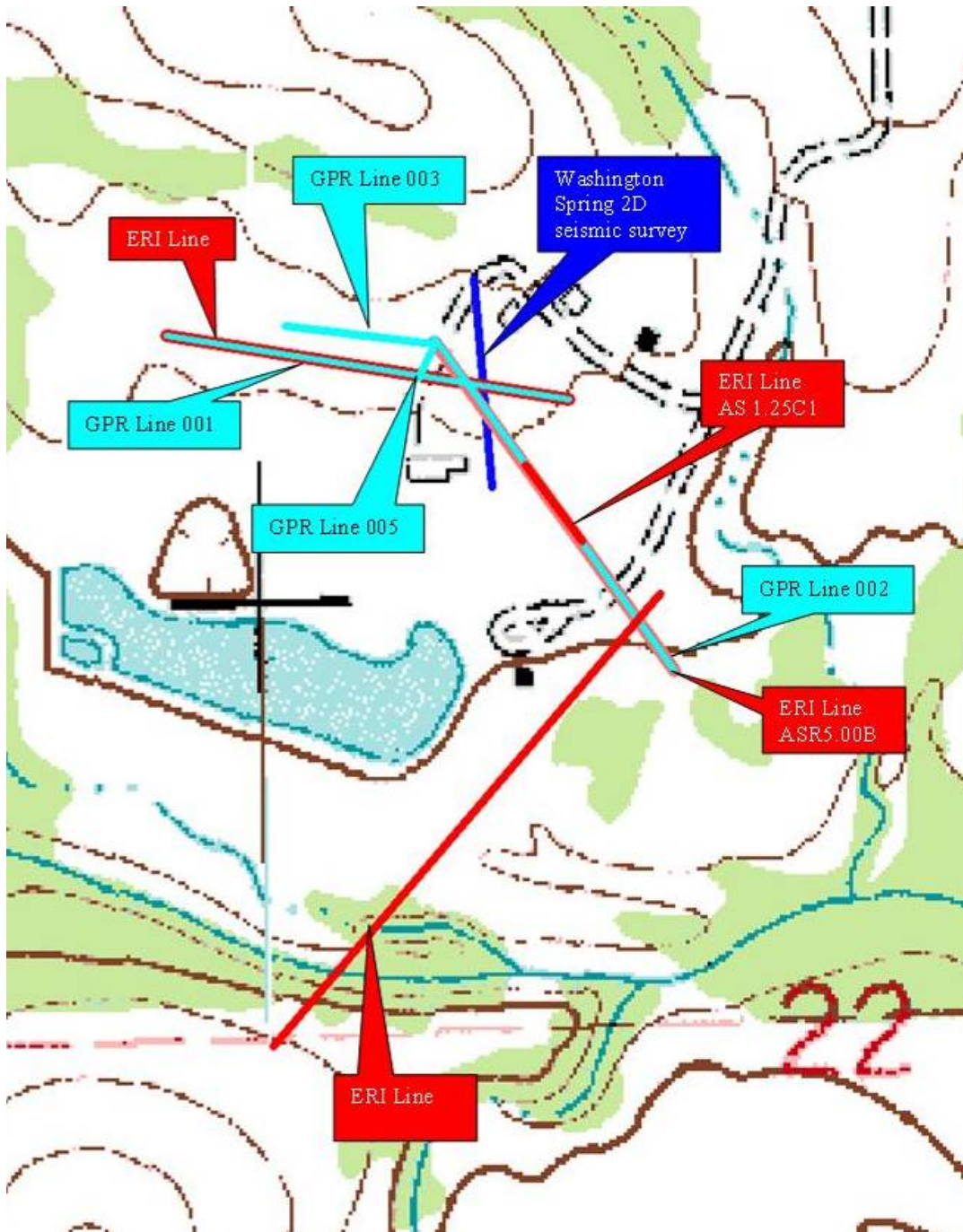


Figure 7: ERI and GPR locations at the Arbuckle-Simpson Ranch and Devil's Den sites.

4.2 ERI Data Reduction

Following field data collection, proprietary post-processing techniques were used to develop a final electrical resistivity image of the subsurface for each survey.

The raw data files collected in the field were post processed, including a more thorough review of data quality and integrity. Data points not meeting an established statistical

error criteria (i.e., typically less than 5 percent of the overall data set) are removed from the data set so that the resulting survey image is not skewed. A final image for each survey was developed which contains a model of the electrical resistivity of the subsurface in units of ohm-meters. Changes in topography along the survey were accounted for using information from a Topcon differential GPS system and a Topcon laser level system during this data processing work.

The final images were developed by contouring and plotting the resistivity data for each survey line using a consistent color scheme for the site to allow for evaluation of the results of all surveys on a comparative basis. For this study, the conductive (i.e., less resistive) areas of the subsurface are illustrated by the blue colors and the more resistive (i.e., less conductive) areas of the subsurface are illustrated by green and orange colors. The resistivity of the sites was so variable, that two color schemes were employed, one for each site.

As a part of overall data quality control process, the resistivity data for the entire site was compiled and then a normalized color scheme for the images was created. This allows consistency in the color scheme so a reviewer can correlate the results from one survey to the results from another survey performed on the same site during the same timeframe.

4.3 ERI Data Interpretation Process

The magnitude of subsurface resistivity values will vary from site to site based on a number of factors, and is related to geological composition and to the chemistry of the groundwater and other fluids trapped in the pore spaces within the soil matrix and the presence or absence of buried debris and structures. For a typical site, fine materials such as clay and silt are generally less resistive (i.e., more conductive) while coarse sand and gravel are generally more resistive (i.e., less conductive). Should the soil (clay or sand) be dry, it will appear more resistive when dry and less resistive when wet.

Should a distinct groundwater table exist in the area being surveyed, the groundwater interface is often not seen in the survey images because the resistivity of the groundwater is often times similar to the resistivity of the soil matrix. Additionally the presence of contaminants within the pore matrix can overshadow (electrically) the presence of groundwater or degree of saturation. The presence of fractures in bedrock geology often appear as a vertically oriented anomaly and may be either conductive or resistive depending on what type of fluid (e.g., clean groundwater and/or unweathered/weathered contamination) is present within the fracture.

ERI survey results do not immediately identify the composition of anomalies which may be caused by variations in geology and/or moisture content (or other factors). Final data interpretation is greatly enhanced by calibrating or benchmarking the electrical resistivity images against existing site data and/or follow-up confirmation boring data. This process lends much greater understanding of the subsurface and the survey images. Ideally, confirmation work is performed as soon as possible following the survey work such that minimal time is allowed for subsurface changes in groundwater quality, etc. that may cause changed electrical conditions in the surveyed areas. For this project, the confirmation data collected previously from direct push borings will be used to evaluate the efficiency of the technique following review of the preliminary interpretations provided

in this report at the Arbuckle Simpson ranch. Since the bedrock is exposed at the Devil's Den site, the features in the bedrock were recorded to compare with the ERI data.

4.4 Electrical Resistivity Imaging Results

Seven transect lines of data were collected. The entire dataset was of good quality with resulting inversion RMS errors between 3 and 6.5%. Processing of Arbuckle Simpson Ranch data eliminated 10-20% of noisy data, which is quite reasonable for these types of data., At the Devil's Den site, only 6% of the data was eliminated in processing for the line that was collected directly on bedrock. For the site collected on soil, 30% of the data was lost due to the extremely high resistivity contrast between the soil and the bedrock.

The interpretations of the datasets are as follows:

ERI Line AS2.5A1: This dataset was collected at the Arbuckle-Simpson Ranch. The image indicates three electrical layers, a conductive (0-250 ohm-meters) soil zone that extends to a depth of approximately 3 to 4 meters on the image. Below the soil zone is the slightly more resistive epikarst zone that extends to a depth of approximately 4 to 9 meters. Underneath the epikarst is a more resistive layer (>850 ohm-meters) indicating more intact zones of bedrock with possible fracturing between the distances of 30-40 meters and 70-75 meters on the image. This image comprised what is believed to be the background lithologic properties at the site.

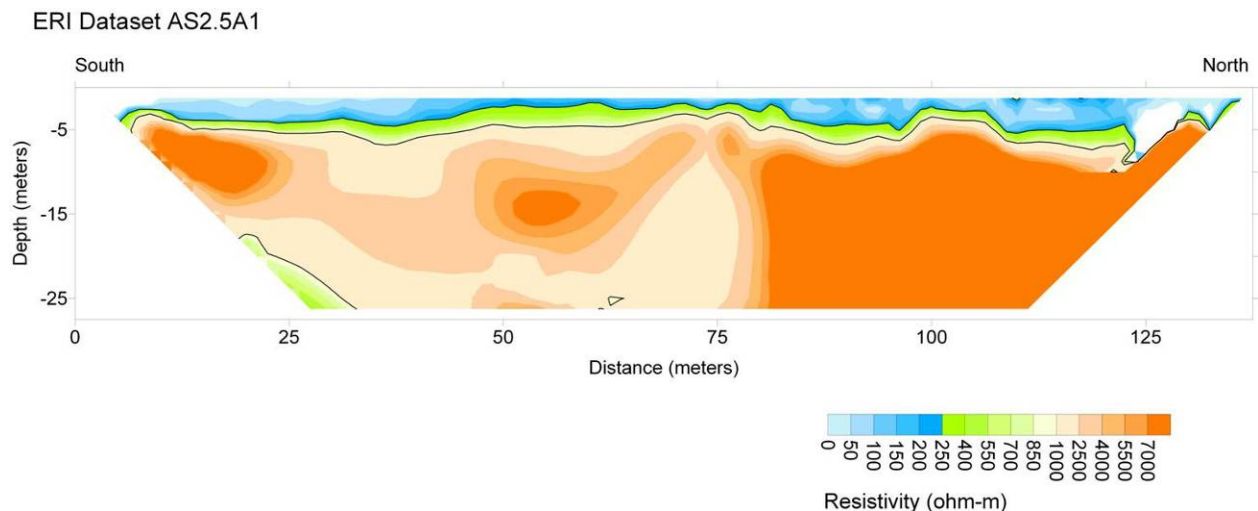


Figure 8: Image of ERI Line AS2.5A1

ERI Line AS1.25C1: This dataset was collected at the Arbuckle-Simpson Ranch. The image indicates two electrical layers, a soil zone less than 250 ohm-meters that extends down to an elevation of approximately 306 meters. This layer was evaluated with direct push cores and determined to be the extent of the soil layer (Sample, 2008). The next layer is more resistive (250-1000 ohm-meters) and extends downward to approximately 294 meters. The conductive area (0-250 ohm-meters) starting at the elevation 300m

going downward indicates an area of potentially increased weathering of the bedrock and a prospective pathway for fluids.

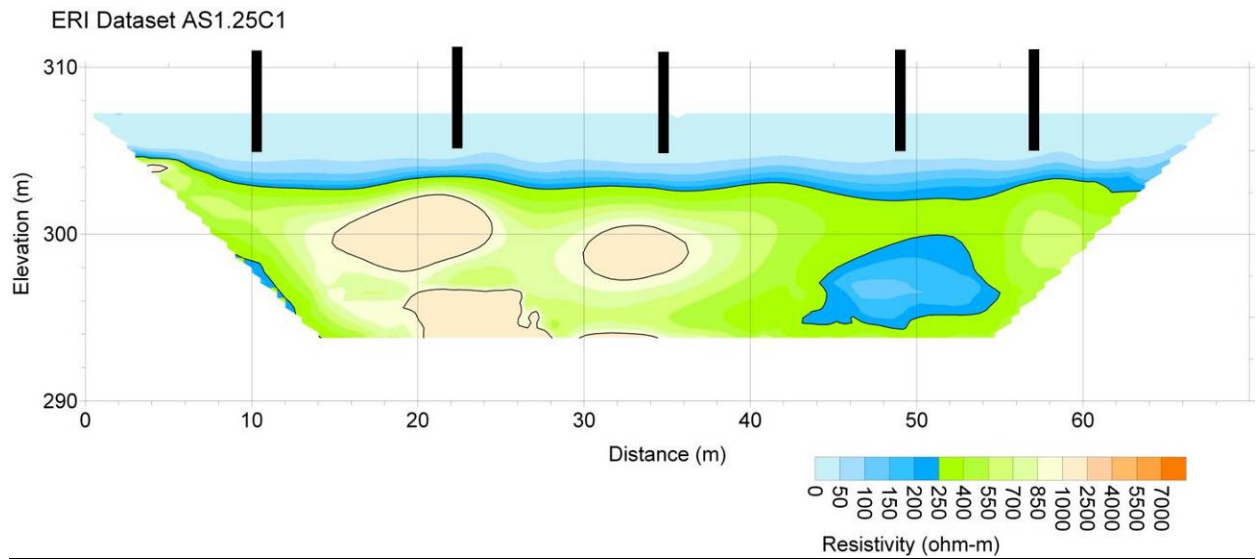


Figure 9: Image of ERI Line AS1.25C1

ERI Line ASR5.00B and ASRWE01A: These dataset were taken nearly orthogonal to each other on the Arbuckle-Simpson Ranch. Both images indicate three electrical layers, a conductive (0-250 ohm-meters) soil zone that extends to an elevation of approximately 300 meters on each image. At the 190 meter distance, both images indicates a fault zone extending vertically through the images. The resistivity values also indicate that an additional weathered zone exists for 100-150 meters away from the fault zone. This fault also corresponds to an inferred fault in the region.

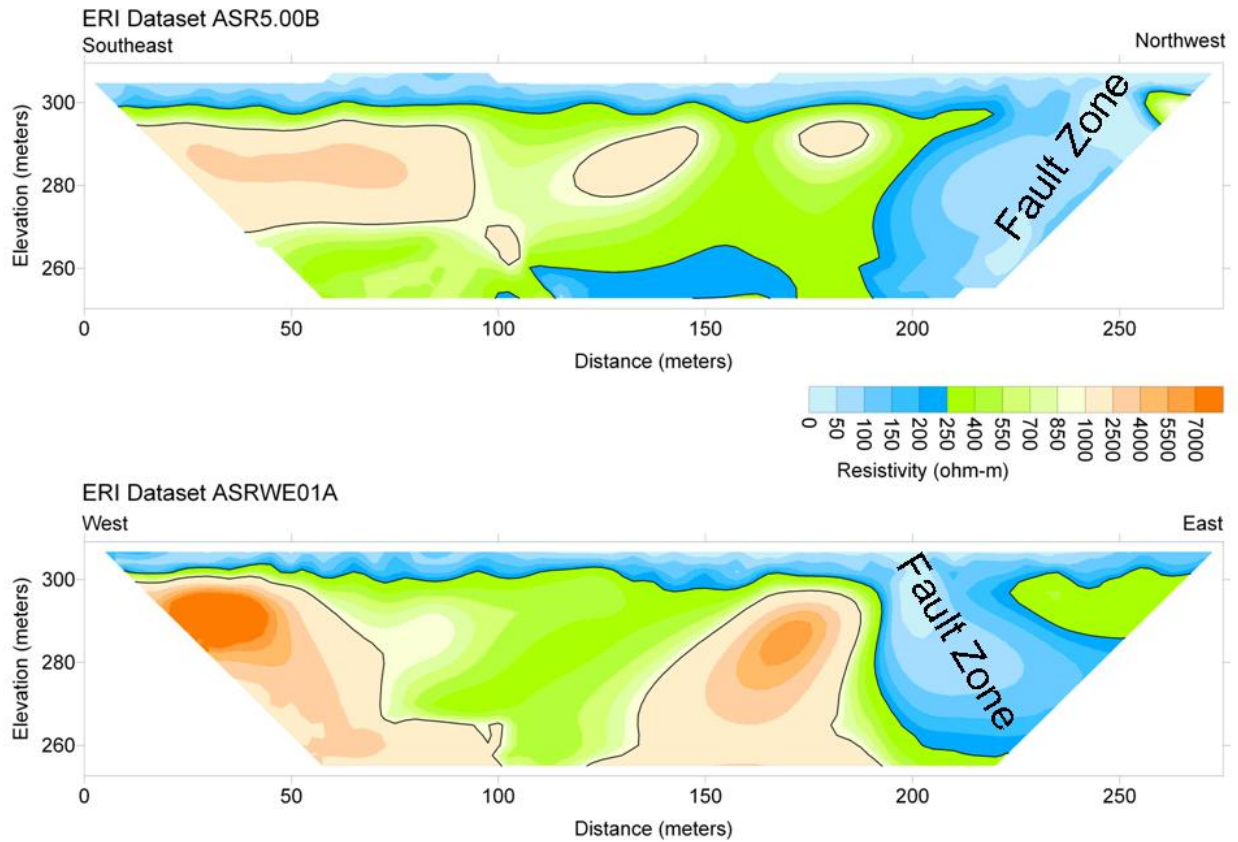


Figure 10: Images of ERI Line ASR5.00B and ASRWE01A

ERI Line QTZSG01: This dataset extends over the Blue River on the Arbuckle Simpson Ranch. This image indicates three electrical layers a conductive soil layer that extends down to 265-275 meters on the first 280 meters of the image. A more resistive layer of rock is found from 345-500 meters on the image and can be observed outcropping at the surface. Below 265 meters the image indicates variable resistivity in the data. Inferred flow paths for springs are indicated in the conductive areas (green and blue tones). The image suggests that the springs are not connected to the Blue River and that at this location, the Blue River is not well connected to the groundwater system.

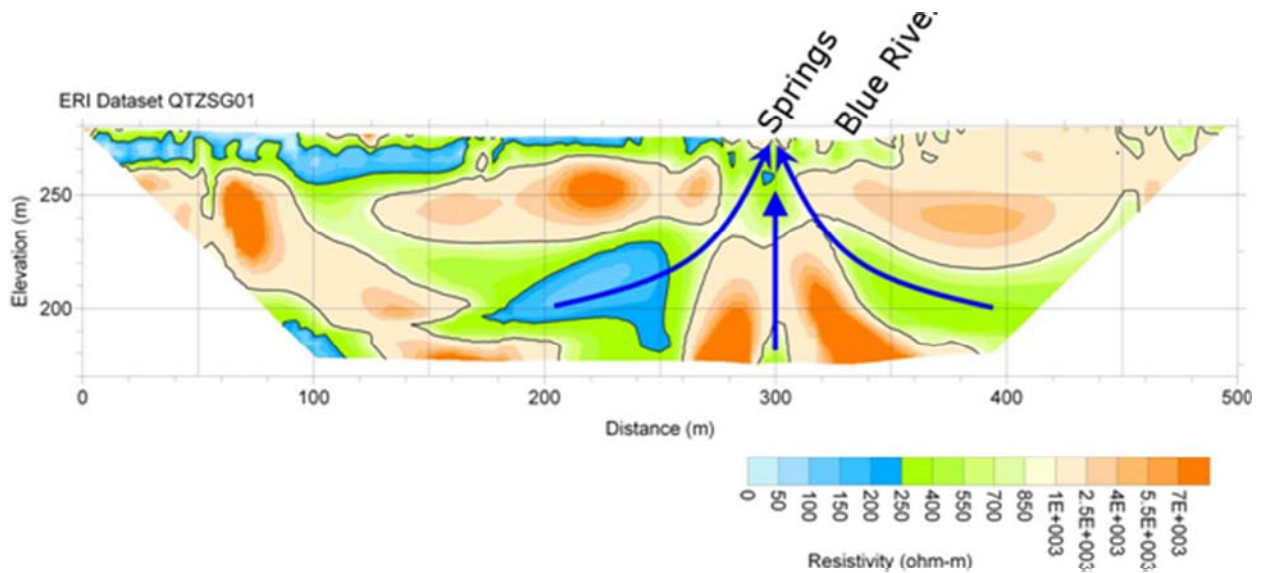


Figure 11: Image of ERI Line QTZSG01:

DEV0102: This data set was taken on exposed granite at the Devil's Den site. The resistivity scale was modified from the Arbuckle Simpson Ranch to accommodate extremely high resistivity values. This image indicates two electrical layers, a somewhat more resistive fractured layer extending down to an elevation of approximately 200 meters. Below the fractured layer is a more resistive less fractured layer extending down to an elevation of 189 meters. At the 40 meter and approximately 45 meter distance on the image granite dikes are indicated by elevated resistivity in the images. These dikes were also visible at the surface. The boundary between the layers may be a fracture zone caused by exposure of the granite.

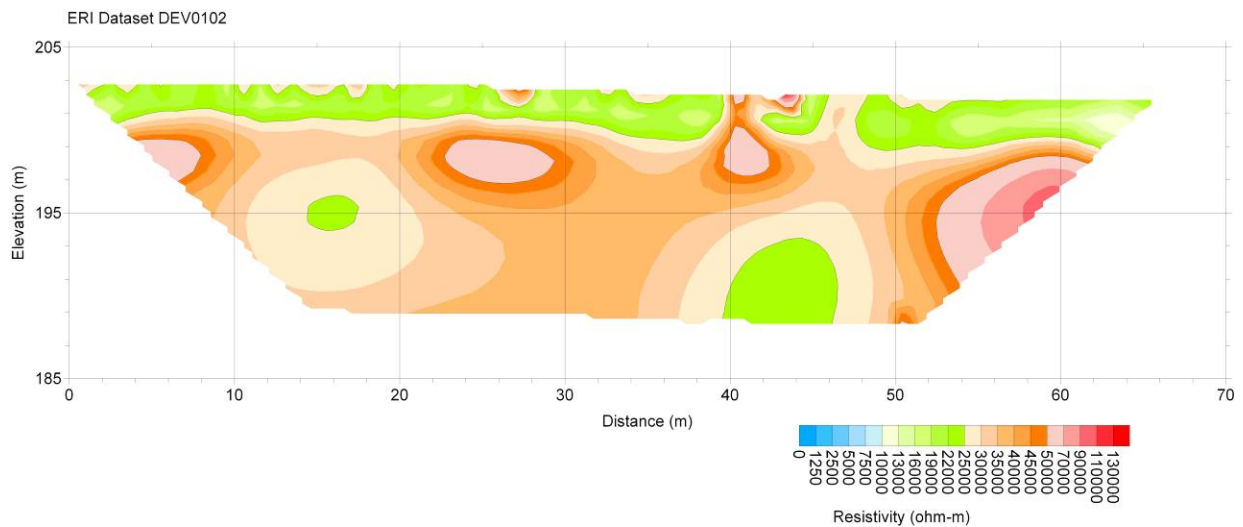


Figure 12: Image of DEV0102

DEV03: This dataset was taken over soil near the exposed granite at the Devil's Den site. This image indicates three electrical layers. For this dataset; a conductive and fractured zone (0-10000 ohm-meters) extends to an approximate elevation of 200 meters. Beneath the conductive zone is a more resistive zone (10,000-130,000 ohm-meters) indicating less fractured bedrock. The deeper conductive area may correspond to a fractured portion of the bedrock.

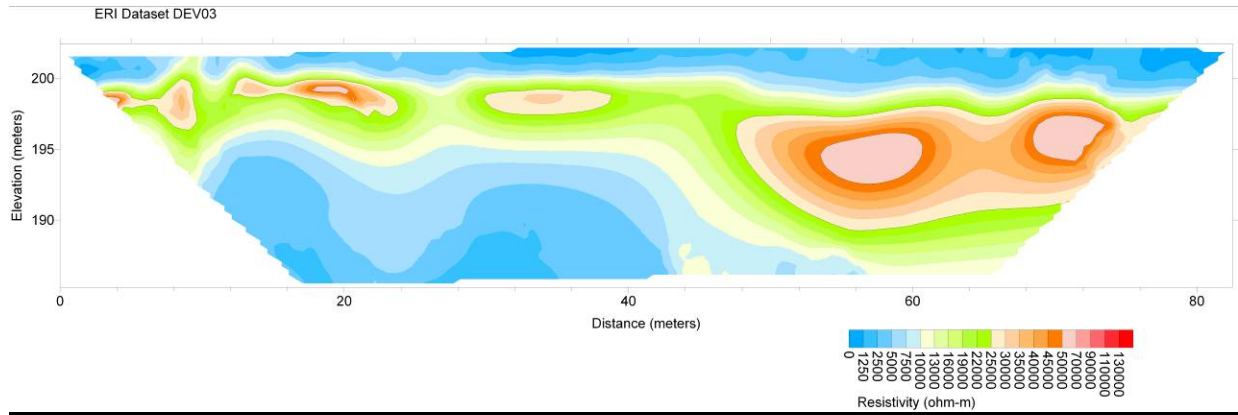


Figure 13: Image of DEV03

5.0 Geophysical and Geological Data Integration

5.1 A comparison of stratigraphic imaging by ERI and GPR methods

The focus of the present project is the correspondence of geological boundaries and vertical discontinuities as seen on the ERI resistivity inversion and on the GPR sections. The A-S Ranch has two coincident ERI and GPR surveys. Guided by the conceptual geological model at the site (Sample, 2008), we have compared the resistivity inversion and the reflection image for one of these pairs.

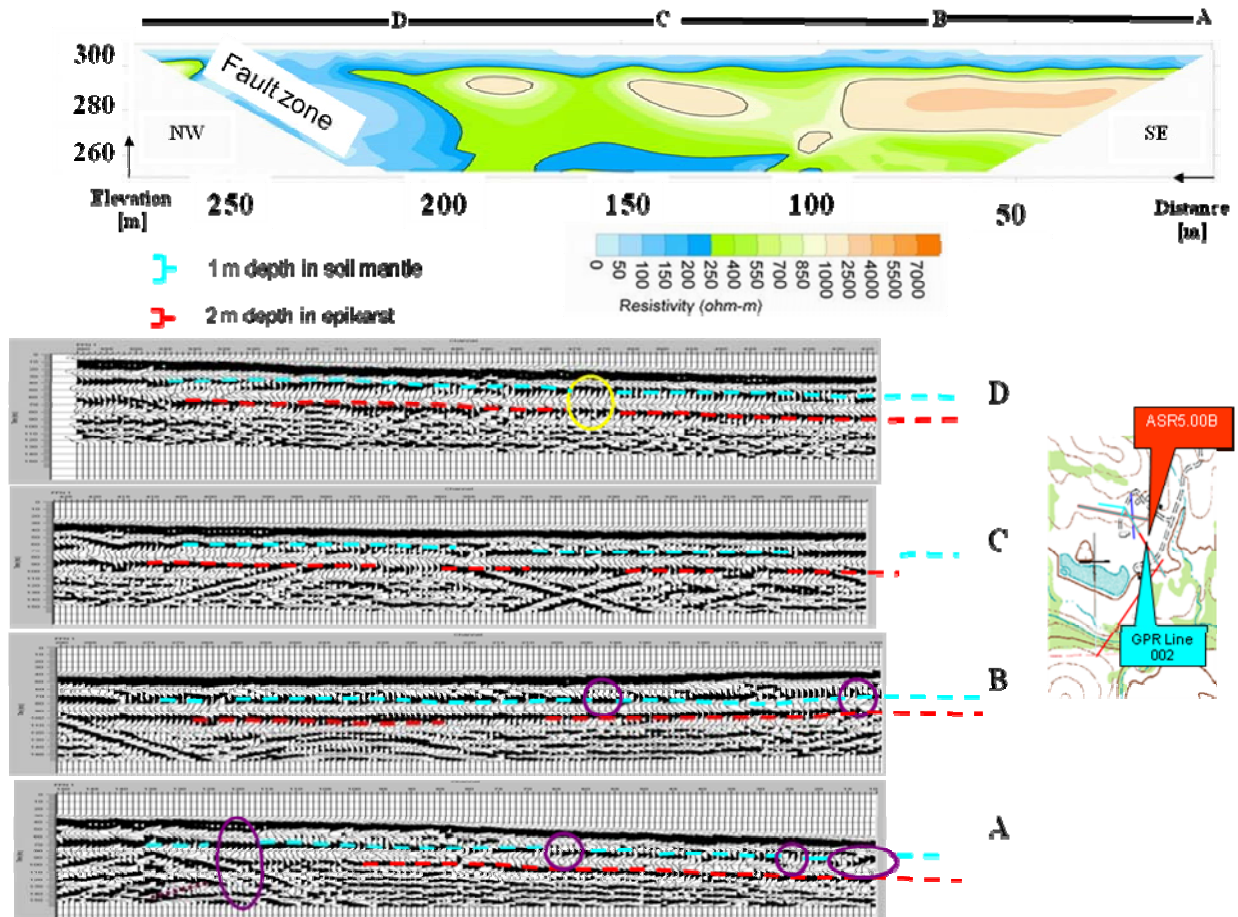


Figure 14: Comparison of ERI and GPR lines at the A-S Ranch. Upper (blue) and lower (red) boundaries are seen on both the ERI inversion (top) and the GPR reflection section (below).

A striking aspect of this comparison is that the two ERI resistivity boundaries—at 200 ohm-m and at the zone of rapid increase in resistivity from 200 to 2000 ohm-m—have a distinct appearance on the GPR line. The 5 m station spacing of the resistivity section does not see the lateral detail of the GPR reflections having a spacing of .5 m, but the blue dashed boundary occurs at a depth of approximately 2-3 m and the red dashed boundary approximately 2 m deeper on both lines.

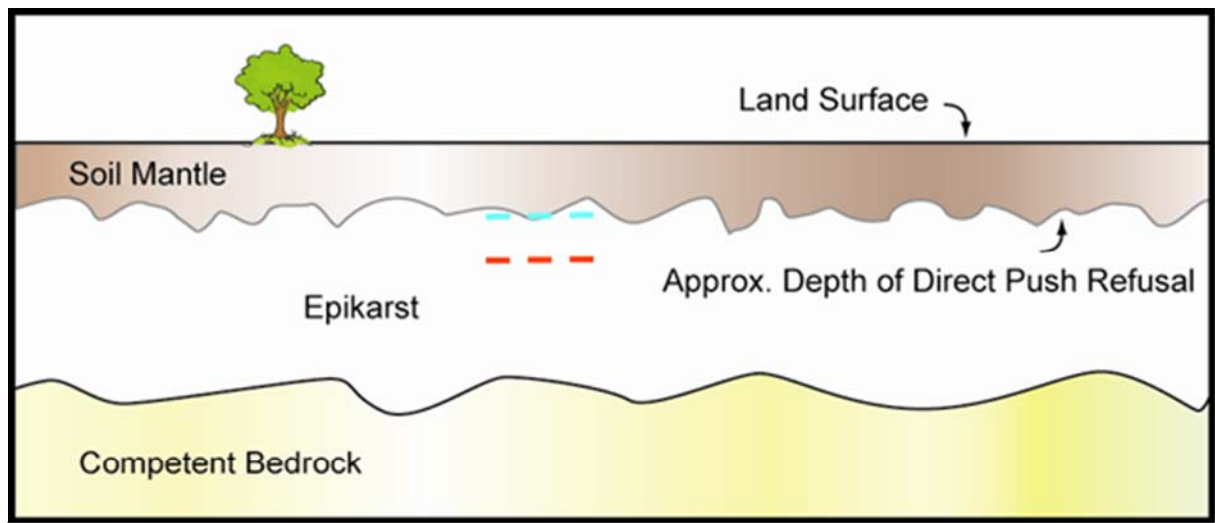


Figure 15: Conceptual model of the stratigraphy at the A-S Ranch (Sample, 2008). Base of the soil mantle (blue dashes) and a boundary within the epikarst (red dashes) are the same boundaries recognized on Figure 14.

Figure 15 indicates that the two geophysical boundaries correspond to the base of the soil mantle and to a boundary within the uppermost epikarst in the conceptual model. Geoprobe cores and logs (Sample, 2008) both indicate an abrupt change from soil to carbonate at a depth of approximately 2 m. (The location in the data is shown by the short red line in the Figure 14 inset.) This is also the depth at which the coring barrel was refused by a much more dense lithology (Sample, 2008). Because the ERI measurements are controlled by resistivity, GPR by permittivity, and core refusal by density one would expect somewhat different depths to these changes in physical properties. Water content would also effect the resistivity—and hence the ERI inversion—more than the permittivity and the GPR section.

Although both methods detect the presence of a fault beneath segment D, the broader delineation by the ERI inversion may be due to water saturation in the fault zone that has less effect on the GPR reflections.

5.2 A comparison of fracture detection by GPR methods and mapped fracture orientations

After processing all GPR lines at Devil's Den (Appendices A, B, and C), Kirchhoff 2D poststack time migration (Yilmaz, 2001) was applied to each line and the lines were combined into a 3D volume using the Kingdom Suite interpretation software (Davogusto and Young, in preparation). Finally, application of the maximum curvature attribute (Marfurt, 2006; Chopra and Marfurt, 2007) localizes the response of the fractures in the volume.

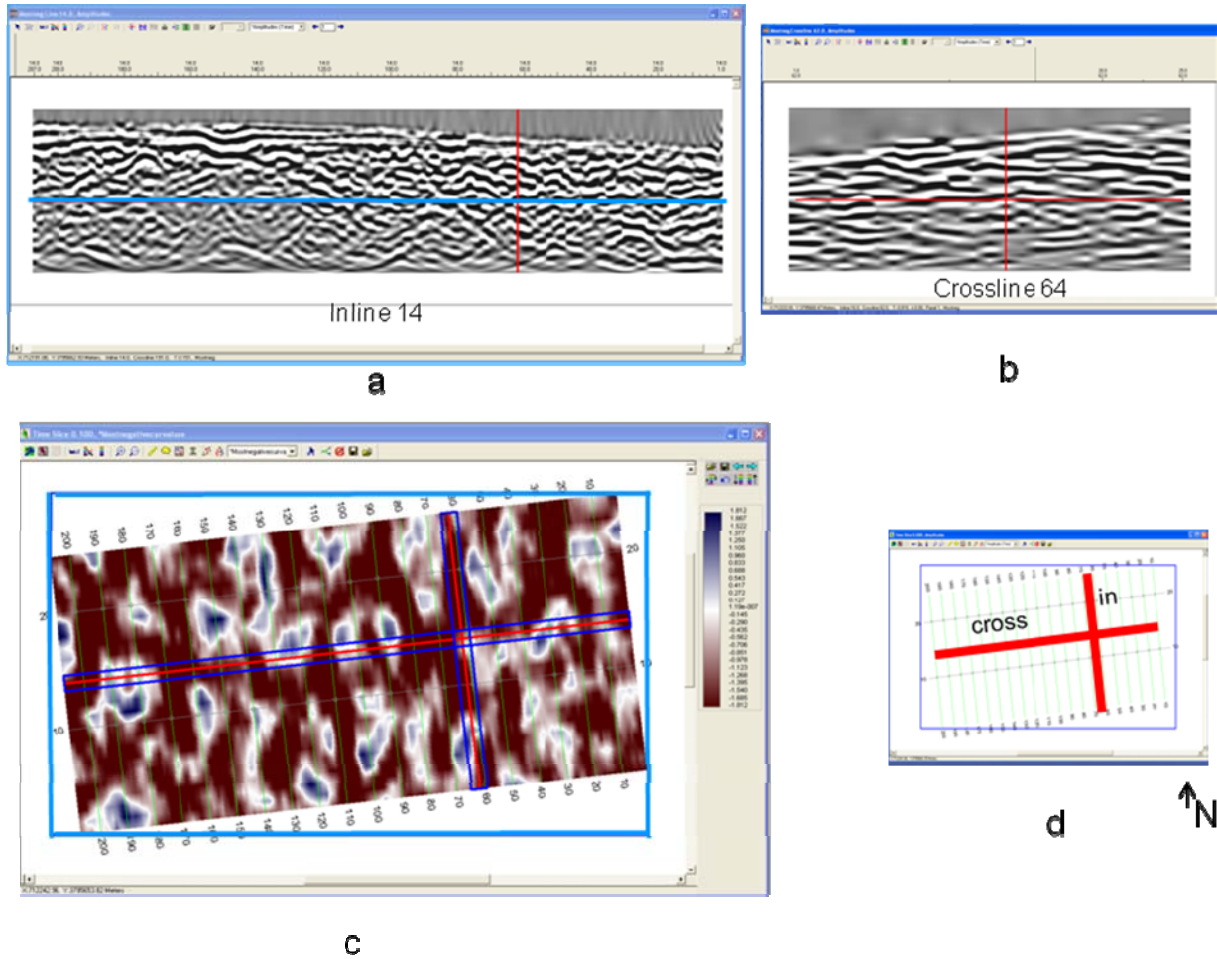
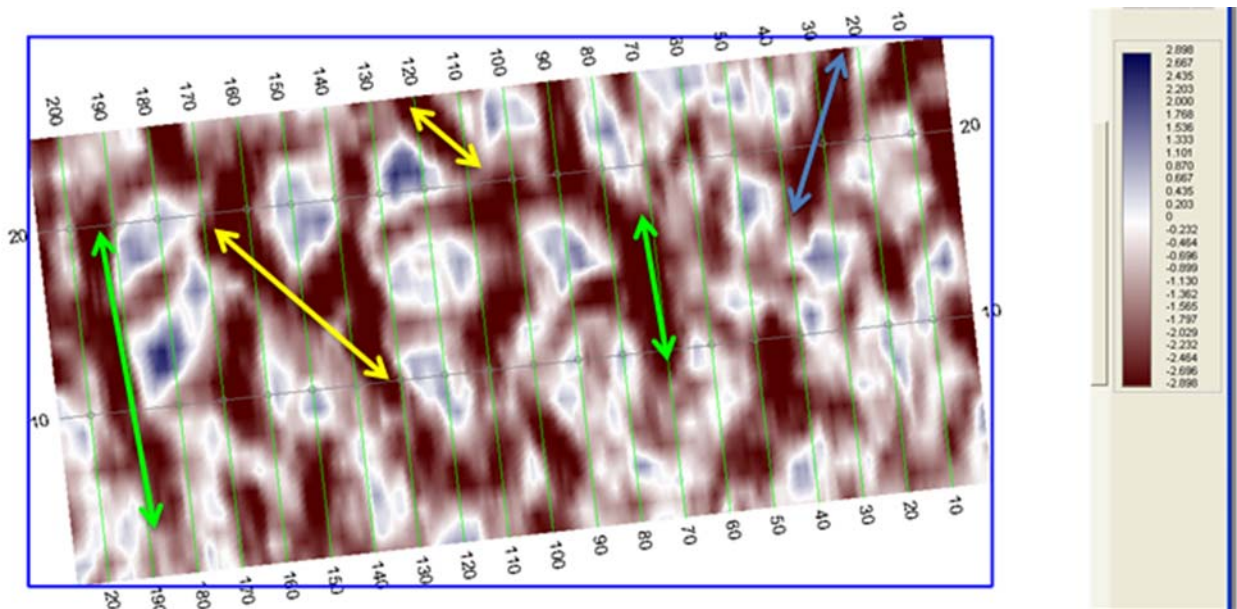
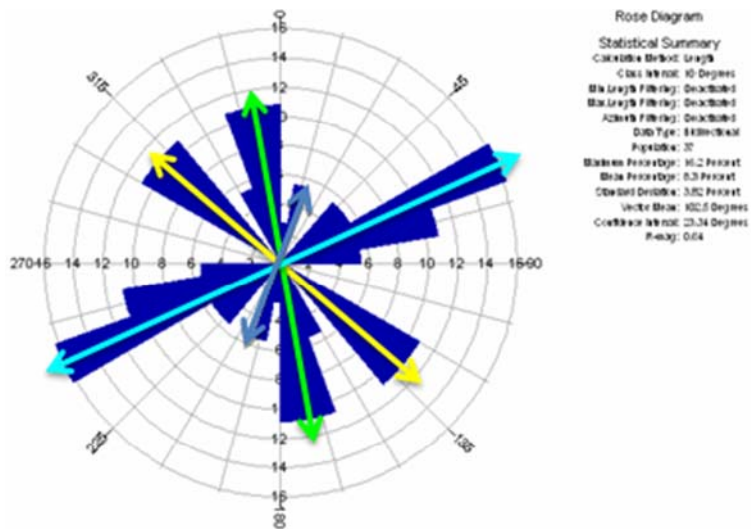


Figure 16: Three slices through the GPR volume . The inset (d) shows the locations of (a) inline 14 and (b) crossline 64 within the 3D survey. A time slice through the most negative curvature volume (c) at 100 ns (blue line on (a)) shows linear patterns not easily recognized on (a) and (b).

Figure 16a and b show two orthogonal lines (Figure 16d) from the GPR volume. A time slice through this volume (Figure 16c) shows linear patterns that we believe to be associated with the mapped fractures.

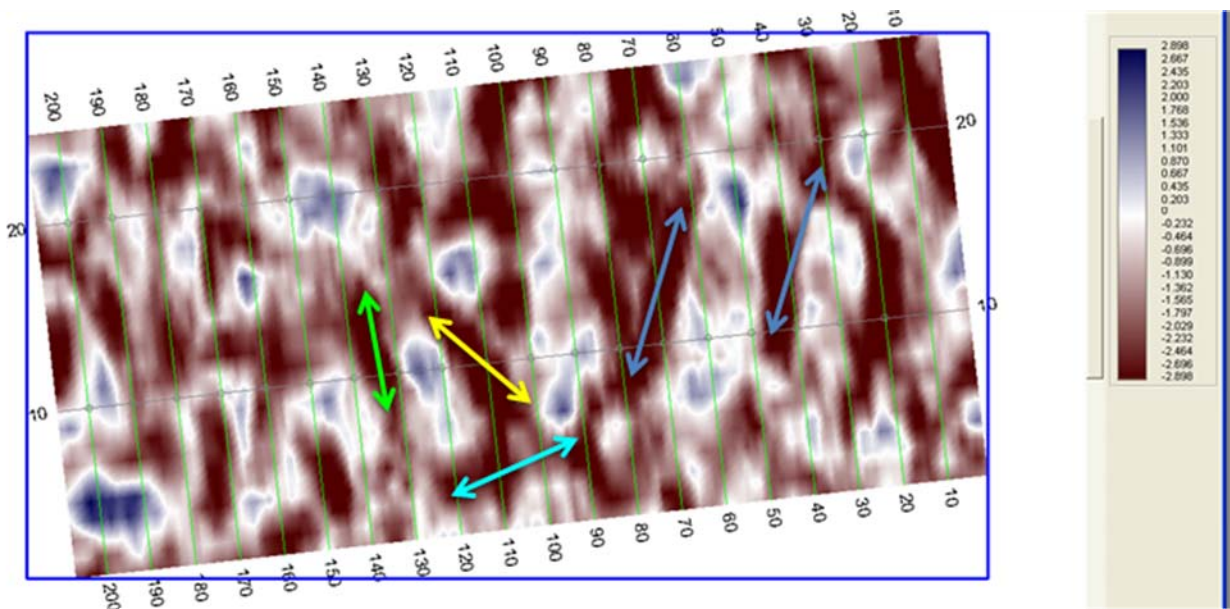


A)

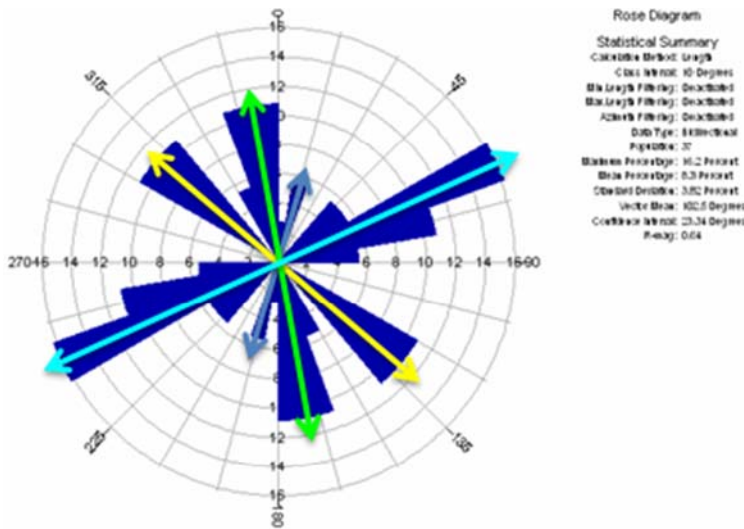


B)

Figure 17: (A) Time slice at 120 ns slice through the least curvature attribute volume. (B) Measured fracture directions are shown in the rose diagram. Principal strike directions of measured fracture sets are recognizable on the time slice as lineations of large negative curvature.



A)



B)

Figure 18: (A) Time slice through least curvature attribute volume at 140 ns. (B) Measured fracture directions are shown in the rose diagram. Principal strike directions of fracture sets are recognizable on the time slice as lineations of large negative curvature.

The linear patterns appear even more clearly in time slices at other times than in Figure 16. Figure 17 and 18 are time slices at 120 and 140 ns, respectively, and for each the measured fracture directions in the rose diagram appear as high amplitude lineations on the time slices. All four directions in the rose diagram are represented in the lineations. Interestingly, the most populous fracture direction (blue in the rose diagram) is not represented in Figure 17A. Particular directions seem to be localized in different sectors

of the time slice, so a future task is to subdivide the fractures represented in the rose diagrams into outcrop locations where they were measured.

5.2 Uncertainties in conceptual models

Our operational model of fracture formation is that it is homogeneous over the surface of an outcrop area 50 m by 100 m. Given this assumption, a comparison of a rose diagram of fracture direction and intensity to patterns seen on time slices of GPR attribute volumes is sensible. However, expert opinion (David London, 2008, personal communication) suggests that preferred fracture packets exist over granite quarry floors elsewhere but that there is also variation in fracture intensity and in orientation over the quarry floor. In such a case, it would be important to break out the fracture information into location within the outcrop.

Perhaps the pattern variability suggested above is due to mining explosions used to quarry the granite and is of little relevance to fracture patterns on an unmined outcrop, such as at Devil's Den, where fractures are inherited from regional stress histories. In our examination of the GPR data at Devil's Den, though, we need to be guided by a clearer understanding of the fracturing process itself.

6.0 Conclusions

5.1 Relevance of combined ERI and GPR to fracture definition in the Arbuckle-Simpson Group

Collisional plate-tectonics affecting the interior of the North American craton caused faulting that disrupted the basement boundary (Ham et al., 1964). Reactivation of these basement faults in the Pennsylvanian and in younger tectonic episodes has resulted in the propagation of these faults upward through overlying formations. This fault reactivation is seen on exploration-scale seismic surveys in central Texas where the same sort of sub-vertical faults displace the basement and also overlying layers (Marfurt, 2006). Indeed, an exploration-scale 2D seismic survey acquired in 1980 by Anschutz across the eastern half of the Hunton Anticline in Oklahoma shows exactly the same sort of disruption by basement-penetrating faults. It also has the same fracture intensity (Kennedy and Young, in preparation). In both the Texas and Oklahoma cases equivalent rocks (the Ellenberger in Texas and the Arbuckle-Simpson in Oklahoma) are involved in the deformation, but in Oklahoma the deformed carbonate section is exposed at the surface. This offers a special opportunity to see if fracture patterns observed on the surface today can be linked to much earlier deformation at basement depths. This, in fact, is possible with the data from the present project. Data from the A-S Ranch comes from a stratigraphic position in the Arbuckle-Simpson Group that is 3000 ft above the base of the Group at its basement contact.

Encouragement that a link from the base of the Arbuckle-Simpson to a stratigraphic position 3000 ft higher is possible comes from an analysis of seismic data on the Hunton Anticline acquired at the A-S Ranch, the Spears Ranch, and the Anschutz 2D seismic line (Kennedy and Young, in preparation). These three locations represent shallow, intermediate, and deep seismic images, respectively, through this 3000 ft section of the Arbuckle-Simpson Group.

Further analysis of the fracture orientation in the present data and its relationship to fracturing extending from the surface to the basement leads to the exciting possibility that shallow geophysics could be a key to determining heretofore unmapped fracture locations in the Arbuckle-Simpson aquifer. Such information is valuable to definition of aquifer reservoir models constructed for flow simulations.

5.2 Enhancing initial success at geophysical imaging in carbonates and basement

The ERI method is a relatively new method that has just recently seen wide use in hydrologic surveys. The GPR method is somewhat more mature, but there is a paucity of published studies comparing results by both ERI and GPR methods over the same terrain.

The present 3D GPR survey on the Tishomingo granitic basement is the only such survey known to the authors. Others have investigated GPR imaging both on the ground surface and in boreholes for which logs are available in order to assess fracture density for the purpose of siting nuclear waste disposal chambers (Holloway et al., 1992). In

addition, underground surveys using GPR have been conducted in order to answer questions of roof stability in potash mining (Gendzwill, 1982).

Pioneering studies such as ours provide unusual new data and suggest new ways of answering important geological questions. However, seeing that ERI and GPR image stratigraphic or lithologic variation in the epikarst at the A-S Ranch, as we have done, is not equivalent to explaining the change in physical properties that is responsible for these observations. Converting the new observations to answers is a task that must build over time as the data is completely digested and geological patterns emerge from the geophysical representations.

Likewise, modern 3D GPR interpretation of fractures (eg., McClymont et al., 2008) takes its direction from innovations in the interpretation of 3-D seismic data using volume based attribute measurements (Marfurt, 2006). An early application of attribute analysis to 3D GPR data acquired over fractured fluvial sandstones (Young et al., 1997) revealed displacements in faulted horizons. The work at Devil's Den is more challenging as no layering exists and one must image diffractions from the fault itself. The work presented here is preliminary but points in a direction of further analysis (Davogustto and Young, in preparation).

7.0 References

- Annan, A.P, 2005, Chapter 11: Ground penetrating radar, in *Near-surface geophysics,, Investigations in Geophysics, vol. 13, Society of Exploration Geophysicists [ed., Dwain K. Butler],357-438.*
- Archie, G. E., 1942, The electrical resistivity log as an aid to determining some reservoir characteristics.: Transactions of the American Institute of Mechanical Engineers, v. 146, p. 389-409.
- Chopra, S., Marfurt, K. (2007). Seismic curvature attributes for mapping faults/fractures, and other stratigraphic features: CSEG RECORDER, 32 (9), 37-41.
- Daily, W., A. Ramirez, A. Binley, and D. LaBrecque, 2004, Electrical resistance tomography: The Leading Edge, p. 438-442.
- Gendzwil, D. J., 1982, Induced earthquakes at a potash mine near Saskatoon, Canada, Canadian Journal of Earth Science, 19, 466-475.
- Ham, W.H., Denison, R.E., and Merritt, C.A., 1964, Basement rocks and structural evolution of Southern Oklahoma, Oklahoma Geological Survey Bull. 95, 302 pp.
- Herwanger, J. V., M. H. Worthington, R. Lubbe, and A. Binley, 2004, A comparison of cross-hole electrical and seismic data in fractured rock: Geophysical Prospecting, v. 52, p. 109-121.
- Holloway, A.L., Stevens, K.M., Lodha, G.S., 1992, The results of surface and borehole radar profiling from permit area B o the Whiteshell Research Area, Manitoba, Canada, Fourth International Conference on Ground Penetrating Radar, Rovaniemi, Finland, conference proceedings [ed. Pauli Hanninen and Sini Autio], Geological Survey of Finalnd, Special Paper 16, 329-337.
- Marfurt, K.J, (2006), Seismic attribute mapping of structure and stratigraphy, Distinguished Instructor Series, No. 9, Society of Exploration Geophysicists, 226 pp.
- McClymont, A.F., Green, A.G., Streich, R., Horstmeyer, H., Tronicke, J., Nobes, D.C., Pettinga, J., Campbell, J., Langridge, R., 2008, Visualization of active faults using geometric attributes of 3D GPR data: An example from the Alpine Fault Zone, New Zealand, Geophysics, 73, 2, B11-B23.
- Niwas, S., and O. A. L. de Lima, 2003, Aquifer parameter estimation from surface resistivity data: Ground Water, v. 41, p. 94-99.
- Purvance, D. T., and R. Andricevic, 2000a, Geoelectric characterization of the hydraulic conductivity field and its spatial structure at variable scales: Water Resources Research, v. 36, p. 2915-2924.
- Purvance, D. T., and R. Andricevic, 2000b, On the electrical-hydraulic conductivity correlation in aquifers: Water Resources Research, v. 36, p. 2905-2913.
- Ramirez Meija, D., and Young, R.A., Fracture orientation in sedimentary rocks using multi-component ground-penetrating radar measurements, *The Leading Edge*, 26, 8, 1010-1017.
- Ramirez, A., W. Daily, D. LaBrecque, E. Owen, and D. Chesnut, 1993, Monitoring an underground steam injection process using electrical resistance tomography, Water Resources Research, United States, American Geophysical Union: Washington, DC, United States, p. 73.
- Sample, M.A., 2008, Characterization of the Epikarst over the Hunton Anticline, Arbuckle-Simpson Aquifer, Oklahoma, MS Thesis, School of Geology, Oklahoma State University, , 220 pp.

- Suneson, N. H., 1997, Pontotoc and Johnston Counties, Oklahoma. An Introduction and Field-Trip Guide: Prepared for the Annual Meeting of the Oklahoma Chapter of The Nature Conservancy.
- Stollar, R. L., and P. Roux, 1975, Earth resistivity surveys; a method for defining ground-water contamination, Ground Water, United States, National Water Well Association, Ground-Water Technology Division : Urbana, IL, United States, p. 145.
- Van Nostrand, R. G., and K. L. Cook, 1966, Interpretation of Resistivity Data, Geological Survey Professional Paper, United States Government Printing Office, Washington, United States Geological Survey.
- Yilmaz, O (2001). *Seismic Data Analysis: Processing, Inversion and Interpretation of Seismic Data Volume I*, Tulsa: Society of Exploration Geophysicists.
- Young, R.A., Sun, J., 1999, Revealing stratigraphy in ground-penetrating radar data using domain filtering, Geophysics, 64, 2, 435-442
- Young, R.A., Deng, Z., Marfurt, K.J., and Nissen, S.E., 1997, 3-D dip filtering and coherence applied to GPR data: a study, The Leading Edge, 1011-1018.

Appendix A

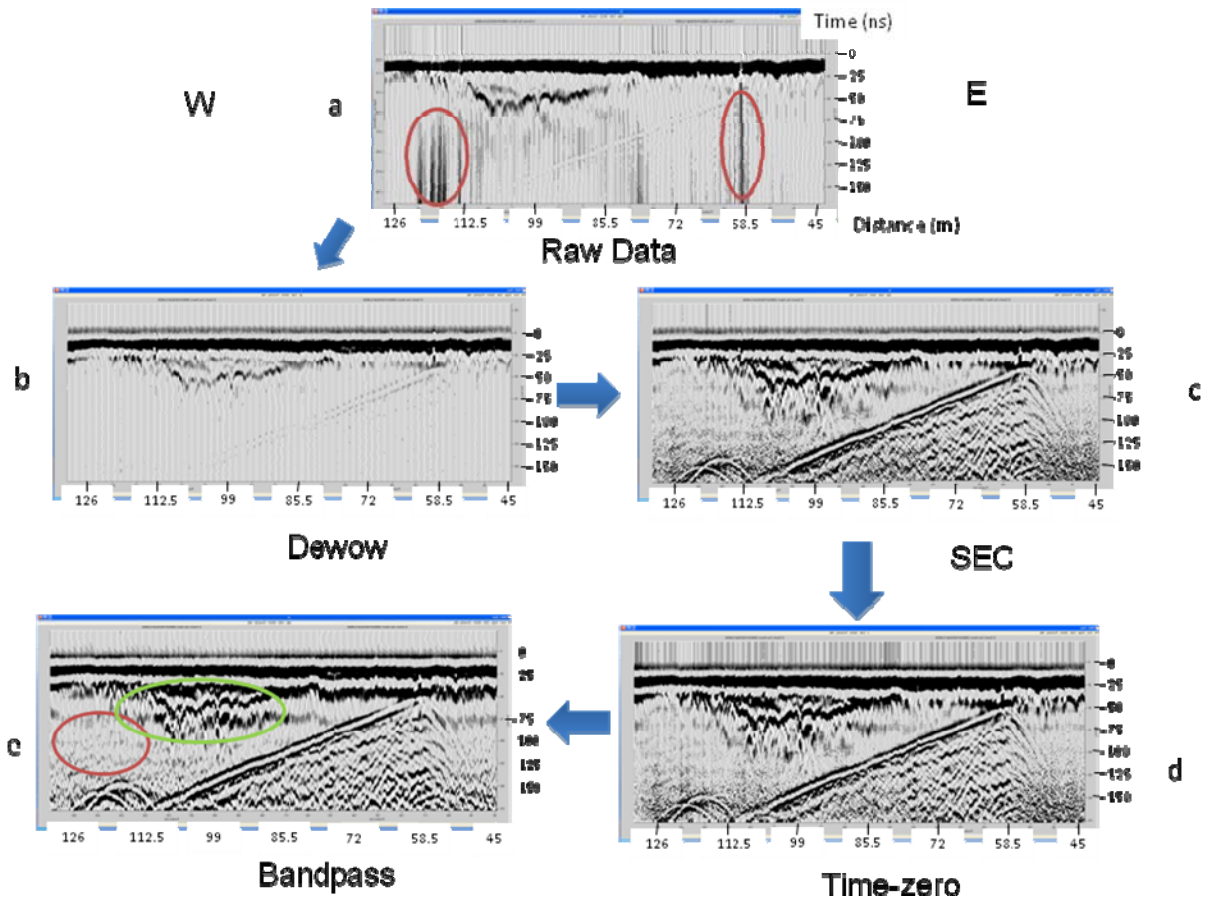
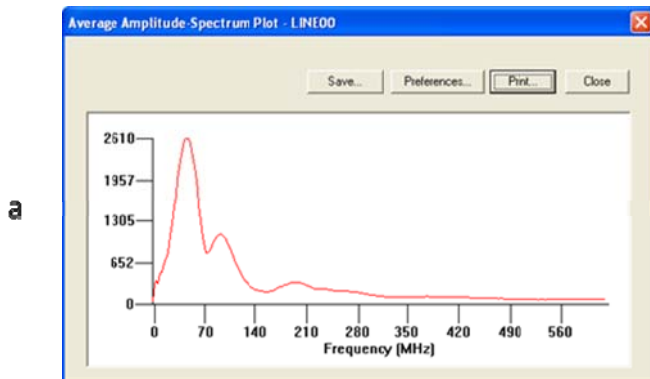


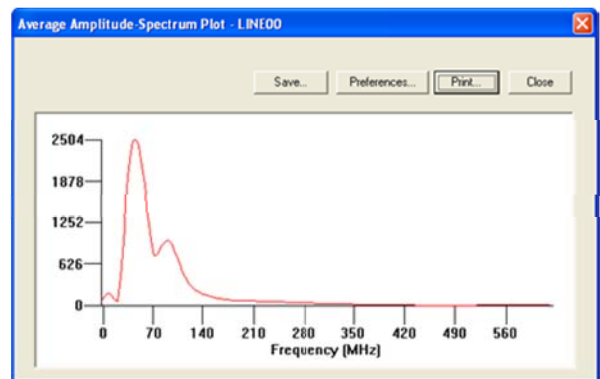
Figure A1: Processing steps for the Arbutle-Simpson Ranch data. (a) A segment of raw data for GPR Line 2 between 45 and 126 m. (b) Data after dewow filter applied. The dewow filter is used to remove very low frequency components of the data associated with inductive phenomena or dynamic range limitations of the equipment (red ellipses in (a)). (c) Spherical and Exponential Compensation restores amplitude attenuation of the signal as it propagates through the ground. After the SEC is applied, features in the middle and deep part of the record are enhanced (green ellipses). Noise is also introduced (yellow arrows). (d) Time-zero correction aligns the airwave reflection starting time (yellow) on all traces. (e) Band pass filtering removes the background noise (yellow arrows in (d)) and high frequency noise revealed by the SEC gain (yellow arrows in (c)) thus giving a cleaner record (red ellipses).



Before Bandpass



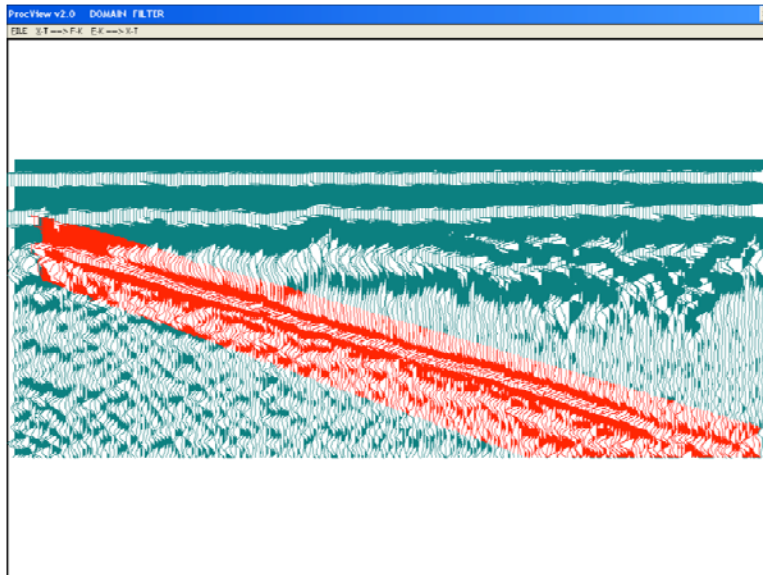
b



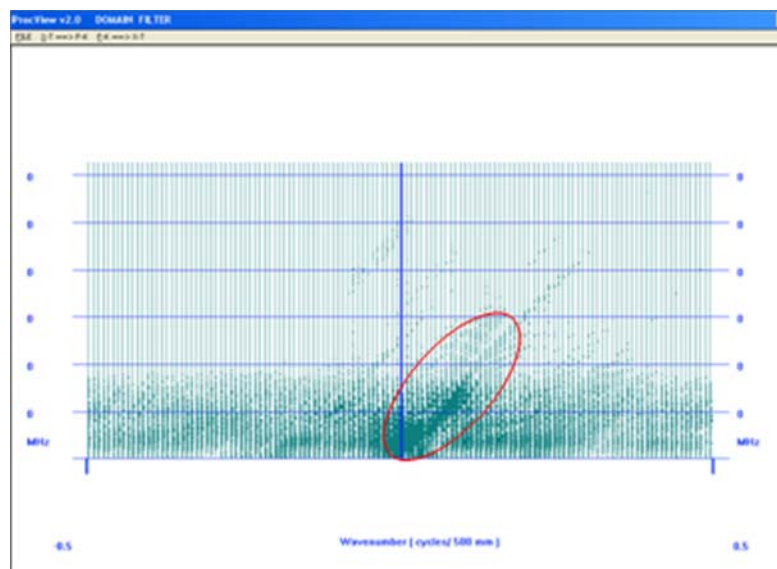
After Bandpass

Figure A2: (a) Amplitude spectrum of the record before band pass filtering. Corner frequencies are 20 – 40 – 100 and 200 MHz. Notice the two imprints of noise: a low frequency slope (0 – 10 MHz) and a high frequency peak (150 - 280 MHz). The spectrum is broad with a maximum at about 60 MHz (b) Amplitude Spectrum after band pass filtering. Low frequency slope and high frequency peak are effectively suppressed. Spectrum has become more narrower—indicating a shorter reflection wavelet.

Appendix B

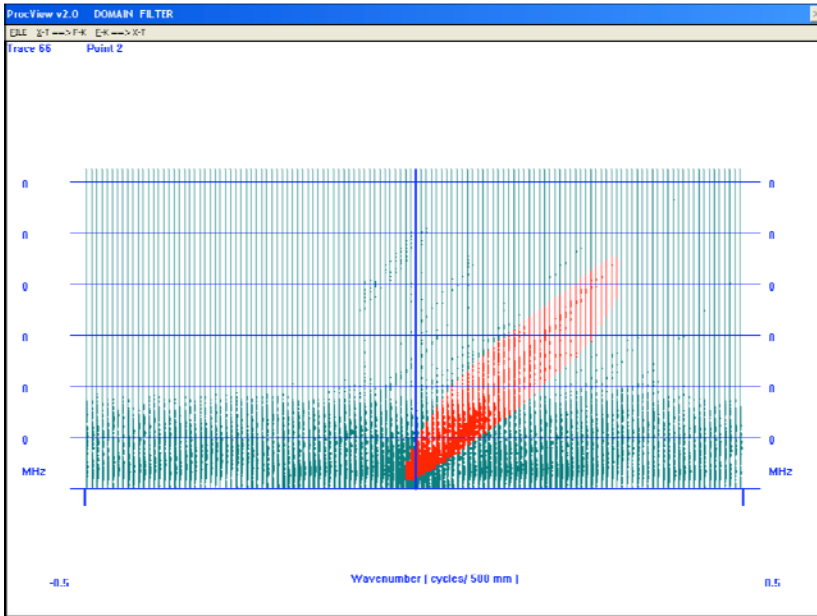


a)

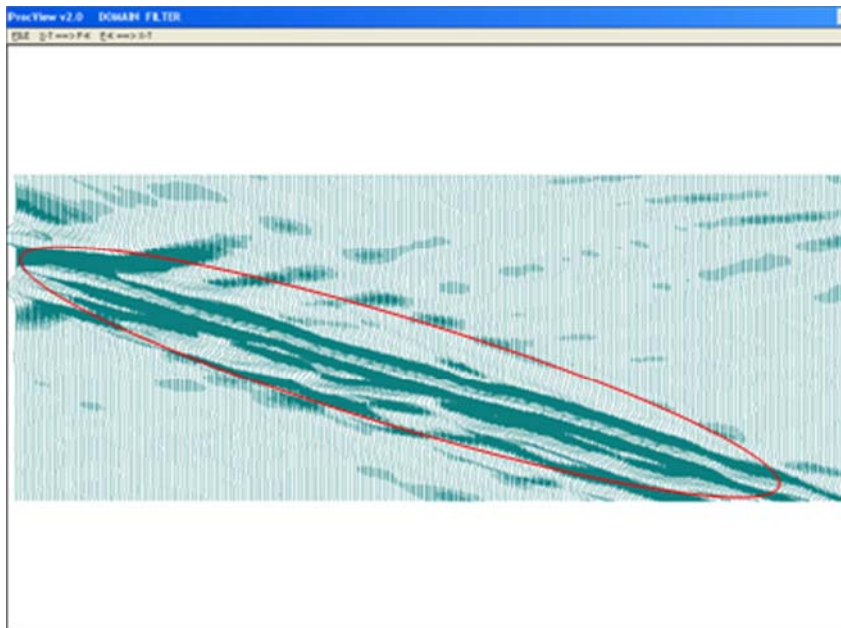


b)

Figure B1: The process of filtering by the Domain Filter. (a) Highlighted part of the record (red) is interpreted as noise. (b) The selected part of the record is displayed in the FK domain. Notice the high-amplitude dipping trend (red ellipse) that is the F-K equivalent of the red part highlighted in (a).

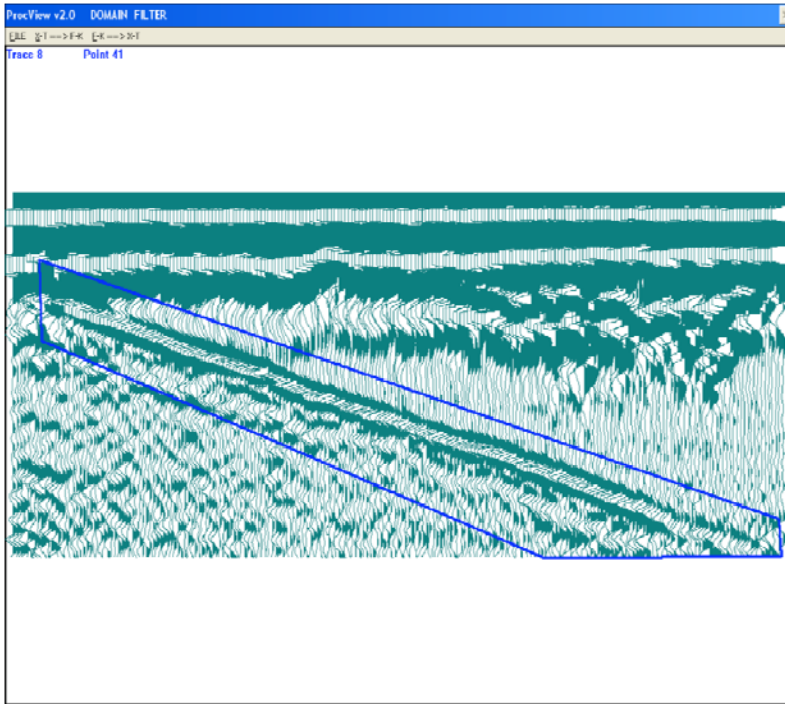


a)

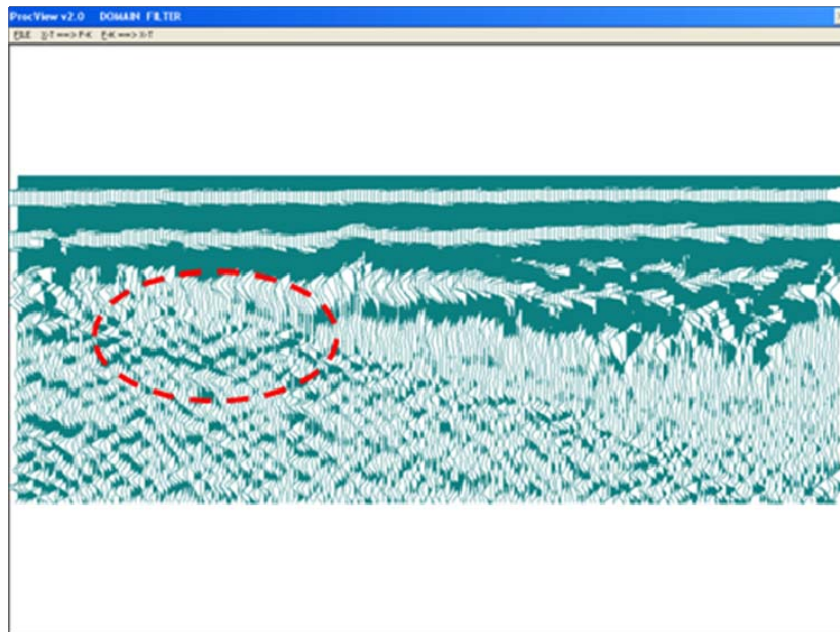


b)

Figure B2 (a) The selected part that is to be transformed back to the XT domain is highlighted in red. (b) After transformation, this is the part of the record (red ellipse) corresponding to the highlighted area that will be removed. Notice the FK transform artifacts outside the red ellipse.



a)



b)

Figure B3: (a) Record before the removal and (b) after the removal. Notice that the non-geological feature (blue rectangle) has been completely removed. The record has not been “damaged” by the artifacts introduced by the transforms when the filtering was performed. A stratigraphic sag (red dashed ellipse) is now apparent.

Appendix C

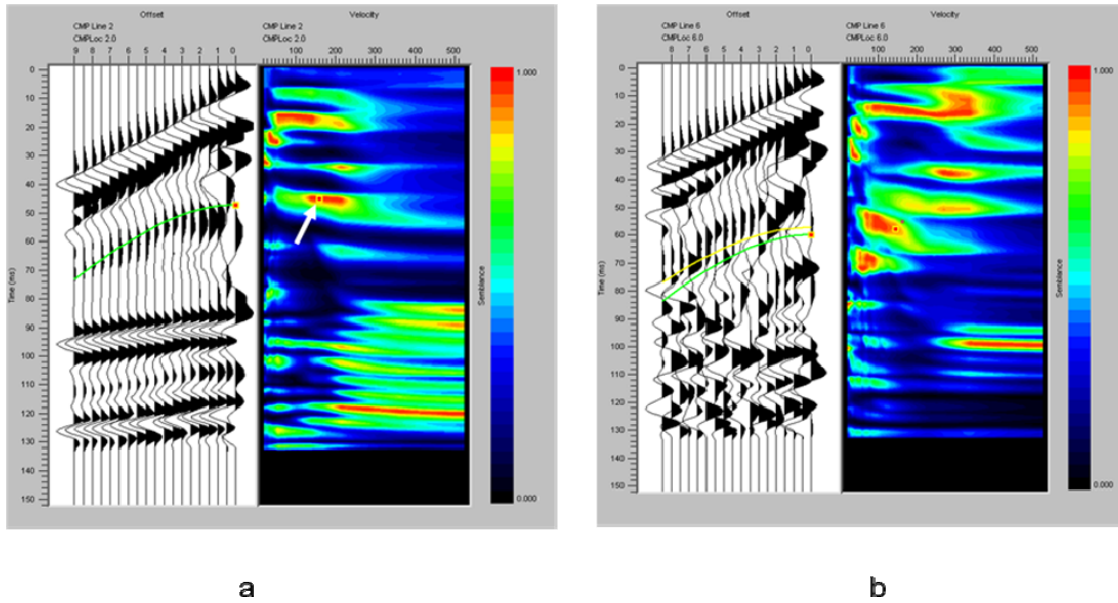


Figure C1: (a) CMP 2---The red contour (right-hand side) of plot shows a large semblance value at 47 ns indicating an RMS velocity of .16 m/ns (white arrow). The corresponding reflection (left-hand side) fits the data well. (b) CMP 6---The RMS velocity indicated at 57 ns is .15 m/ns.

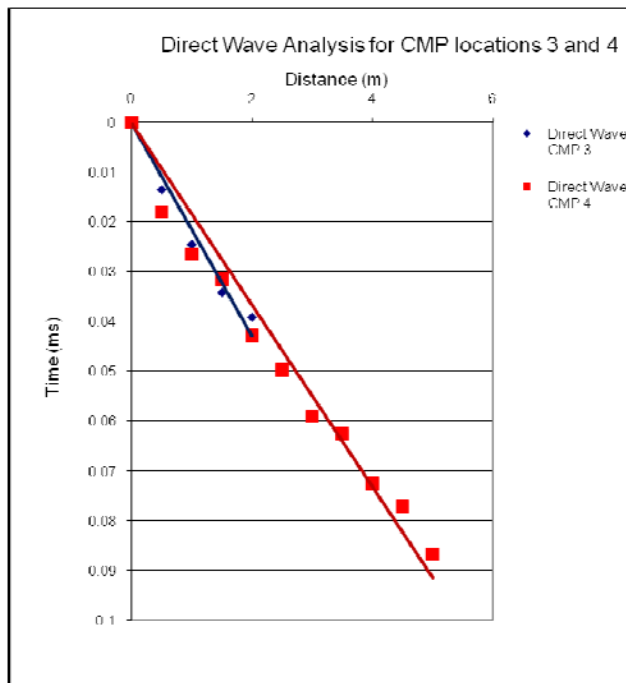


Figure C2: A least-squares fit to the travel times of the direct wave through the ground gives the velocity of the soil mantle.

Appendix D

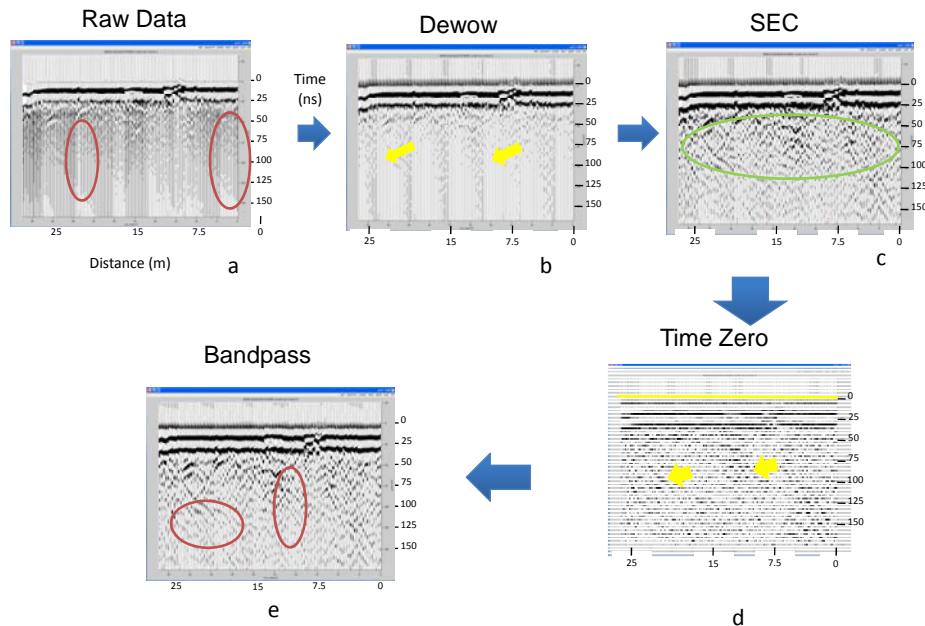
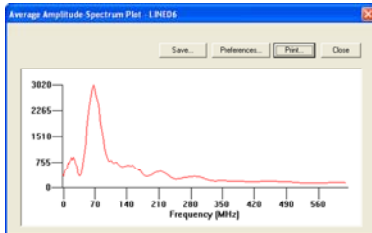
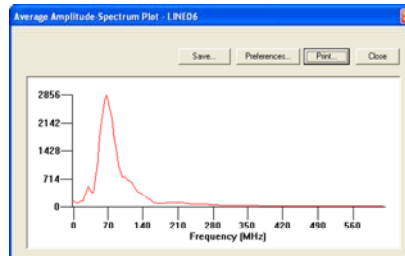


Figure D1: Processing steps for the Devils Den data. (a) Raw data. (b) Data after dewow filter applied. Dewow filter is used to remove very low frequency components of the data (red ellipses). Notice that there is still some low frequency component present (yellow arrows). (c) Spherical and Exponential Compensation restores amplitude attenuation of the signal as it propagates through the ground. After the SEC is applied, features in the middle and deep part of the record are enhanced (green ellipses). (d) Time-zero correction aligns the airwave reflection starting time (yellow) on all traces. (e) Band pass filtering removes the background noise (yellow arrows in (d)) and high frequency noise revealed by the SEC gain (yellow arrows in (c)) thus giving a cleaner record (red ellipses).

Appendix D



Before Bandpass



After Bandpass

Figure D2: (a) Amplitude spectrum plot of the record before the band pass filter cut frequencies are 20 – 40 – 100 and 200 MHz. Notice the low frequency peaks (0 – 10 MHz) and the high frequency peak (150 - 350 MHz). The spectrum is broad with a maximum at about 70 MHz (b) Amplitude Spectrum after band pass filtering. High frequency components are effectively suppressed as well as the low frequency components. The spectrum has become narrower with the maximum at about 70 MHz.

Appendix E

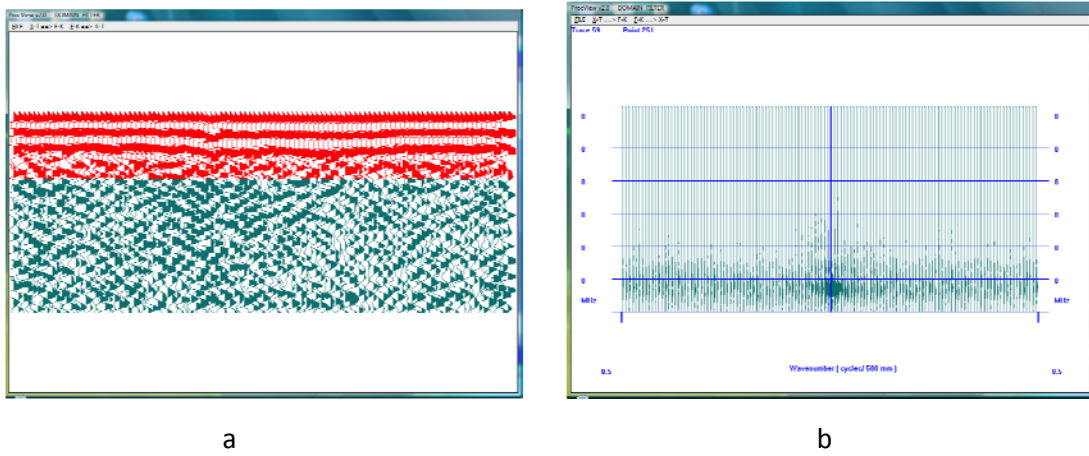
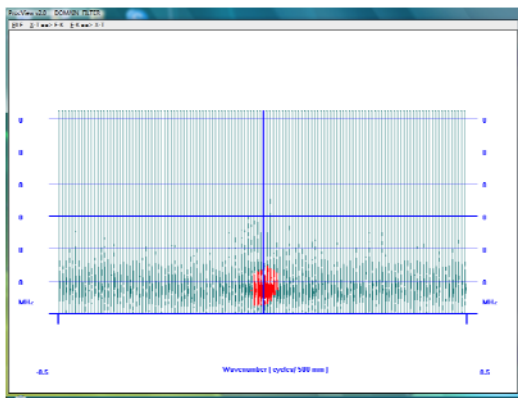
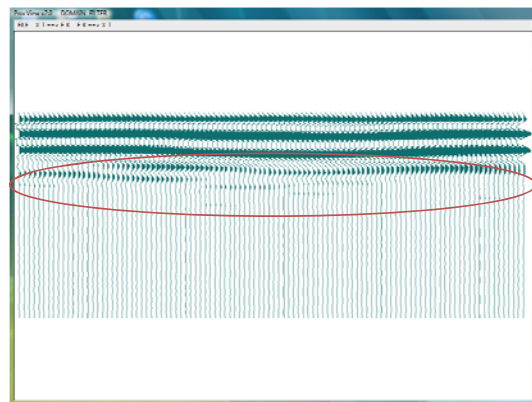


Figure E1: (a) The highlighted part of the record (red) is interpreted as noise. This is the airwave direct arrival which is very strong in the shallow part of the record and might be masking some horizontal fractures or other features. (b) The selected part of the record is displayed in the FK domain.

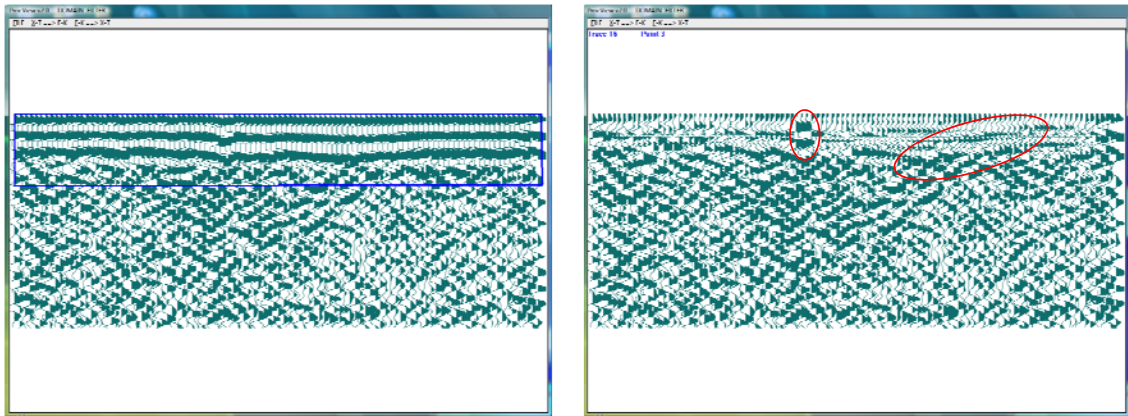


a



b

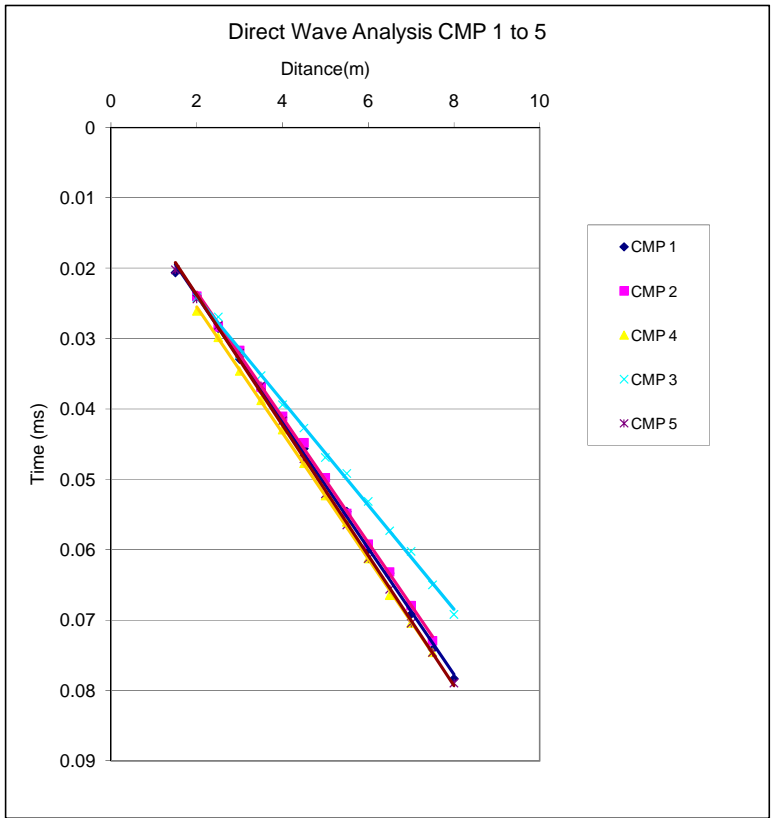
Figure E2: (a) The selected part that is to be transformed back to the XT domain is highlighted in red. (b) After transformation the part of the record (red ellipse) corresponding to the highlighted area that will be removed. Notice the FK transform artifacts outside the red ellipse that are of minor relevance.



a

b

Figure E3: Record before the removal (a) and after the removal (b) of the airwave. The airwave is gone and the record has not been “damaged” by artifacts introduced by the transforms. Shallow diffractions due to fractures at the surface of the outcrop have been revealed (red circles).



Velocity CMP 1 = 0.111 m/ns

Velocity CMP 2 = 0.112 m/ns

Velocity CMP 3 = 0.135 m/ns

Velocity CMP 4 = 0.112 m/ns

Velocity CMP 5 = 0.108 m/ns

Figure F1: Velocity of the Tishomingo granite at Devil's Den determined from the GPR direct arrival at 5 different locations on the outcrop.

Evaluation of Water Use Monitoring by Remote Sensing ET Estimation Methods

Basic Information

Title:	Evaluation of Water Use Monitoring by Remote Sensing ET Estimation Methods
Project Number:	2008OK104B
Start Date:	3/1/2008
End Date:	2/28/2009
Funding Source:	104B
Congressional District:	4
Research Category:	Climate and Hydrologic Processes
Focus Category:	Water Use, Agriculture, Hydrology
Descriptors:	ET, remote sensing, irrigation, water use
Principal Investigators:	Yang Hong, Baxter Vieux

Publication

1. Yang Hong, S. Khan, and B. Vieux (2008), Integrating Remotely Sensed and Hydrological Modeled ET for Better Water Resources Management in Oklahoma, Eos Trans. AGU, 89(53), Fall Meet. Suppl., Abstract H32B-08, SF, CA, 2008
2. Sadiq Khan, Yang Hong, and Baxter Vieux, Integrating Remotely Sensed and Hydrological Modeled ET for Water Use Management in Oklahoma, Governor Conference on Water, Oct. 2008, Oklahoma City, OK

Evaluation of Water Use Monitoring by Remote Sensing ET Estimation Methods

Final Report

Submitted to:

Oklahoma State University Environmental Institute
United States Geological Survey

Authored by:

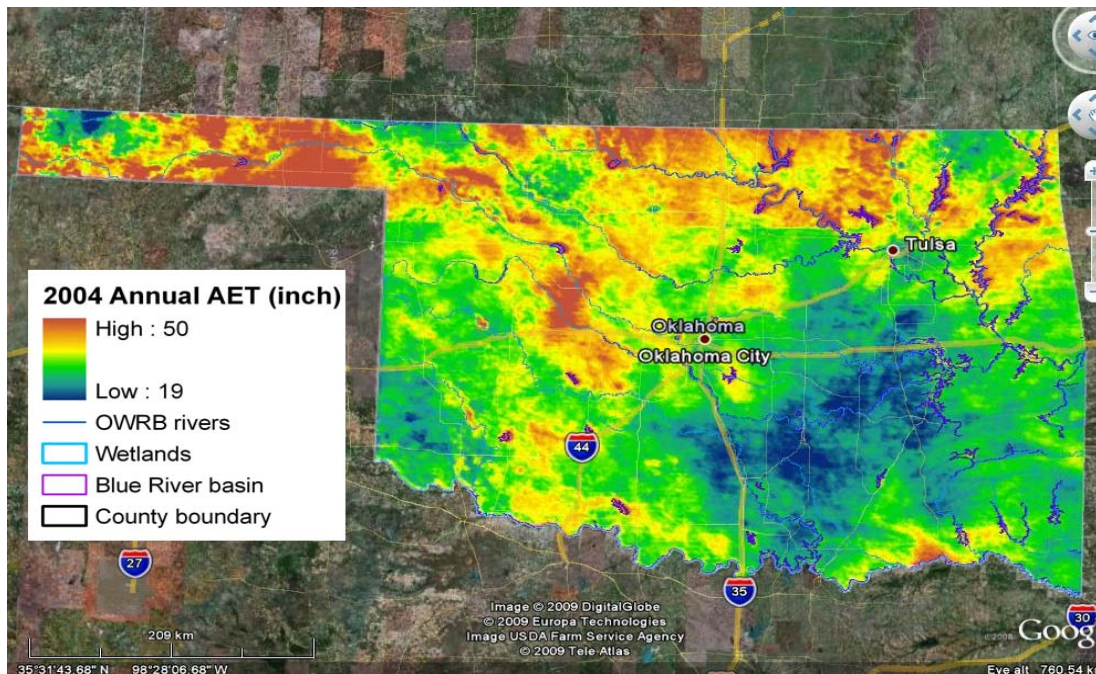
Yang Hong, Associate Professor
Baxter Vieux, Professor
Sadiq Khan, Ph.D. Student
Wenjuan Liu, Ph.D. Student

School of Civil Engineering and Environmental Science, The University of Oklahoma
Natural Hazards and Disaster Research Center, Suite 3630, National Weather Center,
120 David L. Boren Blvd., Norman, OK 73072

Collaborators:

David Dillon, Oklahoma Water Resources Board
Kenneth Crawford, Oklahoma Climate Survey

May 31, 2009



SYNOPSIS

Title: Evaluation of Water Use Monitoring by Remote Sensing ET Estimation Methods

Start Date: (03/01/2008)

End Date: (02/28/2009)

Congressional District: Oklahoma, Third.

Focus Category: Water Use, Agriculture, Hydrology, Drought, Model, Groundwater

Descriptors: Development and Evaluation of Remote Sensing Evapotranspiration (ET) Methods for Monitoring Agricultural Water Use in Oklahoma

Principal Investigators: Yang Hong, Associate Professor, University of Oklahoma

Problem Statement:

Irrigation consumes the highest share of fresh water around the world as well as US, according to the World Bank estimates 70% of fresh water use is for agriculture. The U.S. irrigates over 50 million acres of agricultural land and 32 million acres of recreational landscapes. In Oklahoma, irrigation accounts the largest water use. The hydrologic conditions in irrigated areas of Oklahoma, viz. Tillman and Texas Counties, dictate that irrigation pumped from aquifers and to a limited degree, streamflow, must supplement or entirely satisfy the crop water requirements of corn, wheat, soybeans, and other high value crops. Due to scarcity of water resources in Tillman County, the allocation by OWRB is limited to 1 ac-ft rather than 2 ac-ft that are allocated in Texas County. As the Olagalla aquifer and other sources of water supply continues to decline through exploitation, resource conflicts will arise that exacerbate the difficult allocation of insufficient water resources.

As demand for water increases, water managers need to know how much water is actually consumed in agriculture, urban, and natural environments. Increased demand for scarce water supplies has shifted water management strategy from increasing water supply to innovatively managing water use at sustainable levels. However, in order to more effectively allocate limited water, water resources managers must understand water consumption patterns over large geographical areas. There is a particular need to understand and measure the EvapoTranspiration (ET) flux where irrigated agriculture is the primary consumptive use in Oklahoma. At broader scale, measurement of ET flux would be useful in all watersheds where streamflow must satisfy demand by current and future permitted users and the ecological functions that minimum baseflow must satisfy.

The ability to monitor ET and the hydrologic water balance through the proposed approach will improve our ability to manage scarce water resources. For vegetated and agricultural land, the conversion of water into water vapor by the dual process of evaporation from the soil and the transpiration from plants' stomata, is synonymous with water consumption. Additionally, ET plays a critical role in controlling soil moisture and affecting both surface runoff and ground water flow to river channel, lakes and reservoirs.

The current Oklahoma ET model operated by the Oklahoma Climate Survey (Mesonet, 2007) estimates daily reference ET of uniform length grasses at each individual Mesonet site. Weakness of the ET Model is that it estimates the hypothetical reference ET not actual ET, and that the estimates are sparsely located across the State. First, the hypothetical uniform crop coefficient of 1.0 is not representative of the diversity of plant types in an irrigated area or watershed, thus unable to obtain actual ET to account for spatial variability of water deficit/surplus. Second, both crop coefficients and actual *ET*

are inherently variable because of crop variety, irrigation methods, weather, soil types, salinity and fertility, and/or field management that can be very different from the field used to derive the reference values. Thus, the inevitable spatial variability of actual ET in large irrigation schemes makes reference ET practice almost impossible to accurately monitor water use over large regions.

Project Objectives:

The overall objective of this project was to assess the ability and usefulness of the remote sensing ET estimation techniques/methods for monitoring regional ET and water use in Oklahoma that does not require placement of in-situ monitoring/metering devices in every field. The test beds chosen for this investigation are located in Texas and Tillman County. Towards this goal, study activities are scheduled into three phases:

- 1) We first reviewed and evaluated current remote sensing ET estimation methods used in Idaho, New Mexico, and California.
- 2) Then we calibrated and improved existing remote sensing ET estimation algorithm, with focus on surface irrigation water usage, specifically for applications in Oklahoma agricultural counties (e.g. Texas and Tillman) given its unique climate, soil, and land surface types. As a result, an improved remote sensing ET algorithm will be developed to provide actual ET that can be utilized for monitoring water use in Oklahoma.
- 3) As a natural extension, we also attempted to combine the actual ET estimation with a water balance model *Vflo*TM and evaluate the consistency between estimates of actual

ET produced from basin-scale water balance modeling with those derived from remotely sensed estimates.

The specific objectives are:

1. Estimate the actual **ET** by integrating the **MODIS** (Moderate Resolution Imaging Spectroradiometer) daily products and Oklahoma environmental observational network with 5-minute data acquisition through a **Modified Surface Energy Balance** approach in Oklahoma (thereinafter **M/M-ET**);
2. Evaluate the robustness of the M/M-ET approach using site-based flux tower observations and basin-scale water balance modeling results; and
3. Assess the feasibility of implementing the M/M-ET for an operational actual ET estimation algorithm appropriate for regional scales (e.g., the scale of irrigation projects, rather than individual fields) in real-time.

Methodology:

The M/M-ET algorithm mainly solve the Surface Energy Balance (SEB) of the land surface for latent heat flux (LE) at the time of satellite overpass and extrapolate instantaneous LE to daily ET values. The central scientific basis of SEB methods is to compute the *LE* as the residual of the energy balance equation:

$$LE = R_n - H - G \quad (1)$$

Whereas the available net radiant energy R_n (Wm^{-2}) is shared between the soil heat flux G and the atmospheric convective fluxes (sensible heat flux H and latent heat flux LE ,

which is readily converted to ET). The R_n and other components (H and G) of SEB can be derived through remote sensing information and surface properties such as albedo, leaf area index, vegetation cover, and surface temperature (T_s) etc. The following components of energy balance were solved and are explained here

Net Radiation (R_n)

R_n is computed by subtracting all outgoing radiant fluxes from all incoming radiant fluxes and includes solar and thermal radiation

$$R_n = RS\downarrow - \alpha RS\downarrow + RL\downarrow - RL\uparrow - (1 - \epsilon_o)RL\downarrow \quad (2)$$

Where $RS\downarrow$ =incoming short-wave radiation (Wm^{-2}); α =surface albedo (dimensionless);

$RL\downarrow$ =incoming long-wave radiation (Wm^2); $RL\uparrow$ =outgoing long-wave radiation (Wm^2);

and ϵ_o =broad-band surface thermal emissivity (dimensionless). The $(1-\epsilon_o) RL\downarrow$ term represents the fraction of incoming long-wave radiation reflected from the surface.

Soil Heat Flux (G)

Soil Heat Flux (G) is the rate of heat storage in the soil and vegetation due to conduction.

General applications compute G as a ratio G/R_n using an empirical equation by Bastiaanssen (2000) representing values near midday

$$G = (T_s - 273.16) (0.0038 + 0.0074\alpha) (1 - 0.98NDVI^4) R_n \quad (3)$$

Where T_s is surface temperature (K), and α =surface albedo. The Normalized Difference Vegetation Index (NDVI) is used to predict surface roughness and emissivity.

Sensible Heat Flux (H)

Sensible Heat Flux (H) is defined by the bulk aerodynamic resistance equation, which uses aerodynamic temperature (T_{aero}) and aerodynamic resistance to heat transfer (r_{ah}):

$$H = \rho_{air} C_{pa} (T_{aero} - T_a) / r_{ah} \quad (4)$$

where: ρ_{air} is air density (kg m^{-3}), C_{pa} is specific heat of dry air ($1004 \text{ J kg}^{-1} \text{ K}^{-1}$), T_a is average air temperature, (K), T_{aero} is average aerodynamic temperature (K), which is defined for a uniform surface as the temperature at the height of the zero plane displacement (d , m) plus the roughness length (Z_{oh} , m) for sensible heat transfer, and r_{ah} is aerodynamic resistance (s m^{-1}) to heat transfer from Z_{oh} to Z_m [height of wind speed measurement (m)].

From instantaneous ET_i to daily accumulated ET

At the instant of the satellite image, Latent Heat (LE) is calculated for each pixel from Equation (1-4) and is converted to instantaneous ET (ET_{inst}) in mm h^{-1} by dividing LE by latent heat of vaporization:

$$ET_{inst} = (3600 \times LE) / (\lambda \rho_w) \quad (5)$$

Where ρ_w =density of water ($\sim 1000 \text{ kg m}^{-3}$); 3,600 converts from seconds to hours; and latent heat of vaporation (J kg^{-1}) representing the heat absorbed when a kilogram of water evaporates and is computed as

$$\lambda = [2.501 - 0.00236 \times (T_s - 273.15)] \times 10^6 \quad (6)$$

Reference ET fraction (ET_{rF}) is the ratio of ET_{inst} to the reference ET_r that is defined by the American Society of Civil Engineers and can also be computed using the standard Penman-Monteith alfalfa reference method (ASCE-EWRI, 2005) at overpass time (hourly average). Finally, the computation of daily or 24-h ET (ET_d), for each pixel, is performed as:

$$ET_d = ET_{rF} \times ET_r \times 24 \quad (7)$$

Accuracy of the estimated ET, runoff, and soil moisture results were evaluated at both field and catchment scales using available Mesonet weather station and other in-situ observations. Given future funding availability, this project will further assimilate the seamless satellite-based actual ET estimates into a distributed high-resolution water balance model. Compared with traditional applications of water balance models (i.e. without the satellite-based actual ET assimilation), the combined procedure can provide significant improvements in understanding the latent heat fluxes (i.e. ET) with application to estimation of water usage by irrigated crops. Therefore, applications in watershed studies, water resource allocation, and operational flood forecasting are follow-on contributions expected from the proposed research.

Publications:

Referred Journal Papers:

Khan, S. (student), Y. Hong, B. Vieux, and W. Liu (student), Development and Evaluation of an Actual Evapotranspiration Estimation Algorithm Using Satellite Remote Sensing and Meteorological Observational Network in Oklahoma, International Journal of Remote Sensing Special Issue (submitted)

Liu, W (student), Y. Hong, S. Khan (student), P. Adhikari (student), and M. Huang, Evaluation of Global Daily Reference ET's Hydrological Utility using Oklahoma's Environmental Monitoring Network-MESONET, Water Resources Research, (submitted)

Referred Conference Paper:

Yang Hong, S. Khan, and B. Vieux (2008), Integrating Remotely Sensed and Hydrological Modeled ET for Better Water Resources Management in Oklahoma, Eos Trans. AGU, 89(53), Fall Meet. Suppl., Abstract H32B-08, SF, CA, 2008

Conference Abstract and Presentation:

Sadiq Khan, Yang Hong, and Baxter Vieux, Integrating Remotely Sensed and Hydrological Modeled ET for Water Use Management in Oklahoma, Governor Conference on Water, Oct. 2008, Oklahoma City, OK

Abstracts of Journal Papers generated from this project

Khan, S. (student), Y. Hong, B. Vieux, W. Liu (student),

Development and Evaluation of an Actual Evapotranspiration Estimation Algorithm
Using Satellite Remote Sensing and Meteorological Observational Network in Oklahoma,
International Journal of Remote Sensing Special Issue (submitted)

Abstract

In the past few years satellite remote sensing applications in actual Evapotranspiration (ET) estimation have opened frontiers in water management at local and regional scales. However previous applications have been retrospective in nature, in part because of the lack of timely availability of polar-orbiting satellite sensor in relatively high spatiotemporal resolution. Furthermore, many ground networks do not provide data in near real-time, so that the ET estimates, though useful in retrospective studies, cannot be used in operational water management decision making. **The main objective of this paper is to develop and evaluate a real-time ET estimation algorithm by integrating satellite remote sensing and environmental monitoring network in Oklahoma, USA for operational daily water management purpose.**

First, a surface-energy-balance ET estimation algorithm, MODIS/METRIC (M/M-ET), is implemented for the estimation of actual ET by integrating ET by integrating the MODIS twice daily products and Oklahoma environmental observational network with 5-minute data acquisition through a simplified Surface Energy Balance approach METRIC in

Oklahoma (i.e. MOD/METRIC and thereafter M/M-ET). Second, accuracy of the estimated ET is evaluated at the site scale using AmeriFlux tower's latent heat flux and Mesonet site crop ET on daily, 8-day and seasonal basis. The results show that M/M-ET estimation agrees with these ground observations, with daily ET bias less than **15%** and seasonal bias less than **8%**. Additionally, modeled actual ET from a water balance budget analysis in a heavily instrumented basin is compared favorably (bias <**3%**) with the M/M-ET at catchment scales on the order of several hundreds of square kilometers.

This study demonstrates that (1) the M/M-ET estimation is acceptable for daily and seasonal actual ET estimation and (2) it is feasible to implement the proposed M/M-ET algorithm at real-time rather than retrospective manner for irrigational water resources management at the scale of irrigation projects in Oklahoma.

Keyword: Evapotranspiration; MODIS; Oklahoma; Remote Sensing

Liu, W (student), Y. Hong, S. Khan (student), P. Adhikari (student), and M. Huang

**Evaluation of Global Daily Reference ET's Hydrological Utility using Oklahoma's
Environmental Monitoring Network-MESONET, *Water Resources Research*,**
(submitted)

Abstract

The central objective of this study is to evaluate the potential hydrological utility of the National Oceanic and Atmospheric Administration's Global Data Assimilation System (GDAS) 1-degree daily reference Evapotranspiration (ET₀) products by using Oklahoma world-class environmental monitoring network (MESONET) daily ET₀ over two year period (2005-2006). It showed a close match between the two independent ET₀ products, with bias within a range of 10% for most of the sites and the overall bias of -2.80%. The temporal patterns between GDAS ET₀ and MESONET ET₀ are strongly correlated, with correlation coefficient above 0.9 for all groups. This study further proposed a MODIS Land Surface Temperature (LST)-guided downscaling scheme that utilizes the MODIS 1-km LST products to disaggregate the 1-degree GDAS ET₀ to 1-km spatial resolution. Compared to a linear downscaling method as a benchmark, the MODIS LST-guided scheme not only improved the temporal correlations but also reduced the bias, absolute bias and root mean square error by 18.6%, 22.5% and 17.9%, respectively. In summary, we conclude that (1) the consistent low bias shows the original 1-degree GDAS ET₀ products have high potentials to be used in climate modeling particularly for macro-scale land surface and regional climate modeling; (2) the high temporal correlations demonstrate the capability of GDAS ET₀ to represent the major atmospheric processes

that controls the daily variation of surface hydrology; (3) with a proper downscaling method, a global daily high-spatial resolution (e.g. 1 km) of ET₀ can be derived from the GDAS ET₀ dataset and can be potentially used for a number of hydrologic applications and water resources management practices at a much improved spatial scales. The prospect of availability of global daily 1-km ET₀ has an enormous potential in hydrologic and water resources modeling because for practical purpose various techniques estimate actual ET as a fraction of ET₀ based on the soil-water content and vegetation conditions. However, additional evaluation and downscaling of GDAS ET₀ in different hydro-climatic zones should be emphasized before its hydrological utility can be fully realized.

Keywords: Evapotranspiration (ET) · Reference ET · GDAS · Oklahoma · MODIS.

Principal Findings

Mapping actual ET with satellite remote sensing eliminates a lot of expensive equipments and other time intensive tasks. Applications of the accurate and high-resolution remote sensing ET in watershed studies, water resource allocation, and operational flood forecasting are follow-on contributions expected from the proposed research.

This project demonstrated that 1) Satellite remote sensing-based ET estimation methods can be used to monitor water use in Oklahoma; 2) it is feasible for us to develop and implement a real-time remote sensing-based actual ET estimation system for water managers to monitor actual water use and thus better regulate water rights in Oklahoma.

Significance:

ET is among the most important processes in the hydrologic cycle and considered as a critical component in diverse disciplines such as those involved in water resource management, agriculture, ecology, and climate science. ET is a good measurement of irrigation effectiveness and the most important component of total water consumption in agriculture. Moreover, it is projected that climate change will influence the global water cycle and intensify ET globally. Water regulators have long wanted an efficient and inexpensive procedure to accurately map ET (irrigation consumption) over large regions and thus to improve water use regulation given limited water supply.

Results of this study show substantial promise to implement a high-resolution satellite remote sensing ET estimation system as an efficient, accurate, and inexpensive approach

to estimate the actual ET over irrigated lands in Oklahoma. Prospects of the project are very attractive for water users and managers as they cover large areas and can provide estimates at a very high resolution (30m and daily). Intensive field monitoring is also not required, although some ground-truth measurements can be critical in interpreting the satellite images. In summary, remote sensing ET estimation method compliments or even replaces conventional procedures used by state and other management ministries that solely rely on land surface point-based ET estimation approaches.

Success of this project guarantees data assimilation of the seamless actual ET products into distributed high-resolution water balance models to improve predictions of hydrologic cycle. Further applications in watershed studies, water resource allocation, and operational flood forecasting are follow-on added-value contributions expected from this research.

Students supported by this program

Student Status	Number	Disciplines
Undergraduate	1 (partial support)	Environmental Science
M.S.	0	
Ph.D.	2 (partial support for the second one)	Geography; Agriculture and Forestry Science
Post Doc	0	
Total	3	

List of Figures

Figure 1: Oklahoma’s World-Class Network of Environmental Monitoring Stations (red asterisks) with station ID’s. At the right is the 10-meter tall monitoring tower and instrumentations.....	6
Figure 2: ARM SGP Burn Site.....	9
Figure 3: ARM SGP Main Site.....	9
Figure 4: The ET is computed as a residual of the surface energy balance budget....	17
Figure 5: Study Area with AmeriFlux towers, Mesonet sites and Blue River Basin...	27
Figure 6: 2004 comparisons of daily and 8-day mean actual ET from AmeriFlux tower observations and the M/M-ET estimates through the Simplified Surface Energy Balance (SSEB) approach at ARM SGP Lamont site (when available).. Panels (a) and (b) shows the daily time series and scatter plot comparison; (c) and (d) are for every 8-day.....	29
Figure 7: Comparisons of actual ET from AmeriFlux tower observations and SSEB-based M/M-ET estimates at ARM SGP El-Reno site. Panels (a) and (b) shows the daily time series and scatter plot comparison for 2005; (c) and (d) are for 2006.....	30
Figure 8: Comparisons of crop ET (wheat) and SSEB-based M/M-ET estimates at ARM SGP Medford site. Panels (a) and (b) shows the 2004 time series and scatter plot; (c) and (d) are for 2005.....	31
Figure 9: Comparisons of crop ET (wheat) and SSEB-based M/M-ET estimates at ARM SGP EL-Reno site. Panels (a) and (b) shows the 2005 time series and scatter plot; (c) and (d) are for 2006.....	32

Figure 10: 2004 Seasonal Actual ET based on M/M with mesonet sites locations at Grant and Canadian Counties..... 34

Figure 11: Comparison of the ET estimates from SSEB-based M/M –ET approach and Water-balance budget Analysis for 2005 monthly average at Blue River Basin (Bias ratio = 2.1%)..... 36

Figure 12: Temporal comparison of spatially averaged crop/vegetation index NDVI and actual ET estimates from SSEB approach over Blue river basin during 2004, 2005 and 2006 (Growing season typical has high NDVI and high actual ET; also noticeable dry year 2006 has less crop/vegetation but slightly higher actual ET due to sufficient supply from ground water)..... 37

Figure 13: 2005 Seasonal Actual ET (inch) for Tillman County 40

Figure 14: 2005 Seasonal Actual ET (inch) for Texas County 41

List of Tables

Table 1: Satellite sensor used for rainfall, ET and soil moisture estimation.....	4
Table 2: ET-Relevant NASA MODIS data products	8
Table 3: Validation locations of ARM SGP AmeriFlux towers and Mesonet sites	10
Table 4: Comparisons of daily and 8-day mean actual ET estimates with AmeriFlux observations at ARM SGP Lamont site for year 2004.....	27
Table 5: Comparisons of daily actual ET estimates with AmeriFlux observations at ARM SGP, El-Reno site for year 2005	28
Table 6: Comparisons of actual ET estimates with crop ET at Medford site and El Reno site for wheat growing seasons.....	33
Table 7: Data for Blue River Basin used for the Water Balance.....	35
Table 8: Oklahoma Mesonet Stations located in Texas and Tillman County.....	39

Table of Contents

SYNOPSIS.....	ii
Problem Statement:.....	ii
Project Objectives:	iv
Methodology:.....	v
Net Radiation (Rn)	vi
Soil Heat Flux (G)	vi
Sensible Heat Flux (H).....	vii
From instantaneous ET _i to daily accumulated ET.....	vii
Publications:.....	ix
Refereed Journal Papers:	ix
Refereed Conference Paper:.....	ix
Conference Abstract and Presentation:.....	ix
Abstracts of Journal Papers generated from this project	x
Principal Findings	xiv
Significance:	xiv
Students supported by this program.....	xv
List of Figures	xvi
List of Tables	xviii
Table of Contents	xix
1. Introduction	1
1.1 Overview.....	1
1.2 Scope of the study.....	2
1.3 Proposed Studies.....	2
1.4 Justification of the Study	3
2. Study Area and Data.....	4
2.1 Study Area	4
2.2 Data sets	5
2.2.1 Oklahoma Meteorological Observations: Mesonet	5
2.2.2 Satellite Remote Sensing Data.....	7
2.2.3 AmeriFlux Data	8

3.	Evaluation of SEB methods for Oklahoma	11
3.1	Net Radiation R_n Calculation	11
3.2	Soil Heat Flux (G).....	12
3.3	Sensible Heat (H).....	13
3.4	Integrating MODIS data for higher temporal resolution	14
3.5	Weather Station Measurement and Ground Verification.....	15
4.	M/M-ET: (Actual ET Estimation from MODIS and Mesonet).....	17
4.1	Estimation of instantaneous actual ET using SEB approach	17
4.2	Oklahoma Mesonet Reference ET Model.....	22
5.	Results and Evaluation	24
5.1	Evaluation Indices.....	24
5.1.1	Relative bias (Bias):.....	24
5.1.2	Absolute bias (Abs. bias):.....	25
5.1.3	Root Mean Square Error (RMSE):	25
5.1.4	Correlation coefficient (CC):	25
5.2	Validation at AmeriFlux sites	26
5.3	Validation with Crop ET at Mesonet sites.....	31
5.4	Validation at Blue River Basin	35
6.	Actual ET for two counties in Oklahoma:.....	38
7.	Summary.....	42
8.	Future Work.....	43
9.	Acknowledgement:	46
10.	Reference	47

1. Introduction

1.1 Overview

Evapotranspiration (ET) is among the most important processes in the hydrologic cycle and considered as a critical component in diverse disciplines such as those involved in water resource management, agriculture, ecology, and climate science. Estimation of spatially distributed ET from agricultural areas is important as irrigation consumes the largest share in water use (Glenn et al. 2007, Shiklomanov 1998). Particularly in arid and semi arid biomes, around 90% or more of the annual precipitation can be evapotranspired, and thus ET determines the freshwater recharge and discharge from aquifers in these environments (Huxman et al. 2004). Moreover, it is projected that climate change will influence the global water cycle and intensify ET globally (Meehl et al. 2007; Huntington et al. 2006), consequently this will impact the scarce water resources.

Today, ET estimation from satellites remote sensing data in Idaho and California shows substantial promise as an efficient, accurate, and inexpensive approach to estimate the actual ET from irrigated lands throughout a growing season. Particularly, *the Idaho state-university partnership providing near-real time actual ET that helps manage irrigation water demand is among the 2007 Top 50 Government Innovations named by the Ash Institute for Democratic Governance and Innovation at Harvard University's John F. Kennedy School of Government today.* Similar water resources scarcity and need for improved estimation of available water for management of permitted water use exists in the South Central Plains, especially in Oklahoma.

1.2 Scope of the study

Remote sensing methods can provide ET maps over large areas at very high resolutions (30m and daily) although some ground-truth measurements can be critical in interpreting the satellite images. However, transforming remotely sensed images into quantitative water use information at scales relevant to water management agencies is a primary goal that has not been fully realized. Main objective of this project is to evaluate and improve the ability and usefulness of the remote sensing ET estimation algorithms in Oklahoma that does not require placement of in-situ monitoring/metering devices.

This project combined the seamless satellite observations and our existing knowledge for water balance modeling by assimilating the remote sensing ET estimates into a distributed water balance model. Compared with traditional applications of water balance models (i.e. without the satellite-based actual ET assimilation), the combined procedure can provide significant improvements in understanding the latent heat fluxes (i.e. ET) with application to estimation of water usage by irrigated crops. Application in watershed studies, water resource allocation, and operational flood forecasting are follow-on contributions expected from the proposed research.

1.3 Proposed Studies

We will first review and evaluate the remote sensing ET algorithms that have only been applied to western U.S. Then we calibrated and improved remote sensing algorithms, with focus on surface irrigation water usage, specifically for applications in Oklahoma agricultural counties (e.g. Texas and Tillman) given its unique climate, soil,

and land surface types. As a natural extension, we also proposed to combine a water balance model *Vflo* with remote sensing estimates of ET to provide more accurate prediction of runoff, soil moisture etc for better water use management. Accuracy of the estimated ET, runoff, and soil moisture results will be evaluated at both field and catchment scales using available Mesonet weather station and other in-situ observations.

Deliverables:

1) Evaluation of current satellite remote sensing-based ET estimation algorithms to monitor water use in Oklahoma; 2) Calibration of an improved algorithm to estimate seamless high-resolution actual ET for irrigation land in OK; 3) Assessment of the feasibility of implementing a real-time remote sensing-based ET estimation system for water managers to better monitor actual ET and thus regulate water use in Oklahoma.

1.4 Justification of the Study

Recent developments in ET monitoring by remote sensing methods has been applicable in the western U.S. and such technology especially benefits management of water demand in agricultural areas that depend on irrigation. However, transforming remotely sensed images into quantitative water use information at scales relevant to water management agencies is a primary goal that has not been fully realized in Oklahoma. With the advent of new satellite technology and comprehensive water balance and runoff models, opportunities exist to develop algorithms and apply remote sensing information for the benefit of water resources management. Some of the potential sensors that are used and can be utilized in Oklahoma for water resource management are listed in table 1.

Table 1: Satellite sensor used for rainfall, ET and soil moisture estimation.

Satellite	Repeat cycle	Spatial resolution	Parameters
TMI/PR/GOES	3-hour	4-km	Rainfall, soil moisture, vegetation index and fraction, Thermal Infrared, Surface Skin Temperature, air temperature, infrared/clouds, incident solar and atmospheric radiations, albedo, leaf area index, land cover and land use, sensible heat and latent heat fluxes.
AMSR-E	Daily	25km	
MODIS	0.5 day	250m	
AVHRR	0.5 day	1100m	
GOES	15 minutes	4000m	
LANDSAT 5	16 days	30m	
LANDSAT 7	16 days	30m	
ASTER	16 days	15m or 60m	

2. Study Area and Data

2.1 Study Area

Oklahoma provides a unique setting to implement and evaluate remote sensing ET estimation methods. The region has an extensive and well distributed meteorological observation network, known as Mesonet stations (Figure 1). In addition to Mesonet towers, there are a fair number of surface flux observation stations (AmeriFlux towers) in the Southern Great Plain (SGP), the first field measurement site is established by USA

DOE's Atmospheric Radiation Measurement (ARM) Program. AmeriFlux, part of the global Fluxnet network that was established in 1996 provide continuous observations of ecosystem level exchange of CO₂, water, energy and other climatological variables (<http://www.daac.ornl.gov/FLUXNET/fluxnet.html>). Moreover, Oklahoma has several heavily instrumented watersheds, which enable us to compare the remote sensing actual ET estimates with water balance modeled results at the catchment scale. The Blue River basin is located in south central Oklahoma, covering an approximate area of 1,200 km². The upper part of the basin overlies the Arbuckle-Simpson aquifer, which provides water to streams and rivers as baseflow, constituting the principal water source of many towns in the Chickasaw National Recreation area, including Ada and Sulphur, where the water is used for public water supply, irrigation, recreation, agriculture, industrial use and mining. Map of the study area, AmeriFlux towers, Mesonet sites, and the Blue River basin characteristics are shown in (Figure 5). The study area extends over the states of Oklahoma with longitude from 94.4° W to 103.0° W and latitude from 33.6° N to 37.0° N.

2.2 Data sets

2.2.1 Oklahoma Meteorological Observations: Mesonet

The Oklahoma Mesonet is a world-class network of environmental monitoring stations jointly managed by the University of Oklahoma (OU) and Oklahoma State University (OSU). Established as a multipurpose network, it operates more than 120 automated surface observing stations covering the state of the Oklahoma and measures comprehensive meteorological, hydrological, and agricultural variables since the early

1990's. These monitoring sites have collected Over 3,758,558,640 observations since January 1st, 1994. (<http://www.mesonet.org>; McPherson et al. 2007). At each site, the environment is measured by a set of instruments located on or near a 10-meter-tall tower. The measurements are packaged into "observations" every 5 minutes; then the observations are transmitted to a central facility every 5 minutes, 24 hours per day year-round. The Oklahoma Climatological Survey (OCS) at OU receives the observations, verifies the quality of the data and provides the data to Mesonet customers. It only takes 5 to 10 minutes from the time the measurements are acquired until they become available to the public.

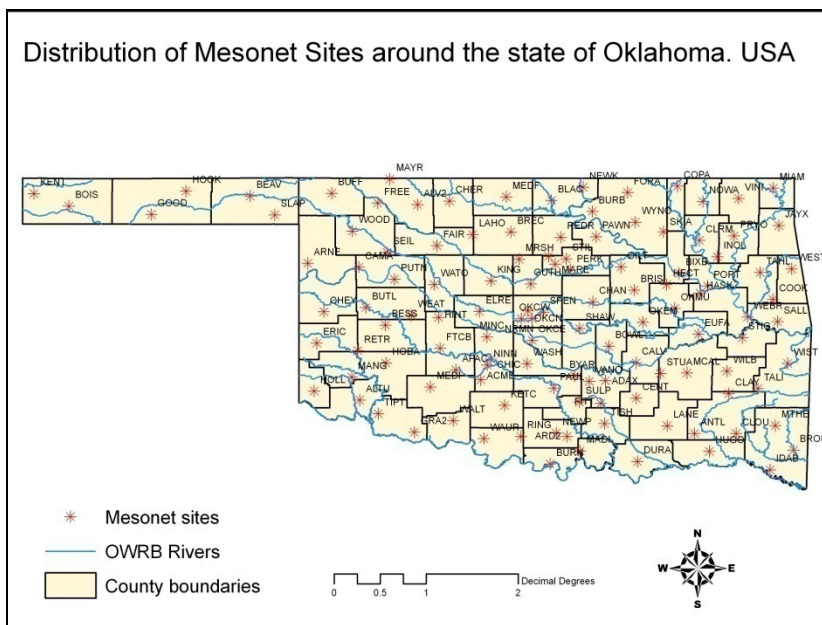


Figure 1: Oklahoma's World-Class Network of Environmental Monitoring Stations (red asterisks) with station ID's. At the right is the 10-meter tall monitoring tower and instrumentations.

2.2.2 Satellite Remote Sensing Data

The MODIS (Moderate Resolution Imaging Spectroradiometer) sensors, with 36 spectral bands (20 reflective solar and 16 thermal emissive bands), provide unprecedented information regarding vegetation and surface energy (Justice et al. 2002), which can be used to develop a remotely sensed ET model (Mu et al. 2007). ET-relevant MODIS data used in this study are listed in (Table 2). Wan and Li (1997) described the retrieval of MOD11 land surface temperature (LST) and emissivity from MODIS data. Detailed information about MOD09 surface reflectance products is provided in Vermote et al. (1997) and Xiong et al. (2007). The algorithm for retrieving the Vegetation Index (MOD13) is presented by Huete et al. (2002). The computation of broadband Albedo (MOD43B3) by integrating bi-hemispherical reflectance data modeled over MODIS channels 1-7 (0.3-5.0 μm) is explained in Schaaf et al. (2002). All NASA MODIS land products include so called Quality Assessment Science Data Sets (QA-SDS), which considers the atmospheric conditions in term of cloud cover and aerosol content, algorithm choices, processing failure, and error estimates (Colditz et al. 2006). These data products were extracted and processed from the Land Processes Distributed Active Archive Center (LP DAAC) at the USGS EROS Data Center), with the standard Hierarchical Data Format (<http://LPDAAC.usgs.gov>). For more information on MODIS, please refer to <http://modis.gsfc.nasa.gov>.

Table 2: ET-Relevant NASA MODIS data products

Product ID	Layer	Spatiotemporal resolution	MODIS QA-SDS ^a Analysis (Quality flags passed)
MOD11A2	Land Surface Temperature (LST)	1-km ^b , overpass	General quality: good
	Emissivity	1-km, overpass	
	View Angle	1-km, overpass	
	Recording time	1-km, overpass	
MOD13Q1	Vegetation index	1-km, 16-day	quality: good ~ perfect mixed clouds: no
	NDVI		
MOD43B3	Albedo	1km, 16-day	Quality: good and acceptable Snow: no
MOD09Q1	Red reflectance	250m, 8-day	Quality: good Clouds: clear Band quality: highest
	NIR reflectance		
MOD15A2	Leaf Area Index (LAI)	1km, 8-day	Quality: good Cloud: clear or assumed clear
MOD12Q1	Land Cover Type	250m, annual	Quality: good

^aQuality Assessment Science Data Sets

^bThe swath products were gridded using the MODIS reprojection tool (MRT)

^cThe view angles were analyzed to remove effects from scan geometry caused by increasing IFOV towards the edges of the scan lines

2.2.3 AmeriFlux Data

The location and general site characteristics are summarized in (Figure 5) and (Table 3).

Table 2 lists the two Atmospheric Radiation Measurements (ARM) SGP eddy covariance tower sites, located at the ARM SGP extended facilities in Lamont and El Reno, Oklahoma, respectively. The two Mesonet sites at El Reno and Medford with Crop ET data are also selected for comparison.

ARM SGP Burn (OK, USA) and ARM SGP Control (OK, USA)

Both of these sites are inactive at the moment but we used the available data sets from previous years. The ARM SGP Burn and control sites are located in Canadian county and are very close to each other. The coordinated are latitude 35.54 and longitude 98.04. The elevation of the both areas is 421 meters (Table 3). IGBP classifies the vegetation in the both area as grassland.



Figure 2: ARM SGP Burn Site

ARM SGP Main (OK, USA)

The IGBP classifies the vegetation type as croplands, and AmeriFlux website classifies the vegetation type as agricultural and dominant vegetation types are wheat, corn, and soybean that have periodic rotation. The elevation of the area is 315 meters (Table 3). The canopy height of the area is ranging from 0 to 0.5m. The soil type of the area is silty clay loam, fine mixed thermic Underitic Paleustolls. Climate of the area is classified as temperate continental. Total precipitation is not very high; in 2003-2004 the range of annual sums were 552-901. Seasonal temperatures vary greatly such as



Figure 3: ARM SGP Main Site

the maximum air temperature in 2003-2004 was 43.6 °C and the minimum air temperature is -17.5 °C.

Table 3: Validation locations of ARM SGP AmeriFlux towers and Mesonet sites

ARM SGP Site	Elevation (m)	County	Vegetation
El Reno	421	Canadian	Pasture (ungrazed)
Lamont	315	Grant	Pasture and wheat
Mesonet Site	Elevation (m)	County	Ecosystem
Medford	332	Grant	Wheat and Pastures
El Reno	419	Canadian	Pasture

3. Evaluation of Surface Energy Balance methods for Oklahoma.

3.1 Net Radiation R_n Calculation

As modification of Equation 1 in previous section, in practice net radiation R_n is computed from the land surface radiation balance as:

$$R_n = (1 - \alpha) R_s + (\varepsilon L_{in} - L_{out}) \quad (8)$$

Where α is surface albedo, R_s is solar radiation (Wm^{-2}), ε is land surface emissivity and L_{in} and L_{out} are incoming and outgoing longwave radiation (Wm^{-2}). The α is determined by integrating spectral reflectance in the six shortwave bands of the Landsat images, and L_{in} and L_{out} are computed as functions of surface temperature derived from the satellite images. The ε is computed from vegetation indices derived from two of the shortwave bands. First, it requires radiometric and atmospheric calibration of satellite images for estimating spatial ET using METRIC. For this purpose, the digital numbers (DN) stored in the satellite image are first converted into radiance (L_b), for each band as $L_b = (\text{gain} \times \text{DN}) + \text{bias}$, then at 'sensor' or 'Top-of-the-Atmosphere' (TOA; exoatmospheric) reflectance values for the shortwave bands are estimated. Reflectance values are calculated by dividing the detected radiance at the satellite (for each band) by the incoming energy (radiance) in the same shortwave band. The incoming radiance is a function of mean solar exoatmospheric irradiance, solar incidence angle, and the inverse

square of the relative earth-to-sun distance. In case of the thermal band, the spectral radiance values are converted into effective at-satellite temperatures of the viewed earth-atmosphere system under an assumption of unity for surface emissivity and using pre-launch calibration constants by means of an inverted logarithmic formula. Subsequently, surface reflectance values are computed after applying atmospheric interference corrections, on the TOA reflectance image, for shortwave absorption and scattering using narrowband transmittance values for each band. Radiative transfer models will be used in the parameter calibration.

3.2 Soil Heat Flux (G)

For several applications of Equation 3 in western U.S., approximate values of $G=0.5R_n$ has been generally assigned for water and snow. Snow is distinguished according to T_s 277 K, NDVI=0 and high surface albedo, and water is distinguished as NDVI=0 and low albedo. However, the $G =0.5R_n$ for water should be refined according to the depth and turbidity of water bodies and time of season (Allen and Tasumi 2005). For example, G/R_n will be less than 0.5 for turbid or shallow water bodies due to the absorption of short-wave radiation near the water surface for turbid water and the reflection of solar radiation from and warming by the bottom for shallow systems. For 24 h periods, G/R_n will be less than the instantaneous value for water. The G/R_n ratio for snow for 24 h periods is assumed to be nearly zero or slightly positive during snowmelt. Alternative methods to derive G will be calibrated by USDA-ARS for irrigated crops at Texas and Tillman Counties:

$$G = R_n (0.05 + 0.18e^{-0.521 \text{ LAI}}) \text{ (LAI} \geq 0.5) \quad (9a)$$

$$G = (1.80 (T_s - 273.15) + 0.084 R_n \text{ (LAI}<0.5)) \quad (9b)$$

Eq. 9a indicates that G/R_n decreases with increasing leaf area, for the same reason, and Eq. 9b indicates that for bare soil G increases in proportion to surface temperature. Eq. 9 has been used with applications in Idaho, California, and New Mexico (all desert or semi-arid soils). When applying METRIC to semi-arid soils where near-surface thermal conductivities are most likely smaller than tilled soils due to cracks, delaminated crust, lack of structure, or very low soil water content, the G/R_n from Eq. 9b is limited and even reduced for T_s of the dry hot pixel. Thus, modifications and re-calibration are necessary when the surface is covered by vegetation that functions as an insulator on the surface.

3.3 Sensible Heat (H)

Remote sensing algorithms obtain ET as the residual of the SEB after measuring and/or modeling net radiation R_n , ground heat flux G , and sensible heat flux H . Among these fluxes, H is the most complex to estimate and its value is associated with greater uncertainty. In practice, METRIC estimates H from wind speed and surface temperature using a unique “internal calibration” of the near surface to air temperature difference (dT) as modified from Equation 4 (Bastiaanssen et al. 2005):

$$H = \rho_{\text{air}} C_{p\text{a}} (a + bT_s) / r_{\text{ah}} = (\rho_{\text{air}} c_p dT) / r_{\text{ah}} \quad (10)$$

Where a and b are empirical coefficients. dT (K) is a parameter that represents the near surface temperature difference between surface and near surface at height about 2m, and that the indexing of dT to T_s does not rely on absolute values of T_s , which allegedly reduces the error in calculating H substantially. While apply the equation to agricultural

lands in OK, coefficient a and b are required to be calibrated for different land surface types from the remote sensing images. The determination of a and b involves locating a hot (dry) pixel in an agricultural field with higher T_s and a cold (wet) pixel with a lower T_s (typically one in an irrigated agricultural setting) in the remote sensing image. Once these pixels have been identified, the energy balance of Equation (1) can be solved as:

$$H_{cold} = (R - G)_{cold} - LE_{cold} \quad (11)$$

$$H_{hot} = (R - G)_{hot} - LE_{hot} \quad (12)$$

Where H_{hot} and H_{cold} are the sensible heat fluxes for the hot and cold pixel, respectively. A hot, dry pixel (typically a dry, bare soil surface) is selected as the “hot pixel”, and latent heat flux LE_{hot} from the pixel is assumed zero, which means that all available energy is partitioned to the sensible heat H . And the H , from the cold pixel is assumed zero ($LE=R_n-G$). With the calculation of H_{hot} and H_{cold} , the coefficients a and b can be calibrated for other pixels within the same remote sensing image using a linear interpolation based on T_s between these two extreme pixels where H and dT are known. However, LE_{hot} can be non-zero and can be calculated according to a soil water budget if rainfall has occurred shortly before the image acquisition date. Therefore, we propose to use Antecedent Precipitation Index (API) from radar and satellite rainfall to adjust the LE_{hot} . As an extension of this project, we plan to incorporate the ET estimates into a distributed water balance model *Vflo* in order to validate the components of water balance budget (see Section 4.4 for detail).

3.4 Integrating MODIS data for higher temporal resolution

In Equation 6-7, the instantaneous ET_{inst} or ET_{iF} values at the satellite image time are assumed to be equal to values representing the ET for the 24 h period. The ASTER and Landsat satellites are polar orbiters and revisit the same path every 16 days. The frequency is also decreased by cloudy condition. Thus, monthly and seasonally ET are estimated by linearly interpolating the ET_{rF} values for periods in between two consecutive images. However, this linear interpolation does not account for the daily wetting and drying events of individual fields that are not captured by Landsat images. Therefore, the interpolation generates uncertainty in the ET estimates, especially for short time periods. We will use MODIS surface skin temperature data with 1-2 day revisit period to increase the temporal resolution of ET estimates from LANDSAT and ASTER.

3.5 Weather Station Measurement and Ground Verification

We will use measurements of Lysimeters and Scintillometers from the Oklahoma Mesonet network, a system of 115 automated measurement stations across Oklahoma. These measurements will verify the remote sensing estimates of boundary layer fluxes of sensible, latent, and ground heat, as well as the radiation balance. Particularly, the weather stations used in this project are listed in Table 3. We will use spatially distributed meteorological weather stations (one of the advantages of OK state) to measure energy balance components (R, G, and H) and determine in particular how the H is related to temperature lapse rate, wind speed, water vapor deficit, and vegetation heights. First, the weather station measurements H will be used to validate estimates derived from the remote sensing ET estimation (METRIC) algorithm applied on data from synchronous ASTER and MODIS satellite overpasses. Second, parameters in the METRIC algorithm

for Texas county high terrain lapse rates, wind speeds, and surface roughness will be critically calibrated and improved by considering meteorological measurements and archived numerical weather model data. Through this work we will make a lasting contribution to ET estimation from METRIC and other SEB-based remote sensing algorithms for current and future satellite mission.

4. M/M-ET: (Actual ET Estimation from MODIS through a Modified SEB-METRIC Approach)

4.1 Estimation of instantaneous actual ET using SEB approach

In this paper we utilized a simplified version of the Surface Energy Balance (SEB) approach to estimate actual ET while maintaining and extending the major assumptions in the SEBAL and METRIC method. The central scientific basis of SEB is to compute the ET as the residual of the energy balance equation:

$$LE = \lambda ET = R_n - G - H \quad (13)$$

ET is calculated as a “residual” of the energy balance

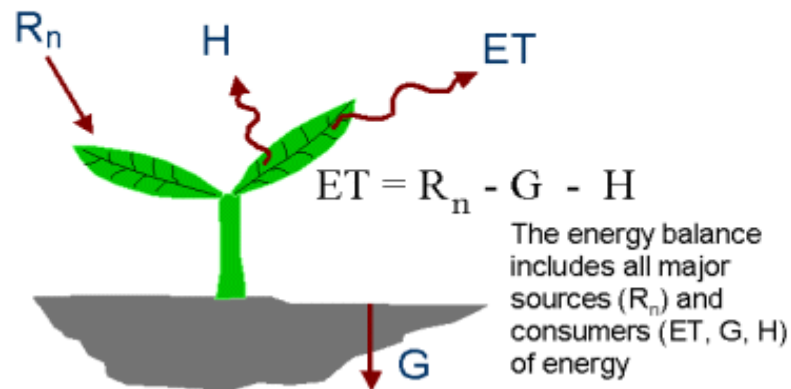


Figure 4: The ET is computed as a residual of the surface energy balance budget.

where λ is the latent heat of water evaporation constant; R_n is net radiation flux; G is soil heat flux; and H is sensible heat flux to the atmosphere (units are Wm^{-2}). Thus, ET is calculated as the residual amount of energy remaining from the surface energy balance budget, where the available R_n is shared between the G and the atmospheric convective fluxes (sensible heat H and latent heat LE). The R_n and other components (i.e. G) of SEB can be derived through remote sensing information and surface properties such as albedo, leaf area index, vegetation cover, surface temperature, and meteorological observations within the study area (Su et al. 2002; Bastiaanssen et al. 2005; and Allen et al. 2007). The equation to calculate the net radiation flux is given by

$$R_n = (1 - \alpha) \cdot R_{swd} + \varepsilon \cdot R_{lwd} - \varepsilon \cdot \sigma \cdot T_s^4 \quad (14)$$

Where α is surface Albedo; R_{swd} and R_{lwd} are incoming shortwave and longwave radiation respectively; ε is surface emissivity; σ is the Stefan-Boltzmann constant, and T_s is the land surface temperature. Soil heat flux (G) was modeled as a function of R_n , vegetation index, surface temperature, and surface albedo (Bastiaanssen, 2000):

$$G = R_n \cdot [(T_s - 275.15) \cdot (0.0038 + 0.0074\alpha) \cdot (1 - 0.98NDVI^4)] \quad (15)$$

where, NDVI is the Normalized Difference Vegetation Index $[(R-NIR)/(R+NIR)]$. R is reflectance in the red band and NIR is reflectance in the near infrared band.

Sensible heat flux (H) is defined by the bulk aerodynamic resistance equation, which uses aerodynamic temperature (T_{aero}) and aerodynamic resistance to heat transfer (r_{ah}):

$$H = \rho_a \cdot Cp_a (T_{aero} - T_a) / r_{ah} \quad (16)$$

where: ρ_a is air density (kg m^{-3}), Cp_a is specific heat of dry air ($1004 \text{ J kg}^{-1} \text{ K}^{-1}$), T_a is average air temperature (K), T_{aero} is average aerodynamic temperature (K), and r_{ah} is aerodynamic resistance (s m^{-1}) to heat transport. In SEBAL and METRIC (Allen et al. 2005; Tasumi et al. 2005), H usually results from dividing the gradient of vertical temperatures (dT) by the aerodynamic resistance of heat transport (r_{ah}), without needing to know T_a or T_{aero} .

$$H = \rho_a \cdot Cp_a \left(\frac{dT}{r_{ah}} \right) \quad (17)$$

Allen et al. (2007a) explained that dT (K) is a parameter that represents the near surface temperature difference between two different elevation z_1 and z_2 , and that the indexing of dT to T_s does not rely on absolute values of T_s , which allegedly reduces the error in calculating H substantially. One key assumption of SEBAL and METRIC is the linear relationship between dT and T_s land surface temperature (Bastiaanssen et al. 1998; Allen et al. 2005), characterized in Equation (18).

$$dT = a + b \cdot T_s \quad (18)$$

where a and b are empirically determined constants.

The determination of a and b in Equation (18) involves locating dry or wet limiting cases, a dry-limit pixel with high T_s and a wet-limit pixel with low T_s . Thus, the linear equation can be computed using the two anchor points. Typically a dry bare soil surface is selected as the “hot pixel”, and latent heat flux LE_{dry} from the pixel is assumed zero, which means that all available energy is partitioned to the sensible heat H_{dry} . Therefore, at the dry limit,

the latent heat (or the evaporation) becomes zero due to the limitation of soil moisture, and the sensible heat flux is at its maximum value. Once these pixels have been identified, the energy balance of Equation (13) can be solved for

$$LE_{dry} = (R_n - G)_{dry} - H_{dry} \equiv 0 \text{ or } H_{dry} = (R_n - G)_{dry} \quad (19)$$

And for the wet-limit, the H_{wet} is assumed zero and LE_{wet} is assumed to have an LE value equal to 1.05 times that expected for a tall reference crop (i.e., alfalfa; Allen et al., 2007a). Therefore, the energy balance of Equation (13) for the wet-limit can be solved as:

$$LE_{wet} = (R_n - G)_{wet} - H_{wet} = (R_n - G)_{wet} = 1.05 \cdot ET_{reference} \quad (20)$$

With the determination of H_{dry} and H_{wet} , proportional coefficients of other pixels can be calibrated within the same remote sensing image using a linear interpolation based on LST between these two extreme pixels. For more detail, please refer to Bastiaanssen et al. (1998) and Allen et al. (2005). Here we adopted the METRIC approach to identify hot and cold pixels. The landscape is simplified as a mixture of vegetation and bare soil. Fractional canopy coverage f_c , whose value is between 0 and 1, is related to MODIS Normalized Difference Vegetation Index (NDVI):

$$f_c = \frac{NDVI - NDVI_{min}}{NDVI_{max} - NDVI_{min}} \quad (21)$$

The surface energy balance computation is then based on the determination of the relative instantaneous ET fraction (ET_f) given by:

$$ET_f = \frac{\lambda E}{H + \lambda E} = \frac{\frac{H_{dry} - H}{H_{dry} - H_{wet}} \cdot \lambda E_{wet}}{R_n - G} \quad (22)$$

Eqs. (13) – (22) above constitute the basic formulation of SEB. The actual sensible heat flux H is obtained by solving a set of non-linear equations and is constrained in the range set by the sensible heat flux at the wet-limit H_{wet} and the dry-limit H_{dry} . An alternative to compute the ET_f is to assume, according to Senay et al. 2008 that dry-hot pixels experience very little ET and wet-cold pixels represent maximum ET throughout the study area, and the temperature of hot and cold pixels can be used to calculate proportional fractions of ET on a per pixel basis. Thus, the ET_f can also be calculated for each pixel by applying the following equation (Equation 23) to each of the MODIS land surface temperature grids:

$$ET_f = \frac{T_{hot} - T_{i,j}}{T_{hot} - T_{cold}} \quad (23)$$

Where T_{hot} is the average of the *hot* pixels selected for a given scene; T_{cold} is the average of the *cold* pixels selected for that scene; and $T_{i,j}$ is the MODIS land surface temperature value for any pixel in the composite scene.

In practice, the ET_f is used in conjunction with reference ET (ET_r) described in the following 3.2 section to calculate the per pixel instantaneous actual ET (ET_a) values in a given scene according to METRIC in Allen et al. 2005:

$$ET_a = ET_f \cdot ET_r \quad (24)$$

A key assumption of the method is that the ET_f is nearly constant, which is often observed to be the case according to [Shuttleworth *et al.* 1989; Sugita and Brutsaert, 1991; Brutsaert and Sugita, 1992; Crago, 1996]. This allows instantaneous estimates of the ET_f at MODIS overpass times to be extrapolated to estimate daily average ET. The daily ET can thus be determined as:

$$ET_{daily} = \sum_{i=1}^{day} (ET_f \times ET_r^i) \quad (25)$$

Where ET_{daily} is the actual ET on a daily basis (mm d^{-1}), i is temporal resolution of computed reference ET (e.g. hourly or 5-minute), the λ is the latent heat of vaporization (JK g^{-1}), ρ_w is the density of water (Kgm^{-3}) and $\overline{R_n}$ is the daily net radiation flux.

4.2 Oklahoma Mesonet Reference ET Model

The Oklahoma reference ET calculations are based on the standardized Penman-Monteith reference ET equation recommended by the American Society of Civil Engineers (ASCE) and the computational procedures found in [Allen et al.](#) (1994a, 1994b) based on the experimental work in Kimberly, Idaho ([Wright](#), 1996):

$$\text{Reference ET} = \frac{0.408\Delta(R_n - G) + \gamma \frac{C_n}{T + 273} u_2 (e_s - e_a)}{\Delta + \gamma(C_d u_2)} \quad (26)$$

Where:

Reference ET = Standardized reference evapotranspiration (mm d^{-1} for daily or mm h^{-1} for hourly time steps),

R_n = Calculated net radiation at the crop surface ($\text{MJ m}^{-2} \text{d}^{-1}$ for daily time steps or $\text{MJ m}^{-2} \text{h}^{-1}$ for hourly time steps),

G = Soil heat flux density at the soil surface ($\text{MJ m}^{-2} \text{d}^{-1}$ for daily time steps or $\text{MJ m}^{-2} \text{h}^{-1}$ for hourly time steps),

T = Mean daily or hourly air temperature at 1.5 to 2.5-m height ($^{\circ}\text{C}$),

u_2 = Mean daily or hourly wind speed at 2-m height (m s^{-1}),

e_s = Saturation vapor pressure at 1.5 to 2.5-m height (kPa), for daily computation, the value is the average of e_s at maximum and minimum air temperature,

e_a = Mean actual vapor pressure at 1.5 to 2.5-m height (kPa),

Δ = Delta, the slope of the saturation vapor pressure-temperature curve ($\text{kPa } ^{\circ}\text{C}^{-1}$),

γ = Psychrometric constant ($\text{kPa } ^{\circ}\text{C}^{-1}$),

C_n = Numerator constant that changes with reference type and calculation time step, and

C_d = Denominator constant that changes with reference type and calculation time step.

5. Results and Evaluation

We implemented the above mentioned M/M-ET estimation algorithm for three years (2004-2006) based on MODIS remote sensing data listed in (Table 2) and Oklahoma Mesonet observational network shown in (Figure 1). For more details of the 5-minute Mesonet weather variables, please refer to (<http://mesonet.org>). In this study M/M-ET estimates are evaluated on daily, 8-day and seasonal basis at both field and catchment levels.

5.1 Evaluation Indices

For the evaluation, we employed commonly used performance indicators: bias, absolute bias, root mean square error and correlation coefficient for each of the two years and two years combined.

5.1.1 Relative bias (Bias):

It is a measure of total volume difference between two time series. The bias between observations (A) and estimates (B) were then calculated as:

$$\text{Bias (\%)} = \frac{\sum_{i=1}^N A_i - \sum_{i=1}^N B_i}{\sum_{i=1}^N B_i} \times 100 \quad (27)$$

5.1.2 Absolute bias (Abs. bias):

It is a measure of timing difference between the two time series besides the volume difference. For example, if the percent bias measure between two time series is small and at the same time, the absolute percent bias measure is large, then one can say the two time series have close total volume but their timing are not as close. A good agreement between the two requires both percent bias and absolute percent bias are small. The absolute percent bias is always greater than or equal to percent bias.

$$\text{Abs. bias (\%)} = \frac{\sum_{i=1}^N |A_i - B_i|^2}{\sum_{i=1}^N B_i} \times 100 \quad (28)$$

5.1.3 Root Mean Square Error (RMSE):

RMSE measures the average error of magnitude between the two datasets. The comparison between the observation and estimates were evaluated as:

$$\text{RMSE (\%)} = \frac{\sqrt{\frac{\sum_{i=1}^N (A_i - B_i)^2}{N}}}{\frac{N}{B}} \times 100 \quad (29)$$

5.1.4 Correlation coefficient (CC):

The correlation coefficient (CC) is used to assess the relation between observations and estimation values.

$$CC = \frac{\sum_{i=1}^N (A_i - \bar{A}) \cdot \sum_{i=1}^N (B_i - \bar{B})}{\sqrt{\sum_{i=1}^N (A_i - \bar{A})^2 \cdot \sum_{i=1}^N (B_i - \bar{B})^2}} \quad (30)$$

5.2 Validation at AmeriFlux sites

Two different field sources described below are used to compare the estimated results: one with AmeriFlux towers for latent heat flux observation and the other with Mesonet sites for crop ET.

The ARM instruments and measurement applications (<http://www.arm.gov>) are well established and have been used for validating estimates of net primary productivity, evaporation, and energy absorption that are being generated by sensors on the NASA TERRA satellite (<http://public.ornl.gov/ameriflux/>) in many studies (Heilman & Brittin, 1989, Halldin & Lindroth, 1992; Lewis, 1995; Shuttleworth, 1991 Venturini et al. 2008). The ARM stations are widely distributed over the whole study domain but only two provides the latent flux data for the study time period. Thus, ET estimates were compared with the flux tower observations at Lamont and El-Reno as shown in (Figure 6) and (Figure 7), respectively.

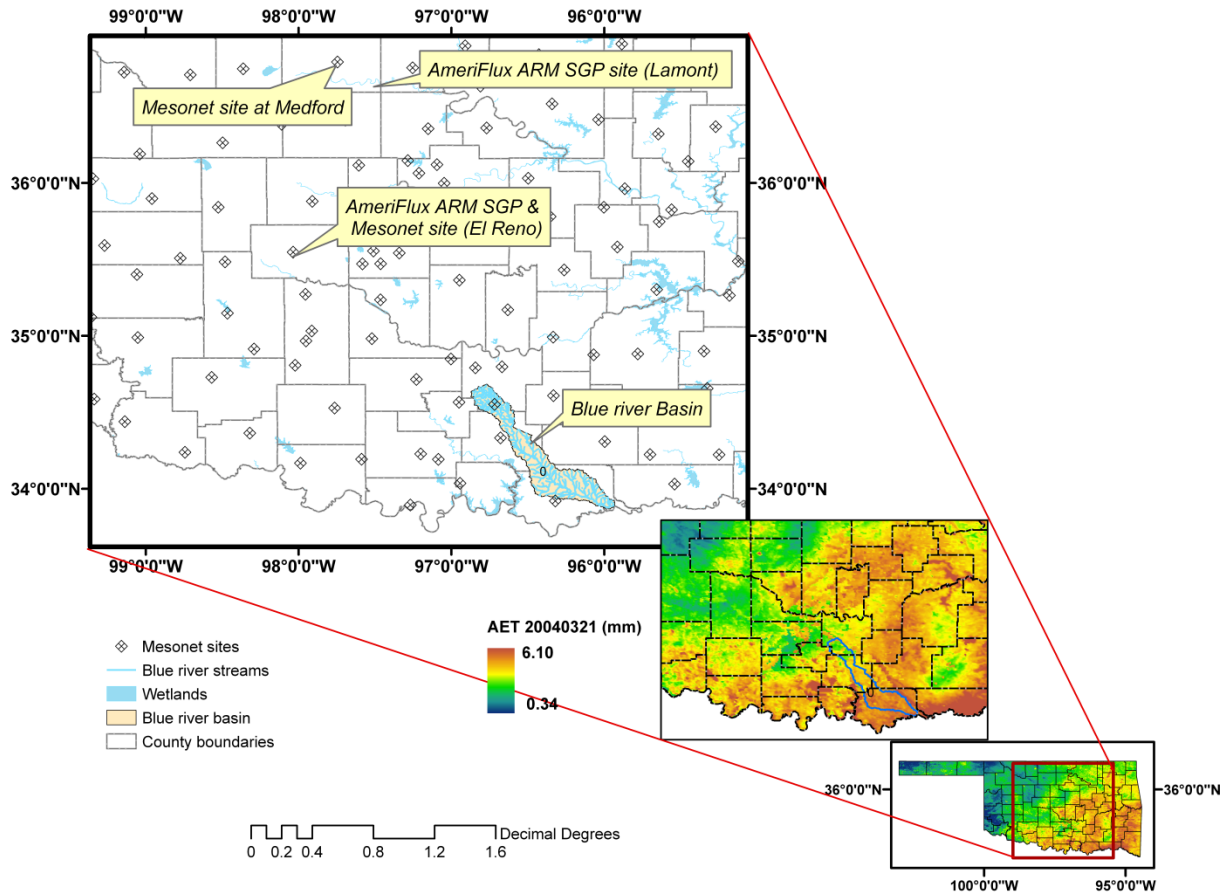


Figure 5: Study Area with AmeriFlux towers, Mesonet sites and Blue River Basin.

Table 4: Comparisons of daily and 8-day mean actual ET estimates with AmeriFlux observations at ARM SGP Lamont site for year 2004

Lamont site	AmeriFlux mean (mm)	M/M mean (mm)	Bias (mm)	Bias ratio	CC
Daily	1.63	1.87	0.28	14.72	0.64
8-day	1.46	1.70	0.24	13.44	0.77
Summer	2.46	2.62	0.16	6.45	-
Fall	1.70	1.83	0.13	7.97	-

Table 4 provides statistical variability for observed and estimated actual ET for the defined temporal scales. In Table 4, the bias ratio, and correlation coefficients are presented for each day, every 8 day and for summer and fall seasons. In general, bias ratios are less than 15% of the mean values for daily and 8-day with a correlation of 0.64 and 0.77, respectively. These values indicate the ET estimates correlate relatively well with the measurements. It should be noted that daily and 8 day results are impacted by the image quality in terms of cloud cover. Therefore, the daily and 8-day bias and RMSE for those days tend to be larger than the seasonal values. The bias ratios are less than 8% at Lamont site for both summer and fall season.

Table 5: Comparisons of daily actual ET estimates with AmeriFlux observations at ARM SGP, El-Reno site for year 2005

El Reno site DOY	AmeriFlux mean (mm)	M/M mean (mm)	Bias (mm)	Bias ratio	CC	% RMSE
20050424 - 20050527	2.49	2.68	0.19	7.626	0.86	27.50
20060424 - 20060605	3.04	3.22	0.17	5.90	0.75	28.15

Table 5 lists the comparison results for another AmeriFlux tower site at El-Reno for growing seasons in 2005 and 2006. Both seasons show relative small bias ratio (7.6% and 5.9%), high correlation (0.86 and 0.75), and low RMSE (27% and 28%).

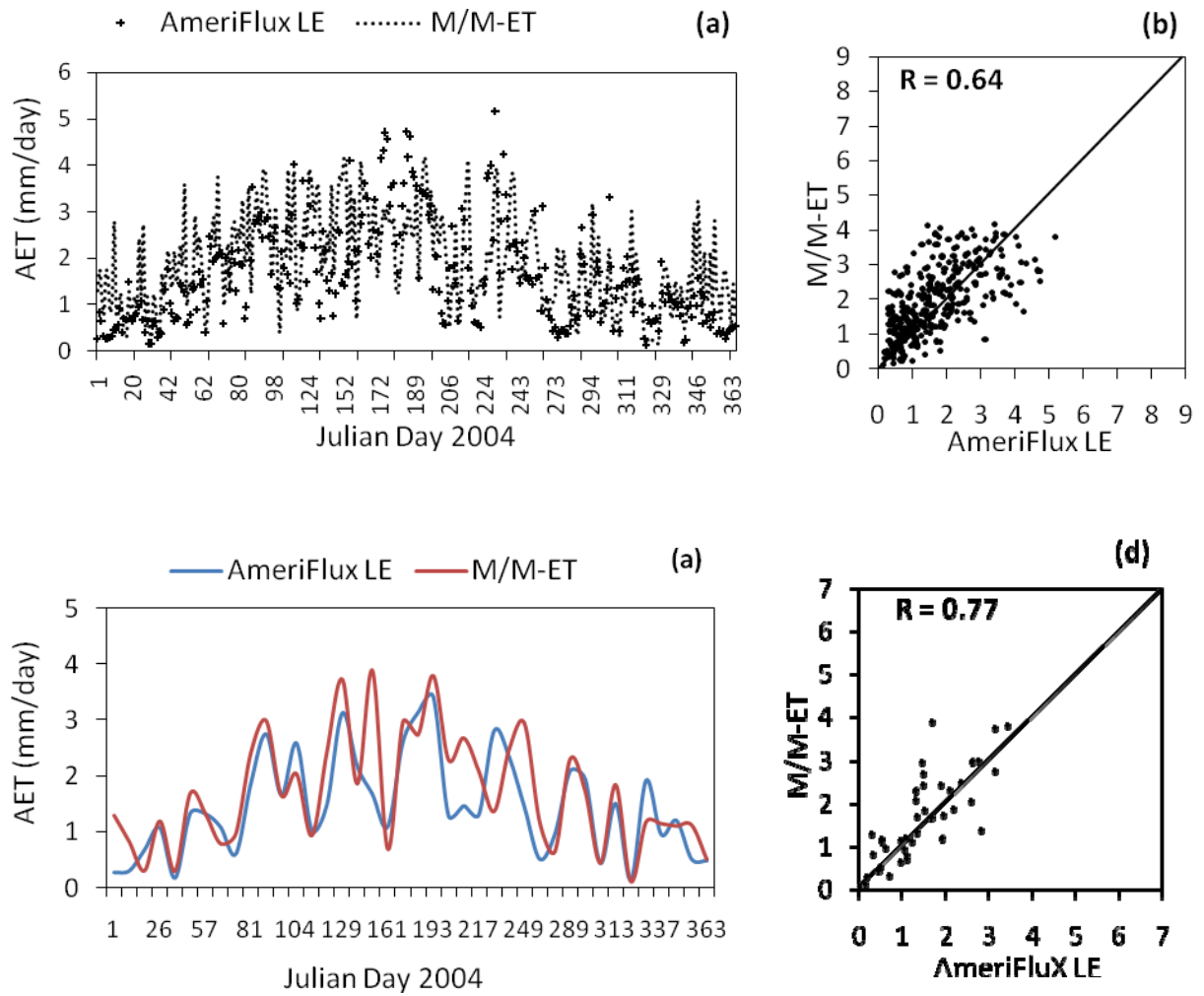


Figure 6: 2004 comparisons of daily and 8-day mean actual ET from AmeriFlux tower observations and the M/M-ET estimates through the Simplified Surface Energy Balance (SSEB) approach at ARM SGP Lamont site (when available). Panels (a) and (b) shows the daily time series and scatter plot comparison; (c) and (d) are for every 8-day.

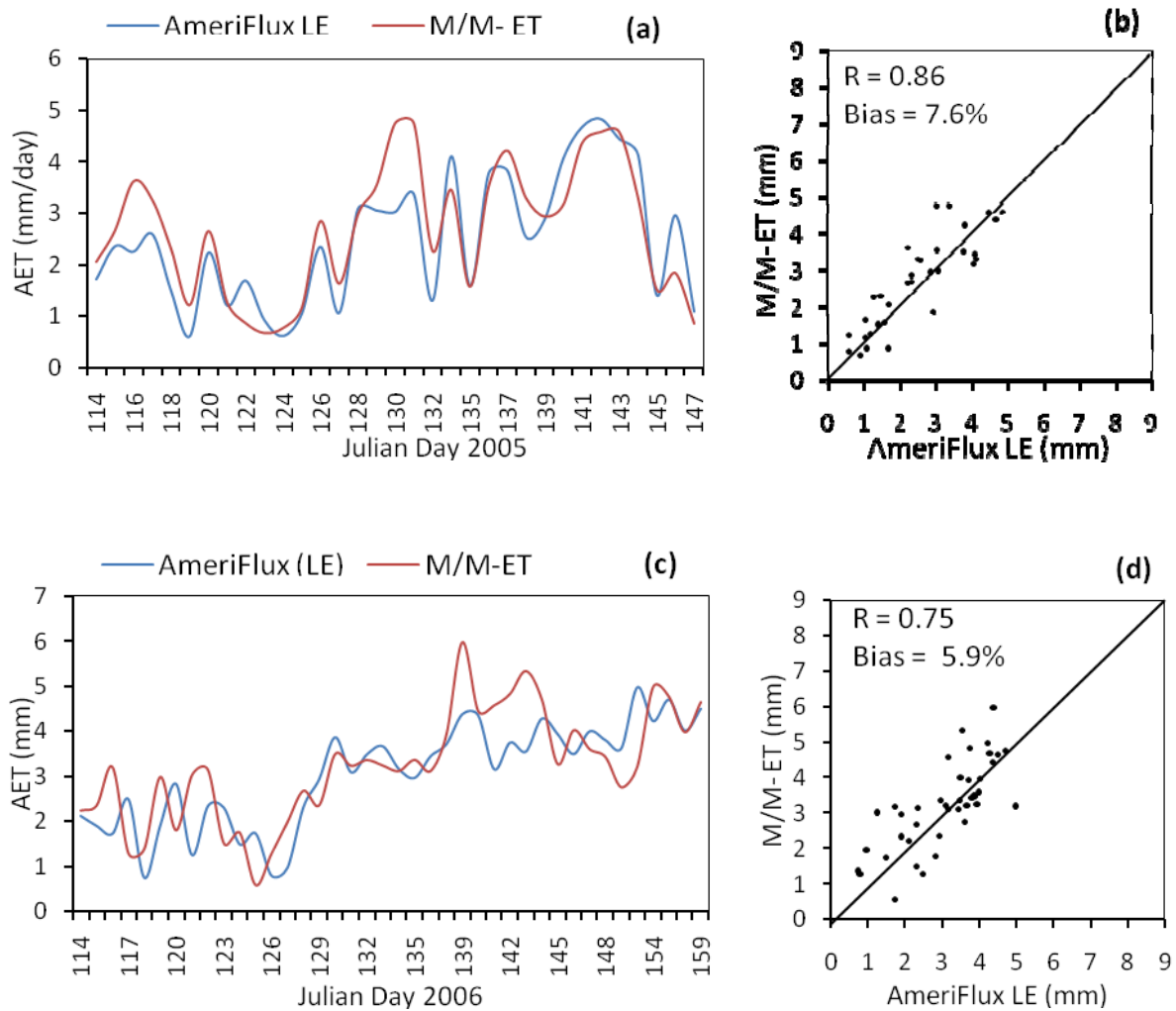


Figure 7: Comparisons of actual ET from AmeriFlux tower observations and SSEB-based M/M-ET estimates at ARM SGP El-Reno site. Panels (a) and (b) shows the daily time series and scatter plot comparison for 2005; (c) and (d) are for 2006.

5.3 Validation with Crop ET at Mesonet sites

The ET estimates are also evaluated with the crop ET at Grant (Medford site) and Canadian (El-Reno site) Counties (Figure 1 and Table 3) during wheat growing season in 2004-2006.

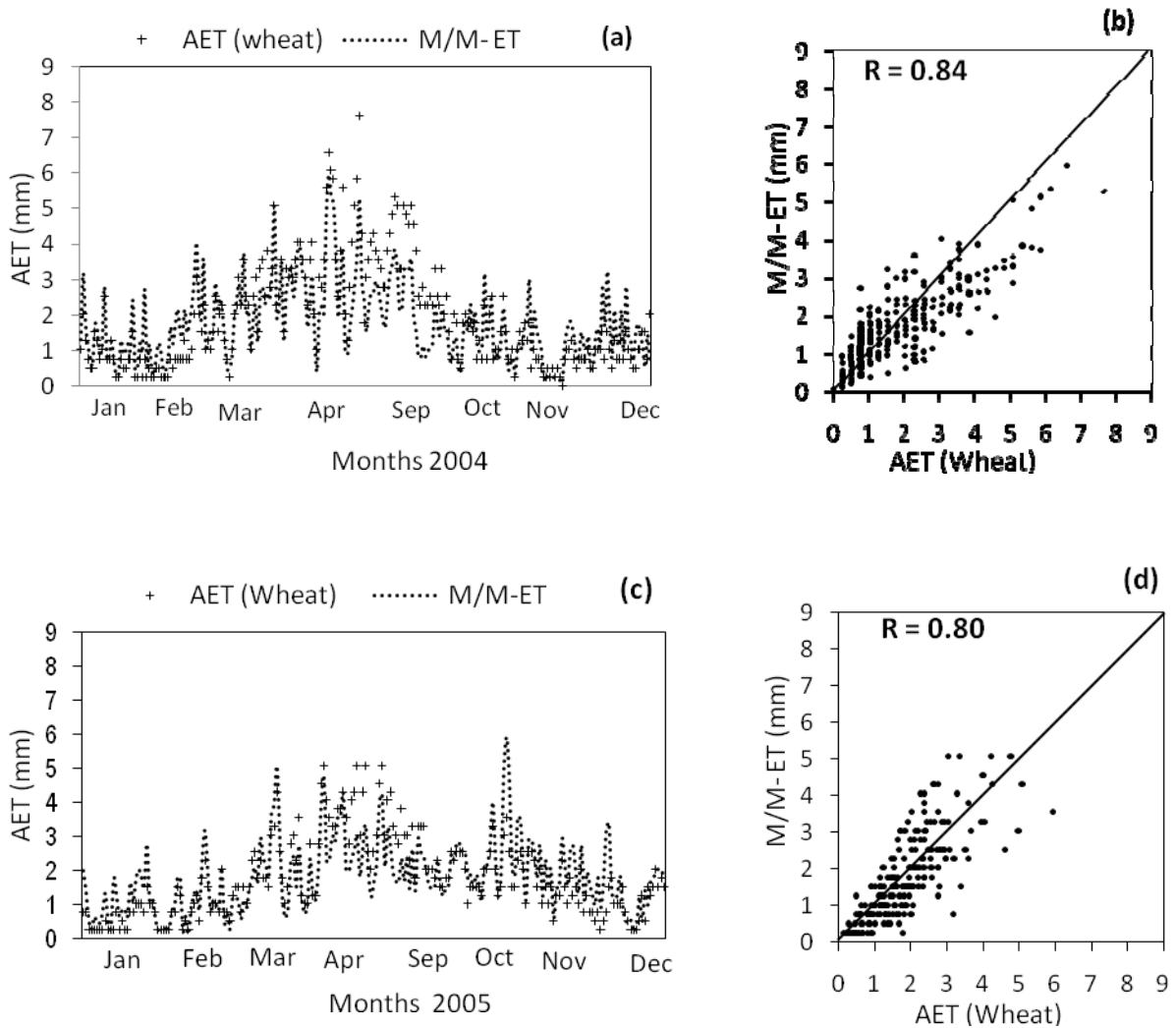


Figure 8: Comparisons of crop ET (wheat) and SSEB-based M/M-ET estimates at ARM SGP Medford site. Panels (a) and (b) shows the 2004 time series and scatter plot; (c) and (d) are for 2005.

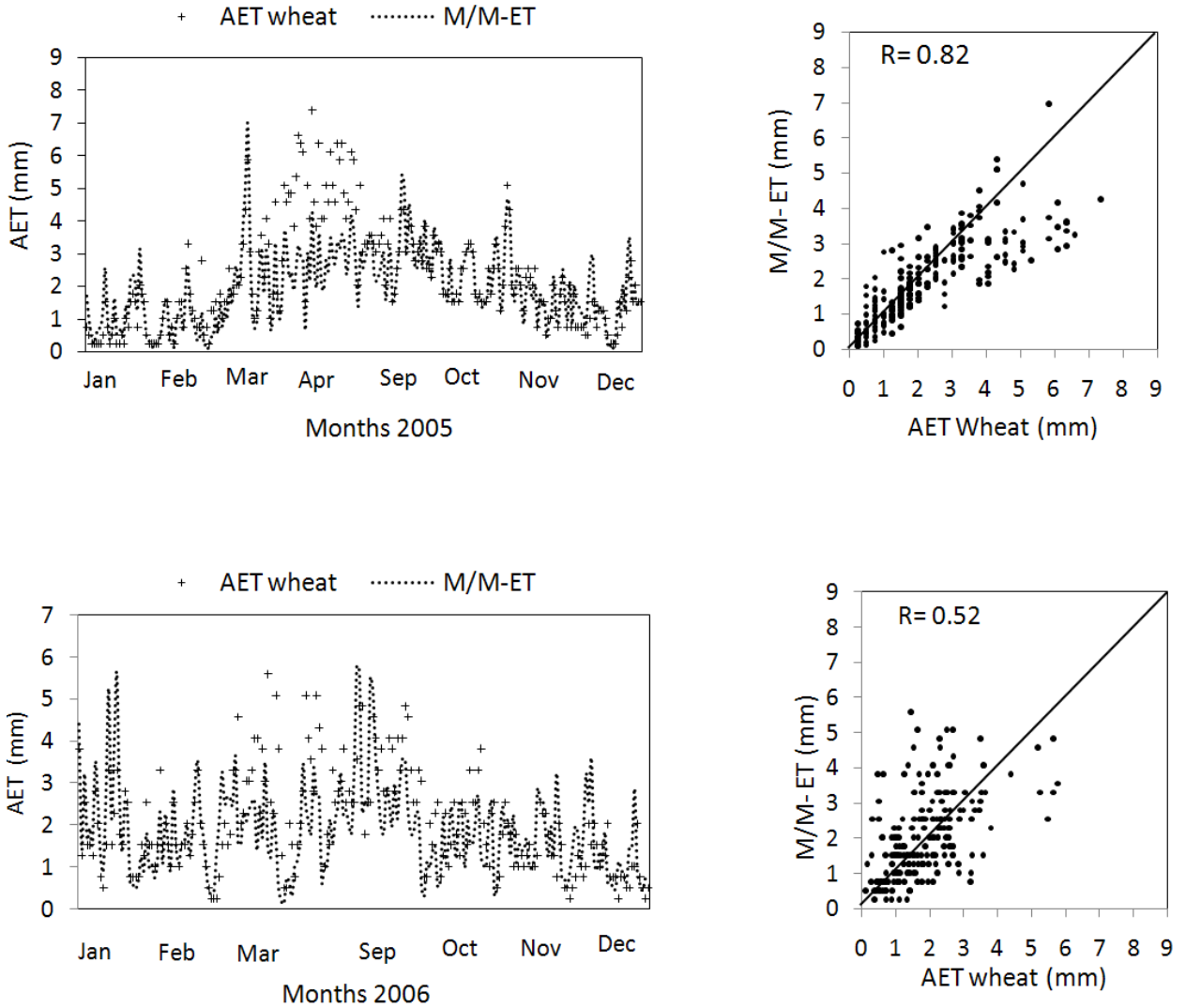


Figure 9: Comparisons of crop ET (wheat) and SSEB-based M/M-ET estimates at ARM SGP EL-Reno site. Panels (a) and (b) shows the 2005 time series and scatter plot; (c) and (d) are for 2006

Figure 8 and Figure 9 shows the daily time series and scatter plots for the sites, respectively. There is a good agreement as the scatter graphs correspond well with the in-situ crop ET observations from the Agweather site

(<http://agweather.mesonet.org/index.php/data/section/crop>).

Table 6: Comparisons of actual ET estimates with crop ET at Medford site and El Reno site for wheat growing seasons.

1) Medford site	ET Wheat crop mean (mm)	M/M mean (mm)	Bias	Bias ratio	CC	% RMSE
2004 wheat crop season	1.91	1.77	-0.14	-7.46	0.84	42.65
2005 wheat crop season	1.77	1.83	0.06	3.55	0.80	41.58
2) El-Reno site						
2005 wheat growing season	2.28	1.97	-0.31	-13.73	0.82	42.50
2006 wheat growing season	2.06	1.87	-0.19	-9.46	0.51	54.56

Table 6 summarizes the comparisons at both Medford and El-Reno site. The bias ratios are around -7% and 3% at Medford site for 2004 and 2005 respectively. Similarly, the correlation coefficients indicate the ET estimates correlate strongly with values of 0.84 and 0.80 for 2004 and 2005 observations at Medford site. M/M-ET estimates at El-Reno show slightly higher biases but in general agreement with the measurements. The correlation coefficient also indicate the ET estimates correlate relatively well with values of 0.82 and 0.51 for 2005 and 2006 measurements at El-Reno site.

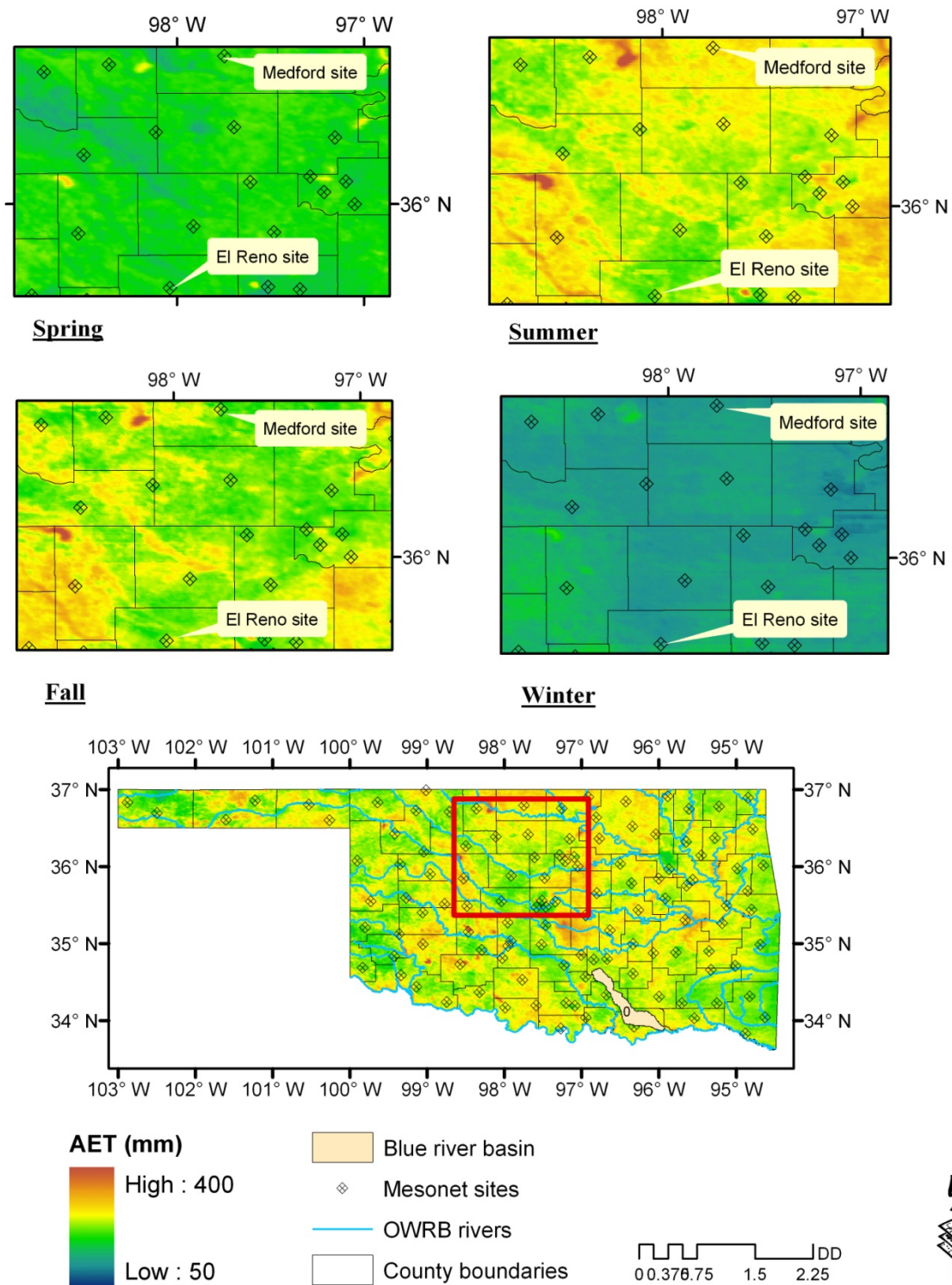


Figure 10: 2004 Seasonal Actual ET based on M/M with mesonet sites locations at Grant and Canadian Counties. The bottom panel shows the statewide summer ET.

5.4 Validation at Blue River Basin

In this study the water balance budgeted ET from a parallel study in the Blue River basin was used to compare the M/M-ET. Shown in Table 7, several hydro-meteorological records for the period 2004-2006 are collected to conduct water budget analysis for the basin. One fundamental assumption of the water balance analysis is that over a period of multiple years when the change in storage becomes relatively insignificant the ET can be assumed equal to the difference of the precipitation and runoff (Morton 1983). Pan evaporation observations were also incorporated to calculate the ET. Shown in Figure 12, monthly comparison between M/M-ET and water balance budget ET shows favorable agreement, with bias ratio less than 3% at the catchment scale.

Table 7: Data for Blue River Basin used for the Water Balance.

COMPONENT	DATA	Blue River near Connerville	
Precipitation (P)	Rainfall from radar, local bias corrected	Station (s)	Radar KTLX and the following Mesonet stations: Centrahoma, Tishomingo, Sulphur, Ada, Ardmore, Lane, Madill, Newport, and Pauls Valley
		Period	Jan 2004 – Dec 2006
Baseflow (Gw)	Derived from streamflow using the <i>PART</i> program	Station (s)	USGS 07332390
		Period	Jan 2004 – Dec 2006
Direct Runoff (R)	Streamflow daily time series, baseflow removed	Station (s)	USGS 07332390
		Period	Jan 2004 – Dec 2006
Potential Evapotranspiration (pET)	Monthly Pan Evaporation	Station (s)	Mesonet station
		Period	Jan 2004 – Dec 2006

We compared the spatially varied parameters used in the determination of actual ET such as NDVI and spatially averaged actual ET over Blue river basin for three years. As shown in Figure 13, it reconfirms a strong correlation of ET with vegetation indices in this mixed natural ecosystems and agricultural areas as previous studies (Seevers and Ottomann, 1994; Szilagyi, 2000, 2002; Nagler et al. 2005; Choudhury et al. 1994; Bausch, 1995; Hunsaker et al. 2003, 2005; Houborg and Soegaard, 2004; Senay et al. 2007). The existence of a clear spatial and temporal pattern in the NDVI-ET relationship may help define biophysical conditions prerequisite for the successful application of vegetation indices in basin-based water-balance modeling (Szilagyi, 2002).

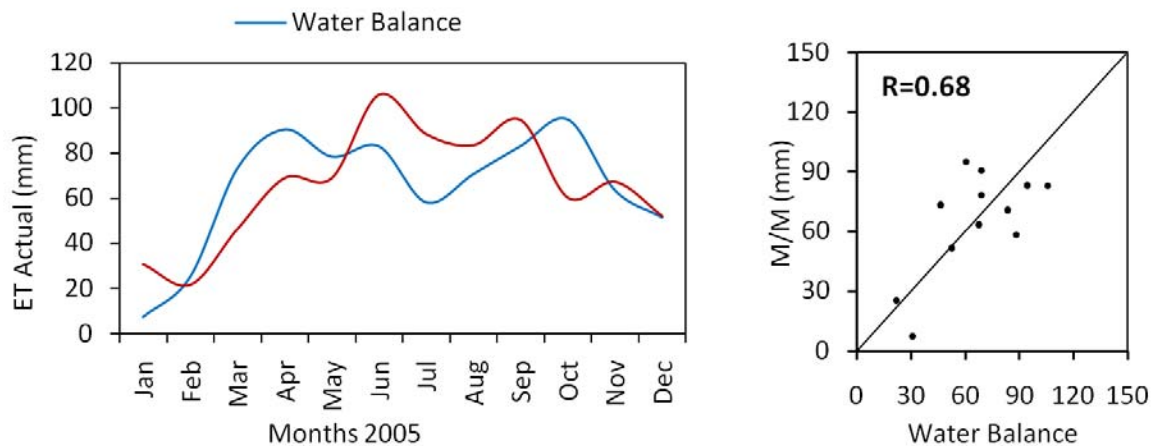


Figure 11: Comparison of the ET estimates from SSEB-based M/M –ET approach and Water-balance budget Analysis for 2005 monthly average at Blue River Basin (Bias ratio = 2.1%).

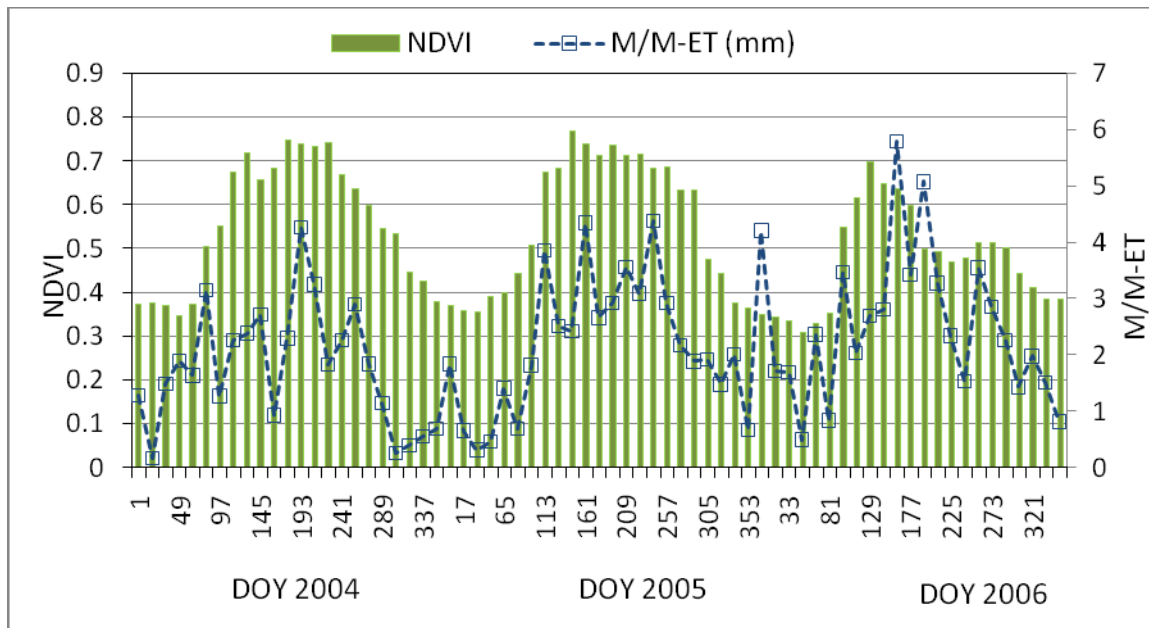


Figure 12: Temporal comparison of spatially averaged crop/vegetation index NDVI and actual ET estimates from SSEB approach over Blue river basin during 2004, 2005 and 2006 (Growing season typical has high NDVI and high actual ET; also noticeable dry year 2006 has less crop/vegetation but slightly higher actual ET due to sufficient supply from ground water).

6. Actual ET for two counties in Oklahoma:

Several ET estimation algorithms, including METRIC, have only been applied in the western U.S. (Idaho, California, and New Mexico) and have not been evaluated for the advective conditions of the great plain. Both the test beds (Texas and Tillman counties) (Table 8) have distinct characteristics of climate, soils, vegetation, geomorphology, and drainage types in contrast to the western US, thus, our M/M-ET algorithm has been calibrated by local surface observations in the Great Plain. During the calibration processes, several key surface energy balance components and processes were evaluated and improved by considering meteorological measurements and archived numerical weather model data.

Through this work we developed an improved ET estimation algorithm (i.e. M/M-ET) for applications in the Southern Great Plains and demonstrated in two counties in Oklahoma. Site details for these locations are listed in Table 8. The seasonal dynamics of Actual ET accumulated from daily at these two counties are show in the Figures 13 and 14.

Table 8: Oklahoma Mesonet Stations located in Texas and Tillman County

County	Location	Site #	Lat.	Long.	Elev.
Texas	Hooker	48	36° 51' 18" N	101° 13' 31" W	912m
Texas	Goodwell	41	36° 36' 6" N	101° 36' 4" W	997m
Tillman	Grandfield	117	34° 14' 21" N	98° 44' 39" W	341m
Tillman	Tipton	94	34° 26' 22" N	99° 8' 15" W	387m

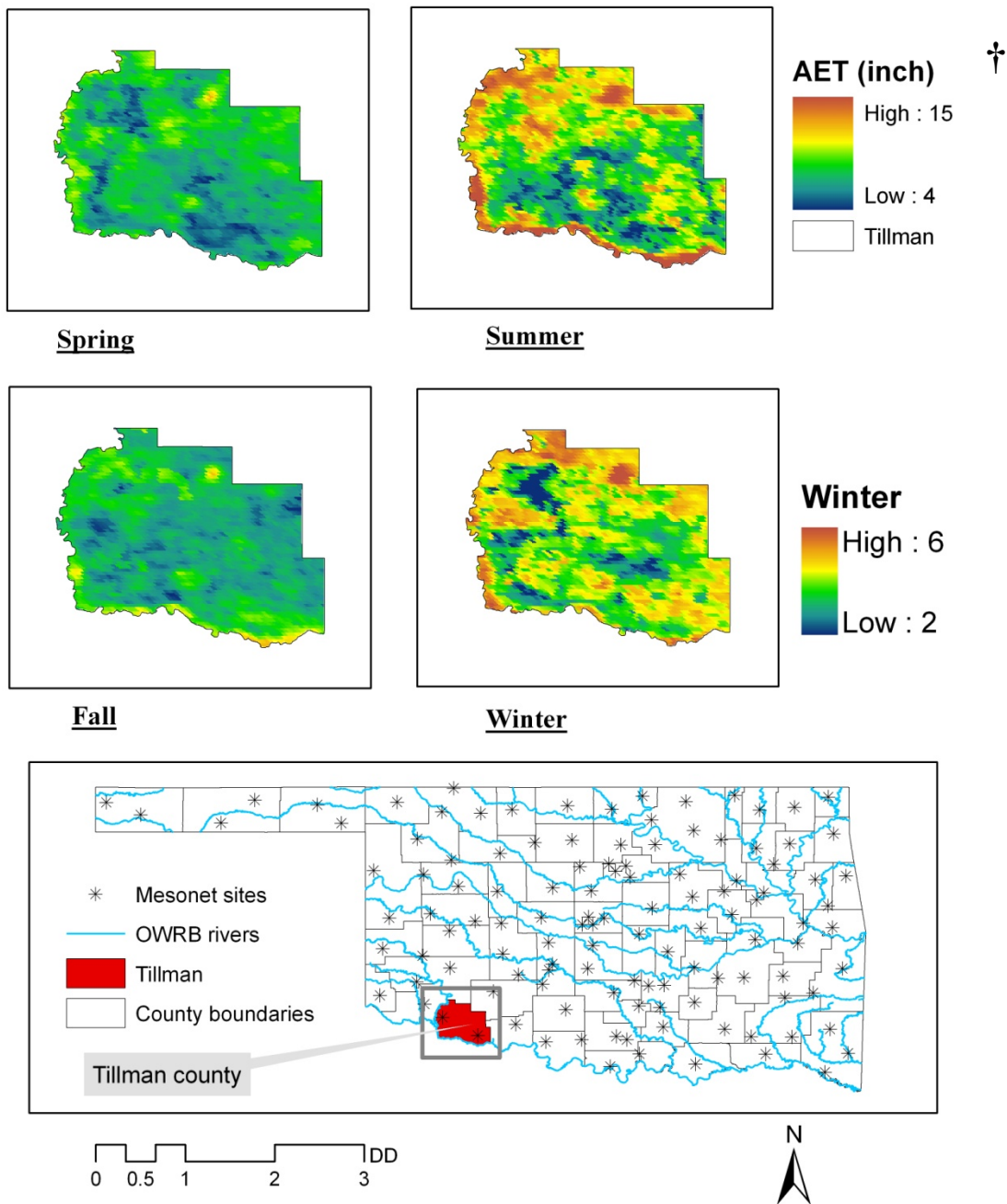


Figure 13: 2005 Seasonal Actual ET (inch) for Tillman County.

†. The 1st color scheme is for spring summer and fall and the 2nd one is for winter season.

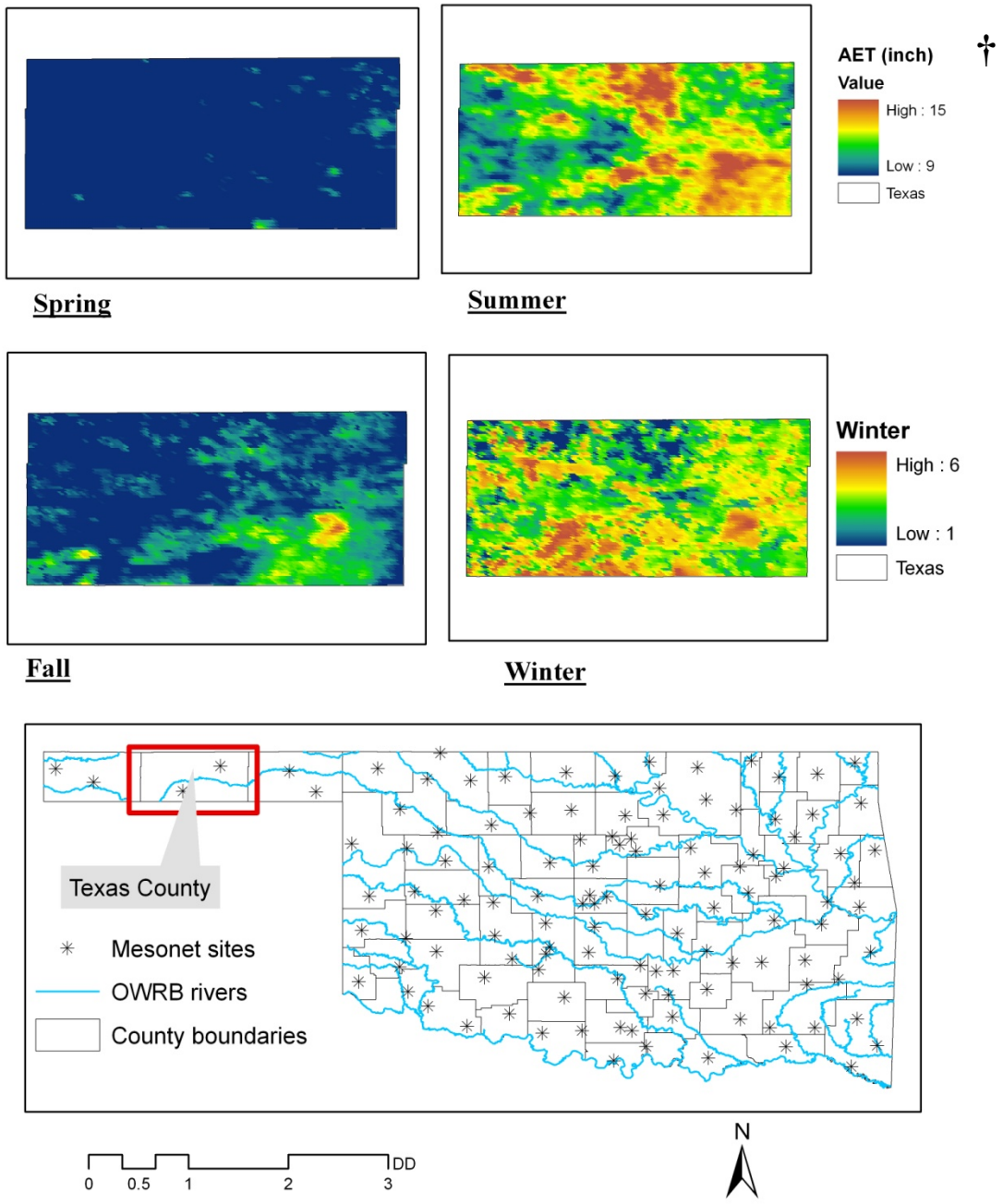


Figure 14: 2005 Seasonal Actual ET (inch) for Texas County

†. The 1st color scheme is for spring summer and fall and the 2nd one is for winter season.

7. Summary

In the past few years satellite remote sensing applications in actual ET estimation have opened frontiers in water management at local and regional scales. However previous applications have been retrospective in nature, in part because of the lack of timely availability of satellite images in relatively high spatiotemporal resolution. Furthermore, many ground observational networks do not provide data in real-time, so that the ET estimates, though useful in retrospective studies, cannot be used in real-time water management decision making (Tang et al., 2009). With the availability of the world-class environmental monitoring network from Mesonet (<http://mesonet.org>) at every 5-minute acquisition frequency, Oklahoma provides a unique setting to develop and apply a real-time ET estimation algorithm for timely water use and irrigation management. Therefore, the central objective of this study is to answer the question: is it possible to implement a real-time actual ET estimation algorithm in Oklahoma for daily operational water use management purpose?

In doing so, we first developed a surface-energy-balance ET estimation algorithm, M/M-ET, by integrating the daily open-access MODIS products and the Oklahoma's well-distributed quality-controlled Mesonet data (every 5-minute acquisition frequency) through a Modified METRIC method. A comprehensive evaluation of the M/M-ET estimates has been conducted on daily, 8-daily, and seasonal basis for multiple years (2004-2006) using AmeriFlux tower's latent flux observations, Mesonet in-situ crop ET database, and water-balance-model-derived catchment-scale ET. The results show that

M/M-ET estimation agrees with these ground observations, with daily ET bias less than **15%** and seasonal bias less than **8%**. Additionally, hydrological modeled actual ET in Blue River basin is also compared favorably with the M/M-ET at catchment and monthly scale (bias ratio < **3%**).

Results from this study demonstrate that (1) the calculated daily ET through the simplified surface-energy-balance approach (i.e. M/M-ET) is acceptable for actual ET estimation given its accuracy within the range (15%) reported by several studies around the world and (2) it is feasible to implement the proposed M/M-ET estimation algorithm at real-time rather than retrospective manner for operational irrigational water resources management in Oklahoma. This operational ET estimation system will be useful at the scale of irrigation projects, rather than individual fields. At the time of writing of this paper, the M/M-ET estimation algorithm is being implemented for entire Oklahoma State with a focus on growing season.

8. Future Work

Integration of the proposed ET scheme with a water balance model will enhance the estimation and validation of ET estimates derived from satellite. Coupling of the two approaches will afford the comparison of the estimated actual ET with computed soil moisture availability. The water balance and soil moisture module of Vflo will be coupled and operated independently of runoff generation for the test beds. As described in Vieux et al. (2006a, b), this model has been setup and evaluated for a range of climatic conditions and used to verify runoff, and indirectly, ET and soil moisture including locations across Oklahoma.

The theoretical basis for tracking soil moisture in *Vflo* is the Green and Ampt infiltration equation and a single-layer soil depth that relies on soil properties estimated from county-level soil survey maps. Infiltration rate and saturation excess runoff is computed in each grid cell as a function of soil properties and antecedent conditions. Once the soil moisture storage capacity is filled, then saturation excess runoff is computed. When the soil moisture is modeled over time, the infiltration rate is adjusted to account for a range of soil moisture. Impervious area and initial abstraction may be set to account for urbanization effects and ponding on the land surface. The rate of soil moisture depletion is limited by the climatologically ET rate and available soil moisture. A limitation of this approach is the knowledge of field-specific or even regional ET fluxes during a specific season, especially where irrigation water is applied to supplement soil moisture deficits.

Assimilation of actual ET into the model can be accomplished by updating time series input to *Vflo*. The computation will track the depletion of soil moisture through ET and replenishment by distributed radar rainfall input affects runoff volume and deep percolation/recharge for the testbed. Climatic controls, soil properties, and vegetative characteristics exert an effect on soil moisture and runoff that becomes apparent during simulations. Model tracking of the soil moisture state is performed efficiently by modifying potential or climatological ET (Vieux, 2004). The model can produce more reliable and site-specific results if ET estimated over each grid is available. The land surface characteristics affecting soil moisture are soil properties including depth, vegetative cover, and atmospheric forcing of ET. While potential ET is used by the model to estimate actual ET constrained by available soil moisture rainfall, a more direct approach can be planned for this proposed approach of using satellite-based ET estimates.

Future studies can utilize the available distributed rainfall derived from radar maps generated at hourly time steps in support of simulations during the year with focus on the growing season when irrigation is prevalent in the test bed areas.

9. Acknowledgement:

This work was financed by the Oklahoma Water Resources Research Institute and Oklahoma Water Resource Board. Partial funding for this research is provided by NASA Earth Science Fellowship. The authors also would like to extend their appreciation to Oklahoma MESONET for providing meteorological data required for the study. We are thankful to Professor Margaret Torn, Lawrence Berkeley, National Laboratory Earth Science, Division Berkeley, CA, for ARM SGP AmeriFlux sites data.

10. Reference

- ALLEN, R. G., M. TASUMI, and R. and TREZZA, 2007, Satellite-Based Energy Balance for Mapping ET with Internalized Calibration, METRIC Model, *J. Irrigation and Drainage Engineering*, **4**, pp. 380-394.
- ALLEN, R.G., M. SMITH, L.S. PEREIRA, and A. PERRIER, 1994b, An update for the calculation of reference evapotranspiration. *ICID Bulletin*, **43**, pp. 35-92.
- ALLEN, R.G., SMITH, M., PERRIER, A and L.S. PEREIRA., 1994a, An update for the definition of reference evapotranspiration. *ICID Bulletin*, **43**, pp. 1-34.
- ALLEN, R.G., TASUMI, M., MORSE, A., TREZZA, R., 2005, A Landsat based energy balance and evapotranspiration model in Western US rights regulation and planning. *Irrig. Drain. Syst.* **19**, pp. 251–268.
- BALDOCCHI, D. D., FALGE, E., GU, L. H., OLSON, R., HOLLINGER, D., RUNNING, S., *et al.* 2001, FLUXNET: A new tool to study the temporal and spatial variability of ecosystem-scale carbon dioxide, water vapour and energy flux densities. *Bulletin of the American Meteorological Society*, 82, 2415–2434.
- BASTIAANSEN, W.G.M., AHMED, M.-UD-D. and CHEMIN, Y., 2002, Satellite surveillance of evaporative depletion across the Indus Basin. *Water Resources Research*. **38**, pp.1273–1282.
- BASTIAANSEN, W.G.M., MENENTI, M., FEDDES, R.A., HOLTSLANG, .AA.,1998, A remote sensing surface energy balance algorithm for land (SEBAL): 1. Formulation. *J Hydrol* 212–213:198–212
- BASTIAANSEN, W.G.M., NOORDMAN, E.J.M., PELGRUM, H., DAVIDS, G., THORESON, B.P. and ALLEN, R.G., 2005, SEBAL model with remotely sensed data to improve water-resources management under actual field conditions. *ASCE J Irrigation Drainage Eng* **131**, pp. 85–93.
- BATRA, N., ISLAM, S., VENTURINI, V., BISHT, G., and JIANG, L. 2006, Estimation and comparison of evapotranspiration from MODIS and AVHRR sensors for clear sky days over the southern Great Plains. *Remote Sensing of Environment*, **103**, pp.1–15
- BAUSCH, W. 1995, Remote sensing of crop coefficients for improving the irrigation scheduling of corn. *Agric Water Manage.* **27** pp. 55–68.

- BOUWER, L. M., BIGGS, T. W., and AERTS J. C. J. H, 2007, Estimates of spatial variation in evaporation using satellite-derived surface temperature and a water balance model, *Hydrol. Process.*, **22**, pp. 670–682.
- BRUTSAERT, W.H. and SUGITA, M., 1992, Application of self-preservation in the Diurnal evolution of the surface energy budget to determine daily evaporation. *Journal of Geophysical Research*, **97**, pp. 18377–18382.
- CHOUDHURY, B., AHMED, N., IDSO, S., REGINATO, R., and DAUGHTRY, C. 1994. Relations between evaporation coefficients and vegetation indices studied by model simulations. *Remote Sensing of Environment*, **50**: pp 1–17.
- CLEUGH, H. A., LEUNING, Q. M.U. and RUNNING S. W., 2007, Regional evaporation estimates from flux tower and MODIS satellite data, *Remote Sens. Environ*, **106**, pp. 285–304.
- COLDITZ, R.R., CONRAD, C., WEHRMANN, T., SCHMIDT, M., and DECH, S.W., 2006. Generation and assessment of MODIS time series using quality information. In: *IEEE International Conference on Geoscience and Remote Sensing, IGARSS 2006*, (Denver, CO), pp. 779–782.
- CRAGO, R.D. 1996. Comparison of the evaporative fraction and the Priestley–Taylor α for parameterizing daytime evaporation. *Water Resources Research*, **32**, pp. 1403– 1409.
- DÖLL, P., and SIEBERT, S., 2002, Global modeling of irrigation water requirements, *Water Resources Research.*, **38**, 1037.
- GLENN, E. P., HUETE, A. R., NAGLER, P.L., HIRSCHBOECK, KATHERINE K. and BROWN, PAUL, 2007, Integrating Remote Sensing and Ground Methods to Estimate Evapotranspiration. *Critical Reviews in Plant Sciences*, 26 (3), 139-168.
- GOWDA, P., CHAVEZ EGUEZ, J.L., COLAIZZI, P.D., EVETT, S.R., HOWELL, T.A., and TOLK, J.A. 2008, ET mapping for agricultural water management: Present status and challenges. *Irrigation Science*. **26**, pp, 223-237
- HALLDIN and LINDROTH, 1992, Errors in net radiometry: comparison and evaluation of six radiometer designs, *Journal of Atmospheric and Oceanic Technology*, **9**, pp. 762–783.
- HOUBORG, R., and SOEGAARD, H. 2004, Regional simulation of ecosystem CO₂ and water vapor exchange for agricultural land using NOAA AVHRR and Terra MODIS satellite data. Application to Zealand, Denmark. *Remote Sensing of Environment*, **93**, pp.150–167.

- HUETE, A., DIDAN, K., MIURA, T., RODRIGUEZ, E. P., GAO, X., and FERREIRA, L. G. 2002, Overview of the radiometric and biophysical performance of the MODIS vegetation indices. *Remote Sensing of Environment*, **83**, pp, 195–213.
- HUNSAKER, D., PINTER, P., and KIMBALL, B. 2005, Wheat basal crop coefficients determined by normalized difference vegetation index. *Irrigation Science*. 24: 1–14.
- HUNSAKER, D., PINTER, P., BARNES, E., and KIMBALL, B., 2003, Estimating cotton evapotranspiration crop coefficients with a multispectral vegetation index. *Irrigation Science*. **22**, pp, 95–104.
- HUNTINGTON, T., 2006, Evidence for intensification of the global water cycle: review and synthesis. *Journal of Hydrology*. **319**, pp, 83–95.
- HUXMAN, T., WILCOX, B., BRESHEARS, D., SCOTT, R., SNYDER, K., SMALL, E., HULTINE, K., POCKMAN, W., and JACKSON, R., 2005, Ecohydrological implications of woody plant encroachment. *Ecology*, **86**, pp, 308–319.
- IMMERZEEL, W.W. and DROOGERS, P., 2008. Calibration of a distributed hydrological model based on satellite evapotranspiration. *Journal of Hydrology* **349**, p.p 411–424.
- J.L. HEILMAN and BRITTIN C.L., 1989, requirements for Bowsen ratio measurements of latent and sensible heat fluxes, *Agricultural and Forest Meteorology*, **44** pp. 261–273.
- JACKSON, R., 1986, Estimating aerial evapotranspiration by combining remote sensing and ground-based data. In: A. Johnson and A. Rango (eds.), *Remote Sensing Applications for Consumptive Use (Evapotranspiration)*, *American Water Resources Association Monograph Series No. 6*, Bethesda, Maryland, pp. 13–24.
- JIANG, H., *et al.*, 2004, The influence of vegetation type on the hydrological process at the landscape scale, *Canadian Journal of Remote Sensing*, **30**, pp. 743–763.
- JIANG, L., ISLAM, S., 2001, Estimation of surface evaporation map over southern Great Plains using remote sensing data. *Water Resources Research*, **37**, pp. 329–340.
- JUSTICE, C.O., TOWNSHEND, J.R.G., VERMOTE, E.F.E. MASUOKA, R.E., WOLFE, N.Z. EL SALEOUS, D.P., and MORISETTE J.T., 2002, An overview of MODIS land data processing and product status, *Remote Sensing of Environment*, **83**, pp. 3–15.

- KITE, G.W. and PIETRONIRO, A., 1996, Remote sensing applications in hydrological modeling. *Hydrological Sciences Journal*, **41**, pp. 563-592
- KUITTINEN, R. 1992., Remote Sensing for Hydrology Progress and Prospects, *WMO Operational Hydrology report*, No. 36, WMO-No. 773, Geneva, Switzerland,
- LEWIS J.M., 1995., The story behind the Bowen ratio, *Bulletin of the American Meteorological Society* **76** pp. 2433–2443.
- MCPHERSON, R. A., and COAUTHORS., 2007, Statewide monitoring of the mesoscale environment: A technical update on the Oklahoma Mesonet. *Journal of Atmospheric and Oceanic Technology*, **24**, pp 301–321.
- MEEHL, G.A., T.F. STOCKER, W.D. COLLINS, P. FRIEDLINGSTEIN, A.T. GAYE, J.M. GREGORY, A. KITO, R. KNUTTI, J.M. MURPHY, A. NODA, S.C.B. RAPER, I.G. WATTERSON, A.J. WEAVER and ZHAO Z.C., 2007, Global Climate Projections. In: *Climate Change 2007: The Physical Science Basis. Contribution of Working Group I to the Fourth Assessment Report of the Intergovernmental Panel on Climate Change* [Solomon, S., D. Qin, M. Manning, Z. Chen, M. Marquis, K.B. Averyt, M. Tignor and H.L. Miller (eds.)]. Cambridge University Press, Cambridge, United Kingdom and New York, NY, USA.
- MU, Q., F.A. HEINSCH, M. ZHAO, S.W. RUNNING., 2007, Development of a global evapotranspiration algorithm based on MODIS and global meteorology data. *Remote Sensing of Environment*, **111**, pp, 519-536
- NAGLER, P., CLEVERLY, J., LAMPKIN, D., GLENN, E., HUETE, A., and WAN, Z. 2005, Predicting riparian evapotranspiration from MODIS vegetation indices and meteorological data. *Remote Sensing of Environment*, **94**, pp, 17–30.
- NAGLER, P.L., GLENN, E.P., KIM, H., EMMERICH, W., SCOTT, R.L., HUXMAN, T.E., HUETE, A.H., 2007, Relationship between evapotranspiration and precipitation pulses in a semiarid rangeland estimated by moisture flux towers and MODIS vegetation indices. *Journal of Arid Environments*, **70**, pp, 443–462.
- NISHIDA, K., NEMANI, R. R., RUNNING, S. W., and GLASSY, J. M., 2003, An operational remote sensing algorithm of land surface evaporation, *Journal of Geophysical Research*, 108(D9), 4270,
- NORMAN, J. M., ERSON, M. C., KUSTAS, W. P., RENCH, A. N., MECIKALSKI, TORN, J., R., DIAK, G. R. SCHMUGGE, T. J. and TANNER, B. C. W., 2003, Remote sensing of surface energy fluxes at 101-m pixel resolutions, *Water Resources Research*, **39**, pp. 1221

- PELGRUM, H. and BASTIAANSEN, W. G. M., 1996, An Intercomparison of Techniques to Determine the Area-Averaged Latent Heat Flux from Individual in Situ Observations: A remote Sensing Approach Using the European Field Experiment in a Desertification-Threatened Area Data, *Water Resources Research*, **32** pp., 2775–2786.
- RANGO, A. and SHALABY, A. I., 1998., “Operational Applications of Remote Sensing in Hydrology: Success, Prospects and Problems,” *Hydrological Sciences Journal*, **43**, pp. 947-968.
- SANTANELLO J.A., LIDARD C.D., GARCIA M.E., MOCKO, D.M., TISCHLER, M.A., M. and MORANTHOMA, D.P., 2007, Using remotely-sensed estimates of soil moisture to infer soil texture and hydraulic properties across a semi-arid watershed, *Remote Sensing of Environment*, **110**, pp. 79-97
- SCHAAF, C. B., GAO, F., STRAHLER, A. H., LUCHT, W., LI, X., TSANG, T., *et al.*, 2002, First Operational BRDF, albedo and nadir reflectance products from MODIS. *Remote Sensing of Environment*, **83**, 135–148
- SEEVERS, P., and OTTMOANN, R. 1994, Evapotranspiration estimation using a normalized difference vegetation index transformation of satellite data. *Hydrological Sciences Journal*. **39**, pp. 333–345.
- SEGUIN, B., COURAULT, D. and GUÉRIF, M., 1994, Surface temperature and evapotranspiration: Application of local scale methods to regional scales using satellite data. *Remote Sensing of Environment* , **49**, pp. 287-295.
- SENAY, GABRIEL B.; BUDDE, MICHAEL; VERDIN, JAMES P.; MELESSE, ASSEFA M.. 2007. "A Coupled Remote Sensing and Simplified Surface Energy Balance Approach to Estimate Actual Evapotranspiration from Irrigated Fields." *Sensors*. **6**: pp 979-1000
- SHIKLOMANOV, I.A., 1998, World water resources: A new appraisal and assessment for the 21st century. Paris (UNESCO).
- SHUTTLEWORTH W.J., 1991, Insight from large-scale observational studies of land/atmosphere interactions, *Surveys in Geophysics* **12** (1991), pp. 3–30
- SHUTTLEWORTH, W. J., GURNEY, R. J., HSU A. Y. and ORMSBY J. P., 1989, FIFE: The variation in energy partition at surface flux sites, in *Remote Sensing and Large-Scale Processes*, edited by A. Rango, Proc. of the IAHS Third International Assembly, Baltimore, Md., IAHS Publ., **186**, pp 67–74.

- SOBRINO, J.A., GÓMEZ, M., JIMÉNEZ-MUÑOZ, J. C., OLIOSO, A., 2007, Application of a simple algorithm to estimate the daily evapotranspiration from NOAA-AVHRR images for the Iberian Peninsula *Remote Sensing of Environment* , **110**, pp 139-148.
- STEWART J.B, C.J. WATTS, J.C. RODRIGUEZ, H.A.R. DE BRUIN, A.R. VAN DEN BERG and GARATUZ-PAYAN J., 1999, Use of satellite data to estimate radiation and evaporation for northwest Mexico. *Agricultural Water Management*, **38** , pp. 181–193.
- SU, B., 2002, The surface energy balance system (SEBS) for the estimation of turbulent heat fluxes. *Hydrology and Earth System Sciences*. **6**, pp.85–99.
- SUGITA, M. and BRUTSAERT, W., 1991, Daily evaporation over a region from lower boundary layer profiles measured with radiosondes. *Water Resources Research*. **27**, pp. 747-752.
- SZILAGYI, J., 2000, Can a vegetation index derived from remote sensing be indicative of areal transpiration? *Ecological Modelling* **127**, pp. 65–79.
- SZILAGYI, J., 2002, Vegetation indices to aid areal evapotranspiration estimations. *Journal of Hydrologic Engineering*. **7**, pp. 368–372.
- TANG, Q., PETERSON, S., CUENCA, R. H., HAGIMOTO, Y. and LETTENMAIER, D. P., 2009, Satellite-based near-real-time estimation of irrigated crop water consumption, *Journal of Geophysical Research*., 114 D05114.
- VENTURINI, V., ISLAM, S. and RODRIGUEZ, L., 2008, Estimation of evaporative fraction and evapotranspiration from MODIS products using a complementary based model, *Remote Sensing of Environment*, **112**, pp. 132-141
- VERMOTE, E. F., and VERMEULEN A., 1999, Atmospheric correction algorithm: Spectral reflectances (MOD09), ATBD version 4.0, University of Maryland, Dept of Geography., College Park. Available online at: http://modis.gsfc.nasa.gov/data/atbd/atbd_mod08.pdf
- VIEUX, B.E., 2004, *Distributed Hydrologic Modeling Using GIS*. Second edition, Kluwer Academic Publishers, Norwell, Massachusetts, Water Science Technology Series, Vol. 48. ISBN 1-4020-2459-2, p. 289. CD-ROM including model software and documentation.
- VIEUX, B.E., and J.E. VIEUX, 2006a. Advanced Hydrologic Prediction for Event and Long-term Continuous Operations. *3rd Federal Interagency Hydrologic Modeling Conference*, Reno Nevada, April 2-6, 2006. Presentation and Refereed Abstract.

- VIEUX, B.E., and J.E. VIEUX, 2006b. Evaluation of a Physics-Based Distributed Hydrologic Model for Coastal, Island, and Inland Hydrologic Modeling. Published in *Coastal Hydrology and Processes* (ed. by V. P. Singh & Y. J. Xu), Water Resources Publications, LLC, Highlands Ranch, CO 80163-0026, USA. pp. 453-464.
- WAN, Z., Y. ZHANG, Q. ZHANG, and LI, Z. L., 2004, Quality assessment and validation of the MODIS global land surface temperature, *Int. J. Remote Sens.*, 25, 261–271.
- WANG, K., P. WANG, Z. LI, M. SPARROW, and M. Cribb., 2007, A simple method to estimate evapotranspiration from a combination of net radiation, vegetation indices and temperatures. *Journal of Geophysical Research*, 112, D15107, DOI: 10.1029/2006JD008351.
- WRIGHT, J. L., 1996, Derivation of alfalfa and grass reference evapotranspiration. Evapotranspiration and irrigation scheduling, C. R. Camp, E. J. Sadler, and R. E. Yoder, eds., In ., *Int. Conf., ASAE*, San Antonio, 133–140.
- XIONG, X., SUN, J., BARNES, W., SALOMONSON, V., ESPOSITO, J., ERIVES H., and GUENTHER B., 2007, Multiyear On-Orbit Calibration and Performance of Terra MODIS Reflective Solar Bands, *IEEE Transactions on Geoscience and Remote Sensing.*, 45, pp. 879-889.

Decision Support Model for Evaluating Alternative Water Supply Infrastructure Scenarios

Basic Information

Title:	Decision Support Model for Evaluating Alternative Water Supply Infrastructure Scenarios
Project Number:	2008OK105B
Start Date:	3/1/2008
End Date:	2/28/2009
Funding Source:	104B
Congressional District:	3
Research Category:	Social Sciences
Focus Category:	Management and Planning, Water Supply, Water Quantity
Descriptors:	Decision Support, Regionalization, Planning, Modeling
Principal Investigators:	Brian Whitacre, Dee Ann Sanders, Arthur Stoecker

Publication

1. Lea, Mike. 2009. M.S. Thesis. Use of hydraulic simulation software to evaluate future infrastructure upgrades for a municipal water distribution system in Beggs, OK. Dept. of Civil and Environmental Engineering, Oklahoma State University, Stillwater, OK. 130 pages.

Title: Decision Support Model for Evaluating Alternative Water Supply Infrastructure Scenarios

Start Date: 3/1/2008

End Date: 12/31/2009

Congressional District: Federal Congressional District #3 (Payne County, Oklahoma)

Focus Category: MET, MOD, WS, M&P, ECON

Descriptors: Infrastructure evaluation, rural water system, distribution system

Principal Investigators: Brian Whitacre, Oklahoma State University
Art Stoecker, Oklahoma State University
Dee Ann Sanders, Oklahoma State University

Publications:

Lea, Mike. 2009. M.S. Thesis. "Use of hydraulic simulation software to evaluate future infrastructure upgrades for a municipal water distribution system in Beggs, OK." Dept. of Civil and Environmental Engineering, Oklahoma State University, Stillwater, OK. 130 pages.

Bhadbhade, Neha; Sanders, Dee Ann; Stoecker, Art. 2009. "Analysis of water infrastructure upgrade options in Oilton, OK" In 2009 Oklahoma Water Research Symposium, Oklahoma Water Research Resources Institute, Stillwater, OK (to be submitted May 2009).

Lea, Mike; Sanders, Dee Ann; Stoecker, Art. 2009. "Evaluation of future infrastructure upgrades using WaterCAD and EPANET" In 2009 Oklahoma Water Research Symposium, Oklahoma Water Research Resources Institute, Stillwater, OK (to be submitted May 2009).

Problem and Research Objectives:

This project addresses the lack of a documented plan for assessing future water infrastructure needs among the nation's many rural water districts. The objective is to create a process that allows a rural water system to assess their own infrastructure and consider different avenues for funding potential enhancements.

Methodology:

The following steps were taken to initiate this process:

- 1) Meet with the Director of the Oklahoma Rural Water Association to solicit input on the project and select tentative test systems. The meeting resulted in a list of three test systems, each using a different type of source water (surface, ground water, purchased water).

- 2) Establish contact with the directors of the three systems to gain their concurrence. In this step, one water system was removed because of non-interest on the part of the system manager, and another system of the same type was substituted.
- 3) Develop a list (and sources) of data for modeling possible upgrades, including census block population changes, future industrial growth, terrain maps, and road networks.
- 4) Document a streamlined methodology for analyzing the existing distribution system using WaterCAD and EPANET.
- 5) Develop a method for estimating capital and operating and maintenance costs for alternative treatment options using WaterCAD.
- 6) Integrate steps 3 – 5 into a computerized tool: the Decision Support System.

The above general steps were refined as discussed below for the three systems evaluated.

Progress and Initial Findings:

It is possible to develop GIS-based water system simulations for small towns and rural communities at reasonable cost. This can be accomplished with a combination of public domain software, relatively low cost web-based systems such as Google Earth®, GIS software, and macro driven spreadsheets.

The EPANET freeware program is capable of providing useful simulations of piping layouts, pumping demands, spatial analysis of water pressures and water ages in pipeline systems, and calculating operational costs (electricity for pumps) for small towns and rural areas. This software developed by EPA is free and reasonably sophisticated. Base systems can be developed and initially calibrated with minimal effort from the communities involved. The models can then be further refined and used to address specific water system planning needs such as excessive water ages, high pumping cost, low and high-pressure zones, and fire fighting capacities.

The most time consuming process is the development and validation of the current water supply system. The problems and their associated solutions differ between small towns and rural water districts. The findings or methods developed for rural water districts are reviewed first, followed by a discussion of small towns.

Rural water Districts. In Oklahoma, the Oklahoma Water Resources Board (OWRB) has developed GIS files of pipelines for rural water districts. Supporting files provide information (generally from the year 1995) on the source of water, type of treatment, number of people served, number of meters, average use, and peak use. The GIS files contain estimates of pipeline location, length and diameter. The files do not contain elevation levels of system elements. The ORWB files show individual pipelines along with the location of their beginning and ending nodes. However, the pipes are not connected in a system that allows modeling using commercial software. Other problems include the presence of numerous duplicate pipes. These problems are

solvable. Steps to fill these data gaps and allow modeling of the systems are outlined below.

1. The estimation of elevation at end nodes for individual pipes is accomplished by overlaying the pipelines on USGS elevation data sets. GIS software is used to overlay the pipeline map on a USGS 1/3 arc second elevation map and add the elevations to the nodes. Critical elevation points along the pipeline can be verified with GPS units when site visits are made.
2. Spreadsheet macros are developed to eliminate duplicate pipes and to join pipes at the appropriate nodes. The process of joining two pipes at a common node consists of replacing the node identification on one of the pipes with the identification of the joining pipe, so that both pipes have the same ending node. The process of joining pipes in the middle (creating a "T") is accomplished by dividing the initial pipe into two shorter ones, and adding the identification of the ending node of the second pipe to the newly created nodes on the pipe which was just divided. This process creates one new pipe whose identification code (along with the identification of its nodes) must be added to the original list of pipes.
3. Initial estimates of rural water demands tied to specific spatial locations are accomplished by overlaying the pipeline maps on annual NRCS one-meter aerial photo files. Census blocks are generally too large geographically to be of use in locating the position of rural households. The initial estimates are used to develop an operating model that will be later revised through site visits, discussions with RWD personnel, and ground-truthing maps. Field GPS units can also be used in this step.
4. An initial analysis of the system under average and peak flow conditions for the current period is modeled, as well as an analysis, without additional major infrastructure additions, for the 2050-2060 time period.
5. Points of high and low pressure, points of constriction along pipelines, problems of pump and water tower cycling, water age in pipes (particularly dead ends) and unacceptable head losses are noted in both evaluations (current and year 2050).
6. From the problem list prepared in step 5, a priority list of problems is developed. Multiple (at least two) specific system changes (such as pipeline replacement, additional pumps, additional above-ground storage) are then modeled and cost data developed based on the required infrastructure changes.
7. The results of the modeling and priority list of infrastructure improvements are presented to the water district personnel.

Small Towns. Many small towns lack accurate water system maps and records. Between personnel limitations and non-availability of funding, the system managers cannot focus on long-term problems. Since the OWRB does not provide maps of small town systems, a different set of procedures is used to model and evaluate small towns.

1. Water managers or city engineers are contacted to determine the approximate locations and diameters of pipelines serving the city. Thus, the first step is to

develop GIS-based pipeline maps. This is done using the freeware program EPANET-Z developed by Zonum Solutions®. This program allows the user to develop a pipeline map of a town using a street grid map obtained from Google Earth. The pipeline diameters must be provided by local officials. It is necessary to check the pipeline lengths using known measurements of square miles or measured highway miles to verify the distances assigned to the pipelines by the software.

2. Census block data from the 2000 census, along with the pipe line map developed in step 1, are used to determine the residential population served at each of the nodes on the pipe network.
3. The remaining steps follow the same procedure as for rural water districts, steps 4-7.

Specific Systems Studies Completed or in Process. EPANET models have been developed for three small individual towns and for a regional water system. These projects are all in different stages and are described below.

1. **Beggs, Oklahoma:** A master's thesis for the City of Beggs (population 1400, located in Okmulgee county), Oklahoma has been completed. The thesis was important in developing the methods described above for small towns. The thesis study demonstrated the feasibility of constructing an EPANET model using limited city records, using GIS methods to develop pipeline maps, and then using the model simulations to identify problems with pressures, water ages, and fire protection. As described above in step 4 for the rural water district studies, model simulations were performed to calibrate model parameters to current operation of the system. Simulations were then run for the year 2050. Results of the modeling showed that the system could be upgraded to provide adequate water in the design year through a combination of (1) replacement of old, small-diameter cast iron water mains with new, larger-diameter PVC lines; (2) elimination of dead ends by completing loops in the systems; and (3) by adding a new above-ground storage tank for finished water. An additional output of the study was a list of data requirements that will typically be required before beginning similar modeling efforts in other rural locations. This list will prove helpful in future studies at other sites.
2. Two additional master's thesis studies are underway, one for the city of **Bragg** (population 300, located in Muskogee County) and one for the city of **Oilton** (population 1100, located in Creek County).
3. **Kaw Tribe-Kaw City in Kay County:** This effort was requested by the Environmental Coordinator for the Kaw Tribe. The main problem facing users of water from Kaw Lake is that of taste, which is in turn mainly due to high levels of manganese in the water. The Kaw Tribe is considering multiple options that will provide water for at least one user in addition to Kaw City (such as another nearby town). By providing water to multiple users, the Tribe hopes to take advantage of economies of scale. The options include supplying water to a

commercial water bottling facility and/or selling water to the nearby towns of Shidler or Newkirk. The specific analysis being developed for the Kaw Tribe are:

- a. Estimate the cost of developing an additional groundwater well, the connecting pipeline, and a treatment facility to be located northwest of Kaw City.
 - b. Estimate and compare the cost of construction and operation of greensand (a natural ion exchange resin) plus a nano-filtration system, with a greensand plus reverse-osmosis treatment plant that would serve populations of 400 (Kaw City only) or populations of 1,500-2,000 (Kaw City plus another town).
 - c. Estimate the cost of linking Shidler and/or Newkirk to the Kaw City Treatment facility.
 - d. Develop and test an EPANET model for the Kaw City Water System.
- 4. Economic Analysis of a Regional Water Use and Treatment System:** The purpose of this phase of the project is to update the cost of a regional pipeline serving communities around Lake Tenkiller in Eastern Oklahoma. The permanent residential and seasonal tourist populations immediately surrounding and extending west and north of Lake Tenkiller are served by approximately 30 water systems. The U.S. Army Corps of Engineers previously estimated the cost of establishing and operating a regional pipeline that would replace the individual systems. This study is being updated as an extension of a related study on the overall management of the Lake Tenkiller water supply for power generation, water supply, and recreation. Specific objectives are:
- a. Estimate monthly and peak daily use of water for individual treatment systems for which monthly treatment plant operations have been filed with the Oklahoma Department of Environmental Quality.
 - b. Develop operational models for the major rural water systems operating in the area for which there are GIS pipeline maps. These models are used to estimate the cost of delivering water through individual pipelines along with points of high and low pressure and water ages in various parts of the pipeline.
 - c. Compare the cost of developing a regional treatment system with the cost of purchasing and operating individual water treatment systems.

EPANET models have been established for the individual systems where GIS pipeline data are available. The EPANET model of the regional pipeline system has also been developed and validated. A statistical analysis of monthly water quantities of water treated by the cities and towns in the regions is being conducted.

Preliminary Findings

Results of the study at Beggs, Oklahoma, indicate that the integration of EPA models, OWRB data, and GIS maps may require a commitment of time and technical expertise that would likely be beyond the capabilities of small water systems. The studies at the

other small communities (Bragg and Oilton) will be refined accordingly to evaluate the feasibility of a simpler process to determine future infrastructure requirements.

At a minimum, this project will produce a clear set of data inputs, modeling criteria, and expected outcomes that can be used in the future by water managers.

An Assessment of Environmental Flows for Oklahoma

Basic Information

Title:	An Assessment of Environmental Flows for Oklahoma
Project Number:	2008OK107B
Start Date:	3/1/2008
End Date:	6/19/2009
Funding Source:	104B
Congressional District:	3
Research Category:	Climate and Hydrologic Processes
Focus Category:	Hydrology, Water Quantity, Ecology
Descriptors:	stream classification, hydrologic indices, modeling eco-hydrology
Principal Investigators:	Don Turton, William Fisher

Publication

**OWRRI Project
Final Report
An Assessment of Environmental Flows for Oklahoma**

Start Date: February 29, 2008

End Date: February 28, 2009

Congressional District: 3

Focus Categories: ECL, HYDROL, MET, SW, WQN, WU

Submitted by:

Co-PIs:

Dr. Don Turton
Associate Professor
Oklahoma State University
Department of Natural Resource Ecology and Management

Dr. Bill Fisher
USGS, NY Coop Research Unit
206F Fernow Hall, Cornell Univ
Ithaca, NY 14850

And:

Titus S. Seilheimer, Ph.D.
Postdoctoral Fellow
OK Cooperative Fish and Wildlife Research Unit
404 Life Sciences West
Oklahoma State University

Rachel A. Esralew
Hydrologist
U.S. Geological Survey
Oklahoma Water Science Center
202 NW66th
Oklahoma City 73116

Publications: none to date

Table of Contents

List of Tables.....	iii
List of Figures.....	iv
Problem and Research Objectives.....	1
Methods and Results of HIP Development Steps 1, 2 and 3.....	4
<i>Step 1: Baseline Period of Record and the Identification of Streams for Classification.....</i>	<i>4</i>
<i>Step 2: Calculation of 171 hydrologic indices using the Hydrologic Index Tool (HIT).....</i>	<i>11</i>
<i>Step 3: Classification of streams and identification of the 10 primary flow indices.....</i>	<i>15</i>
Principal Findings and Significance.....	41
Future Needs.....	43
References.....	44
Appendix.....	47

List of Tables

Table 1: Site code, station ID, and station name of 88 USGS streamflow stations used to classify Oklahoma streams.....	12-14
Table 2: Eigenvalues, percent variance explained, cumulative percent variance, and broken-stick eigenvalues for the first six principal components from the principal components analysis of 160 hydrologic indices and 88 stream gages.....	16
Table 3: Eigenvector loading on the first six principal components for the 27 hydrologic indices used to classify Oklahoma streams. Bold indicate the principal component was selected from.....	19
Table 4: Names and definitions of the 27 hydrologic indices used to classify Oklahoma streamflows grouped primarily by flow category.....	20-21
Table 5: Mean and standard deviation for two cluster classification using 27 hydrologic indices. Significant differences ($\alpha = 0.05$) between groups was tested with the Mann-Whitney test and are indicated by different letters.....	25
Table 6: Mean and standard deviation for the four cluster classification using 27 hydrologic indices. Significant differences ($\alpha = 0.05$) between groups was tested with the Kruskal-Wallis test with post-hoc test to differentiate between groups. Significant differences between groups is indicated by different letters.....	31
Table 7: Mean and standard deviation for the six cluster classification using 27 hydrologic indices. Letters separate significant differences ($\alpha = 0.05$) between groups tested with the Mann-Whitney test for groups 62/63 (a/b) and 65/66 (y/z).....	37
Table A: Final baseline period of record for selected streamflow gaging stations in and near Oklahoma that were considered for use in the HIP Classification.....	48-58

List of Figures

Figure 1. The development and application steps of the Hydroecological Integrity Assessment Process (HIP).....	3
Figure 2. USGS streamflow gaging stations, within a selected analysis extent, having 10 or more years of continuous daily streamflow record and a drainage area of less than 2,600 square miles.....	7
Figure 3. USGS streamflow gaging stations with a baseline period of record of 10 or more years, and the quality ranking of the baseline period for each gage.....	10
Figure 4: Principal components analysis plots A) site scores of streamflow stations and B) eigenvectors of hydrologic indices for the first and second principal components. Percentages indicate proportion of total variation in dataset that is explained by each principal component.....	17
Figure 5: Cluster analysis dendrogram made by using Euclidian distance measure and Ward's method for classification of 88 streams in Oklahoma. Station codes are shown in Table 2.....	23
Figure 6: Cluster analysis dendrogram (Euclidean distance and Ward's method) showing two cluster classification of 88 Oklahoma streamflow stations. Station codes are shown in Table 2.....	26
Figure 7: Map of 88 streamflow station in Oklahoma classified by two group cluster analysis. Red triangles are members of group 21 and blue circles are members of group 22.....	27
Figure 8: Boxplots of hydrologic indices for the two cluster classification of streamflow-gaging stations in Oklahoma. See Table 5 for hydrologic index names and Figure 6 for groups.....	28-29
Figure 9: Cluster analysis dendrogram (Euclidean distance and Ward's method) showing four cluster classification of 88 Oklahoma streamflow stations. Station codes are shown in Table 2.....	32
Figure 10: Map of 88 streamflow stations in Oklahoma classified by four group cluster analysis. Red triangles are members of group 41, yellow pentagons are members of group 42, black diamonds are members of group 43, and blue circles are members of group 44.....	33

Figure 11: Boxplots of hydrologic indices for the two cluster classification of streamflow-gaging stations in Oklahoma. See Table 5 for hydrologic index names and Figure 9 for groups.....34-35

Figure 12: Cluster analysis dendrogram (Euclidean distance and Ward's method) showing six cluster classification of 88 Oklahoma streamflow stations. Station codes are shown in Table 2.....38

Figure 13: Map of 88 streamflow stations in Oklahoma classified by six group cluster analysis. Red triangles are members of group 61, yellow pentagons are members of group 62, purple pentagons with dot are members of group 63, black diamonds are members of group 64, blue circles are members of group 65, and green circles with dot are members of group 66.....39

Figure 14: A comparison of the four-group cluster analysis stream classifications and Level II Ecoregions of Oklahoma. Note that the symbols represent the location of a gaging station at the watershed outlet. The majority of the watershed drained by the stream may lie in a different ecoregion.....42

Problem and Research Objectives:

Background:

The state of Oklahoma is in the process of updating the Oklahoma Comprehensive Water Plan. The water plan was last updated in 1995, and water demand projections for the current plan will be for the next 50 years (<http://www.owrb.ok.gov/supply/ocwp/ocwp.php>, accessed on 27 May 2009). The water plan will focus on development of system-level plans to provide the most water to the majority of Oklahomans. Assessment of current and projected water demands and water supply and availability will be made by 2011 prior to implementation of the water plan. Development of the plan will proceed through three phases. Phase one will focus on developing water demand projections by county and region through year 2060 and a comprehensive inventory and analysis of the state's water supplies. Phase two will identify local and regional problems and opportunities related to the use of water for public supply, agricultural, industrial, recreational, and environmental uses. Phase three will involve implementation of planning initiatives and tools derived from the issues, problems and needs identified in phase two. Technical studies will be needed to identify environmental uses of water, particularly the flows required for fish and other aquatic biota, to aid in planning for Oklahoma's future water needs.

Previous Oklahoma water plans have not recognized environmental flows or made provisions for protecting them. Assessment of current and projected water demands and water supply and availability will be made by 2011 prior to implementation of the water plan. Oklahoma has four fish species and three mussel species that are federally-listed as threatened or endangered and sensitive to alterations in streamflow. It is imperative that environmental flows be assessed and considered in the development of the updated Oklahoma comprehensive water plan to aid in sustaining aquatic life and protecting federally threatened and endangered and state species of greatest conservation concern in Oklahoma.

Alteration of the hydrologic regime of rivers from impoundments and flow diversions modifies the structure and function of river ecosystems (Poff et al. 1997, Rosenberg et al. 2000, Postel and Richter 2003, Poff et al. 2007). Hydrologic alterations such as flow stabilization, prolonged low flows, loss of seasonal flow peaks, rapid changes in river stage, and low or high water temperatures downstream disrupt life cycles of aquatic plants, invertebrates, and fishes resulting in a reduction in species diversity and modifying reproduction and growth rates that oftentimes lead to local extinctions of native species and the invasion and establishment of exotic species (Poff et al. 1997). Large water diversions deplete streamflows, sometimes to damaging levels that affect aquatic and floodplain habitats, aquatic biodiversity, sport and commercial fisheries, natural floodplain fertility, and natural flood control (Postel and Richter 2003). The development of water resources to meet the demands of urban population centers is

growing and threatens the ecological integrity of many freshwater ecosystems (Fitzhugh and Richter 2004).

Water management goals in the new millennium have broadened from traditional societal goals of water supply, flood control, channel maintenance, power production and commerce to include maintenance and enhancement of natural aquatic communities and ecosystem services. This has resulted in a paradigm shift from the simple question of "How much water can be taken from streams and lakes for human use?" to the more complex question of "How much water needs to be left in streams and lakes to sustain critical water-dependent natural resources?" (USFWS and USGS 2004). Evaluation of water use and development projects now requires consideration of effects at multiple scales, including consideration of the whole hydrograph and not simply minimum flows, the dynamic river channel rather than the static channel, the linkage between surface and ground water, and ecological communities rather than single species.

Assessment of environmental flows, traditionally referred to as instream flows, for Oklahoma is needed to aid planners, policy makers and the public in developing of the Oklahoma Comprehensive Water Plan. An initial step in assessing environmental flows for Oklahoma is characterizing and classifying streams and rivers based on their flow regimes. There are currently over 200 methods for evaluating environmental flows, which range from those that determine "minimum" flows to those that mimic the "natural flow regime" (Arthington et al. 2006). Scientists and many managers are now in general agreement that a regulated river needs to mimic the five components of the natural flow regime, including the magnitude, timing, frequency, duration, and rate of change and predictability of flow events, plus the sequence of these conditions (Olden and Poff 2003, Arthington et al. 2006). These more complex methods go beyond developing simple hydrological "rules of thumb" to more comprehensive environmental flow assessment. HIP is a tool developed by the USGS that identifies 10 non-redundant hydrologic indices that are ecologically relevant, specific to stream classes, and characterize the five components of the natural flow regime (Figure 1) (http://www.fort.usgs.gov/Resources/Research_Briefs/HIP.asp, accessed on 27 May 2009). The HIP process can be developed for a state (e.g., Massachusetts, Missouri, New Jersey, Pennsylvania, and Texas, are using HIP), but also can be applied at the stream reach level.

Objectives:

We used the Hydroecological Integrity Assessment Process (HIP) approach developed by the U. S. Geological Survey to assess environmental flows in Oklahoma's perennial streams. The HIP is a modeling tool that identifies 10 non-redundant hydrologic indices that are ecologically relevant, specific to stream classes, and characterize the five components of the natural flow regime. These components are the magnitude, timing, frequency, duration, and rate of change and predictability of flow events, plus the sequence of these conditions. Information derived from the HIP analysis will be used to make environmental flow recommendations for incorporation

into the Oklahoma Comprehensive Water Plan and for future water permitting and planning.

The HIP is a process consisting of four development and two application steps (Figure 1). The objectives of this work were to complete the first 3 steps:

1. Obtain baseline data and identify appropriate streams for classification.
2. Calculate 171 hydrologic indices using the Hydrologic Index Tool (HIT).
3. Classify streams and identify the 10 primary flow indices.

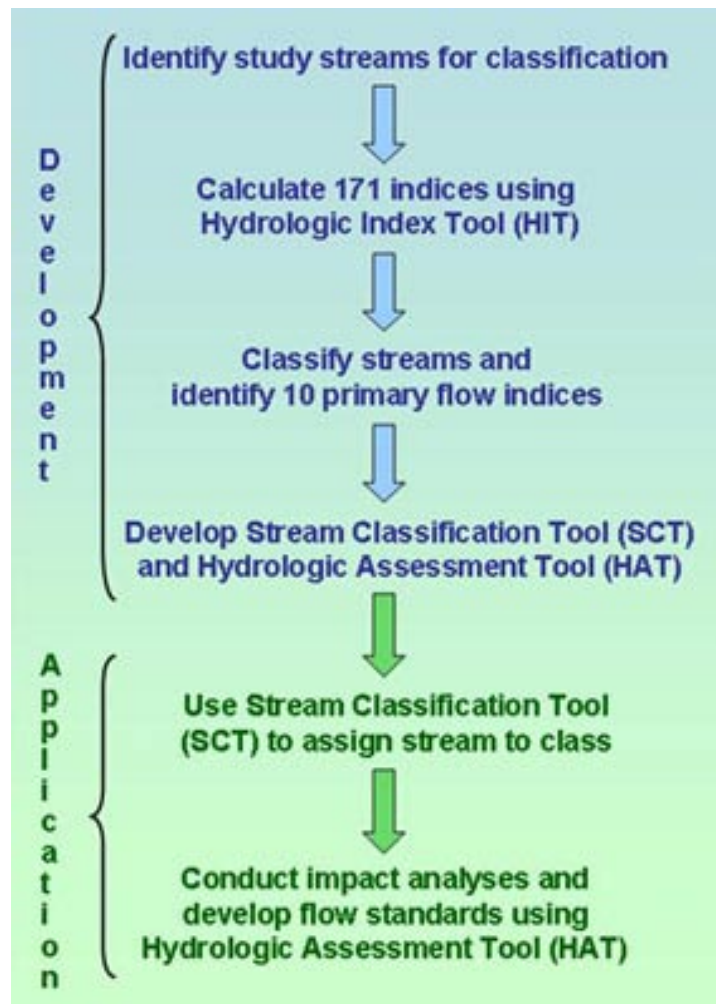


Figure 1. The development and application steps of the Hydroecological Integrity Assessment Process (HIP).

Methods and Results of HIP Development Steps 1,2 and 3

Step 1: Baseline Period of Record and the Identification of Streams for Classification

This section of the report was prepared by the U.S. Geological Survey

Ideally, a HIP classification suite should include long-term continuous streamflow record from the most natural state of streamflow available. This allows for the HIP classification to represent the most “natural” conditions of the basin which can be used as a hydrologic foundation for future assessment of ecological impairment with respect to anthropogenic alteration of the flow regime. Usage of the most natural (or least-altered) streamflow record in the HIP classification also reduces the likelihood that the records will be statistical outliers in the cluster analysis.

In addition to selecting streamflow data from a least-altered period, streamflow records need to be sufficient in length to ensure that typical variations in climate are observed during the selected period. Due to potentially limited gaging record and increasing development of the stream over time, the least-altered period of record for some gages may be relatively short. A sufficient record length would increase the probability that intra-annual variability of the daily hydrograph, which may be affected by recurrent climate cycles, is encompassed by the period chosen for classification. This pre-condition will help to minimize statistical bias and random error in the cluster analysis.

For each USGS streamflow-gaging station with continuous streamflow record selected for use in the HIP classification, a minimum optimal baseline period of record was determined. The baseline period of record can be defined as a period which is both “least altered” by anthropogenic activity and has sufficient record length to represent the extremes of climate variability. By this definition, there is a possibility for streams with continuous streamflow data not to have a period of record that could be considered baseline. For this study, if a streamflow-gaging station had data that either was substantially altered by human activity or did not have a minimum of 10 years of least-altered, then that record was either omitted from use in the HIP classification or downgraded in quality.

In Oklahoma, substantial streamflow alteration can be caused by a variety of human activities. Irrigation with both surface water and groundwater and other consumptive water uses are common throughout Oklahoma and represent the single largest use of water (Tortorelli 2002). Most irrigation water comes from groundwater, primarily from the High Plains aquifer in the panhandle as well as from other parts of western Oklahoma. Surface-water withdrawals, primarily used for consumptive water supply and livestock, are also common throughout the state. Many surface-water diversions in Oklahoma are withdrawn from reservoirs or other impoundments (Tortorelli 2002).

Flood peak reduction, from numerous flood-water retarding structures that serve to decrease main-stem flood peaks and regulate runoff recession of single storm events, also affects streamflow for large areas of Oklahoma (Tortorelli and Bergman 1985; Bergman and Huntzinger 1981).

Few if any streams in or near Oklahoma have been completely free of anthropogenic activity during the last century. Therefore, an allowable amount of anthropogenic alteration must be permitted in order to include sufficiently long-term record in the HIP classification. Long-term record is desired for the classification in order to provide a representative sample of streamflow during variable climate conditions. By accepting some alteration, the goal of the baseline period determination process is to select, for each gage, a sufficiently long period that is "least altered". The selection of a least-altered period of record includes eliminating the period of streamflow data where the degree of alteration is substantially high and that the streamflow record is unacceptable for use in the HIP classification. The degree of anthropogenic alteration varies over time and over a spatial extent. Determining if a period is "natural" or "altered" may require some subjective judgement. In addition, the effects of anthropogenic activity in a stream basin may not occur over the course of one year, but may take many years. Examples would be increasing irrigation development over a period of time, construction of numerous small flood retarding structures in the stream basin, or gradual urban development in a watershed.

Streamflow data have been collected for streams in and near Oklahoma over periods ranging from a few years to nearly a century (U.S. Geological Survey National Water Information System, <http://waterdata.usgs.gov/nwis>, accessed June, 2008). Shorter periods of record may coincide with aberrant climate conditions and streamflow patterns that are not representative of typical conditions. Longer periods of record are more likely to provide a representative sample of central tendencies and variability of streamflow. However, as population increases and agricultural, industrial, and urban development increase in Oklahoma over the course of a century, longer periods of record and more recent periods of record are likely to contain streamflow data that are affected by human activity in the basin.

Based on the potential sources of subjectivity involved with selection of baseline periods for gages as described above, baseline periods of some gages may be more complete than others. Quality assurance and examination of outliers in the HIP classifications may require a qualitative assessment of the data used to develop the model. In order to reduce the subjectivity of selecting a baseline period and enable comparison of the baseline periods from one gage to another, a quality ranking was assigned to each baseline period. The terms in the quality ranking of the baseline period are "excellent", "good", "fair", "poor", or "unusable" and are based on the relative degree of anthropogenic activity, severity of climatic bias for the period with the least anthropogenic activity, and length of the record. The goal of the baseline analysis was to select a period for each stream that had the most favorable quality ranking based on these criteria. Streams where the period of record was determined to be "poor" or "unusable" were entirely omitted from use in the HIP classification.

Methods for Determining the Baseline Period of Record

Streamflow data from gaging stations with a minimum of 10 years of daily streamflow record, and a drainage area that is greater than 1 square mile but less than 2,600 square miles were considered for use in the HIP classification. A minimum period of record of 10 years was assumed to be an adequate minimum record length for determination of the least-altered period. This assumption was based on the use of 10 years of record for the New Jersey statewide HIP classification (Eraslew and Baker 2008 and Kennen et al. 2007). Drainage areas of streams selected for analysis were greater than 1 square mile and less than 2,600 square miles based on drainage area criteria used in previous statistical analysis studies (Tortorelli and Bergman 1985; Tortorelli 1997). Streamgages selected for analysis and contributing drainage area upstream from the streamgage were located within 8-digit hydrologic unit boundaries (based on the 8-digit hydrologic unit codes, or HUC) that were located at least partly in Oklahoma. There were 168 streamgages that met the criteria for analysis. Figure 2 shows the locations of gages that meet these criteria, and were initially included in baseline period determination process.

Streamflow data from substantially altered streams, or periods of streamflow record that were determined to be affected by human alteration, were removed from consideration from the HIP classification after a series of analysis procedures (Figure 1). After this elimination, if the gage did not have at least 10 years of remaining continuous period of record, the streamgage was eliminated from consideration for use in the HIP classification. The methods used to determine a baseline period of record were incorporated from visual and statistical procedures as well as professional judgment.

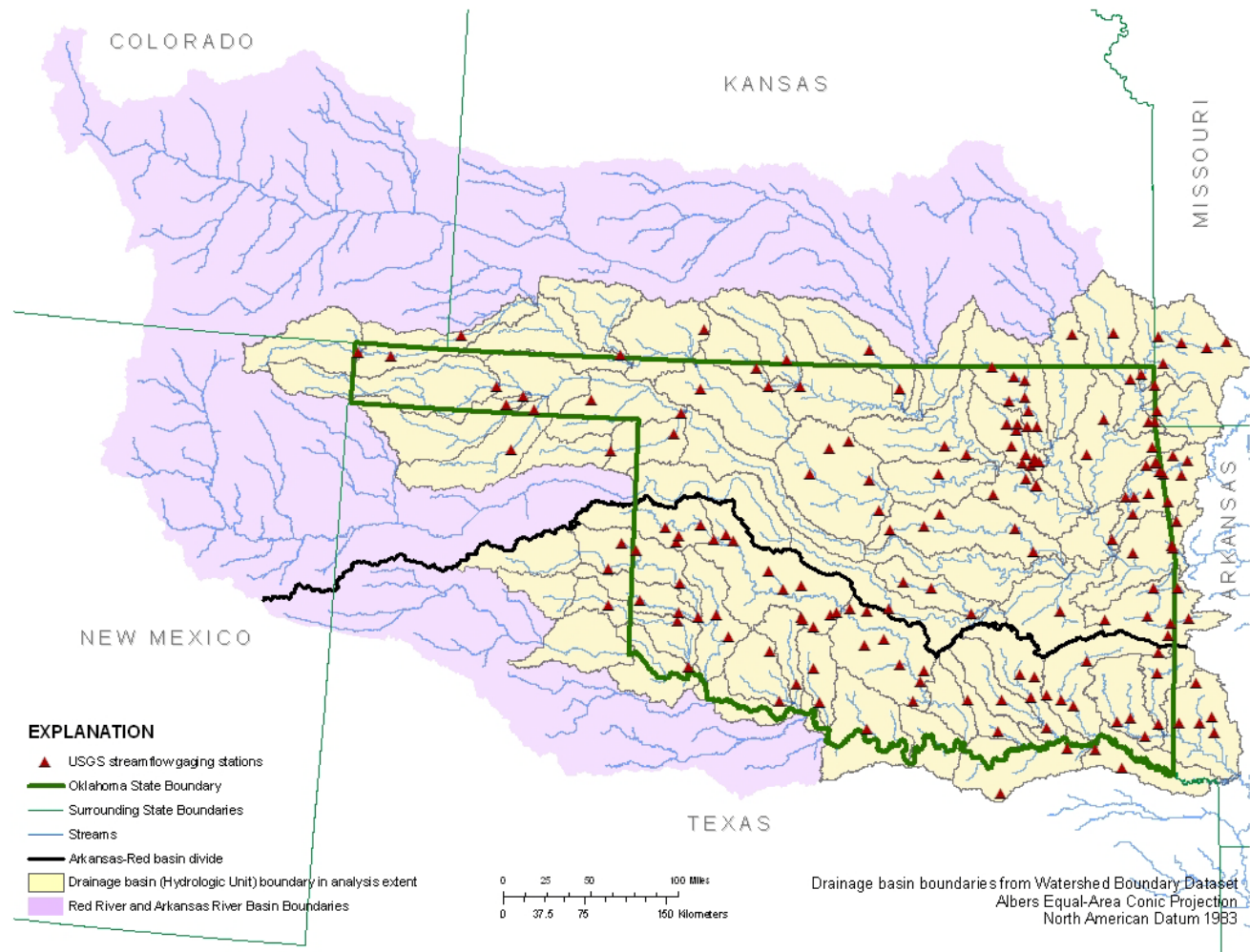


Figure 2. USGS streamflow gaging stations, within a selected analysis extent, having 10 or more years of continuous daily streamflow record and a drainage area of less than 2,600 square miles.

Determination of the Least-Altered Period of Record

Determination of a baseline period was conducted in two phases. In the first phase, least-altered periods were selected for gages that had a minimum record length of 10 years. In the second phase, an optimum minimum period of record was determined for gages in each Climate Division (National Oceanic and Atmospheric Administration, 2008) to determine if 10 years of record sufficiently represented long-term climate variability.

In the first step of the process to determine the least-altered period of record, streamgage information was evaluated using previous publications, historical gage record notes, and information gathered from oral and written communication with data-collection staff familiar with selected gages. Known anthropogenic events in the basin were used to reduce the record to a least-altered period with a minimum of 10 years. If the least-altered period of record included streamflow that was affected by anthropogenic alteration, then the quality ranking was reduced accordingly.

In the second step of the determination of the least altered period, gages that had substantial effects from upstream impoundment were identified by evaluating the location and extent of dams in the drainage basin. Impounded areas were delineated using geographic information system (GIS) software in order to estimate the percent of impoundment in the basin, and how much that percentage changed over time. The percentage of the basin that was impounded was used to determine a preliminary quality ranking for the baseline period. If 20 percent or more of the drainage basin was affected by impoundment, it was eliminated from consideration.

In the third step of the determination of the least-altered period, statistical trend analysis was performed for selected streamgages with 20 or more years of record to detect statistically significant changes in baseflow, runoff, total flow, and baseflow index for selected gages where visual trends in the annual hydrograph were observed. Significant trends in streamflow were compared with trends in precipitation, using visual trend observation and analysis of covariance of double-mass curves, in order to determine if the trend was attributable to climate or possible anthropogenic affects. If trends were suspected to be due to anthropogenic affects and not trends in precipitation, an additional Kendall's tau test was performed for selected datasets to determine if statistically significant trends existed for each of the annual flow parameters (Kendall and Gibbons 1990). If the preliminary baseline period determined from previous steps had a statistically significant trend in the annual hydrograph that was not attributable to climate changes, then the quality ranking was reduced to "poor".

Determination of an Optimum Minimum Period of Record to Encompass Climate Variability

In the second phase, an optimum minimum period of record was determined for each of the least-altered periods to ensure that the selected period had a sufficient record length to provide a representative sample of the extremes of climate variability. An assumption was made in the previous phase that no less than 10 years should be

considered for the baseline period. For each climate division that contained gages that were to be used in the HIP classification, an optimum minimum period of 10 years or more were evaluated by using a Wilcoxon rank-sum test. This test was used to analyze the variability of annual precipitation for selected 5-, 10-, 15-, 25-, and 35-year periods. The results from the test were used to determine how many years of annual precipitation were needed for the distribution of annual precipitation for the selected period to be statistically similar to the distribution of annual precipitation for a longer period, 1925-2007. This period was selected because it encompasses all of the years of streamflow record considered in the baseline analysis. In addition, this longer period was compared to the annual precipitation for the least-altered period to determine if the least-altered period was statistically representative of long-term climate variability. Results of the record-length analysis for each gage are listed in Table A.

For purposes of this study, the baseline period was the same as the least-altered period determined from previous steps because least-altered periods were not eliminated from use in the HIP classification if it did not contain an optimal minimum number of years as a result of the second phase of the analysis process. Instead, the quality ranking was reduced for these periods. If the preliminary baseline period determined from previous steps did not have an optimum minimum period of record or was statistically different from the period 1925-2007, the quality ranking was reduced accordingly. Eliminating gages from the HIP classification where the least-altered period of record was less than the optimum minimum period would substantially reduce the number of stations. Instead of eliminating gages from consideration where the least-altered period of record did not meet these criteria, the quality ranking was lowered by one level (for example a "fair" baseline period would be reduced to a "poor" baseline period). Therefore the difference between the baseline period and least-altered period are only due to the quality ranking and not the number of years.

Final Baseline Period of Record

A final baseline period was determined for each gaging station considered for use in the HIP classification. The baseline period for each station was rated as "excellent", "good", "fair", "poor", or "unusable" by combining the quality rankings determined for the degree of alteration in the basin for the least-altered period of record, and whether or not the least-altered period was long enough to likely be representative of long-term climate variability. The baseline period of record determined for each gage considered for use in the HIP classification, and the associated quality ranking of the baseline period, are presented in Table A and are shown in Figure 3. Gages that were removed from the list because they did not have an adequate baseline period (the baseline period was rated as "unusable") are not listed in Table A or Figure 3.

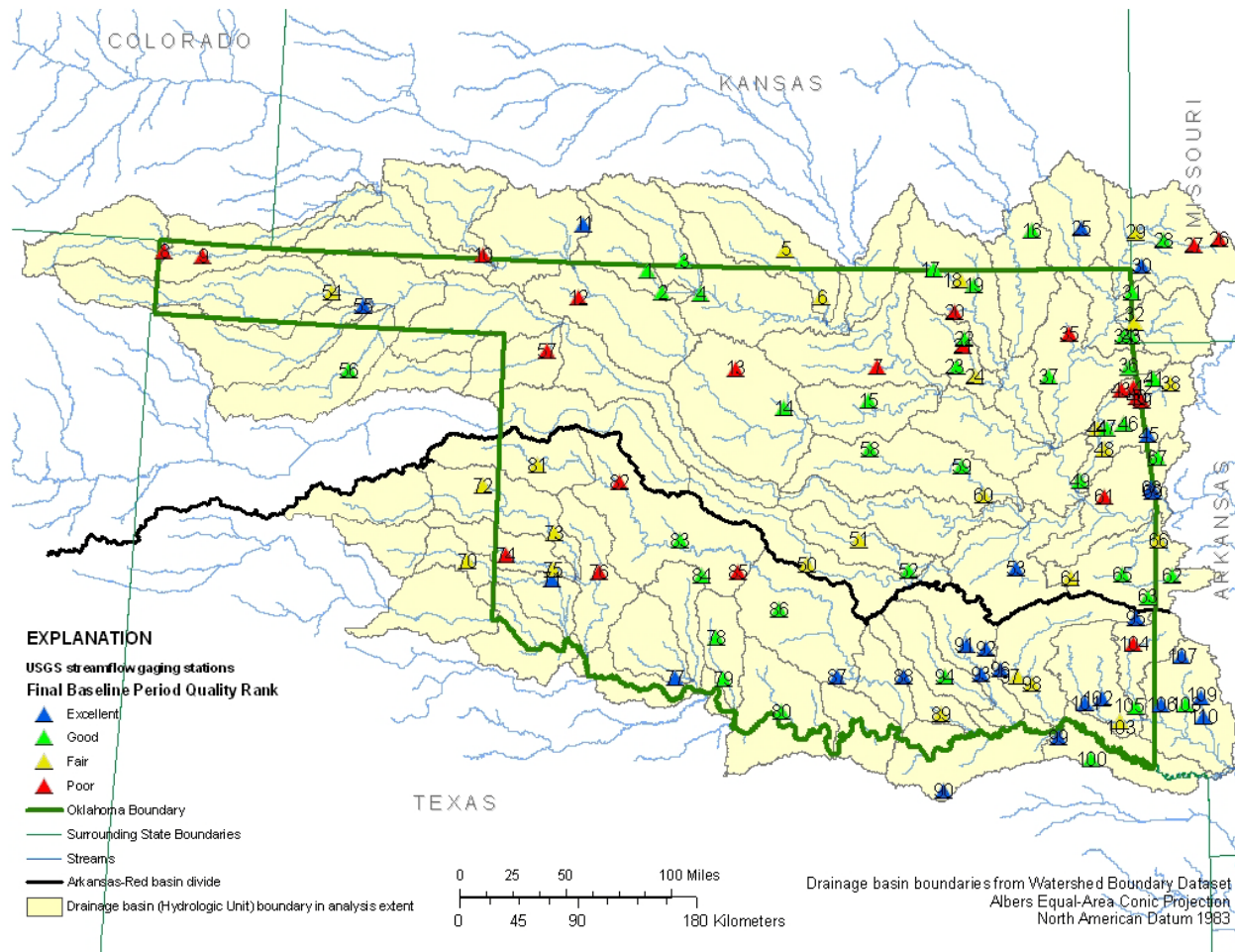


Figure 3. USGS streamflow gaging stations with a baseline period of record of 10 or more years, and the quality ranking of the baseline period for each gage.

Step 2: Calculation of 171 hydrologic indices using the Hydrologic Index Tool (HIT).

We used multivariate statistical analysis on streamflow statistics to describe the variability in the flow regime for reference conditions of Oklahoma rivers (Henriksen et al. 2006; Kennen et al. 2007; Olden and Poff 2003). Classification was completed using data from 88 USGS streamflow stations (Table 1) obtained from the baseline analysis described in the previous section (Table A). The stations were primarily located in Oklahoma (59), along with stations located in bordering states with flows that were relevant to Oklahoma: Kansas (6), Texas (6), Missouri (6), and Arkansas (11).

Flow Regime

Factors such as the quantity of water, the time of the year that high and low flows occur, and how often flow events happen are collectively referred to as the natural flow regime. This set of unique conditions is determined by many factors, such as geology, climate, and vegetation cover (Poff et al. 1997), and can be used to identify groups of streams with similar hydrologic behaviors. In addition to being useful for classification of streams, flow regime is important to biological organisms and the health of aquatic ecosystems, which have adapted over time to those conditions. Impacts to aquatic organisms from flow regime alteration can include the disruption of their life cycle (Scheidegger and Bain 1995), loss of connection and access to wetlands or backwaters (Junk et al. 1989), and change in plant cover types (Auble et al. 1994). Thus to protect ecosystems, the flow regime should be maintained or mimicked to support the natural cycles that species rely on.

The natural flow regime can be described with five categories that cover the natural hydrologic variation that is present in a stream (Poff et al. 1997). Magnitude is a measure of the quantity of water moving past a point per unit time. This category is divided into magnitudes of average (MA), low (ML), and high (MH) flows. Frequency describes how often specified low (FL) and high (FH) flow events occur. Duration describes the length of time that low (DL) and high (DH) flow events occur. Both the frequency and duration categories deal with low (e.g. no flow days) and flood flow events. Timing describes the dates that average (TA), low (TL), and high (TH) flow events occur. The rate of change (RA) describes the rise or fall in streamflow. Streams with high or rapid rate of change can indicate they are "flashy," while low rates may indicate that a stream has "stable" streamflow.

Software

We used the Hydrologic Index Tool (HIT, Version 1.48; USGS, Fort Collins, CO; <http://www.fort.usgs.gov/Products/Software/NATHAT/hitinst.exe>) software to calculate indices from all five classes of streamflow. The HIT software calculates a total of 171 indices (Henriksen et al. 2006; Olden and Poff 2003) with 94 describing magnitude, 14 describing frequency, 44 describing duration, 10 describing timing, and 9 describing rate

Table 1: Site code, station ID, and station name of 88 USGS streamflow stations used to classify Oklahoma streams.

Site Code	Station ID	Station Name
CAVC	07157900	Cavalry Creek at Coldwater, KS
LGHT	07184000	Lightning Creek near McCune, KS
SHOL	07187000	Shoal Creek above Joplin, MO
BRND	07196900	Baron Fork at Dutch Mills, AR
GAIN	07232000	Gaines Creek near Krebs, OK
COLD	07233000	Coldwater Creek near Hardesty, OK
LEES	07249985	Lee Creek near Short, OK
LEEV	07250000	Lee Creek near Van Buren, AR
STRM	07300500	Salt Fork Red River at Mangum, OK
DFCK	07311500	Deep Red Creek near Randlett, OK
CADO	07330500	Caddo Creek near Ardmore, OK
BLUM	07332400	Blue River at Milburn, OK
BDRC	07332600	Bois D'Arc Creek near Randolph, TX
CHCS	07333500	Chickasaw Creek near Stringtown, OK
MCGE	07333800	McGee Creek near Stringtown, OK
MBOG	07334000	Muddy Boggy Creek near Farris, OK
KIAC	07335700	Kiamichi River near Big Cedar, OK
TENM	07336000	Tenmile Creek near Miller, OK
LPIN	07336750	Little Pine Creek near Kanawha, TX
LTRW	07337500	Little River near Wright City, OK
GLOV	07337900	Glover River near Glover, OK
ROLL	07339500	Rolling Fork near DeQueen, AR
COSV	07340300	Cossatot River near Vandervoort, AR
SALD	07341000	Saline River near Dierks, AR
SALL	07341200	Saline River near Lockesburg, AR
SLTW	07148350	Salt Fork Arkansas River near Winchester, OK
SLTA	07148400	Salt Fork Arkansas River near Alva, OK
MEDL	07149000	Medicine Lodge River near Kiowa, KS
SLTC	07149500	Salt Fork Arkansas River near Cherokee, OK
SKEL	07160500	Skeleton Creek near Lovell, OK
CNCL	07163000	Council Creek near Stillwater, OK
BHIL	07170700	Big Hill Creek near Cherryvale, KS
CNYE	07172000	Caney River near Elgin, KS
LCAN	07174200	Little Caney River below Cotton Creek, near Copan, OK
CNDY	07176800	Candy Creek near Wolco, OK
HMNY	07177000	Hominy Creek near Skiatook, OK

Table 1, continued.

Site Code	Station ID	Station Name
SPRC	07185765	Spring River at Carthage, MO
LOST	07188500	Lost Creek at Seneca, MO
CVSP	07189540	Cave Springs Branch near South West City, MO
HONY	07189542	Honey Creek near South West City, MO
SPAV	07191220	Spavinaw Creek near Sycamore, OK
PRYR	07192000	Pryor Creek near Pryor, OK
FLTS	07195800	Flint Creek at Springtown, AR
PECH	07196973	Peacheater Creek at Christie, OK
BRNE	07197000	Baron Fork at Eldon, OK
ILRG	07198000	Illinois River near Gore, OK
LTRS	07231000	Little River near Sasakwa, OK
PALO	07233500	Palo Duro Creek near Spearman, TX
DRYC	07243000	Dry Creek near Kendrick, OK
DFKB	07243500	Deep Fork near Beggs, OK
POTC	07247000	Poteau River at Cauthron, AR
BLFK	07247250	Black Fork below Big Creek near Page, OK
POTW	07248500	Poteau River near Wister, OK
COVE	07249500	Cove Creek near Lee Creek, AR
LBEA	07313000	Little Beaver Creek near Duncan, OK
BVCK	07313500	Beaver Creek near Waurika, OK
MUDC	07315700	Mud Creek near Courtney, OK
COBB	07326000	Cobb Creek near Fort Cobb, OK
LWSC	073274406	Little Washita River above SCS Pond No 26 near Cyril, OK
RUSH	07329000	Rush Creek at Purdy, OK
CBOG	07335000	Clear Boggy Creek near Caney, OK
PCAN	07336800	Pecan Bayou near Clarksville, TX
MTNE	07339000	Mountain Fork near Eagletown, OK
COSD	07340500	Cossatot River near DeQueen, AR
CHCC	07151500	Chickaskia River near Corbin, KS
CHCB	07152000	Chickaskia River near Blackwell, OK
CNYH	07173000	Caney River near Hulah, OK
BRDS	07177500	Bird Creek near Sperry, OK
SPRW	07186000	Spring River near Waco, MO
ELKR	07189000	Elk River near Tiff City, MO
OSAG	07195000	Osage Creek near Elm Springs, AR
ILRT	07196500	Illinois River near Tahlequah, OK
CNYC	07197360	Caney Creek near Barber, OK

Table 1, continued.

Site Code	Station ID	Station Name
WNUT	07229300	Walnut Creek at Purcell, OK
BVRV	07232500	Beaver River near Guymon, OK
DFKD	07244000	Deep Fork near Dewar, OK
FOMA	07247500	Fourche Maline near Red Oak, OK
JMSF	07249400	James Fork near Hackett, AR
STRW	07300000	Salt Fork Red River near Wellington, TX
SWET	07301410	Sweetwater Creek near Kelton, TX
NFRR	07301500	North Fork Red River near Carter, OK Elm Fork of North Fork Red River near
ELMM	07303500	Mangum, OK
WASC	07316500	Washita River near Cheyenne, OK
BLUB	07332500	Blue River near Blue, OK
KIAA	07336200	Kiamichi River near Antlers, OK
KIAB	07336500	Kiamichi River near Belzoni, OK
LTRI	07338500	Little River below Lukfata Creek, near Idabel, OK

of change of streamflow. Categories with many indices, such as magnitude, had sets indices that were calculated for individual months (e.g. January mean flow, May mean minimum flow), and this resulted in many indices in those categories.

We used data from a reference period recorded at USGS streamflow stations. The analysis used two types of data: daily average flows (mean flow in 24 hours in ft³/second), and peak flow (instantaneous ft³/sec) data for each gage, which were required for the calculation of six indices. The length of reference period used in the analysis for all stations had a median length of 22 years and ranged from a minimum of 10 to a maximum of 83 years. A set of eleven indices were not able to be calculated for all 88 stations. This was a result of an error in calculation of indices for some sites due to a zero in denominator of the index equation. Ten of the indices had too many zero flow days in their record (MA6, MA7, MA8, ML18, ML21, FL2, DL6, DL7, DL8, DL17), while one had no zero flow days (DL19). After exclusion of the indices, the available dataset was reduced from 171 to 160, but all five components of flow regime were still represented.

Step 3: Classification of streams and identification the 10 primary flow indices

Data Screening and Standardization

We used the two step process called the Hydroecological Integrity Assessment Process (HIP) for classification of streams based on flow regime from hydrological indices (Henriksen et al. 2006; Kennen et al. 2007; Olden and Poff 2003). The first step uses principal component analysis (PCA) to reduce redundancy in the 171 indices and select hydrologic indices that explain the most variation. The selected indices were then used in the second step in a cluster analysis to classify and group streamflow-gage stations based on similarity between flow regime.

Data standardization was required because the indices used different units (e.g. ft³/second, percent), which can affect the results from the cluster analysis (McGarigal et al. 2000). The standardization procedure we selected was the z-score method, which normalized each column (i.e. hydrologic indices) to have a mean of zero and a standard deviation of one (McCune and Grace 2002). An outlier analysis was also conducted using PC-ORD to remove the confounding influence of multivariate outliers on the principal components analysis and cluster analysis (McCune and Grace 2002). Outliers were defined as indices more than two standard deviations from the mean. The analysis found three indices that were classified as outliers (ML20, FL01, RA08), although they were only slightly over the two standard deviation threshold (2.1, 2.0, and 2.1 respectively). Outliers were flagged and excluded from later analyses. The outliers were not identified as high information variables in the principal components analysis, so no unique information was lost with their exclusion.

Principal Components Analysis

We used principal components analysis (PCA) to identify the hydrologic indices that contained the most information about the flow regime across the region. PCA is an eigenvector method of ordination that is used to reduce a large datasets into a smaller number of synthetic variables that describe the maximum amount of variation in the dataset (McGarigal et al. 2000). The reduced dataset of high information variables can then be used to characterize the flow regime of the selected streams. Variables with high eigenvector values on a principal component (i.e. have high score) contribute more information about the variation in the data than variables with near zero scores. This allows for the heaviest loading variable to be used to explain the ordination of the sites (McGarigal et al. 2000).

We used a PCA on a correlation matrix (PC-ORD) to ordinate 88 stations and 160 hydrologic indices. The first two principal components explain over 50% of the total variation in the dataset. A site's location on the PCA plot represents the centroid of all the hydrologic variables for that site on each plotted principal component (PC; Figure 4a). Stations like SPRC and BRNE both are found on the far left negative end of the first axis, but they do not have high scores on the second axis. The opposite is true for stations like GLOV and MBOG, which have low scores on the first axis but high scores on the second axis. The PCA also produced eigenvectors for the hydrologic indices for

each principal component (Figure 4b). Indices with high loadings on an axis indicate that the index is explaining a larger amount of variation (e.g. high positive on PC1 MA3 in Figure 4b) in the dataset than index scores that are near zero (e.g. DH23 in Figure 4b). Both the lower left and lower right quadrants of the graph have large groups of indices with high loadings on one or both of the first two principal components.

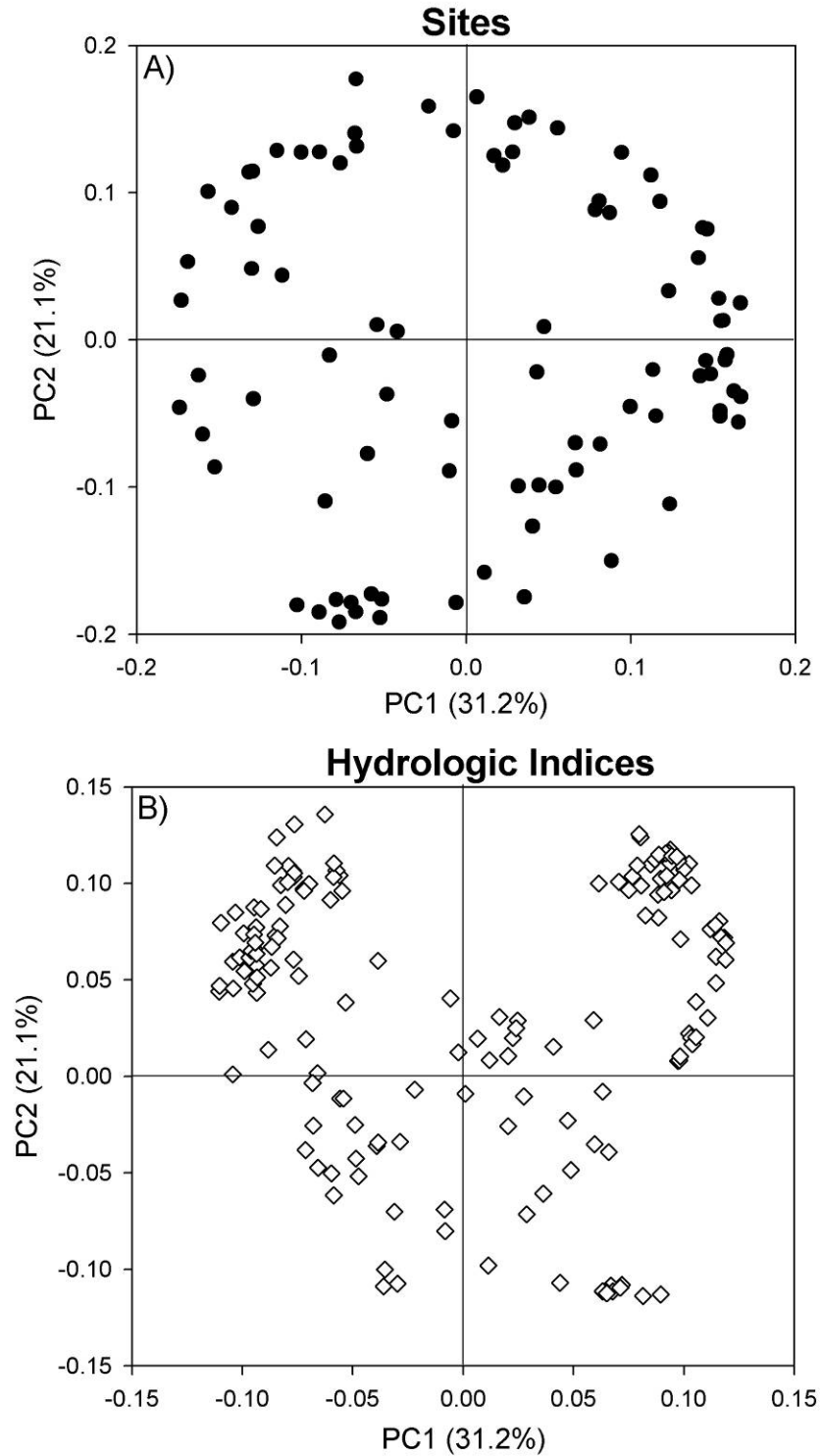
We used the first six principal components as the source for the selection of high information indices. The first two axes explain 52.2% of the variation in the dataset (Table 2). The total variation explained by the first six principal components was 77% (Table 2). We identified the first six principal components as important axes using the brokenstick eigenvalues. Brokenstick eigenvalues are an estimation of the eigenvalues that would be expected from the PCA by chance alone (Jolliffe 1972; King and Jackson 1999). Thus, when the actual eigenvalues are higher than brokenstick eigenvalues, then the patterns observed in the PCA are not random. The first six PC had higher real eigenvalues than brokenstick values and could be used in the selection of the most important hydrologic indices for describing Oklahoma streams (Table 2).

Table 2: Eigenvalues, percent variance explained, cumulative percent variance, and broken-stick eigenvalues for the first six principal components from the principal components analysis of 160 hydrologic indices and 88 stream gages.

Axis	Eigenvalue	Percent Variance	Cumulative Percent Variance	Broken-stick Eigenvalue
1	49.9	31.2	31.2	5.7
2	33.7	21.1	52.2	4.7
3	15.4	9.6	61.8	4.2
4	12.6	7.9	69.7	3.8
5	6.8	4.3	74.0	3.6
6	4.9	3.0	77.0	3.4

The process of index selection seeks to identify indices that contain the maximum amount of information about the flow regime, while removing redundant indices that are highly correlated with each other. One target in the reduction of the number of variables to maintain a 3:1 ratio of sites to indices for the cluster analysis (McGarigal et al. 2000). Based on the number of sites in the dataset (88), we used the target number of 29 hydrologic indices for selection into the cluster analysis. Another guideline was that the selected variables would include each of the ten components of the flow category, in order to include a picture of the entire flow regime in the classification process.

Figure 4: Principal components analysis plots. (A) site scores of streamflow stations and (B) eigenvectors of hydrologic indices for the first and second principal components. Percentages indicate proportion of total variation in dataset that is explained by each principal component.



We selected indices on the first six principal components that were within 15% of the highest absolute loading on each axis. This criterion reduced the total number of variables from 160 to 55. The 55 remaining indices were considered to contain a high amount of information that would be useful for classification of the stations (Table 3). In order to reduce the redundancy between the selected indices, we used a nonparametric correlation analysis (Spearman rho) for indices within each flow category. Indices that were highly correlated (e.g. May and June mean flows) were identified and the least correlated (i.e. most non-redundant) hydrologic indices were selected to be included in the classification portion of the analysis. The subset of 55 variables was further reduced to 27 indices, which was near our target of 29 variables for the 3:1 ratio (Table 4). The five flow components are represented in this set of variables with 8 describing magnitude (3 average magnitude, 2 low magnitude, and 3 high magnitude), 4 describing frequency (1 low flow frequency and 3 high flow frequency), 9 describing duration (3 low flow duration and 6 high flow duration), 3 describing timing (1 in timing of average, low, and high flows), and 3 describing rate of change (Table 4). With this set of variables, we can represent the natural flow regime at the stations and group them based on similarities in streamflow patterns.

Table 3: Eigenvector loading on the first six principal components for the 27 hydrologic indices used to classify Oklahoma streams. Bold indicate the principal component was selected from.

Eigenvector on Principal Component						
	1	2	3	4	5	6
MA01	-0.1023	-0.1104	-0.0178	-0.0466	0.0104	0.0437
MA04	0.0845	-0.1239	-0.0105	-0.0053	-0.0052	0.0342
MA28	0.1043	-0.0596	0.0291	-0.0770	-0.0979	-0.1007
ML01	-0.1119	-0.0764	-0.0392	-0.0151	-0.0169	-0.0798
ML09	-0.1039	-0.0167	-0.1226	0.0055	-0.0532	-0.1487
MH04	-0.0918	-0.1157	-0.0025	-0.0454	0.0169	0.0504
MH14	0.1012	-0.0617	-0.0895	0.0043	-0.0853	0.0208
MH20	-0.0224	-0.0199	-0.0096	0.0838	-0.0275	-0.1808
FL03	0.1032	-0.0850	0.0084	-0.0914	-0.0105	-0.0116
FH01	0.0533	-0.0383	0.1126	-0.1385	-0.1875	-0.0603
FH04	0.0764	-0.1307	-0.0117	0.0472	0.0066	0.0590
FH05	0.0392	0.0360	0.0457	-0.1871	-0.2018	0.0487
DL03	-0.0984	-0.0104	-0.1276	0.0129	-0.0666	-0.1606
DL05	-0.1191	-0.0693	-0.0655	-0.0258	-0.0312	-0.0612
DL18	0.1041	-0.0456	-0.0698	0.0023	0.0275	-0.1287
DH02	-0.0937	-0.1175	-0.0175	-0.0634	0.0092	0.0581
DH07	0.0474	0.0517	-0.1512	-0.1307	0.0636	-0.0131
DH10	0.0678	0.0254	-0.1121	-0.1646	0.0997	-0.0216
DH15	-0.0632	0.0079	-0.0566	0.1627	0.1177	0.0524
DH21	-0.0119	-0.0085	-0.0777	0.1016	0.2081	0.0192
DH23	-0.0164	-0.0309	-0.0516	-0.0595	0.1116	0.1778
TA01	-0.0661	0.0391	-0.1504	0.0121	-0.1354	-0.0533
TL01	-0.0247	-0.0290	-0.1030	0.0737	0.0331	0.0289
TH01	0.0385	0.0342	-0.1024	-0.1718	0.0862	0.0494
RA03	-0.0797	-0.1256	0.0215	-0.0657	0.0128	0.0725
RA05	-0.0488	0.0485	0.0130	-0.1388	-0.1305	0.1567
RA07	0.1097	-0.0797	-0.0244	-0.0403	-0.0630	-0.0568

Table 4: Names and definitions of the 27 hydrologic indices used to classify Oklahoma streamflows grouped primarily by flow category.

Code	Hydrologic Index	Units	Definition
Magnitude			
MA01	Mean daily flows	ft ³ /second	Mean daily flows
MA04	Variability in daily flows 2	Percent	Coefficient of variation of the logs in daily flows corresponding to the {5th, 10th, 15th, . . . , 85th, 90th 95th} percentiles
MA28	Variability in May flows	Percent	Coefficient of variation in monthly flows for May
ML01	Mean minimum January flows	ft ³ /second	Mean minimum monthly flow for January
ML09	Mean minimum September flows	ft ³ /second	Mean minimum monthly flow for September
MH04	Mean maximum April flows	ft ³ /second	Mean of the maximum monthly flows for April
MH14	Median of annual maximum flows	Dimensionless	Median of the highest annual daily flow divided by the median annual daily flow averaged across all years
MH20	Specific mean annual maximum flows	ft ³ /second /mile ²	Mean annual maximum flows divided by catchment area
Frequency			
FL03	Frequency of low flow spells	Events per year	Total number of low flow spells (threshold equal to 5% of mean daily flow) divided by the record length in years
FH01	High flood pulse count 1	Events per year	Mean number of high pulse events, where the 75th percentile is the high pulse threshold
FH04	High flood pulse count 2	Days per year	Mean number of days per year above the upper threshold (defined as 7 times median daily flow), and the value is represented as an average instead of a tabulated count
FH05	Flood frequency 1	Events per year	Mean number of high flow events per year using an upper threshold of 1 times median flow over all years
Duration			
DL03	Annual minima of 7-day means of daily discharge	ft ³ /second	Magnitude of minimum annual flow of 7-day mean daily discharge
DL05	Annual minima of 90-day means of daily discharge	ft ³ /second	Magnitude of minimum annual flow of 90-day mean daily discharge

Table 4, continued.

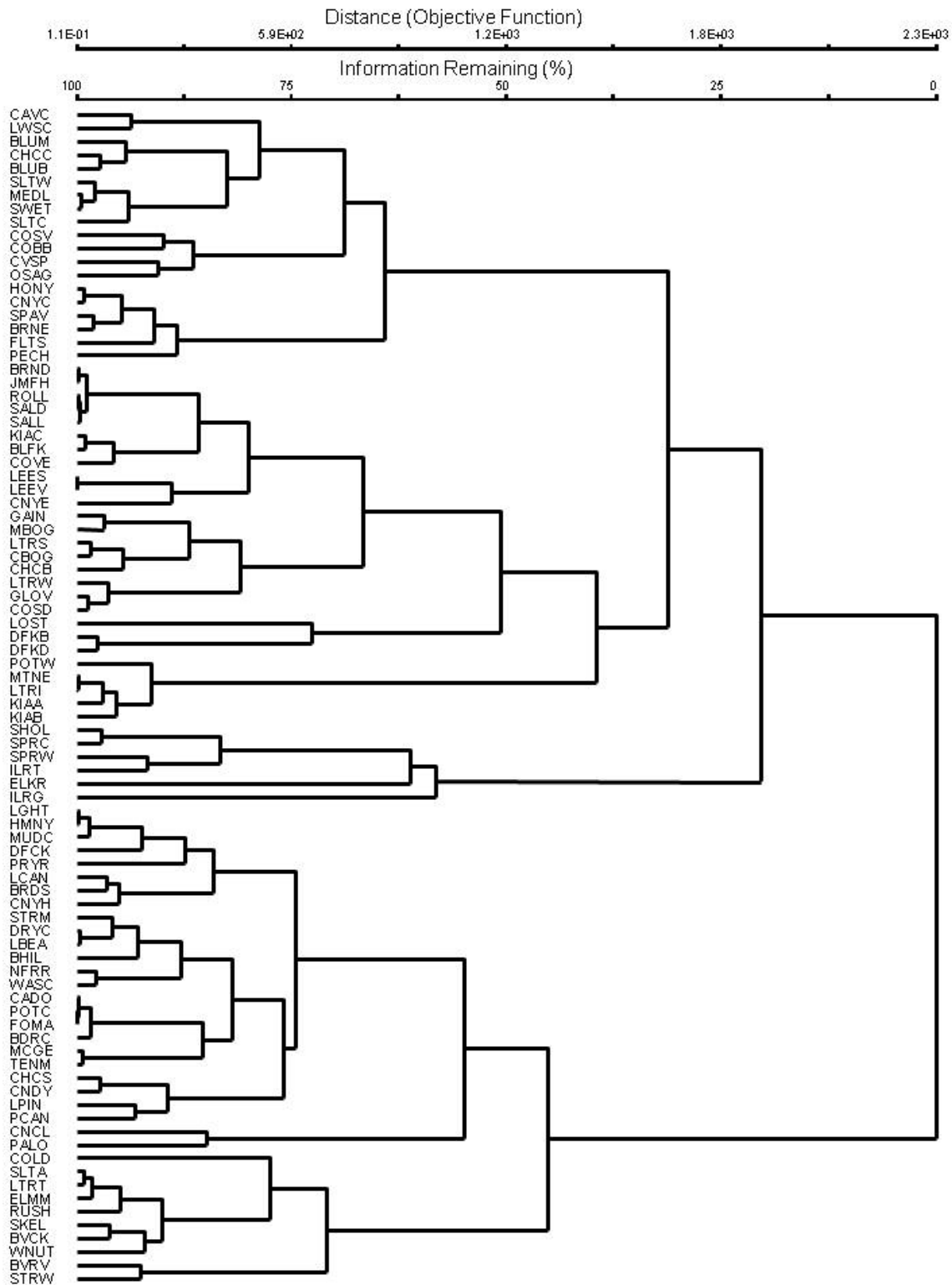
Code	Hydrologic Index	Units	Definition
DL18	Number of zero-flow days	Days per year	Mean annual number of days having zero daily flow
DH07	Variability in annual maxima of 3-day means of daily discharge	Percent	Coefficient of variation in the 3-day moving average flows
DH10	Variability in annual maxima of 90-day means of daily discharge	Percent	Coefficient of variation in the 90-day moving average flows
DH15	High flow pulse duration	Days per year	Mean duration of FH1 (high flood pulse count 1)
DH21	High flow duration 2	Days	Average duration of flow events with flows above a threshold equal to the 25th percentile value for the entire set of flows
DH23	Flood duration 2	Days	Mean annual number of days that flows remain above the flood threshold averaged across all years
Timing			
TA01	Constancy	Dimensionless	See Colwell (1974)
TL01	Julian date of annual minimum	Julian day	The mean Julian date of the 1-day annual minimum flow over all years
TH01	Julian date of annual maximum	Julian day	The mean Julian date of the 1-day annual maximum flow over all years
Rate of Change			
RA03	Fall rate	ft ³ /second /day	Mean rate of negative changes in flow from one day to the next
RA05	No day rises	Dimensionless	Ratio of days where the flow is higher than the previous day
RA07	Change of flow	ft ³ /second /day	Median of difference between natural logarithm of flows between two consecutive days with decreasing flow

Cluster Analysis (CLA)

Cluster analysis is a multivariate statistical method that can be used to identify patterns between many sites using many variables. This study uses a polythetic agglomerative hierarchical clustering that first calculates a dissimilarity matrix with sites and indices. Then, a clustering algorithm is used to group the most similar sites together. In this study, we used Euclidean distance as the measure of dissimilarity and Ward's method (Ward 1963) for the clustering algorithm. This method produced clusters that we were able to classify the stations in a useful and interpretable fashion. The length of the lines on the dendrogram that connect any two stations or groups of stations, indicate the relative similarity of the streamflow, where shorter lines are more similar (CAVC to LWSC) and longer lines are less similar (CAVC to STRW; Figure 5). The selection of clusters was done at levels of information remaining that were the most interpretable for the study. We can divide the cluster dendrogram (Figure 5) in different places to create many combinations of group numbers. The distance function on the top of the graph is measure of the amount of information remaining while the clustering process is being complete (Figure 5; McCune and Grace 2002). The most useful groups produced two clusters at 20% of information remaining, four clusters at 45% of information remaining, and six clusters at 54% of information remaining. These three classification schemes are discussed in the following sections.

We used two nonparametric tests to determine significant differences between the groups identified by the cluster analysis. The Mann-Whitney test was used to compare pairs of groups (i.e. 2 cluster group) and the Kruskal-Wallis with a post-hoc test was used for multiple groups (i.e. 4 cluster group). The Kruskal-Wallis test is similar to the commonly used analysis of variance (ANOVA), but is nonparametric and compares the rank of data in a group rather than actual values (Conover 1999). While the Kruskal-Wallis test can be used to determine if any significant differences were present between the groups. The post-hoc test was used to find the groups that differed between each other, which is similar to the Tukey-Kramer post-hoc test (Conover 1999). The small size of some groups in the 6 cluster classification made statistical analysis not as powerful to compare all the groups, but we did use the Mann-Whitney test to differences in pairs of interest.

Figure 5: Cluster analysis dendrogram made by using Euclidian distance measure and Ward's method for classification of 88 streams in Oklahoma. Station codes are shown in Table 1.



Two-Cluster Classification

The two cluster classification (Figure 6) has a larger cluster (21) with 52 stations and a smaller cluster (22) with 36 stations. The distribution of the sites from both groups are mixed together throughout the region and there is not a clear geographic pattern (Figure 7), although there does appear to be more stations from group 21 in the eastern part of the area. The only stations in the panhandles of Oklahoma and Texas are from group 22, and this area is not well represented in the number of available stations in the analysis.

Statistical analyses with the Mann-Whitney test found that all but 5 indices (MH20, DH21, DH23, TL01, and RA03) were significantly different between groups (Table 5). The stations in group 21 had higher mean flow (MA01) with higher flow during low flow periods (ML01, ML09; Figure 8). The stations in group 22 had more flood events (FH01, FH04, FH05), more days with zero flow (DL18), and more variable flows (TA01; Figure 8).

The cluster analysis shows that 21 had higher flows that were more stable (i.e. perennial streams). The stations in group 22 had lower low flows that stay low for longer and even long periods of zero flows (i.e. intermittent streams). Group 22 also had a greater number of high flow pulses compared to group 21. In general, the streams of group 21 are perennial streams with stable flow, while the streams of group 22 are more intermittent and flashy (Figure 8).

Table 5: Mean and standard deviation for two cluster classification using 27 hydrologic indices. Significant differences ($\alpha = 0.05$) between groups was tested with the Mann-Whitney test and are indicated by different letters.

Index	Unit	21			22		
		Mean	SD		Mean	SD	
MA01	ft ³ /second	482.7	507.2	a	115.6	98.9	b
MA04	Percent	140.0	44.7	a	206.0	45.5	b
MA28	Percent	119.2	34.9	a	209.8	34.2	b
ML01	ft ³ /second	109.9	133.0	a	10.4	8.6	b
ML09	ft ³ /second	26.9	42.5	a	2.2	2.6	b
MH04	ft ³ /second	4671.0	4870.3	a	1604.6	1733.6	b
MH14	Dimensionless	93.5	65.6	a	489.3	333.0	b
MH20	ft ³ /second/mile ²	34.0	58.3		24.6	17.3	
FL03	Events per year	3.4	2.6	a	8.3	2.1	b
FH01	Events per year	2.5	10.2	a	1.8	12.6	b
FH04	Days per year	36.6	21.4	a	62.7	25.8	b
FH05	Events per year	8.4	2.3	a	10.2	3.0	b
DL03	ft ³ /second	18.3	34.4	a	0.9	1.4	b
DL05	ft ³ /second	73.6	76.2	a	12.1	10.2	b
DL18	Days per year	8.5	12.5	a	57.4	39.7	b
DH02	ft ³ /second	8315.0	8491.9	a	3289.0	2570.6	b
DH07	Percent	67.9	17.6	a	84.5	27.4	b
DH10	Percent	57.3	15.5	a	79.2	19.4	b
DH15	Days per year	8.4	2.3	a	6.2	1.4	b
DH21	Days	85.0	28.0		80.3	25.4	
DH23	Days	2.3	1.3		2.3	0.8	
TA01	Dimensionless	0.35	0.11	a	0.28	0.06	b
TL01	Julian day	257.9	11.8		253.8	15.2	
TH01	Julian day	114.5	47.2	a	147.8	36.1	b
RA03	ft ³ /second /day	168.1	156.4		92.1	61.8	
RA05	Dimensionless	0.23	0.04	a	0.22	0.04	b
RA07	ft ³ /second/day	0.12	0.05	a	0.24	0.08	b

Figure 6: Cluster analysis dendrogram (Euclidean distance and Ward's method) showing two cluster classification of 88 Oklahoma streamflow stations. Station codes are shown in Table 1.

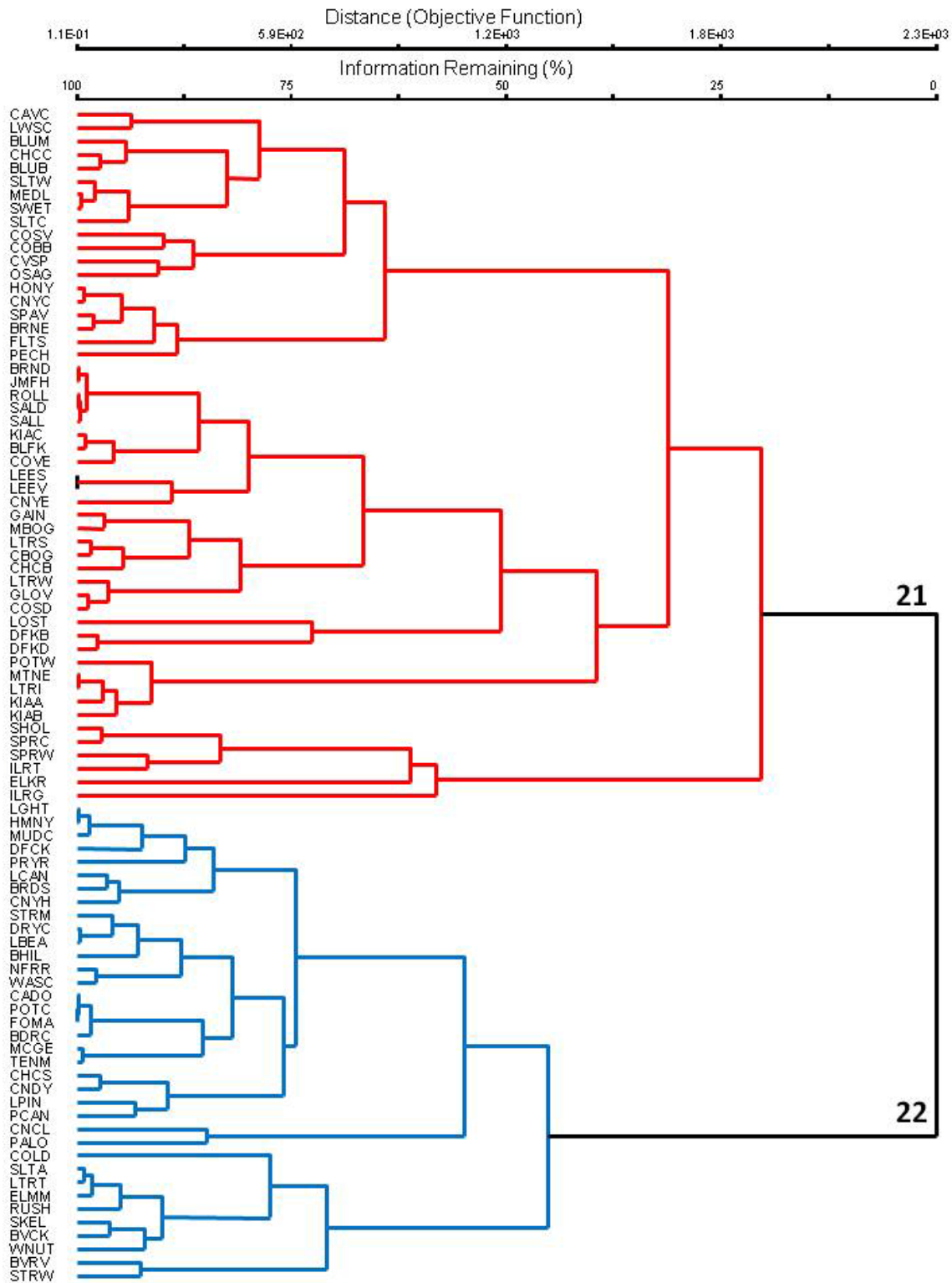


Figure 7: Map of 88 streamflow station in Oklahoma classified by two group cluster analysis. Red triangles are members of group 21 and blue circles are members of group 22.

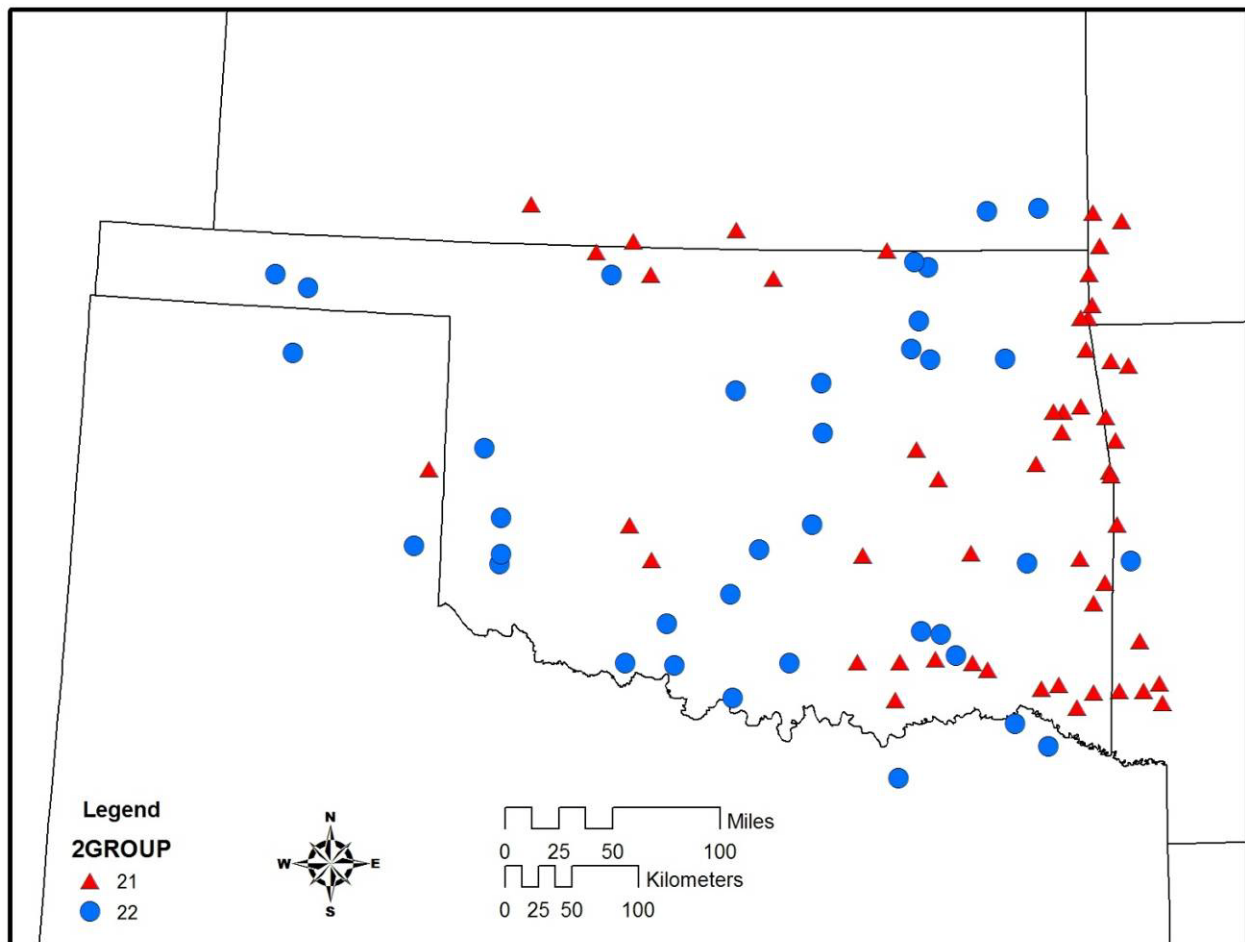


Figure 8: Boxplots of hydrologic indices for the two cluster classification of streamflow-gaging stations in Oklahoma. See Table 4 for hydrologic index names and Figure 6 for groups.

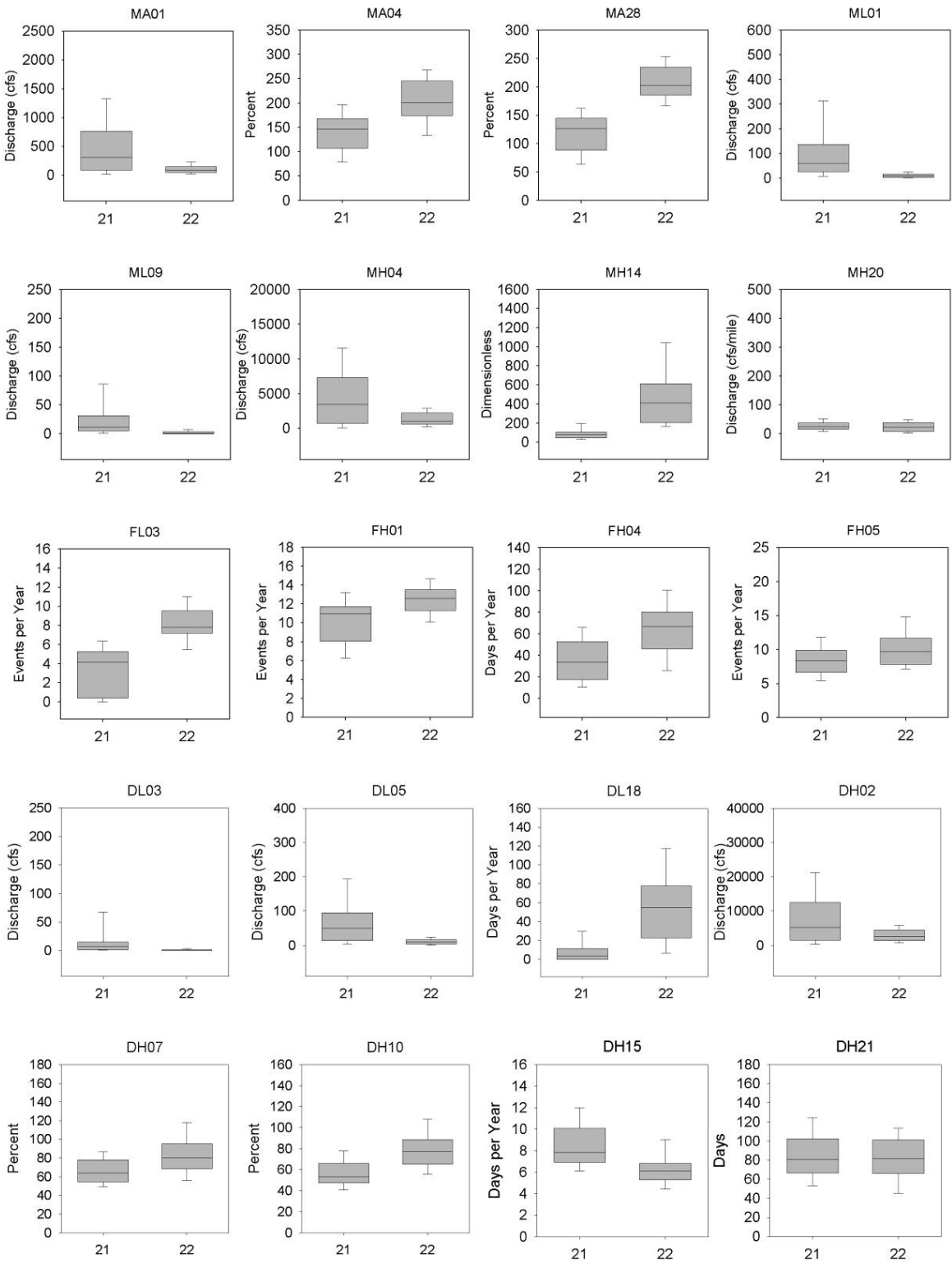
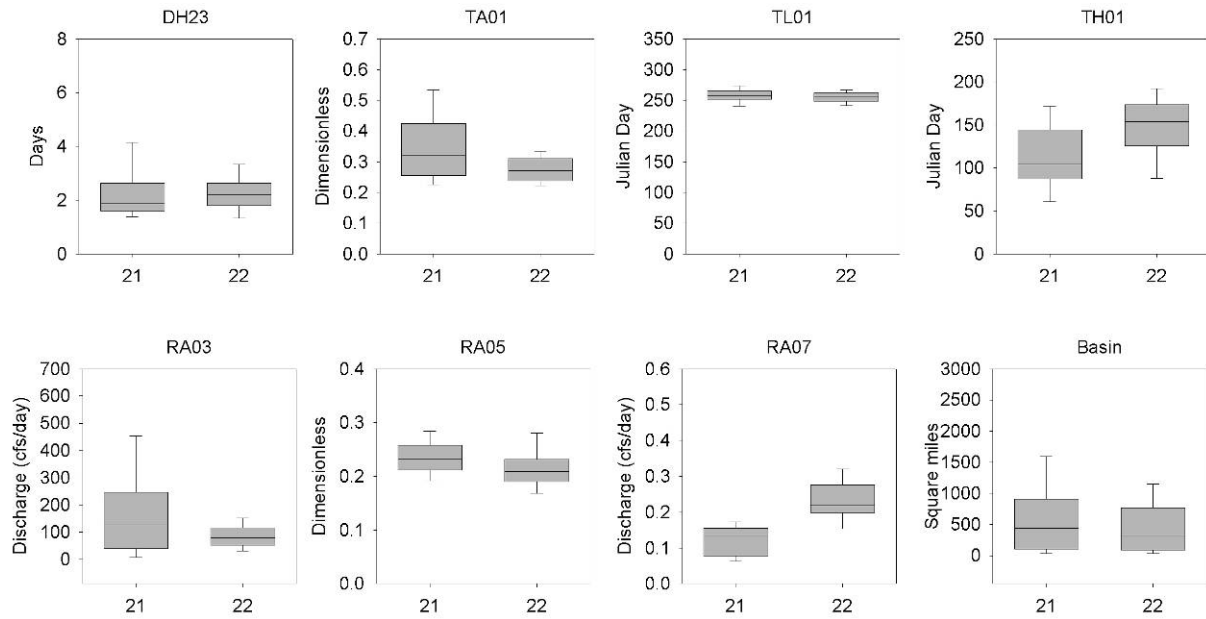


Figure 8, cont.



Four-Cluster Classification

The 4 group dendrogram (Figure 9) is divided with 45% of the information remaining and divided the two cluster classification group 21 into three groups, numbered 41, 42 and 43. Group 41 had 19 stations, group 42 had 27 stations, and group 43 had 6 stations. Group 44 contained 36 stations and is the same as group 22. Group 43 was more dissimilar (longer distance away on the dendrogram) from groups 41 and 42 than the differences between groups 41 and 42. There was a more regional distribution of the sites in the four group classification (Figure 10) than in the two group classification. The group 41 stations were found throughout the study area. Group 42 stations are concentrated in the southeastern part of the region but it also has some stations in the northeast. Group 43 has the fewest number of stations, which are located only in the northeastern part of the region (i.e. Ozark Highlands). The stations in group 44 were the same as group 22 and were located throughout the region.

A statistical comparison of the stations in the four group classifications with the Kruskal-Wallis test and post test show that there were significant differences between groups for all the hydrologic indices (Table 6). Group 41 stations had lower mean flows (MA01) with relatively stable flows (MA04, TA01; Figure 11). Group 42 stations had more frequent (FH01, FH04) and less variable (DH07) high flow events (Figure 11). Group 43 had the highest stability of flows (TA01) with high baseflows (ML01, DL03, DL05), and no zero flow days in the entire record (DL18). There were also similarities for the stations in groups 42 and 43, which had significantly higher mean flows (MA01) with a higher magnitude of maximum flows in April (MH04) than the other groups. When high flow events did occur at these stations, the flows fell quickly (RA03; Figure 11). The stations of group 44 are the same as group 22, so similar patterns are present with a high number of flood events (FH01) and a high number of zero flow days (DL18; Figure 11).

Based on the trends observed between the four groups, we can classify group 41 as perennial run-off streams, while group 42 stations are perennial flashy streams. The stations in group 43 are stable groundwater streams. Group 44 has streams that have many zero flow days and can be classified as intermittent.

Table 6: Mean and standard deviation for the four cluster classification using 27 hydrologic indices. Significant differences ($\alpha = 0.05$) between groups was tested with the Kruskal-Wallis test with post-hoc test to differentiate between groups. Significant differences between groups is indicated by different letters.

		41			42			43			44		
		Mean	SD		Mean	SD		Mean	SD		Mean	SD	
MA01	ft ³ /second	122.2	119.5	a	643.3	519.6	b	901.1	570.4	b	115.6	98.9	a
MA04	Percent	101.8	30.2	a	173.1	29.0	b	112.0	18.8	a	206.0	45.5	c
MA28	Percent	98.7	28.5	a	142.4	23.4	b	79.9	17.4	a	209.8	34.2	c
ML01	ft ³ /second	38.2	31.9	a	118.5	135.4	b	298.6	136.9	c	10.4	8.6	d
ML09	ft ³ /second	16.4	15.5	a	11.9	10.5	a	127.4	57.0	b	2.2	2.6	c
MH04	ft ³ /second	1098.6	1250.1	a	6562.0	4811.6	b	7473.8	6220.6	b	1604.6	1733.6	a
MH14	Dimensionless	57.1	22.8	a	131.6	69.6	b	36.8	12.1	a	489.3	333.0	c
MH20	ft ³ /second/mile ²	18.7	13.5	a	32.6	15.2	b	88.6	168.3	ab	24.6	17.3	ac
FL03	Events per year	1.5	1.7	a	5.3	1.7	b	0.6	0.9	a	8.3	2.1	c
FH01	Events per year	9.7	3.0	a	11.1	1.8	b	7.9	1.7	a	12.6	1.8	c
FH04	Days per year	17.3	8.8	a	53.5	14.4	b	21.1	8.3	a	62.7	25.8	b
FH05	Events per year	9.3	2.9	ab	8.3	1.5	a	6.0	0.9	c	10.2	3.0	b
DL03	ft ³ /second	11.2	12.3	a	5.3	5.5	a	99.6	48.6	b	0.9	1.4	c
DL05	ft ³ /second	32.1	27.6	a	70.9	59.7	b	216.8	81.9	c	12.1	10.2	d
DL18	Days per year	6.7	11.1	ab	11.6	13.8	a	0.0	0.0	b	57.4	39.7	c
DH02	ft ³ /second	2185.4	2282.5	a	11245.0	8162.3	b	14540.8	11605.9	b	3289.0	2570.6	a
DH07	Percent	75.0	20.1	ab	61.0	14.3	d	76.7	9.4	ac	84.5	27.4	bc
DH10	Percent	59.8	19.7	a	55.4	13.8	a	58.2	3.7	a	79.2	19.4	b
DH15	Days per year	8.1	2.7	a	8.1	1.8	ab	10.2	2.1	b	6.2	1.4	c
DH21	Days	75.1	26.5	ab	87.5	28.8	ac	105.3	16.8	d	80.3	25.4	bc
DH23	Days	1.8	0.5	ac	2.6	1.7	ab	2.7	0.8	bd	2.3	0.8	cd
TA01	Dimensionless	0.40	0.11	a	0.28	0.05	b	0.54	0.03	c	0.28	0.06	b
TL01	Julian day	253.0	11.8	a	258.7	10.9	a	269.7	6.5	b	253.8	15.2	a
TH01	Julian day	128.8	55.9	ab	104.5	43.4	a	114.4	19.3	ab	147.8	36.1	b
RA03	ft ³ /second /day	51.3	53.4	a	238.3	161.7	b	222.6	146.4	b	92.1	61.8	c
RA05	Dimensionless	0.24	0.04	a	0.23	0.03	ab	0.24	0.02	ab	0.22	0.04	b
RA07	ft ³ /second/day	0.09	0.03	a	0.16	0.03	b	0.06	0.01	a	0.24	0.08	c

Figure 9: Cluster analysis dendrogram (Euclidean distance and Ward's method) showing four cluster classification of 88 Oklahoma streamflow stations. Station codes are shown in Table 1.

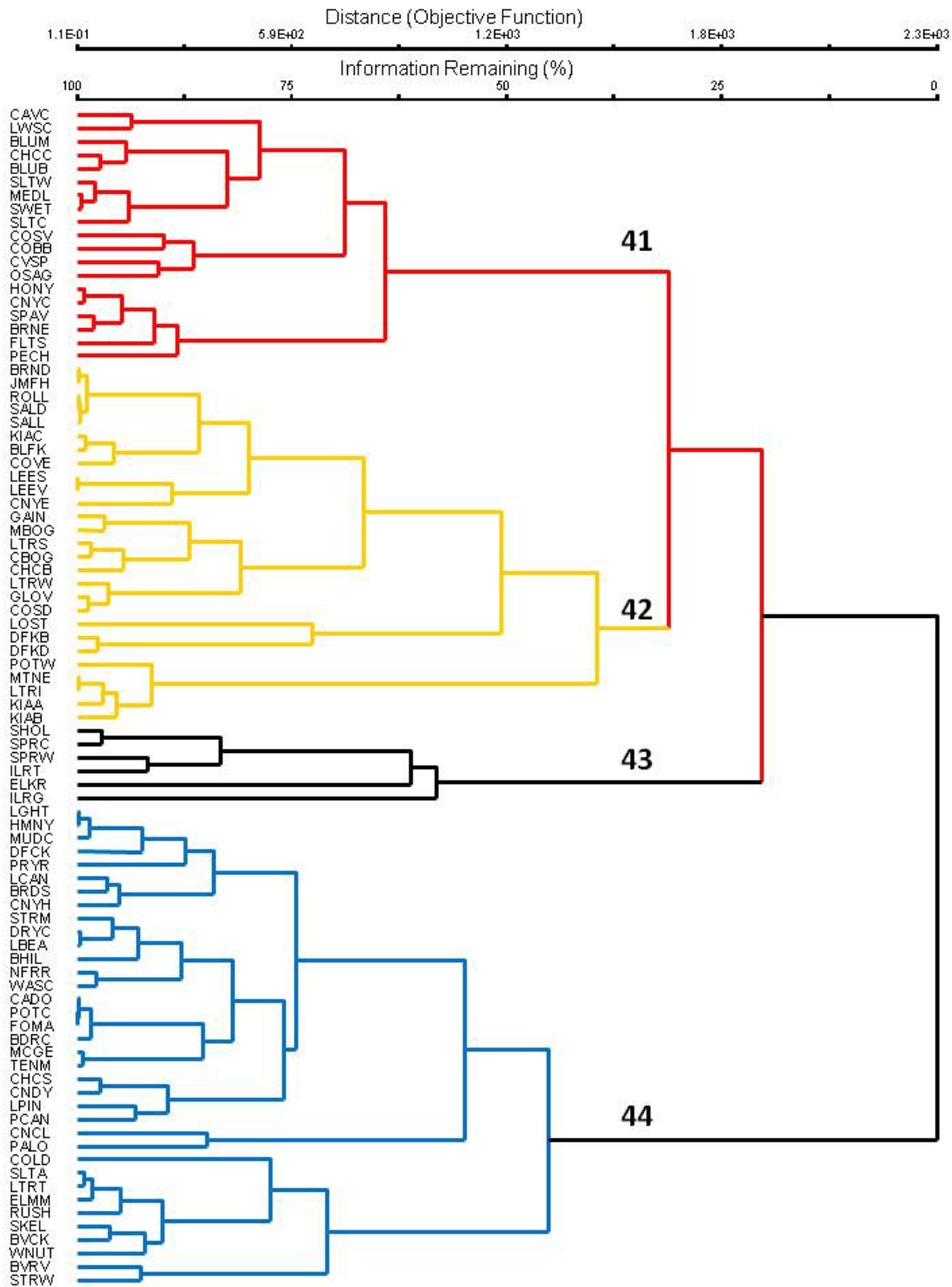


Figure 10: Map of 88 streamflow stations in Oklahoma classified by four group cluster analysis. Red triangles are members of group 41, yellow pentagons are members of group 42, black diamonds are members of group 43, and blue circles are members of group 44.

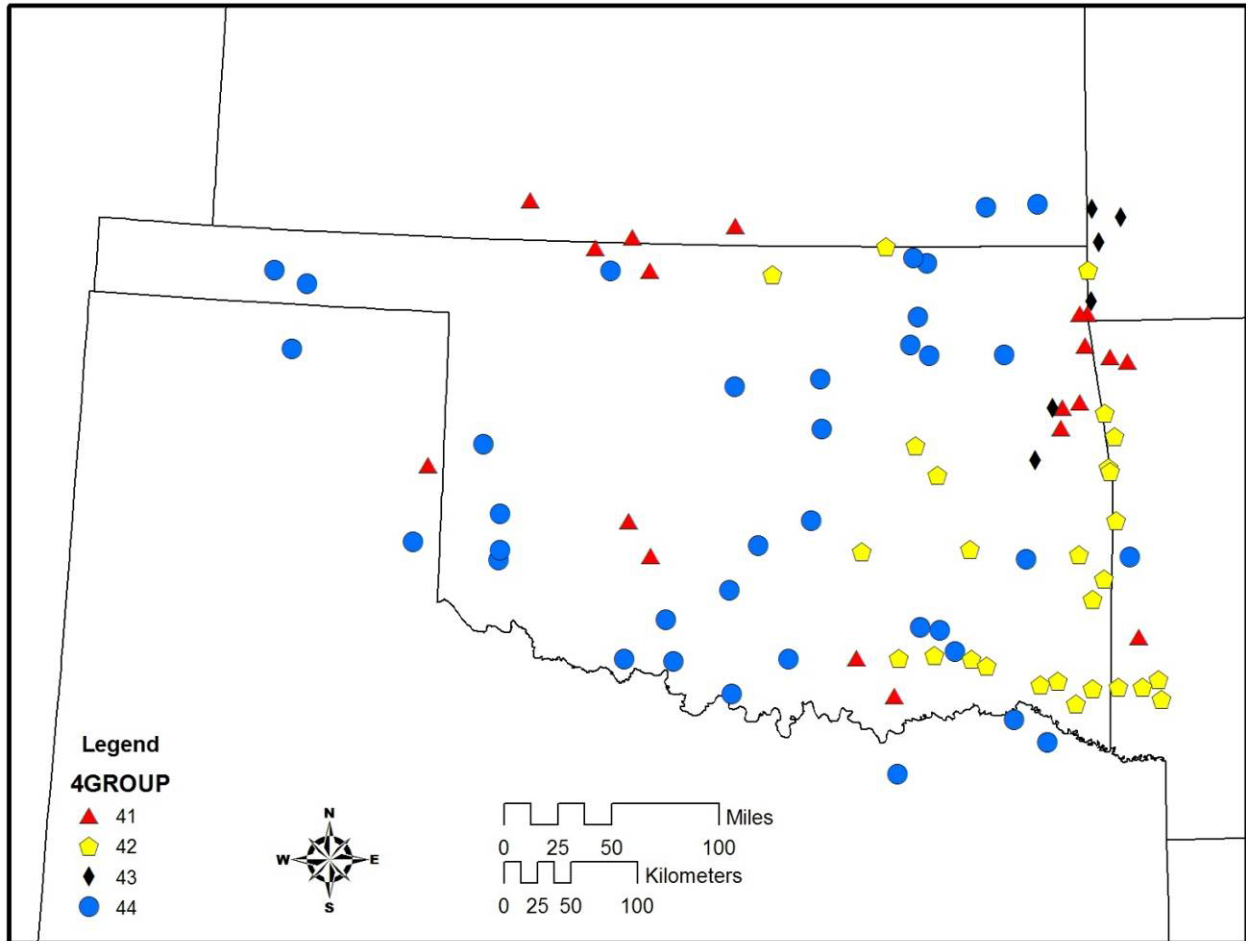


Figure 11: Boxplots of hydrologic indices for the four cluster classification of streamflow-gaging stations in Oklahoma. See Table 4 for hydrologic index names and Figure 9 for groups.

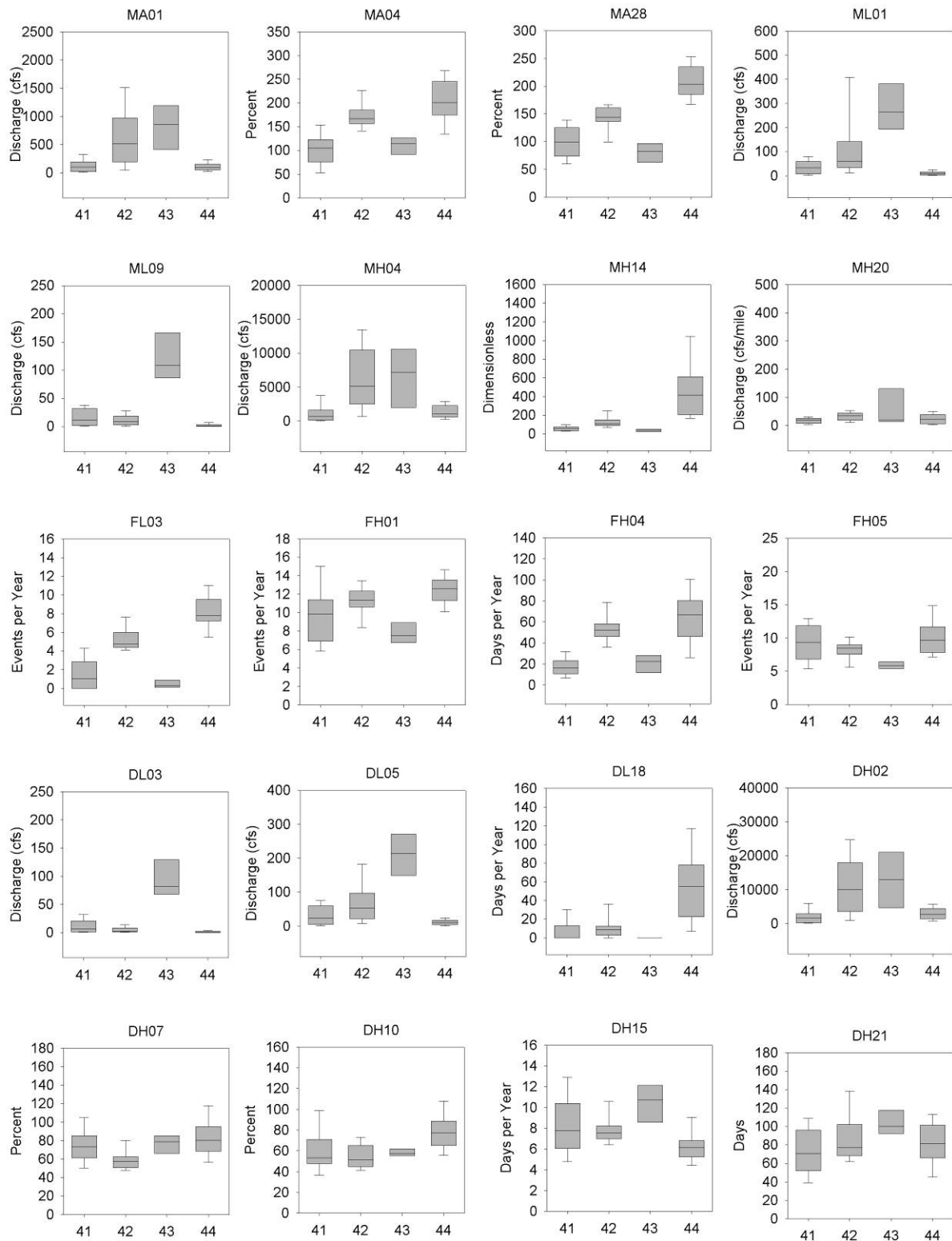
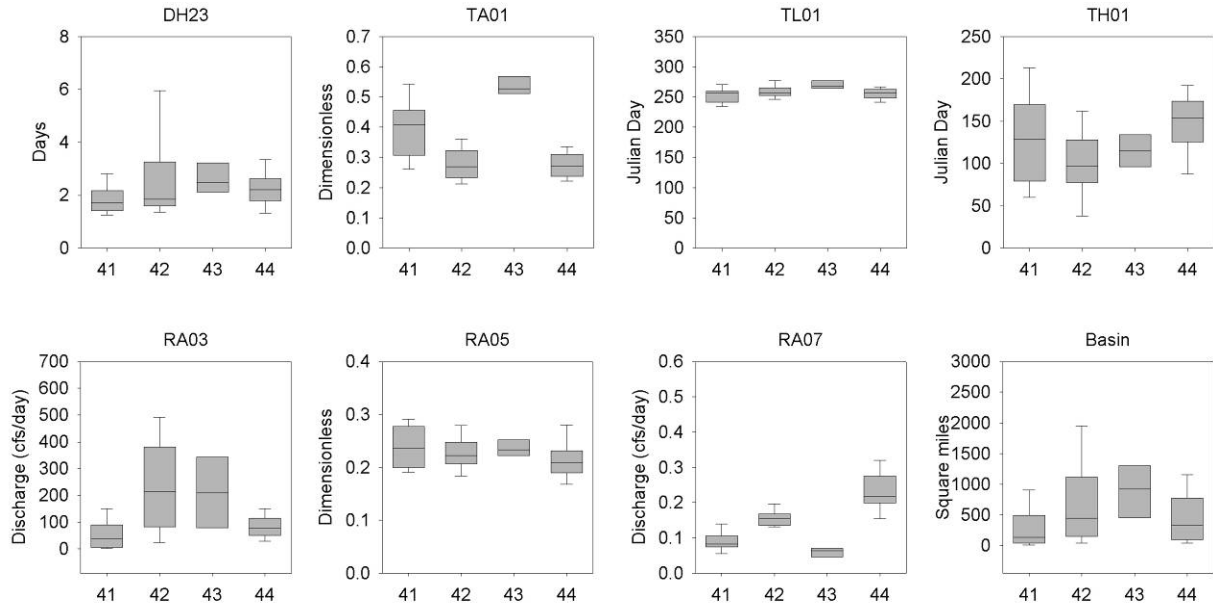


Figure 11, cont.



Six-Cluster Classification

The dendrogram divided at 54% of the information remaining had several smaller clusters compared to the four cluster classification (Figure 12). The group numbers and the number of stations in each group were: 61 (19 stations), 62 (22 stations), 63 (5 stations), 64 (6 stations), 65 (26 stations), and 66 (10 stations). The two changes from the four cluster classification are that group 42 was divided into two groups (62 and 63), and group 44 was divided into two groups as well (65 and 66; Figure 12). We will focus on the differences within groups 62/63 and 65/66 that only occur in the six cluster classification because groups 61 and 64 were discussed in the previous section as 41 and 43, respectively. Group 62 is located primarily in the eastern part of the region, while the five stations of Group 63 are found only in southeastern Oklahoma (Figure 13). The stations of groups 65 and 66 are mixed together around the region (Figure 13). Group 66 stations are mostly in the western part of the region, while stations in group 65 are scattered among the other stations, with a concentration of eight stations in the northeastern part of the region (Figure 13).

Only 10 of the 27 hydrologic indices were significantly different between the groups 62 and 63 when tested with the Mann-Whitney test (Table 7). Group 63 had higher magnitude flows for average (MA01), low (ML01, ML09), and high (MH04) magnitude flows (Table 7). The stations of group 63 had more stable flows (TA01) and a higher fall rate (RA03). There was also a significant difference in basin size (608 miles² in group 62 and 1142 miles² in group 63), which would be linked to the values of the magnitude and other indices. The stations in groups 65 and 66 have been clustered together in both the two cluster classification as 22 (Figure 6) and the four cluster classification as 44 (Figure 9). There were 17 indices that were significantly different between groups 65 and 66 (Table 7). Group 65 stations had more variable daily flow (MA04) and higher mean annual maximum flows (MH14) than group 66. The group also had more low flow spells (FL03) and twice as many zero flow days per year (DL18). Group 66 stations had more frequent (FH05) and longer floods (DH15). The timing of flows for group 66 stations were earlier in the year for low flows (TL01) and later in the year for high flows (TH01) than station in group 66 (Table 7). The group 66 stations also had more days with no rise (RA05) and a lower rate of change between days (RA07) than group 65.

The analysis of the differences between the groups in the six cluster classification indicate that group 62 are perennial streams with smaller watersheds, while group 63 are stations are perennial streams with larger watersheds. The stations in groups 65 and 66 are both intermittent streams. Group 65 appears to be more intermittent flashy streams and group 66 streams are intermittent run-off streams.

Table 7: Mean and standard deviation for the six cluster classification using 27 hydrologic indices. Letters separate significant differences ($\alpha = 0.05$) between groups tested with the Mann-Whitney test for groups 62/63 (a/b) and 65/66 (y/z).

		61		62		63		64		65		66			
		Mean	SD	Mean	SD	Mean	SD	Mean	SD	Mean	SD	Mean	SD		
MA01	ft ³ /second	122.2	119.5	451.7	347.2	a	1486.4	176.9	b	901.1	570.4	124.8	112.2	91.6	46.7
MA04	Percent	101.8	30.2	173.2	31.9		172.9	11.4		112.0	18.8	225.0	35.6	y	156.6 27.7 z
MA28	Percent	98.7	28.5	144.2	25.3		134.5	10.4		79.9	17.4	214.0	36.4		198.9 26.3
ML01	ft ³ /second	38.2	31.9	63.1	44.9	a	362.0	132.9	b	298.6	136.9	9.2	8.8		13.4 7.5
ML09	ft ³ /second	16.4	15.5	10.0	10.0	a	20.6	9.3	b	127.4	57.0	1.3	1.6	y	4.7 3.3 z
MH04	ft ³ /second	1098.6	1250.1	4885.3	3342.4	a	13939.3	2888.4	b	7473.8	6220.6	1828.2	1963.9		1023.2 673.6
MH14	Dimensionless	57.1	22.8	142.7	72.2	a	82.8	20.5	b	36.8	12.1	592.7	337.6	y	220.6 59.2 z
MH20	ft ³ /second/mile ²	18.7	13.5	33.6	16.5		28.5	6.7		88.6	168.3	29.4	17.2	y	12.1 9.8 z
FL03	Events per year	1.5	1.7	5.4	1.8		5.1	1.0		0.6	0.9	8.9	2.1	y	7.0 1.7 z
FH01	Events per year	9.7	3.0	10.9	1.9		12.1	1.0		7.9	1.7	12.1	1.5	y	13.9 1.7 z
FH04	Days per year	17.3	8.8	53.8	15.9		52.5	4.4		21.1	8.3	74.0	20.0	y	33.4 12.2 z
FH05	Events per year	9.3	2.9	8.2	1.7		8.7	0.9		6.0	0.9	9.1	2.2	y	13.3 2.8 z
DL03	ft ³ /second	11.2	12.3	4.6	5.6		8.3	4.1		99.6	48.6	0.4	0.8	y	2.4 1.7 z
DL05	ft ³ /second	32.1	27.6	50.2	39.2	a	162.3	47.5	b	216.8	81.9	10.8	10.9	y	15.7 7.5 z
DL18	Days per year	6.7	11.1	12.2	15.2		9.0	4.6		0.0	0.0	68.7	35.3	y	27.8 36.2 z
DH02	ft ³ /second	2185.4	2282.5	8368.3	5773.0	a	23902.4	3508.2	b	14540.8	11605.9	3478.3	2925.7		2796.7 1244.3
DH07	Percent	75.0	20.1	63.6	14.3	a	49.4	6.7	b	76.7	9.4	79.2	25.3		98.3 29.2
DH10	Percent	59.8	19.7	56.6	14.7		50.0	6.8		58.2	3.7	74.7	16.8		90.9 21.7
DH15	Days per year	8.1	2.7	8.3	2.0		7.3	0.7		10.2	2.1	6.7	1.2	y	4.9 0.8 z
DH21	Days	75.1	26.5	91.0	30.8		72.0	7.1		105.3	16.8	83.0	23.1		73.2 30.9
DH23	Days	1.8	0.5	2.6	1.9		2.5	0.7		2.7	0.8	2.3	0.8		2.4 0.8
TA01	Dimensionless	0.40	0.11	0.27	0.05	a	0.32	0.02	b	0.54	0.03	0.28	0.07		0.29 0.03
TL01	Julian day	253.0	11.8	258.7	11.8		258.5	6.8		269.7	6.5	258.3	8.0	y	242.0 22.5 z
TH01	Julian day	128.8	55.9	106.3	48.0		96.7	7.6		114.4	19.3	138.3	37.1	y	172.5 17.0 z
RA03	ft ³ /second/day	51.3	53.4	178.7	108.6	a	500.5	50.3	b	222.6	146.4	97.2	70.2		78.9 30.1
RA05	Dimensionless	0.24	0.04	0.23	0.04		0.23	0.02		0.24	0.02	0.20	0.02	y	0.26 0.04 z
RA07	ft ³ /second/day	0.09	0.03	0.16	0.03		0.15	0.02		0.06	0.01	0.26	0.08	y	0.18 0.04 z

Figure 12: Cluster analysis dendrogram (Euclidean distance and Ward's method) showing six cluster classification of 88 Oklahoma streamflow stations. Station codes are shown in Table 1.

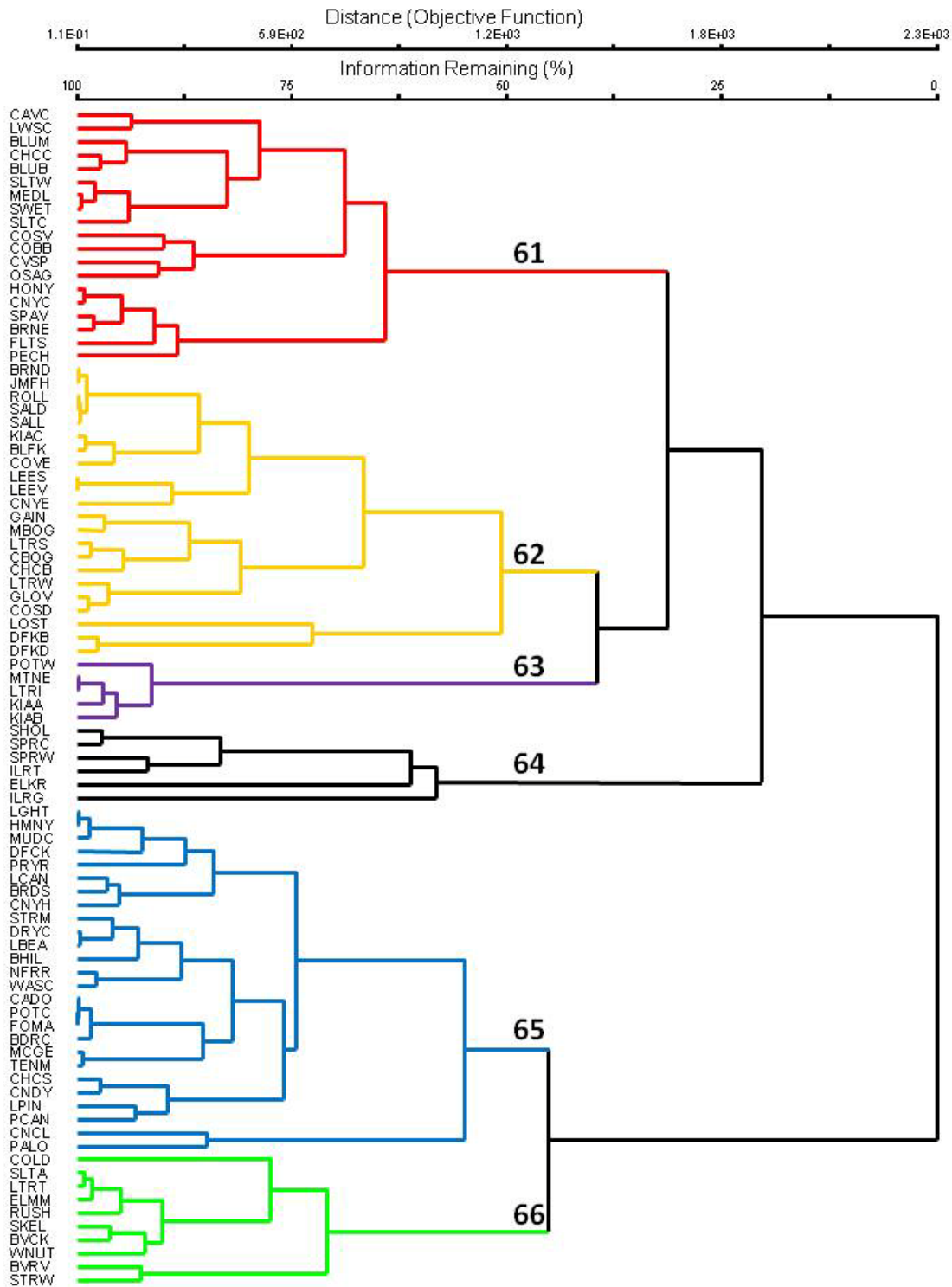
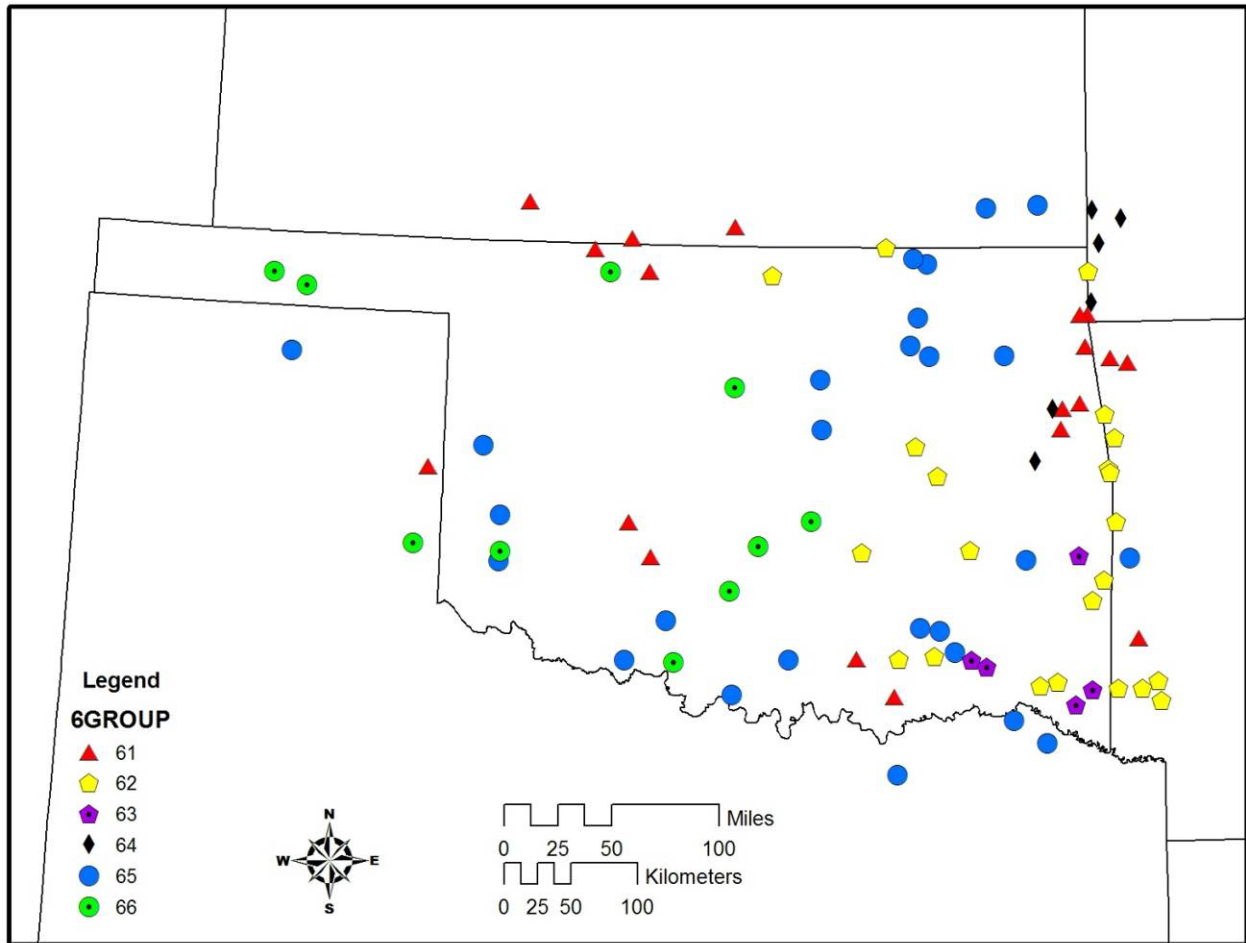


Figure 13: Map of 88 streamflow stations in Oklahoma classified by six group cluster analysis. Red triangles are members of group 61, yellow pentagons are members of group 62, purple pentagons with a dot are members of group 63, black diamonds are members of group 64, blue circles are members of group 65, and green circles with a dot are members of group 66.



Stability of Clusters

We tested how reliable the clusters were using a jackknife method in order to determine if the clusters were dependent on a specific combination of sites and variables (Armstrong et al. 2008; McGarigal et al 2000). Cluster stability was tested by removing individual indices and stations and then running the cluster analysis again. The number of sites that changed cluster membership were then counted. This process was repeated 115 times for each of the 88 sites and 27 indices. The analysis showed that the clusters represent unique groups of stations. The mean stability across all indices and sites was 91% and 94%, respectively. The stability of the clusters from site removal ranged from 73% (with removal of MA04, MA28) to 100%, while the stability of clusters from hydrologic indices ranged from 75% (with removal of SALD, KIAB) to 100%.

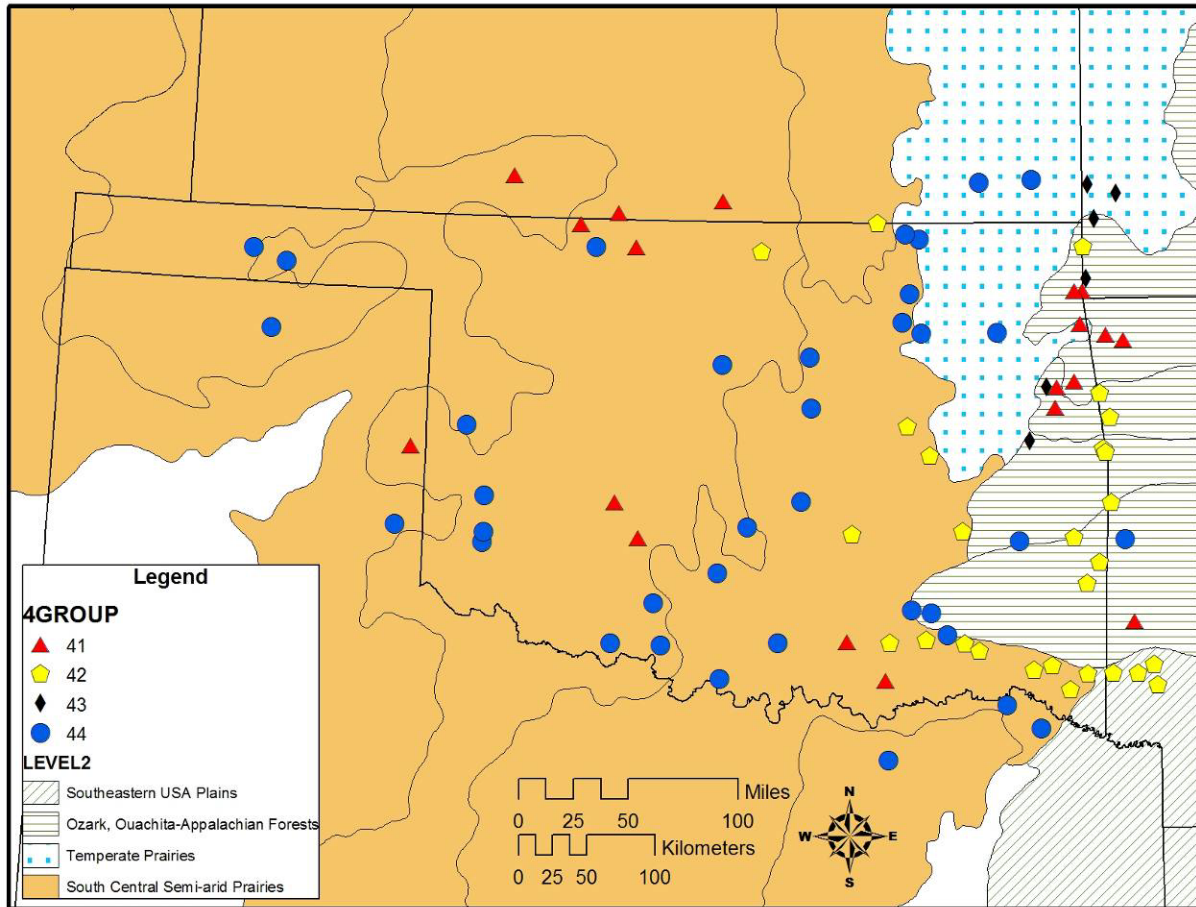
Principal Findings and Significance

This report documents the hydroecological classification of Oklahoma streams based on natural flow regime that incorporates natural flow variability. The classification completes the first 3 development steps of the Hydroecological Integrity Assessment Process (HIP). Completion of the remaining steps of the HIP process will provide tools to water resource managers to include environmental flows to support aquatic life in specific streams as part of Oklahoma's Comprehensive Water Plan.

We calculated 171 ecologically-relevant hydrologic indices for 88 streams across Oklahoma, which described the magnitude, frequency, duration, timing, and rate of change of stream flows. The 27 most non-redundant, high information indices representing all five components of a flow regime were selected for use in the classification of 88 streamflow stations. Cluster analysis was then used to group streamflow stations with similar flow characteristics in two cluster, four cluster, and six cluster groups.

We found that the groupings of streams fell roughly within specific ecoregions of Oklahoma. For example, most of the Group 42 streams (4 cluster analysis) were located in (or the majority of the watershed drained) the Ozark, Ouachita-Appalachian Forests Level II ecoregions (Figure 14). Group 44 streams were located predominately in the Temperate Prairies and South-Central Semi-arid Prairies ecoregions (Figure 14). Ecoregions are based on differences in the inter-related characteristics of climate, geology, soils, and vegetation of a particular location. The hydrologic characteristics of a particular stream (or watershed) are also based on the same characteristics. Therefore we can conclude that the stream groupings generated by the HIT procedure and identification of the primary flow indices represent "real world" differences in the hydrologic characteristics of the watersheds. From a water resources management perspective, this information is vital to develop environmental flow prescriptions that are stream and organism specific.

Figure 14. A comparison of the four-group cluster analysis stream classifications and Level II Ecoregions of Oklahoma. Note that the symbols represent the location of a gaging station at the watershed outlet. The majority of the watershed drained by the stream may lie in a different ecoregion.



Future Needs

In order to gain the maximum amount of usefulness from this work, the remaining steps of the Hydroecological Integrity Assessment Process (HIP) should be completed. The next development step in the HIP is the development of the Stream Classification Tool (SCT) and the Hydrologic Assessment Tool (HAT) for Oklahoma streams. The SCT development further refines the stream classification and provides water resource managers tools to classify streams that were not included in the baseline analysis performed in this project. The HAT is based on the initial classifications created in this report and the SCT procedure. It is used to provide options for setting environmental flow standards and evaluating past and proposed hydrologic modifications for a specific stream reach.

The baseline stream classification developed in this report and further development of the SCT and HAT will also serve to increase our understanding of the link between natural climate variability, or a changed climate under different climate change scenarios and the variability of the hydrologic characteristics of a stream and populations of various aquatic species. This could include state and federally listed species as well as sportfishes.

Overall, the HIP represents an evolution from simple "rules of thumb" minimum flows to a complex system of hydroecologic flow parameters that support aquatic life throughout the life cycle. The HIP will provide water resource managers with better information with which they can better balance water allocation between human and ecological uses.

References

- Auble, G. T., J. M. Friedman, and M. L. Scott. 1994. Relating Riparian Vegetation to Present and Future Streamflows. *Ecological Applications* 4(3):544-554.
- Armstrong, D.S., Parker, G.W., and Richards, T.A., 2008, Characteristics and classification of least altered streamflows in Massachusetts: U.S. Geological Survey Scientific Investigations Report 2007–5291, 113 p.
- Arthington, A. H., S. E. Bunn, N. L. Poff, R. J. Naiman. 2006. The challenge of providing environmental flow rules to sustain river ecosystems. *Ecological Applications* 16:1311-1318.
- Bergman, D. L., and T. L. Huntzinger. 1981, Rainfall-runoff hydrograph and basin characteristics data for small streams in Oklahoma: U.S. Geological Survey Open File Report 81-824, 320 p.
- Colwell RK. 1974. Predictability, constancy, and contingency of periodic phenomena. *Ecology* **55**: 1148–1153.
- Conover, W. J. 1999. Practical nonparametric statistics, 3rd edition. Wiley, New York.
- Esralew, R.A. and R.J. Baker. 2008. Determination of baseline periods of record for selected streamflow gaging stations in New Jersey for determining ecologically relevant hydrologic indices (ERHI). U.S. Geological Survey Scientific Investigations Report 2008-5077, 83p.
- Fitzhugh, T. W., and B. D. Richter. 2004. Quenching urban thirst: growing cities and their impacts on freshwater ecosystems. *Bioscience* 54:741-754.
- Henriksen, J., J. Heasley, J. Kennen, and S. Nieswand. 2006. User's manual for the Hydroecological Integrity Assessment Process software. U.S. Geological Survey Open-File Report 2006–1093:71 p.
- Kendall, M. and J.D. Gibbons. 1990, Rank correlation methods (5th ed.): New York, Oxford University Press, 260 p.
- Kennen, J.G., J.A. Henriksen, and S.P. Nieswand. 2007. Development of the Hydroecological Integrity Assessment Process for Determining Environmental Flows for New Jersey Streams: U.S. Geological Survey Scientific Investigations Report 2007-5206, 65 p.
- Jolliffe, I. T. 1972. Discarding Variables in a Principal Component Analysis .1. Artificial Data. *Journal of the Royal Statistical Society Series C-Applied Statistics* 21(2):160-&.
- Junk, W. J., P. B. Bayley, and R. E. Sparks. 1989. The flood pulse concept in river-floodplain systems. *Canadian Special Publication of Fisheries and Aquatic Sciences* 106:110-127.

- Kennen, J., J. Henriksen, and S. Nieswand. 2007. Development of the Hydroecological Integrity Assessment Process for determining environmental flows for New Jersey streams. U.S. Geological Survey Scientific Investigations Report 2007-5026. 55 p.
- King, J. R., and D. A. Jackson. 1999. Variable selection in large environmental data sets using principal components analysis. *Environmetrics* 10(1):67-77.
- McCune, B., and J. B. Grace. 2002. Analysis of ecological communities. MjM Software Design, Gleneden Beach, OR.
- McGarigal, K., S. Cushman, and S. G. Stafford. 2000. Multivariate statistics for wildlife and ecology research. Springer, New York.
- National Oceanic and Atmospheric Administration (NOAA), 2008: National Climatic Data Center U.S. Climate Monitoring Reports and Products, database available online at <http://www.ncdc.noaa.gov/oa/climate/research/monitoring.html> (Accessed July 1, 2008).
- Olden, J. D., and N. L. Poff. 2003. Redundancy and the choice of hydrologic indices for characterizing streamflow regimes. *River Research and Applications* 19(2):101-121.
- Poff, N. L., J. D. Allan, M. B. Bain, J. R. Karr, K. L. Prestegard, B. D. Richter, R. E. Sparks, and J. C. Stromberg. 1997. The natural flow regime: a paradigm for river conservation and restoration. *Bioscience* 47:769-784.
- Poff, N. L., J. D. Olden, D. M. Meritt, and D. M. Pepin. 2007. Homogenization of regional river dynamics by dams and global biodiversity implications. *Proceedings of the National Academy of Sciences* 104:5732-5737.
- Postel, S., and B. Richter. 2003. Rivers for life: managing water for people and nature. Island Press, Washington D. C.
- Rosenberg, D. M., P. McCully, and C. M. Pringle. 2000. Global-scale environmental effects of hydrological alterations: introduction. *Bioscience* 50: 746-751.
- Scheidegger, K. J., and M. B. Bain. 1995. Larval Fish Distribution and Microhabitat Use in Free-Flowing and Regulated Rivers. *Copeia* (1):125-135.
- Tortorelli, R.L., and D.L. Bergman. 1985, Techniques for estimating flood peak discharges for unregulated streams and streams regulated by small floodwater retarding structures in Oklahoma: U.S. Geological Survey Water Resources Investigations Report 84-4358, 85 p.
- Tortorelli, R. L., 1997, Techniques for estimating peak-streamflow frequency for unregulated streams and streams regulated by small floodwater retarding structures in Oklahoma: U.S. Geological Survey Water-Resources Investigations Report 97-4202, 39 p.
- Tortorelli, R.L., 2002, Estimated Freshwater Withdrawals in Oklahoma: U.S. Geological Survey circular available online at <http://ok.water.usgs.gov/intro.html> (Accessed July 1, 2008)

USFWS (U.S. Fish and Wildlife Service) and USGS (U.S. Geological Survey). 2004. Future challenges project: compendium of challenge summaries. USFWS/USGS Future Challenges Project Workshop Report, Shepardstown, West Virginia.

Ward, J.H. 1963. Hierarchical grouping to optimize an objective function. *Journal of the American Statistical Association* 58: 236-244.

Appendix

Table A: Final baseline period of record for selected streamflow gaging stations in and near Oklahoma that were considered for use in the HIP Classification. *This data was prepared by the US Geological Survey*

Map Number	USGS Station Identifier	Station Name	Climate Division	Drainage Area (Miles ²)	Baseline Period of Record*	Baseline Years	Human Activities	Climate Variability in Baseline?†	Baseline Quality Ranking
1	07148350	Salt Fk Arkansas River near Winchester, OK	OK2	848.7	1960-1993	34	Minor Irrigation	Yes	Good
2	07148400	Salt Fork Arkansas River near Alva, OK	OK2	1007.5	1939-1951	13	Minor Irrigation	Yes	Good
3	07149000	Medicine Lodge River near Kiowa, KS	KS8	908	1939-1950, 1960-1968	21	None to note	Yes	Good
4	07149500	Salt Fk Arkansas River near Cherokee, OK	OK2	2420	1941-1950	10	None to note	Yes	Good
5	07151500	Chikaskia River near Corbin, KS	KS8	833.6	1951-1965, 1976-2007	47	Withdrawal, diversion, and irrigation	Yes	Fair
6	07152000	Chikaskia River near Blackwell, OK	OK2	1921.6	1937-1949	13	Withdrawal, diversion, and irrigation	Yes	Fair
7	07153000	Black Bear Creek at Pawnee, OK	OK3	552.3	1945-1960	16	Minor Regulation	No	Poor
8	07154500	Cimarron River near Kenton, OK	OK1	1140.4	1951-1966	16	Irrigation	Yes	Poor
9	07155000	Cimarron River above Ute Creek near Boise City, OK	OK1	2017.6	1943-1954	12	Irrigation, Diversion	No	Poor

Table A, continued.

Map Number	USGS Station Identifier	Station Name	Climate Division	Drainage Area (Miles ²)	Baseline Period of Record*	Baseline Years	Human Activities	Climate Variability in Baseline?†	Baseline Quality Ranking
10	07157500	Crooked Creek near Englewood, KS	KS7	843.3	1943-1963	21	Irrigation	Yes	Poor
11	07157900	Cavalry Creek near Coldwater, KS	KS8	42.6	1967-1980	14	None to note	Yes	Excellent
12	07157960	Buffalo Creek near Lovedale, OK	OK1	411.7	1967-1993	27	Minor Regulation	Yes	Poor
13	07159000	Turkey Creek near Drummond, OK	OK2	261.4	1948-1970	23	Diversion	Yes	Poor
14	07160500	Skeleton Creek near Lovell, OK	OK5	422.7	1950-1993, 2002-2007	58	None to note	Yes	Good
15	07163000	Council Creek near Stillwater, OK	OK5	30.8	1935-1960	26	None to note	Yes	Good
16	07170700	Big Hill Creek near Cherryvale, KS	KS9	37.8	1958-1980	23	None to note	Yes	Good
17	07172000	Caney River near Elgin, KS	KS9	439.6	1940-1964	25	None to note	Yes	Good
18	07173000	Caney River near Hulah, OK	OK3	729.2	1938-1949	12	None to note	No	Fair

Table A, continued

Map Number	USGS Station Identifier	Station Name	Climate Division	Drainage Area (Miles ²)	Baseline Period of Record*	Baseline Years	Human Activities	Climate Variability in Baseline?†	Baseline Quality Ranking
19	07174200	Little Caney River below Cotton Cr, near Copan, OK	OK3	516.4	1939-1963	24	None to note	No	Good
20	07174600	Sand Creek at Okesa, OK	OK3	141.4	1960-1993	34	Regulation	Yes	Poor
21	07176500	Bird Creek at Avant, OK	OK3	378.1	1946-1967	22	Regulation	No	Poor
22	07176800	Candy Creek near Wolco, OK	OK3	32.2	1970-1980	11	None to note	No	Good
23	07177000	Hominy Creek near Skiatook, OK	OK3	348.9	1945-1980	36	None to note	Yes	Good
24	07177500	Bird Creek near Sperry, OK	OK3	930.5	1939-1957	20	Diversion	No	Fair
25	07184000	Lightning Creek near McCune, KS	KS9	201	1939-1946, 1960-2007	56	None to note	Yes	Excellent
26	07185500	Stahl Creek near Miller, MO	MO4	4.1	1951-1976	26	None to note	No	Poor
27	07185700	Spring River at LaRussell, MO	MO4	313.5	1958-1973, 1976-1980	21	None to note	No	Poor
28	07185765	Spring River at Carthage, MO	MO4	459.4	1967-1980, 2002-2007	20	None to note	No	Good

Table A, continued

Map Number	USGS Station Identifier	Station Name	Climate Division	Drainage Area (Miles ²)	Baseline Period of Record*	Baseline Years	Human Activities	Climate Variability in Baseline?†	Baseline Quality Ranking
29	07186000	Spring River near Waco, MO	MO4	1188.1	1925-2007	83	Minor regulation	Yes	Fair
30	07187000	Shoal Creek above Joplin, MO	MO4	438.5	1942-2007	66	None to note	Yes	Excellent
31	07188500	Lost Creek at Seneca, MO	MO4	41.8	1949-1959	11	None to note	No	Good
32	07189000	Elk River near Tiff City, Mo	MO4	872.7	1940-2007	68	Backwater from Regulation	Yes	Fair
33	07189540	Cave Springs Branch near South West City, MO	MO4	8.2	1997-2007	11	None to note	No	Good
34	07189542	Honey Creek near South West City, MO	OK3	49.9	1997-2007	11	None to note	No	Good
35	07191000	Big Cabin Creek near Big Cabin, OK	OK3	462	1948-2007	60	Effluent, Irrigation	Yes	Poor
36	07191220	Spavinaw Creek near Sycamore, OK	OK3	135	1962-2007	46	None to note	Yes	Good
37	07192000	Pryor Creek near Pryor, OK	OK3	233.3	1948-1963	16	None to note	No	Good
38	07195000	Osage Creek near Elm Springs, AR	AR1	133.3	1966-1975, 1996-2007	22	Effluent, Minor Regulation	Yes	Fair

Table A, continued.

Map Number	USGS Station Identifier	Station Name	Climate Division	Drainage Area (Miles ²)	Baseline Period of Record*	Baseline Years	Human Activities	Climate Variability in Baseline? [†]	Baseline Quality Ranking
39	07195430	Illinois River South of Siloam Springs, AR	AR1	582.5	1996-2006	11	Minor Regulation	No	Poor
40	07195500	Illinois River near Watts, OK	OK6	646.1	1991-2007	18	Diversion	No	Poor
41	07195800	Flint Creek at Springtown, AR	AR1	15.1	1962-1963, 1965-1979, 1981-2007	44	None to note	Yes	Good
42	07195865	Sager Cr near West Siloam Springs, OK	OK3	19.6	1997-2007	11	Effluent	No	Poor
43	07196000	Flint Creek near Kansas, OK	OK3	118.6	1956-1977	22	Irrigation	No	Poor
44	07196500	Illinois River near Tahlequah, OK	OK6	974.9	1936-1977	42	Minor Regulation	Yes	Fair
45	07196900	Baron Fork at Dutch Mills, AR	AR1	42.2	1959-2007	49	None to note	Yes	Excellent
46	07196973	Peach eater Creek at Christie, OK	OK6	25.5	1993-2003	11	None to note	No	Good
47	07197000	Baron Fork at Eldon, OK	OK6	319.7	1949-2007	59	None to note	Yes	Good
48	07197360	Caney Creek near Barber, OK	OK6	92.5	1998-2007	10	None to note	No	Fair
49	07198000	Illinois River near Gore, OK	OK6	1656.8	1940-1951	12	None to note	No	Good

Table A, continued.

Map Number	USGS Station Identifier	Station Name	Climate Division	Drainage Area (Miles ²)	Baseline Period of Record*	Baseline Years	Human Activities	Climate Variability in Baseline?†	Baseline Quality Ranking
50	07229300	Walnut Creek at Purcell, OK	OK5	207.4	1966-1993	28	Backwater from Regulated Stream	Yes	Fair
51	07230500	Little River near Tecumseh, OK	OK5	474.5	1944-1964	21	Irrigation	Yes	Fair
52	07231000	Little River near Sasakwa, OK	OK5	911.4	1943-1961	19	None to note	Yes	Good
53	07232000	Gaines Creek near Krebs, OK	OK6	600.2	1943-1963	21	None to note	Yes	Excellent
54	07232500	Beaver River near Guymon, OK	OK1	1653.5	1938-1960	23	Minor Regulation	Yes	Fair
55	07233000	Coldwater Creek near Hardesty, OK	OK1	1055.5	1940-1964	25	None to note	Yes	Excellent
56	07233500	Palo Duro Creek near Spearman, TX	TX1	640.9	1946-1969	24	Diversion	Yes	Good
57	07236000	Wolf Creek near Fargo, OK	OK1	1511.1	1943-1956	16	Impoundment	Yes	Poor
58	07243000	Dry Creek near Kendrick, OK	OK5	70.1	1956-1994	39	None to note	Yes	Good
59	07243500	Deep Fork near Beggs, OK	OK6	2056.2	1939-1960	22	Minor Regulation	Yes	Good
60	07244000	Deep Fork near Dewar, OK	OK6	2355.5	1938-1950	13	Minor Regulation	No	Fair

Table A, continued.

Map Number	USGS Station Identifier	Station Name	Climate Division	Drainage Area (Miles ²)	Baseline Period of Record*	Baseline Years	Human Activities	Climate Variability in Baseline?†	Baseline Quality Ranking
61	07245500	Sallisaw Creek near Sallisaw, OK	OK6	185.8	1943-1962	20	Diversion	Yes	Poor
62	07247000	Poteau River at Cauthron, AR	AR4	208.8	1940-1963	29	Minor Regulation	Yes	Good
63	07247250	Black Fork below Big Creek near Page, OK	OK9	96.8	1992-2007	16	None to note	Yes	Good
64	07247500	Fourche Maline near Red Oak, OK	OK9	123.5	1939-1963	25	Impoundment	Yes	Fair
65	07248500	Poteau River near Wister, OK	OK9	1019.4	1939-1948	10	None to note	Yes	Good
66	07249400	James Fork near Hackett, AR	AR4	150.5	1959-2007	19	Diversion/Withdrawal	Yes	Fair
67	07249500	Cove Creek near Lee Creek, AR	AR4	35.7	1950-1970	21	None to note	Yes	Good
68	07249985	Lee Creek near Short, OK	OK6	445.3	1931-1936, 1950-1991, 1993-2007	63	None to note	Yes	Excellent
69	07250000	Lee Creek near Van Buren, AR	OK6	449.3	1931-1936, 1951-1992	48	None to note	Yes	Excellent

Table A, continued.

Map Number	USGS Station Identifier	Station Name	Climate Division	Drainage Area (Miles ²)	Baseline Period of Record*	Baseline Years	Human Activities	Climate Variability in Baseline?†	Baseline Quality Ranking
70	07300000	Salt Fk Red Rv near Wellington, TX	TX2	1029.4	1953-1966	14	Irrigation	Yes	Fair
71	07300500	Salt Fork Red River at Mangum, OK	OK7	1380.4	1938-1966	29	None to note	Yes	Excellent
72	07301410	Sweetwater Creek near Kelton, TX	TX2	305	1963-1978	15	Diversion	Yes	Fair
73	07301500	North Fork Red River near Carter, OK	OK4	2155	1938-1961	25	None to note	Yes	Fair
74	07303400	Elm Fk of N Fk Red River near Carl, OK	OK7	449.3	1960-1979, 1995-2007	33	Diversion/Withdrawal	Yes	Poor
75	07303500	Elm Fk of N Fk Red River near Mangum, OK	OK7	868.3	1938-1976	39	Minor Regulation	Yes	Fair
76	07304500	Elk Creek near Hobart, OK	OK7	563.5	1950-1966	17	Irrigation	No	Poor
77	07311500	Deep Red Creek near Randlett, OK	OK7	619.7	1950-1963, 1970-1973	18	None to note	No	Excellent
78	07313000	Little Beaver Creek near Duncan, OK	OK8	160.6	1949-1963	15	None to note	Yes	Good

Table A, continued.

Map Number	USGS Station Identifier	Station Name	Climate Division	Drainage Area (Miles ²)	Baseline Period of Record*	Baseline Years	Human Activities	Climate Variability in Baseline?†	Baseline Quality Ranking
79	07313500	Beaver Creek near Waurika, OK	OK8	579	1954-1976	23	None to note	Yes	Good
80	07315700	Mud Creek near Courtney, OK	OK8	589.3	1961-2007	47	Minor Regulation	Yes	Good
81	07316500	Washita River near Cheyenne, OK	OK4	782.3	1938-1957	18	Irrigation	Yes	Fair
82	07325000	Washita River near Clinton, OK	OK4	1998.8	1936-1955	20	Irrigation, Minor Regulation	Yes	Poor
83	07326000	Cobb Creek near Fort Cobb, OK	OK7	318.8	1940-1950	11	Minor Regulation	No	Good
84	073274406	Little Washita River above SCS Pnd 26 near Cyril, OK	OK7	3.7	1995-2007	13	None to note	No	Good
85	07327490	Little Washita River near Ninnekah, OK	OK5	213.3	1952-1969	18	Irrigation, Minor Regulation	Yes	Poor
86	07329000	Rush Creek at Purdy, OK	OK8	143.3	1940-1953	13	None to note	Yes	Good
87	07330500	Caddo Creek near Ardmore, OK	OK8	304	1937-1950	14	None to note	Yes	Excellent
88	07332400	Blue River at Milburn, OK	OK8	208.5	1966-1986	21	None to note	Yes	Excellent
89	07332500	Blue River near Blue, OK	OK8	489.8	1937-1980	44	Minor Regulation	Yes	Fair

Table A, continued.

Map Number	USGS Station Identifier	Station Name	Climate Division	Drainage Area (Miles ²)	Baseline Period of Record*	Baseline Years	Human Activities	Climate Variability in Baseline? [†]	Baseline Quality Ranking
90	07332600	Bois D'Arc Creek near Randolph, TX	TX3	74	1964-1985	22	None to note	Yes	Excellent
91	07333500	Chickasaw Creek near Stringtown, OK	OK8	33.5	1956-1968	13	None to note	Yes	Excellent
92	07333800	McGee Creek near Stringtown, OK	OK8	91.1	1956-1968	13	None to note	Yes	Excellent
93	07334000	Muddy Boggy Creek near Farris, OK	OK8	1117.1	1938-1958	21	None to note	Yes	Excellent
94	07335000	Clear Boggy Creek near Caney, OK	OK8	731.8	1943-1960	18	None to note	Yes	Good
95	07335700	Kiamichi River near Big Cedar, OK	OK9	40.7	1966-2007	42	None to note	Yes	Excellent
96	07336000	Tenmile Creek near Miller, OK	OK9	70.1	1956-1970	15	None to note	Yes	Excellent
97	07336200	Kiamichi River near Antlers, OK	OK9	1158.3	1973-1982	10	Diversion	Yes	Fair
98	07336500	Kiamichi River near Belzoni, OK	OK9	1452.6	1926-1972	47	Diversion	Yes	Fair
99	07336750	Little Pine Creek near Kanawha, TX	TX4	77.2	1970-1980	11	None to note	Yes	Excellent
100	07336800	Pecan Bayou near Clarksville, TX	TX4	101.5	1963-1977	15	None to note	Yes	Good
101	07337500	Little River near Wright City, OK	OK9	665	1945-1966	22	None to note	Yes	Excellent

Table A, continued.

Map Number	USGS Station Identifier	Station Name	Climate Division	Drainage Area (Miles ²)	Baseline Period of Record*	Baseline Years	Human Activities	Climate Variability in Baseline? [†]	Baseline Quality Ranking
102	07337900	Glover River near Glover, OK	OK9	328.6	1962-2007	46	None to note	Yes	Excellent
103	07338500	Little River blw Lukfata Ck, near Idabel, OK	OK9	1260	1930-1968	39	Diversion/Withdrawal	Yes	Fair
104	07338750	Mountain Fork at Smithville, OK	OK9	330.7	1992-2007	16	None to note	No	Poor
105	07339000	Mountain Fork near Eagletown, OK	OK9	820.5	1930-1968	39	None to note	Yes	Good
106	07339500	Rolling Fork near DeQueen, AR	AR7	188.1	1949-1976	28	None to note	Yes	Excellent
107	07340300	Cossatot River near Vandervoort, AR	AR4	91.4	1967-2007	29	None to note	Yes	Excellent
108	07340500	Cossatot River near DeQueen, AR	AR7	370.6	1939-1974	36	None to note	Yes	Good
109	07341000	Saline River near Dierks, AR	AR7	123.3	1939-1974	36	None to note	Yes	Excellent
110	07341200	Saline River near Lockesburg, AR	AR7	259.3	1964-1974	11	None to note	Yes	Excellent

* A water year is the 12-month period beginning October 1 and ending September 30 and is named for the year in which it ends; %, percent; --, did not exceed indicated percentage; "no change" indicates that the baseline period of record did not change as a result of the assessment of impoundment.

[†]An optimum minimum period of record to encompass climate variability was determined by analyzing variability in annual precipitation for each climate division and determining the minimum number of years where the distribution of annual precipitation in the climate division was similar to the distribution of annual precipitation for a longer period, 1925-2007. If the gage has fewer baseline years than the minimum number of years determined for the climate division that the gage is located in, the quality ranking was reduced.

Information Transfer Program Introduction

Activities for the efficient transfer and retrieval of information are an important part of the OWRRI program mandate. The Institute maintains a website on the Internet (<http://environ.okstate.edu/owrri>) that provides information on the OWRRI and supported research, grant opportunities and deadlines, and upcoming events. Abstracts of technical reports and other publications generated by OWRRI projects are updated regularly and are accessible on the website.

OWRRI Information Transfer Project

Basic Information

Title:	OWRRI Information Transfer Project
Project Number:	2008OK112B
Start Date:	3/1/2008
End Date:	2/28/2009
Funding Source:	104B
Congressional District:	3
Research Category:	Not Applicable
Focus Category:	None, None, None
Descriptors:	None
Principal Investigators:	Will J Focht, Mike Langston

Publication

The OWRRI produces a quarterly newsletter entitled *The Aquahoman* to disseminate research results and provide information on upcoming events and grant competitions. In 2008, *The Aquahoman* was produced three times and distributed to over 1,000 recipients throughout the state.

The OWRRI sponsors a water research symposium in the fall of each year at which OWRRI-sponsored projects are presented, along with many others. This year's water research symposium was held in conjunction with the annual Governor's Water Conference. This three day event drew over 400 academics, professionals, and the interested public.

In addition, to keep state water professionals apprised of our work, updates on current-year projects are presented to the OWRRI's Water Research Advisory Board, which consists of representatives from 24 state and federal water agencies, as well as non-government organizations. The WRAB is a unique gathering of the State's water agencies, Native American tribes, and water-interested NGOs. As such it has not only become a popular meeting for its members (who report that they have no other opportunity to gather with all of the other state's water organizations and agencies), but has also become a popular venue for seeking advice on water related-topics.

This year the WRAB met four times. Meetings in April and May were held to review and provide advice on the state's efforts to revise its comprehensive water plan. The WRAB was chosen as the appropriate venue for such a meeting because of its unique membership. The August meeting was for the purpose of setting funding priorities for OWRRI's annual research competition and the January meeting was to assist with the selection of funded projects. This year the researchers presented the results of their 2007 projects at the August meeting. This year for the first time, five proposals were selected to be presented by their authors at the January meeting for funding consideration.

The OWRRI produced an annual report which included 2007's technical reports from all research projects (both final and interim reports). This was distributed in hard copy to the members of the WRAB and anyone requesting one. These reports are also available on the website.

USGS Summer Intern Program

None.

Student Support					
Category	Section 104 Base Grant	Section 104 NCGP Award	NIWR-USGS Internship	Supplemental Awards	Total
Undergraduate	2	0	0	0	2
Masters	8	0	0	0	8
Ph.D.	3	0	0	0	3
Post-Doc.	1	0	0	0	1
Total	14	0	0	0	14

Notable Awards and Achievements

Notable Achievements

In 2008, OWRI continued its effort to gather public input on policy suggestions for the Oklahoma's update of the comprehensive water plan. The OWRI is under contract with Oklahoma Water Resources Board (OWRB) for this effort and has designed a novel approach for gathering public input. Utilizing the values of the public as well as the best expertise available, the goal of this four and a half year process is to develop a plan that enjoys broad support and is well informed. The effort includes approximately 70 public meetings across the state to gather, consolidate, and prioritize citizens' concerns, and then, develop policy recommendations regarding state water issues.

The first two years have been very successful, consisting of 42 Local Input Meetings followed by 11 Regional Input Meetings across the state. In 2008, approximately 350 people participated in the process by helping to identify the high priority topics for the water plan.

As part of this planning effort, the OWRB has joined the OWRI in funding research to address the state's water planning needs by providing a match to the money granted by the US Geological Survey.

Publications from Prior Years